Ae 237

Non-steady Gasdynamics

Lecture Notes

Ae 237

Discrete Waves in a Medium

Consider a homogeneous material contained in a rigid insulating tube that is open at the right and closed by a rigid, thermally insulating movable piston on the left. Let the density, pressure and temperature be ρ_0, p_0 and T_0 in the medium.

Now let the piston be brought impulsively to a finite constant velocity to the right, u_p. The part of the medium that is immediately adjacent to the piston "knows" about its change of velocity at time $t=0$, but these will be a region in the tube further from the piston where information about the piston motion arrives only after a finite time. We look for discrete waves, so

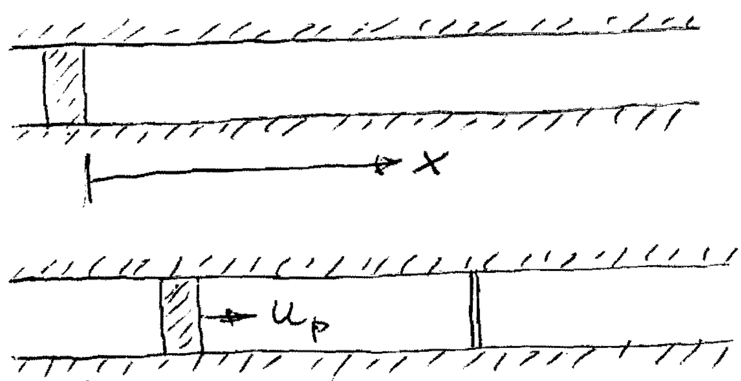

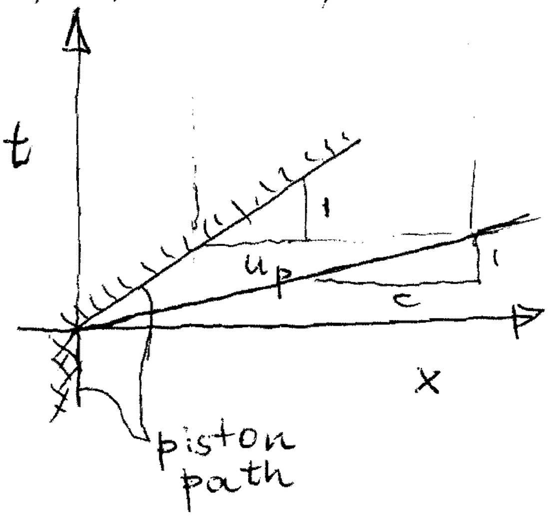

assume that there exist only two states in the medium: One which is completely unaffected by the piston motion, and one which is changed by it. Both regions are uniform and they are separated by a wave travelling ahead of the piston at a wave speed c.

In order to obtain quantitative relations for this situation consider the conservation equations. Consider the time interval between t_1 and t_2

$$\Delta t = t_2 - t_1$$

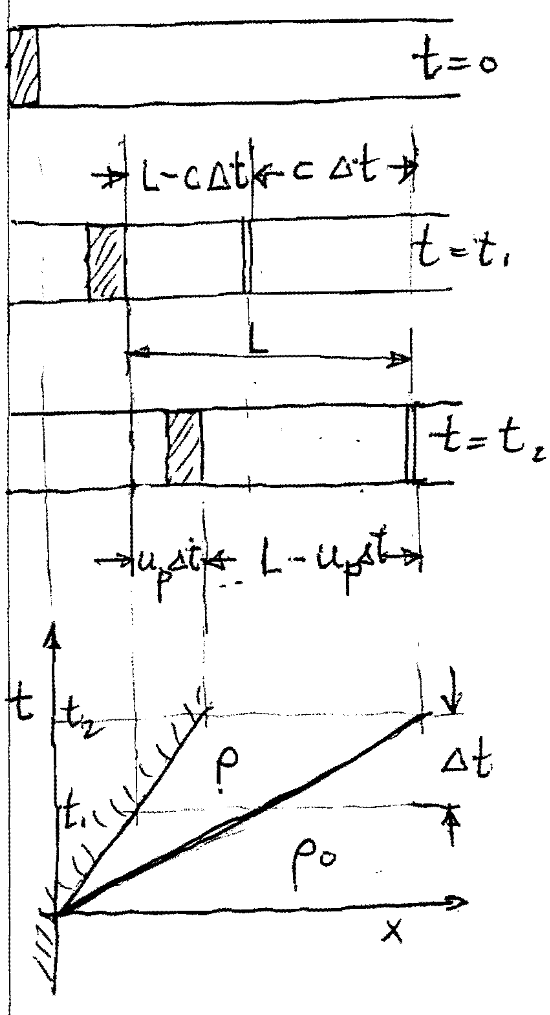

Conserve mass:

Consider the region L of the tube:

$$\rho(L - u_p\Delta t) = \rho(L - c\Delta t) + \rho_o c\Delta t$$

$$\boxed{\rho(c - u_p) = \rho_o c}$$

Or $c(\rho - \rho_o) = \rho u_p$.

Therefore

$$\boxed{\frac{\Delta\rho}{\rho} \equiv \frac{\rho - \rho_o}{\rho} = \frac{u_p}{c} = -\frac{\Delta v}{v_o}}$$

where $v \equiv 1/\rho$ is the specific volume.

Conserve momentum:

Consider the same time interval and demand that momentum increase = $\Delta t \times$ applied force

$$\rho(L-u_p\Delta t).u_p - \rho(L-c\Delta t).u_p = (p-p_0)\Delta t$$

or $$p-p_0 = \rho u_p(c-u_p)$$

$$\boxed{p-p_0 = \rho_0 c u_p}$$

<u>Note</u>: In the limit of very weak waves, the wave propagation speed approaches the speed of sound, a, and $dp = \rho a\, du$. Hence we speak of the acoustic impedance ρa.

We may now form the ratio

$$\frac{\Delta p}{\Delta v} = -\frac{c}{v_0 u_p}\cdot \rho_0 c u_p = -\frac{\rho_0 c^2}{v_0}$$

or $$\boxed{\frac{\Delta p}{\Delta v} = -\rho_0^2 c^2 = -m^2}$$

$m \equiv \rho_0 c$ = mass flux relative to wave = constant!

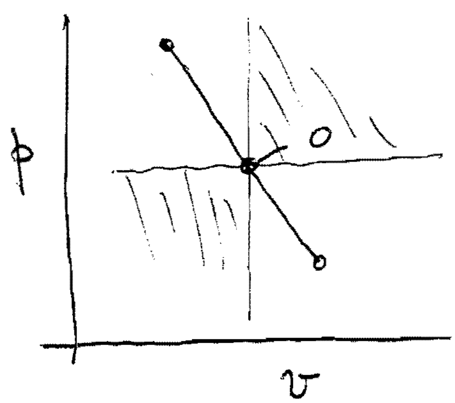

The line joining the upstream and downstream points has a negative slope in vp-space.

Ae 237

We may also form the ratio

$$\frac{\Delta p}{\Delta \rho} = \rho_0 c u_p \cdot \frac{c}{\rho u_p} = \rho(c-u_p)\cdot\frac{c}{\rho}$$

$$\rightarrow \quad \frac{\Delta p}{\Delta \rho} = c(c-u_p)$$

In the weak wave limit: $\frac{dp}{d\rho} = a^2$

<u>Now conserve energy</u>

Note: $\Delta p \Delta v = \rho_0 c u_p \cdot \left(-\frac{v_0 u_p}{c}\right) = -u_p^2$

This shows that Δp and Δv have opposite sign even if $u_p < 0$.

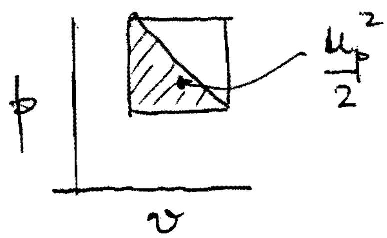

Let $e \equiv$ specific internal energy

Energy conservation:

$$\rho(L-u_p\Delta t)\left(e+\frac{u_p^2}{2}\right) - \left[\rho(L-c\Delta t)\left(e+\frac{u_p^2}{2}\right) + \rho_0 e_0 c\Delta t\right] = p u_p \Delta t$$

$$\underbrace{\rho(c-u_p)}_{\rho_0 c}\left(e+\frac{u_p^2}{2}\right) - \rho_0 e_0 c = p u_p$$

$$\rho_0 c\left(e - e_0 + \frac{u_p^2}{2}\right) = p u_p$$

$$\boxed{e - e_0 + \frac{u_p^2}{2} = \frac{p u_p}{\rho_0 c} = -p\Delta v}$$

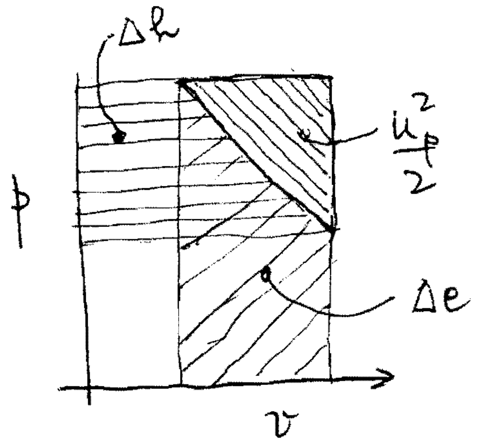

so that

$$\frac{\Delta e}{\Delta v} = -p - \frac{u_p^2}{2\Delta v}$$

$$= -p - \frac{u_p^2}{2}\left(-\frac{\Delta p}{u_p^2}\right)$$

$$= -p + \frac{p - p_0}{2}$$

$$= -\frac{p + p_0}{2} = -\bar{p}$$

$$\boxed{\frac{\Delta e}{\Delta v} = \bar{p}}$$

Note: weak wave: $\left(\frac{\partial e}{\partial v}\right)_s = -p$ ✓

We could also form the specific enthalpy change

$$h - h_0 = e - e_0 + pv - p_0 v_0$$

$$= -\frac{p + p_0}{2}(v - v_0) + pv - p_0 v_0$$

$$= p\left(\frac{v_0}{2} - \frac{v}{2} - v_0\right) + p_0\left(-\frac{v}{2} + \frac{v_0}{2} + v\right)$$

$$= (p - p_0)\,\frac{v_0 + v}{2}$$

$$\boxed{\Delta h = \Delta p\,\bar{v}}$$

Note: weak wave $\left(\frac{\partial h}{\partial p}\right)_s = v$

We now summarize the shock jump conditions. Since we have not made any assumptions about the material properties, these apply quite generally:

Shock jump conditions:
general medium.

$$\boxed{\begin{aligned} \Delta h &= \bar{v}\,\Delta p \quad &(1)\\ \Delta p &= -\rho_0^2 c^2 \Delta v \quad &(2)\\ \Delta v &= -v_0 \frac{u_p}{c} \quad &(3)\end{aligned}}$$

Example: perfect gas

$$\frac{p}{\rho} = RT \qquad h = c_p T = \frac{\gamma}{\gamma-1}\, p v$$

Substitute into (1):

$$\frac{\gamma}{\gamma-1}\left(p v - p_0 v_0\right) = \frac{v+v_0}{2}\left(p-p_0\right)$$

Now write $\quad p = p_0\left(1+\frac{p-p_0}{p_0}\right), \quad v = v_0\left(1+\frac{v-v_0}{v_0}\right)$

So $\quad \frac{\gamma}{\gamma-1}\left[p_0 v_0\left(1+\frac{p-p_0}{p_0}\right)\left(1+\frac{v-v_0}{v_0}\right) - p_0 v_0\right] = \frac{1}{2}\left[v_0\left(1+\frac{v-v_0}{v_0}\right)+v_0\right] \times (p-p_0)$

$$\frac{\gamma}{\gamma-1}\, p_0 v_0 \left[\frac{p-p_0}{p_0} + \frac{v-v_0}{v_0} + \frac{p-p_0}{p_0}\,\frac{v-v_0}{v_0}\right] =$$

$$= \frac{p-p_0}{p_0}\cdot \cancel{p_0 v_0} + \frac{1}{2}\cancel{p_0 v_0}\cdot\frac{v-v_0}{v_0}\cdot\frac{p-p_0}{p_0}$$

$$\frac{p-p_0}{p_0}\left[\frac{\gamma}{\gamma-1}\left(1+\frac{v-v_0}{v_0}\right) - 1 - \frac{1}{2}\,\frac{v-v_0}{v_0}\right] = -\frac{\gamma}{\gamma-1}\,\frac{v-v_0}{v_0}$$

$$\frac{p-p_0}{p_0}\left[\frac{1}{\gamma-1} + \frac{\gamma+1}{2(\gamma-1)}\,\frac{v-v_0}{v_0}\right] = -\frac{\gamma}{\gamma-1}\,\frac{v-v_0}{v_0}$$

Solve

$$\boxed{\begin{aligned} \frac{p-p_0}{p_0} &= -\frac{\gamma \dfrac{v-v_0}{v_0}}{1+\dfrac{\gamma+1}{2}\dfrac{v-v_0}{v_0}} \\ \text{or} \quad \frac{v-v_0}{v_0} &= -\frac{\dfrac{p-p_0}{p_0}}{\gamma+\dfrac{\gamma+1}{2}\dfrac{p-p_0}{p_0}} \end{aligned}} \quad (4) \quad \text{(perf. gas)}$$

To express these in terms of $M_s \equiv \dfrac{c}{a_0}$, use $a_0^2 = \dfrac{\gamma p_0}{\rho_0}$ in (2) & (4)

$$\boxed{\begin{aligned} \frac{p-p_0}{p_0} &= \frac{2\gamma}{\gamma+1}\left(M_s^2-1\right) = -\gamma M_s^2 \frac{v-v_0}{v_0} \\ \frac{v-v_0}{v_0} &= -\frac{2}{\gamma+1}\left(1-\frac{1}{M_s^2}\right) \\ \frac{u_p}{a_0} &= \frac{2}{\gamma+1}\left(M_s-\frac{1}{M_s}\right) \end{aligned}}$$

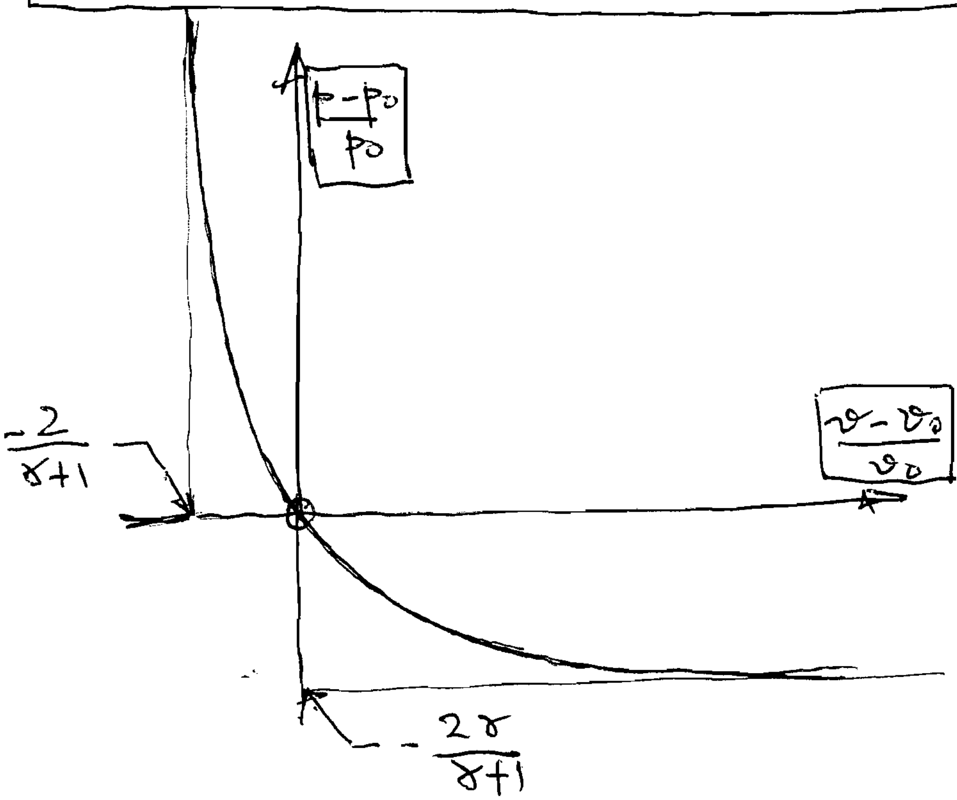

Second Law of Thermodynamics, and causality and stability implications.

To satisfy causality, information must pass from the piston to the wave. Infinitesimally weak waves must therefore catch up with the shock. It follows that

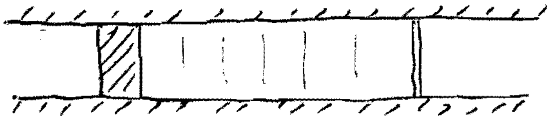

$$\boxed{c - u_p \leqslant a}$$

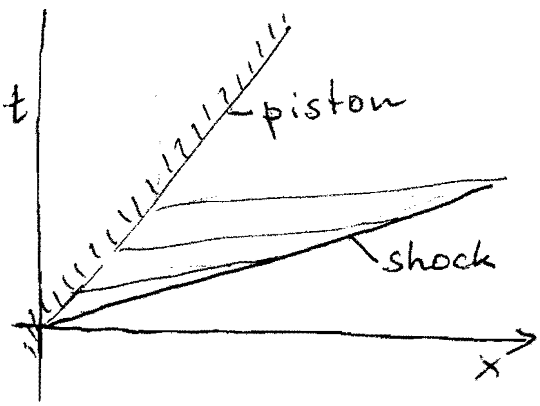

The equal sign corresponds to the weak wave limit or to the Chapman-Jouguet condition (see later)

The alternative condition, that weak waves do not catch up with the shock, violates causality.

To illustrate in vp-space, consider

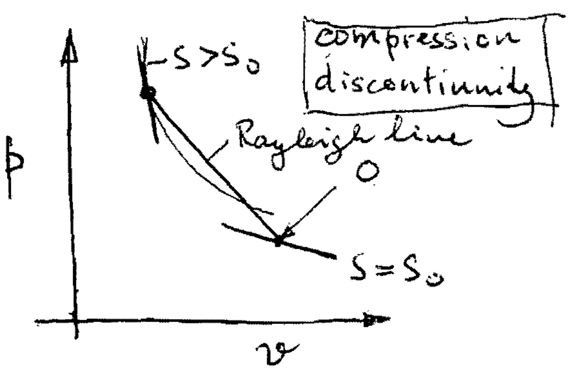

$$\frac{\Delta p}{\Delta v} = -\rho_0^2 c^2 = -\rho^2 (c - u_p)^2$$

$$\left|\frac{\Delta p}{\Delta v}\right| = \rho^2 (c-u_p)^2 < \rho^2 a^2 = \left(\frac{\partial p}{\partial v}\right)_s$$

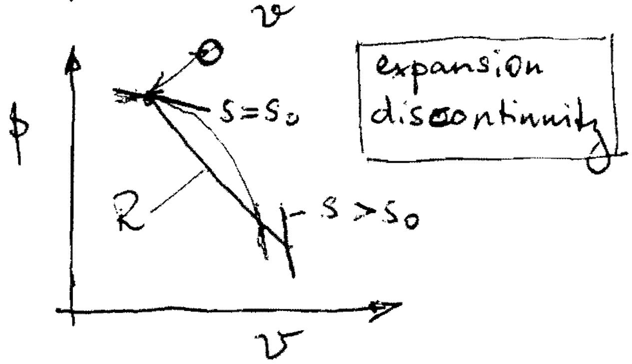

At downstream point isentrope is steeper than the "Rayleigh" line.

Stability

The discrete wave or shock does not split up into more waves. I.e., it does not send signals ahead of itself. Weak disturbances

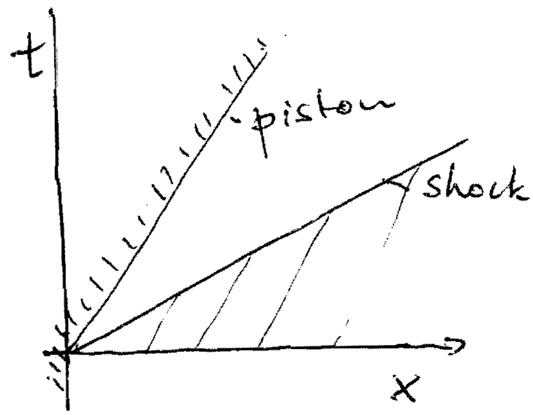

generated along the tube at $t=0$ are caught by the shock. This means that

$$\boxed{c > a_0}$$

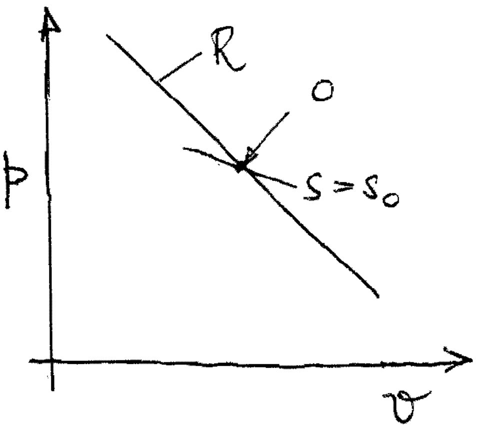

To illustrate this in vp-space, consider the upstream point

$$\left|\frac{\Delta p}{\Delta v}\right| = \rho_0^2 c^2 > \rho_0 a_0^2 = \left|\left(\frac{\partial p}{\partial v}\right)_s\right|_0$$

Rayleigh line is steeper than the isentrope at the upstream point.

Now consider the locus of states reachable from a given initial state by shock waves of different strengths. This curve in vp-space is called the Hugoniot or shock adiabat. Its shape depends on the properties of the medium. We now proceed to construct this by assuming that entropy change is monotonic in the shock strength.

First, review some <u>material properties</u>:

(1) The first question to consider is: In which direction in vp-space does s increase?

Write
$$T\,ds = de + p\,dv$$
or
$$de = T\,ds - p\,dv$$
Integrability of de demands that
$$\left(\frac{\partial T}{\partial v}\right)_s = -\left(\frac{\partial p}{\partial s}\right)_v$$

Therefore,
$$\left(\frac{\partial p}{\partial s}\right)_v = \left(\frac{\partial T}{\partial s}\right)_v\left(\frac{\partial s}{\partial v}\right)_T = \frac{T}{c_v}\left(\frac{\partial p}{\partial T}\right)_v \qquad \text{since } c_v = T\left(\frac{\partial s}{\partial T}\right)_v$$
$$= -\left(\frac{\partial p}{\partial v}\right)_T\left(\frac{\partial v}{\partial T}\right)_p \cdot \frac{T}{c_v} \qquad \text{Integrability of } df = -s\,dT - p\,dv \rightarrow \left(\frac{\partial s}{\partial v}\right)_T = \left(\frac{\partial p}{\partial T}\right)_v$$
$$= -v\left(\frac{\partial p}{\partial v}\right)_T \cdot \frac{1}{v}\left(\frac{\partial v}{\partial T}\right)_p \cdot \frac{T}{c_v}$$

Now, $-\frac{1}{v}\left(\frac{\partial v}{\partial p}\right)_T \equiv k$ is the isothermal compressibility

and $\frac{1}{v}\left(\frac{\partial v}{\partial T}\right)_p \equiv \beta$ is the isobaric volume expansivity

$k > 0$ for material stability and $= \frac{1}{p}$ for a perfect gas.

$\beta \gtrless 0$ and $= \frac{1}{T}$ for a perfect gas.

Return to $\left(\frac{\partial p}{\partial s}\right)_v = \frac{\beta}{k}\frac{T}{c_v}$

so $$\boxed{\left(\frac{\partial s}{\partial p}\right)_v = \frac{k c_v}{\beta T}}$$

If $\beta > 0$ entropy increases in the positive pressure direction and vice versa.

Introduce the Grüneisen parameter G

$$G \equiv v\left(\frac{\partial p}{\partial e}\right)_v = \frac{v}{T}\left(\frac{\partial p}{\partial s}\right)_v$$

Hence $$\boxed{\left(\frac{\partial s}{\partial p}\right)_v = \frac{v}{TG}}$$

Note: $G = \frac{\beta v}{k c_v} = \frac{\beta a^2}{c_v} = \gamma - 1$ for a perfect gas.

(2) Next, we need the sign of $\left(\frac{\partial^2 p}{\partial v^2}\right)_s$, i.e., the curvature of the isentropes in vp-space

Define $$\boxed{\Gamma \equiv \frac{v^3}{2a^2}\left(\frac{\partial^2 p}{\partial v^2}\right)_s = \frac{1}{a}\left(\frac{\partial(\rho a)}{\partial \rho}\right)_s}$$

This is called the fundamental derivative of gasdynamics. For a perfect gas, $\Gamma = \frac{\gamma+1}{2}$ which is positive. However, some materials exhibit $\Gamma < 0$. Depending on material properties we therefore have to distinguish four possible cases depending on the signs of G and Γ.

(I) $\boxed{G > 0, \quad \Gamma > 0}$

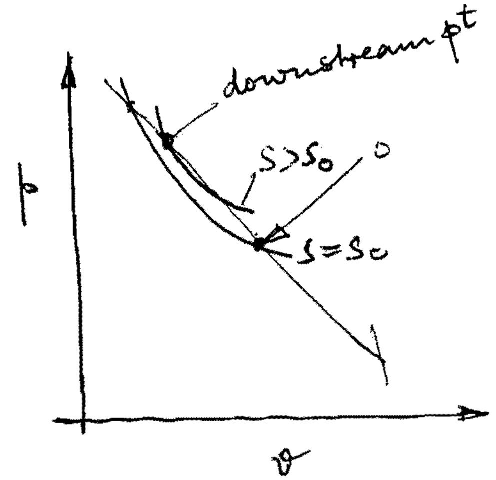

$\left(\frac{\partial^2 p}{\partial v^2}\right)_s > 0$

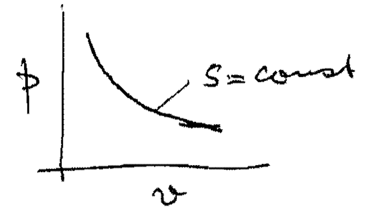

$\left(\frac{\partial s}{\partial p}\right)_v > 0$

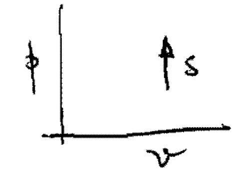

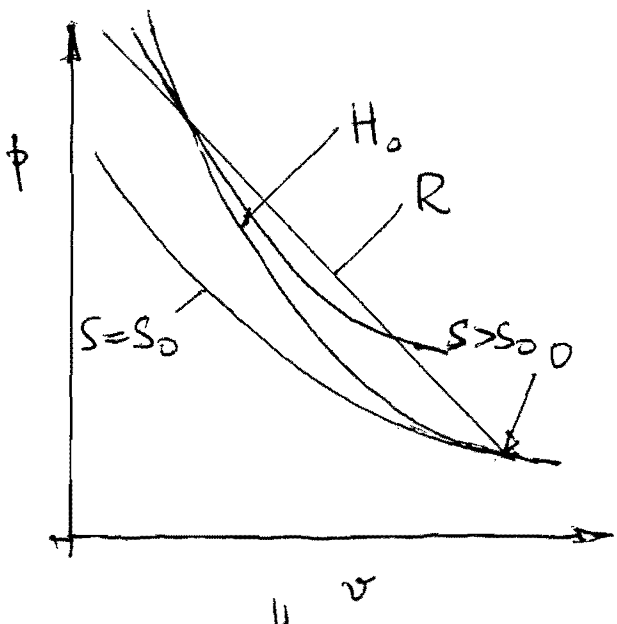

These conditions are satisfied for a <u>compression shock</u>, but not for an expansion shock.

As will be shown later the slope of the Hugoniot at o (H_o) is the same as that of the isentrope at o. At the downstream point s = constant lies between Hugoniot and Rayleigh line.

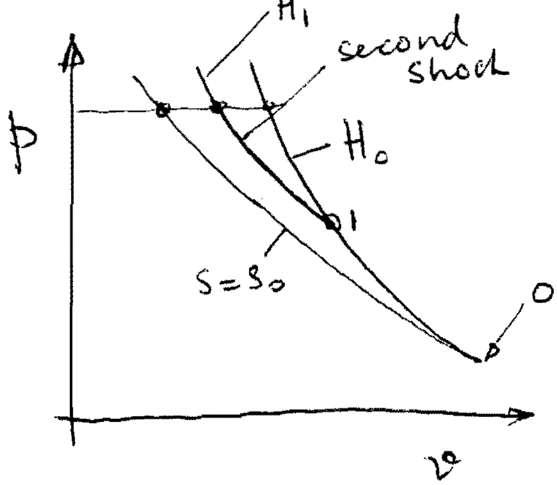

For a given Δp, an isentropic wave gives the largest volume reduction, single shock gives the least (less than multiple shocks)

II $\boxed{G<0\ ,\ \Gamma>0}$

$\left(\frac{\partial^2 p}{\partial v^2}\right)_s > 0$

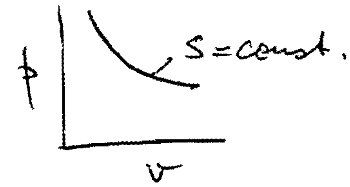

$\left(\frac{\partial s}{\partial p}\right)_v < 0$

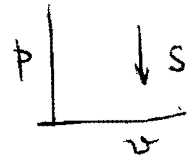

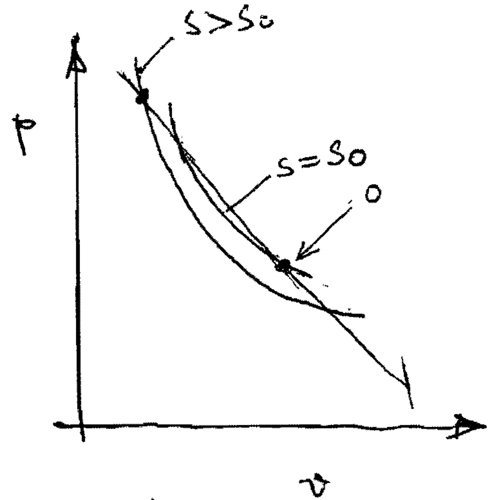

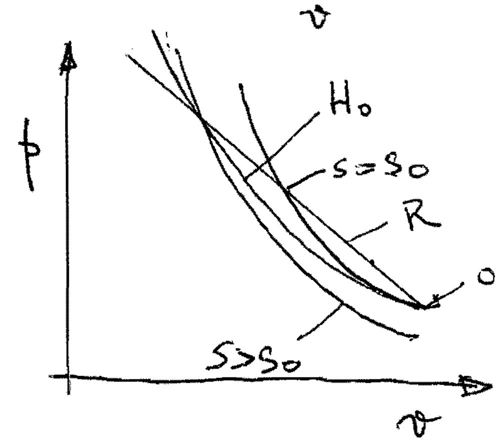

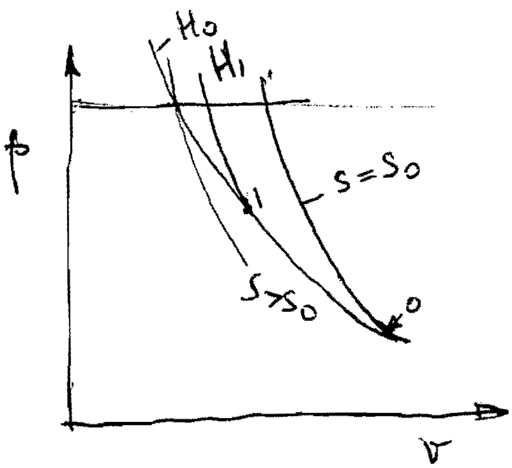

<u>compression shock</u>

This time, at the downstream point, the Hugoniot through 0, H_0, lies between the Rayleigh line and the isentrope.

Because a second shock has to be tangent to the isentrope at <u>its</u> upstream point, a single shock gives greater volume reduction than multiple shocks.

Also, an isentropic wave gives the smallest volume reduction,

(in both cases for a given pressure rise)

III $\boxed{G > 0 \,,\ \Gamma < 0}$

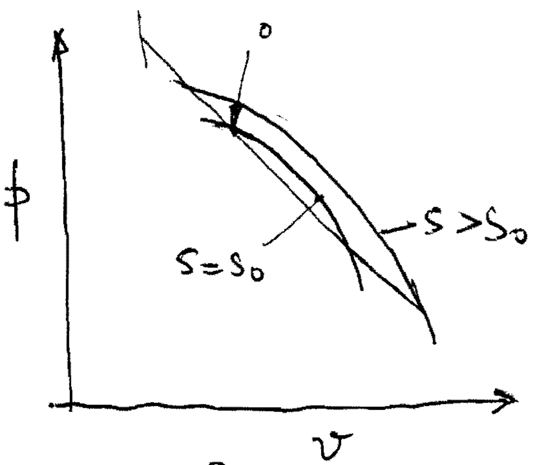

$\left(\frac{\partial^2 p}{\partial v^2}\right)_s < 0$

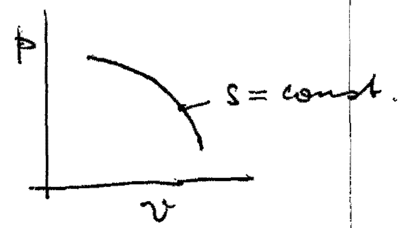

$\left(\frac{\partial s}{\partial p}\right)_v > 0$

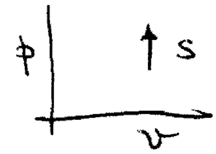

expansion shock

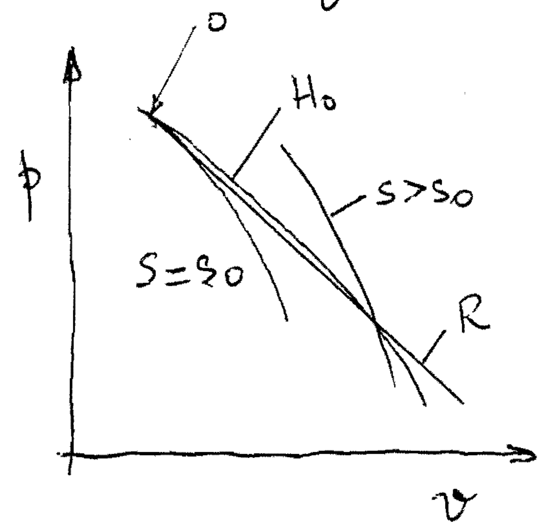

H_0 lies between $s = $ const. and R at the downstream point

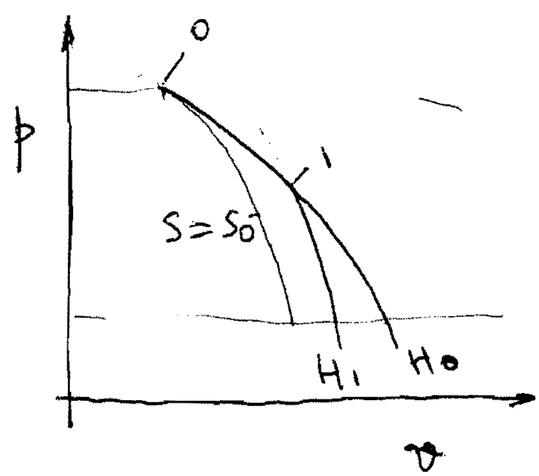

Single shock gives largest volume increase greater than multiple shocks. Isentropic wave gives smallest volume increase.

IV $\boxed{G < 0 \ , \ \Gamma < 0}$

$\left(\dfrac{\partial^2 p}{\partial v^2}\right)_s < 0$

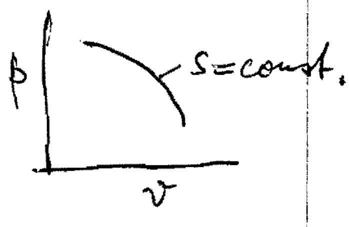

$\left(\dfrac{\partial s}{\partial p}\right)_v < 0$

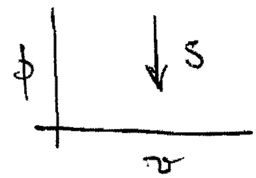

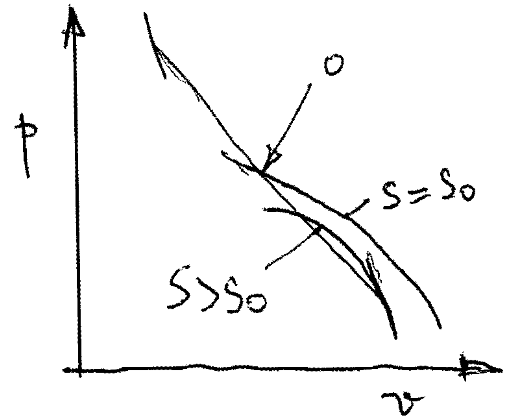

<u>expansion shock</u>

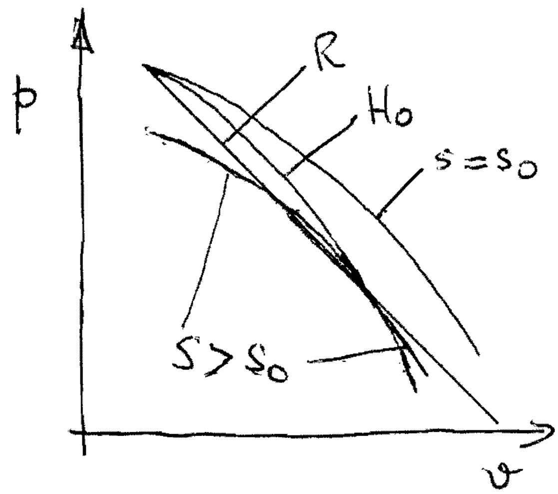

s = constant lies between R and H_0 at downstream point.

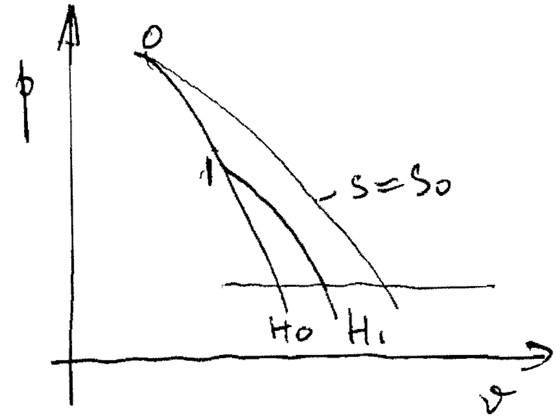

For a given pressure decrease, a single shock gives less volume increase than multiple shocks. The largest volume increase is given by an isentropic wave.

Relation between Hugoniot and isentrope at (o)

Consider the entropy change across a weak shock. From the general shock jump relations (homogeneous single phase)

$$\Delta e = -\bar{p}\,\Delta v = -\frac{p_0 + p}{2}\,\Delta v$$

rewrite

$$\boxed{\Delta e = -\frac{\Delta p}{2}\Delta v - p_0\,\Delta v}$$

Now proceed to obtain Taylor-series expansions of both sides of this equation.

$\boxed{\text{L.H.S.}}$ Consider $e = e(s, v)$:

$$\Delta e = \left.\frac{\partial e}{\partial v}\right|_0 \Delta v + \left.\frac{\partial^2 e}{\partial v^2}\right|_0 \frac{(\Delta v)^2}{2} + \left.\frac{\partial^3 e}{\partial v^3}\right|_0 \frac{(\Delta v)^3}{6} + \dots + \left(\frac{\partial e}{\partial s}\right)_v \Delta s + \dots$$

but $de = T\,ds - p\,dv$, so $\frac{\partial e}{\partial v} = -p$

Hence
$$\Delta e = -p_0\,\Delta v - \left(\frac{\partial p}{\partial v}\right)_s \frac{(\Delta v)^2}{2} - \left(\frac{\partial^2 p}{\partial v^2}\right)_s \frac{(\Delta v)^3}{6} + \dots + T_0\,\Delta s + \dots$$

$\boxed{\text{R.H.S.}}$ Consider $p = p(s, v)$:

$$\Delta p = \frac{\partial p}{\partial v}\Delta v + \frac{\partial^2 p}{\partial v^2}\frac{(\Delta v)^2}{2} + \dots + \frac{\partial p}{\partial s}\Delta s$$

$$-p_0\,\Delta v - \frac{\Delta p}{2}\Delta v = -p_0\,\Delta v - \frac{\partial p}{\partial v}\frac{(\Delta v)^2}{2} - \frac{\partial^2 p}{\partial v^2}\frac{(\Delta v)^3}{4} + \dots - \frac{\partial p}{\partial s}\Delta s\frac{\Delta v}{2} + \dots$$

equate LHS and RHS expansions

$$\boxed{T_0\,\Delta s = -\frac{1}{12}\left(\frac{\partial^2 p}{\partial v^2}\right)_s (\Delta v)^3 = -\frac{\Gamma}{6}\,a_0^2\left(\frac{\Delta v}{v_0}\right)^3}$$ — near (0)

This shows that the Hugoniot is isentropic to second order! at the upstream point, and brings out the importance of Γ.

Since Δs must be positive (Second Law) a positive value of Γ requires Δv to be negative (compression shock) while negative Γ gives rise to expansion shocks.

Now form the difference between $p_H(v)$ along the Hugoniot and $p_s(v)$ along the isentrope. Since Δp_H and Δp_s differ only by $\left(\frac{\partial p}{\partial s}\right)_v \Delta s$, (see previous page)

$$\boxed{\begin{aligned} p_H - p_s &= -\frac{1}{12 T_0}\left(\frac{\partial p}{\partial s}\right)_v \left(\frac{\partial^2 p}{\partial v^2}\right)_s (\Delta v)^3 \\ p_H - p_s &= -\frac{\Gamma G}{6}\, \rho_0 a_0^3 \frac{(\Delta v)^3}{v^3} \end{aligned}} \text{ — near (0)}$$

An alternative way to obtain the result at the bottom of p. 16 is as follows:

Differentiating $\quad \Delta h = \bar{v}\Delta p\,, \quad$ —— (1)

we get $\quad \dfrac{dh}{\Delta h} = \dfrac{1}{2}\dfrac{dv}{\bar{v}} + \dfrac{dp}{\Delta p}.$

The d implies "along the Hugoniot" here.

Using (1) again,

$$dh = \bar{v}\,dp + \frac{1}{2}\Delta p\,dv.$$

Substitute this into

$$T\,dS = dh - v\,dp$$

$$= \frac{v+v_0}{2}\,dp + \frac{1}{2}\Delta p\,dv - v\,dp$$

$$= -\frac{\Delta v}{2}\,dp + \frac{1}{2}\Delta p\,dv \qquad \text{(i)}$$

Differentiate this twice w.r.t. v along the Hugoniot:

$$\frac{dT}{dv}\frac{dS}{dv} + T\frac{d^2S}{dv^2} = -\frac{1}{2}\Delta v\frac{d^2p}{dv^2} - \cancel{\frac{1}{2}\frac{dp}{dv}} + \cancel{\frac{1}{2}\frac{dp}{dv}} \qquad \text{(ii)}$$

$$\frac{d^2T}{dv^2}\frac{dS}{dv} + 2\frac{dT}{dv}\frac{d^2S}{dv^2} + T\frac{d^3S}{dv^3} = -\frac{1}{2}\Delta v\frac{d^3p}{dv^3} - \frac{1}{2}\frac{d^2p}{dv^2} \qquad \text{(iii)}$$

Now evaluate (i), (ii) and (iii) at the upstream point (o) where $\Delta p = \Delta v = 0$.

(i) $\rightarrow$ $\quad T_0\left(\frac{dS}{dv}\right)_0 = 0$

(ii) $\rightarrow$ $\quad T_0\left(\frac{d^2S}{dv^2}\right)_0 = 0$

(iii) $\rightarrow$ $\quad T_0\left(\frac{d^3S}{dv^3}\right)_0 = -\frac{1}{2}\left(\frac{d^2p}{dv^2}\right)_0 = -\frac{1}{2}\left(\frac{\partial^2 p}{\partial v^2}\right)_S = -\frac{a_0^2}{v_0^3}\Gamma$

It follows that (Taylor expansion)

$$T_0\,\Delta S = -\frac{1}{12}\left(\frac{\partial^2 p}{\partial v^2}\right)_S (\Delta v)^3 = -\frac{\Gamma}{6}\frac{a_0^2}{v_0^3}(\Delta v)^3$$

as before.

Example: Perfect gas, $\Gamma = \frac{\gamma+1}{2}$

$$\frac{\Delta v}{v_0} = -\frac{2}{\gamma+1}\left(1-\frac{1}{M_S^2}\right)$$

$$T_0\,\Delta S = -\frac{(\gamma+1)}{12}\left(\frac{\gamma p_0}{\rho_0}\right)\left(\frac{-2}{\gamma+1}\right)^3\left(1-\frac{1}{M_S^2}\right)^3$$

$$\boxed{\frac{\Delta S}{R} = \frac{2}{3}\frac{\gamma}{(\gamma+1)^2}\left(\frac{M_S^2-1}{M_S^2}\right)^3}\text{ — near (0)}$$

since this applies only near (0), i.e. for very weak waves, $M_S \doteq 1$

$$\frac{\Delta S}{R} \doteq \frac{2}{3}\frac{\gamma}{(\gamma+1)^2}\left(M_S^2-1\right)^3$$

In the limit of $M_S \to 1$, the wave is isentropic (acoustic limit).

Experimental determination of Hugoniot

In gases and liquids, shocks of different strengths are generated in a shock tube, and the pressure is measured at the shock tube wall at two places. As the shock passes across the pressure transducer, the pressure jumps. This gives Δp. The time interval between the pressure jumps at the two transducers gives the shock speed c. Knowledge of the upstream conditions, together with the shock jump relations then gives the remaining information to draw the Hugoniot. Show example from Griffiths, Sandeman, Hornung.

In the case of solids, one side of a "test" plate of the medium is suddenly loaded, either by a shock wave or by impact of another "striker plate". In the case of shock impingement, measure u_p and c, and hence get Hugoniot, see sketch on left.

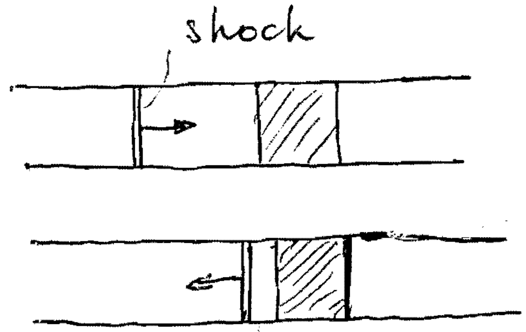

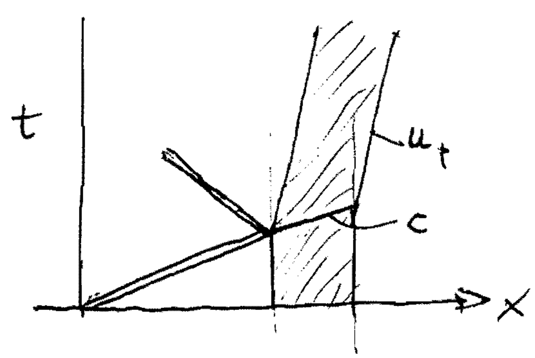

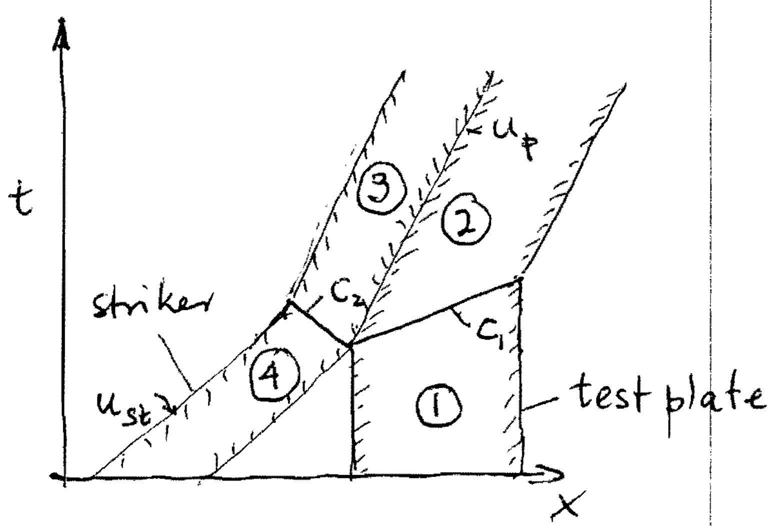

In the case of a striker plate, $p_2 = p_3$ since interface is not accelerated. Therefore

$$\rho_1 c_1 u_p = \rho_4 c_4 (u_{st} - u_p)$$

If the materials are the same, $\rho_1 = \rho_4$, $c_1 = c_4$

$$u_p = \tfrac{1}{2} u_{st} \quad . \quad \text{Measure } c_1, u_{st} .$$

Ae 237

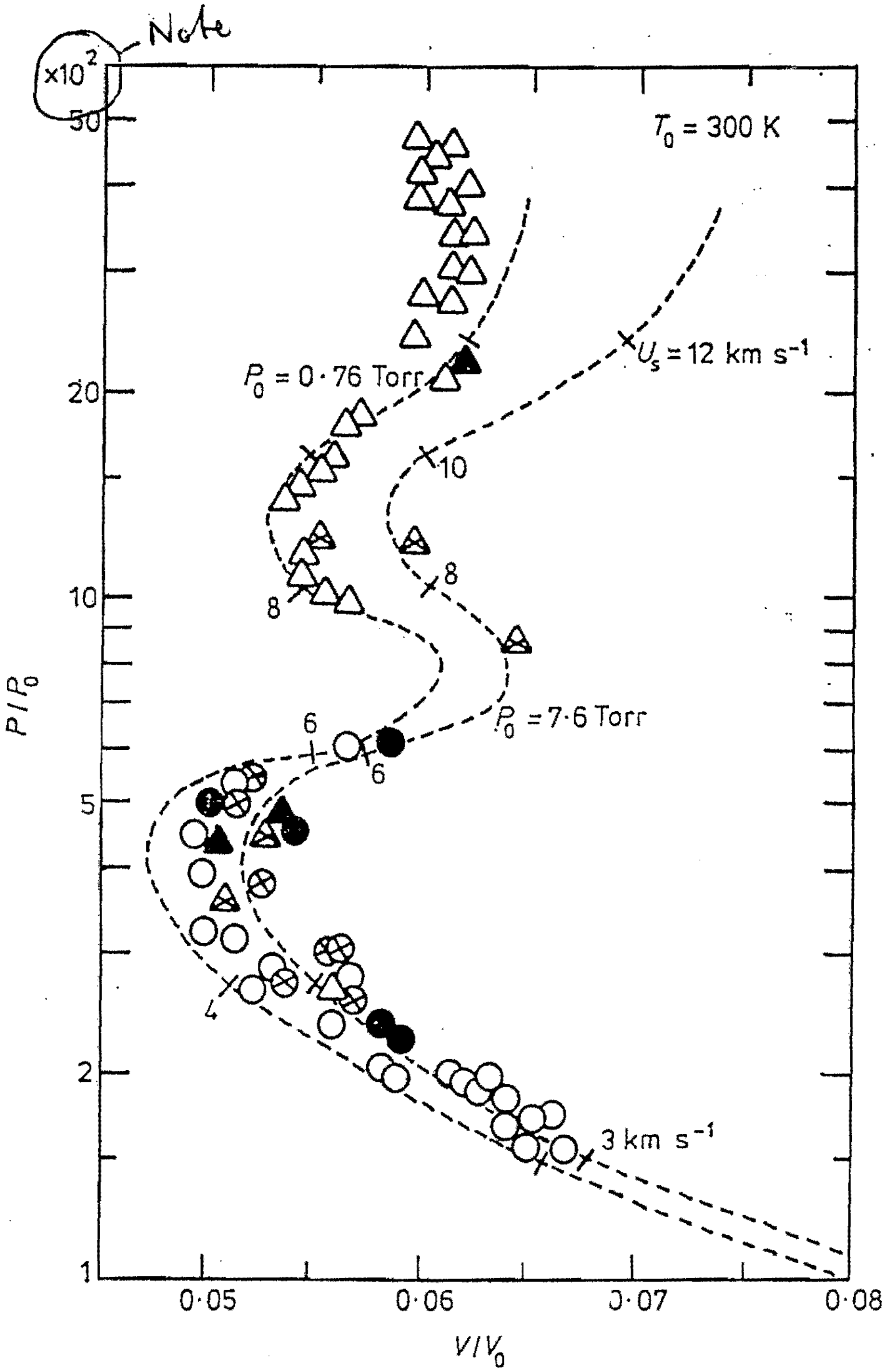

Figure 6. Experimental stability results for shock waves in CO_2 superimposed on the computed (normalized) equilibrium Hugoniot curves. Solid, crossed and open symbols show cases classed as 'unstable', 'doubtful' and 'stable' shocks respectively. △ DD operation; ○ SD operation.

From Griffiths, Sandeman & Hornung
J. Phys. D.: Appl. Phys. Vol. 8 p1681, 1975

The figure from G., S., + H. shows that the Hugoniot can double back on itself. In such cases a faster shock may give a smaller Δv, compare shock 2 with shock 1.

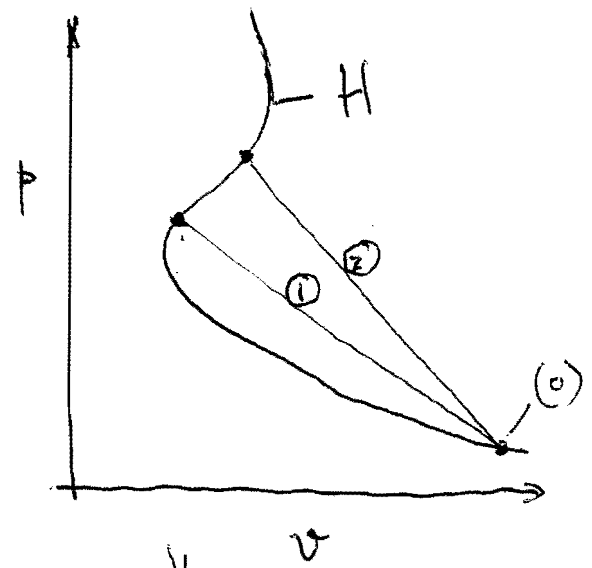

Note: In the experimental results it looks as if the Rayleigh line could intersect the Hugoniot twice, as shown in the sketch on the left.

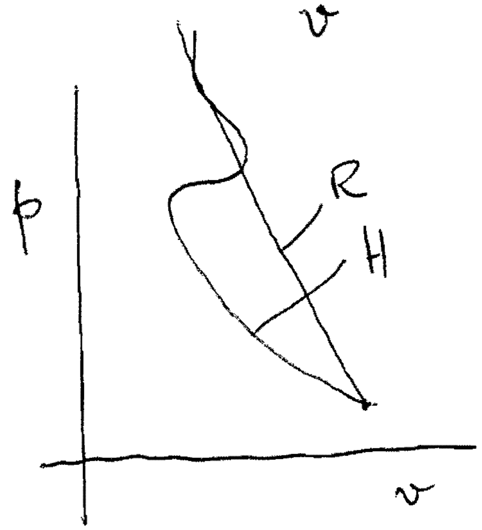

However, this is not the case. The logarithmic plot makes it look like that. In the vicinity of $p/p_0 = 1000$, the Hugoniot slope is $\sim -40{,}000$ while the Rayleigh line slope is ~ -1000.

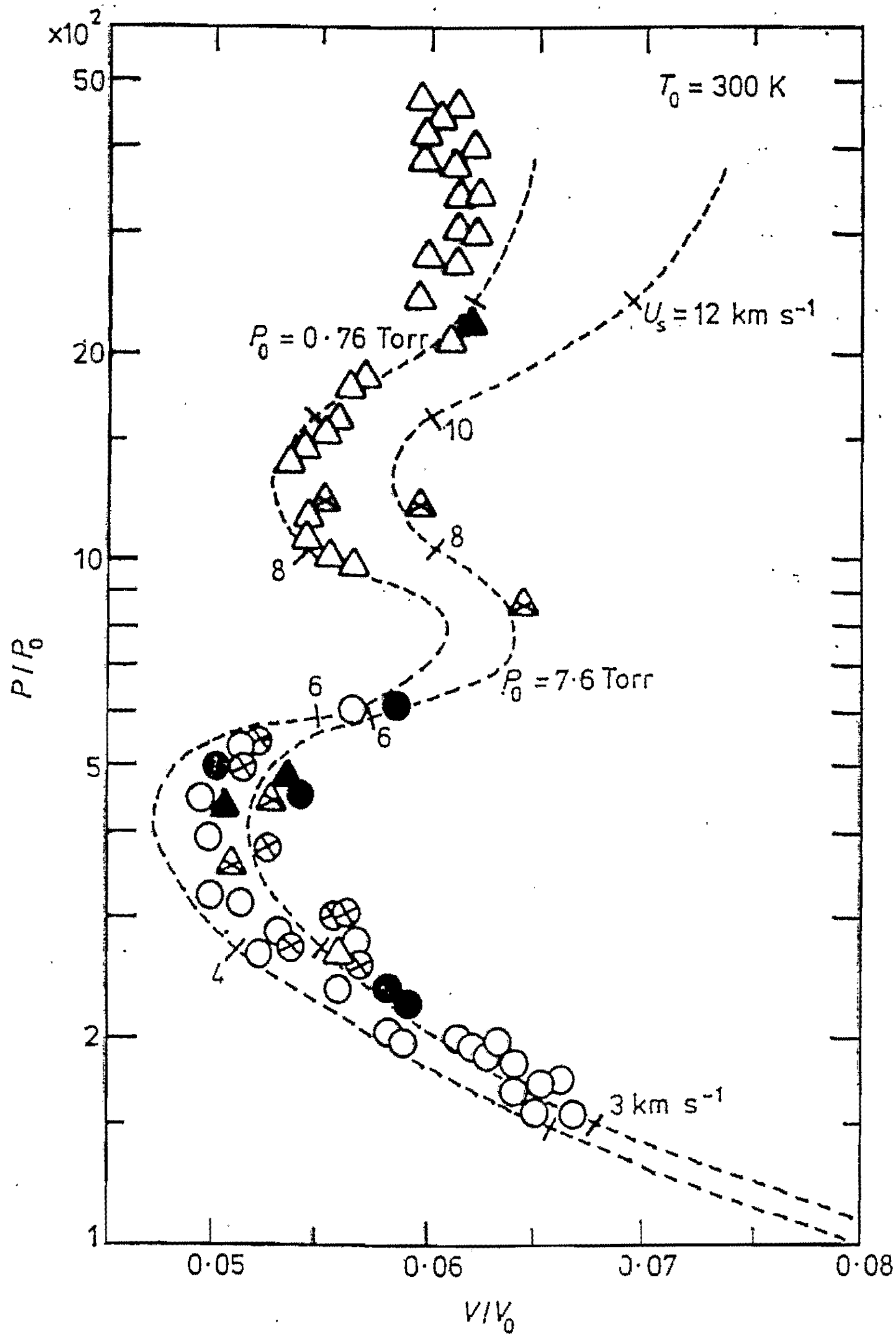

Figure 6. Experimental stability results for shock waves in CO_2 superimposed on the computed (normalized) equilibrium Hugoniot curves. Solid, crossed and open symbols show cases classed as 'unstable', 'doubtful' and 'stable' shocks respectively. △ DD operation; ○ SD operation.

General properties of the Hugoniot

If a chemical reaction can occur or if a phase transition is possible between the upstream and downstream states, then the downstream state lies on a curve which does not pass through the upstream state. In the example of a chemical reaction, one might model the reactants and the products to each behave as a perfect gas so that the enthalpy is given by

$$\frac{\gamma}{\gamma-1} p v + \text{const.}$$

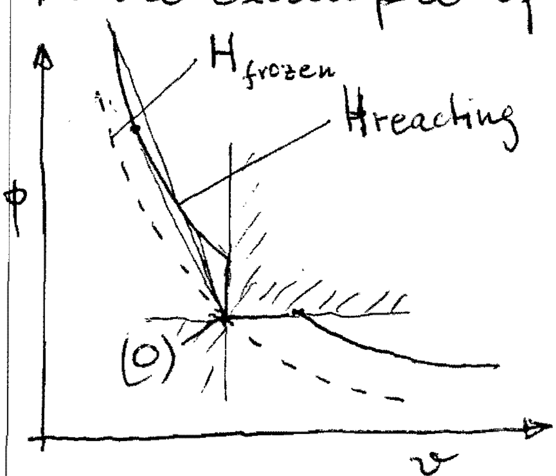

exothermic case

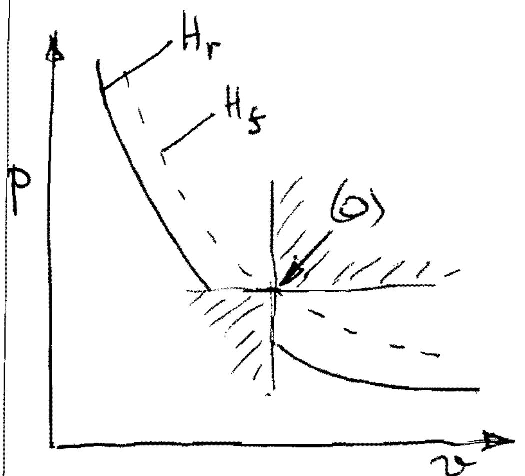

endothermic case

but the constant for the downstream state differs from that of the upstream state by the heat of reaction. For exothermic reaction, the reacting case Hugoniot lies above the frozen (no reaction) Hugoniot, for endothermic reaction below. Consider first the exothermic case for compression waves.

Reserve the word "shock" for H through (0)

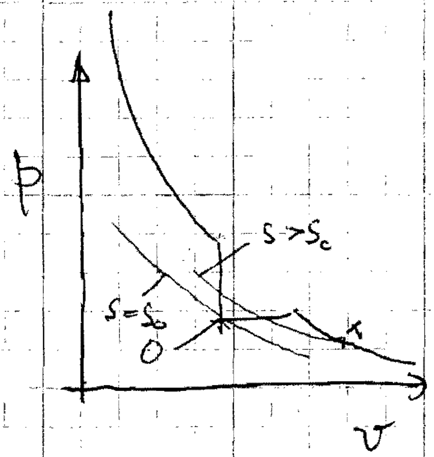

Now, even with

$$\frac{\partial^2 p}{\partial v^2} > 0$$

expansion waves are possible because the entropy is higher at x than at o

~~2806~~

7/0 3/0

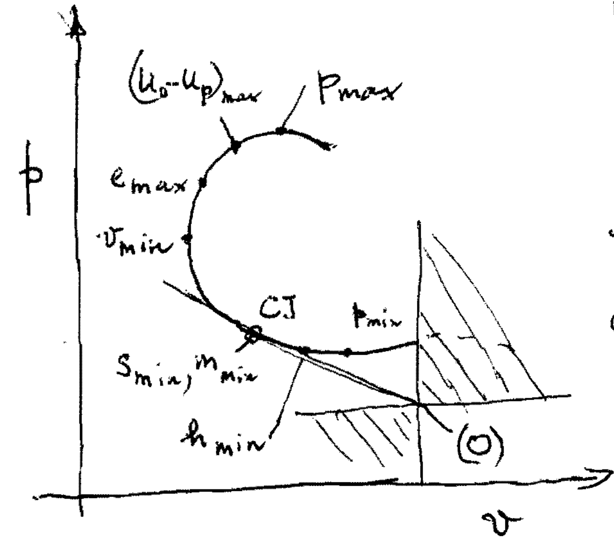

Exothermic compression wave

We now proceed do find the points on the Hugoniot at which different quantities have extrema.

To do this, consider the shock jump conditions and use them to form differentials along the Hugoniot. From the first,

$$\boxed{\begin{aligned} \frac{\Delta p}{\Delta v} &= -m^2 \\ \frac{\Delta e}{\Delta v} &= -\bar{p} \\ \frac{\Delta h}{\Delta p} &= \bar{v} \end{aligned}}$$

$$\frac{dp}{\Delta p} - \frac{dv}{\Delta v} = -2\,\frac{dm}{m}$$

multiply by $\frac{\Delta p}{dv}$

$$\frac{dp}{dv} - \frac{\Delta p}{\Delta v} = -2\,\frac{\Delta p}{m}\,\frac{dm}{dv}$$

This shows that mass flux minimum $(dm=0)$ occurs when

$$\boxed{\frac{dp}{dv} = \frac{\Delta p}{\Delta v}\,,\quad dm=0}$$

i.e. where the Rayleigh line is tangent to the Hugoniot. This point is called Chapman-Jouguet point or CJ-pt.

Now form $\quad \frac{dh}{\Delta h} - \frac{dp}{\Delta p} = \frac{1}{2}\,\frac{dv}{\bar{v}}$

or $$dh = \frac{\Delta h}{\Delta p} dp + \frac{1}{2} \frac{\Delta h}{\bar{v}} dv$$
$$= \bar{v}\, dp + \frac{\Delta p}{2} dv .$$

Substitute into $T ds = dh - v dp$

$$T ds = \frac{\Delta p}{2} dv - \frac{\Delta v}{2} dp .$$

This shows that $\boxed{ds = 0 \quad \text{when} \quad \frac{\Delta p}{\Delta v} = \frac{dp}{dv}.}$

At the CJ point we therefore have

$$\frac{\Delta p}{\Delta v} = \frac{dp}{dv} = \left(\frac{\partial p}{\partial v}\right)_s$$

and $$-\rho_0^2 c^2 = -\rho^2 (c - u_p)^2 = -\rho^2 a^2$$

$$\therefore c - u_p = a .$$

Recall the causality condition $c - u_p \leq a$.

The CJ point is right on the edge of causality.

$\boxed{\text{At the CJ point the speed of the downstream flow relative to the wave is sonic.}}$

Now consider h: $dh = \bar{v} dp + \frac{\Delta p}{2} dv$

This shows that at $dv = 0$, $\frac{dh}{dp} > 0$

$$dh = T ds + v dp .$$

This shows that at $ds = 0$, $\frac{dh}{dp} > 0$ still.

and that at $dp = 0$, $\frac{dh}{ds} > 0$ so that $\frac{dh}{dv} > 0$,

since $\frac{ds}{dv} > 0$ on the Hugoniot between s_{min} and p_{min}. It follows that h decreases as we move from p_{min} to s_{min} and it also decreases as we move from s_{min} to p_{min}. Therefore there must be a minimum in h between s_{min} and p_{min}.

Now consider

$$de = \bar{p}\, dv - \frac{\Delta v}{2}\, dp$$

At $dp=0$, $\frac{de}{dv} > 0$ and at $dv=0$, $\frac{de}{dp} < 0$

It follows that p_{max} and v_{min} enclose an internal energy maximum.

With such arguments we can find the other extrema shown in the sketch on p. 24.

Similar arguments for exothermic expansion waves lead to the situation sketched here.

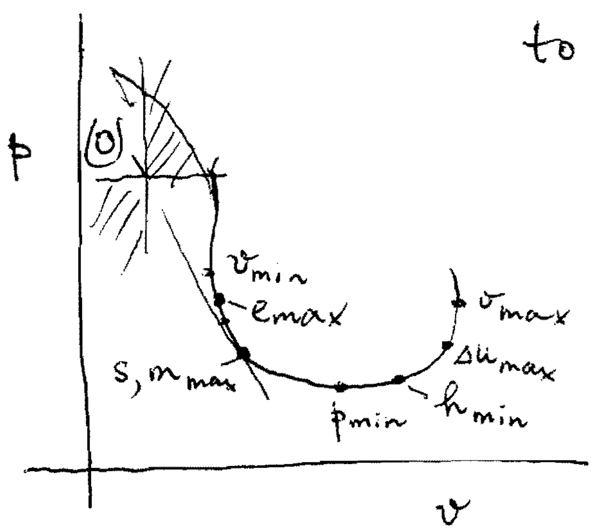

In the above we have written ordinary derivatives for variations along the Hugoniot. This is permissible because if there exists a relation between the two independent variables in $f(x,y)$, e.g. $y = g(x)$, then f may be expressed as $f(x, g(x)) = h(x)$. The ordinary derivative implies "along the Hugoniot".

So, for example, we could express

$$T\,ds = \frac{\Delta p}{2}\,dv - \frac{\Delta v}{2}\,dp,$$

which applies along the Hugoniot, by using

$$dp = \left(\frac{\partial p}{\partial s}\right)_v ds + \left(\frac{\partial p}{\partial v}\right)_s dv,$$

as

$$T\,ds = \frac{\Delta p}{2}\,dv - \frac{\Delta v}{2}\left[\left(\frac{\partial p}{\partial s}\right)_v ds - \left(\frac{\partial p}{\partial v}\right)_s dv\right],$$

or

$$\frac{T\,ds}{\frac{\Delta v}{2}\left(\frac{\Delta p}{\Delta v} - \left(\frac{\partial p}{\partial v}\right)_s\right)} = \frac{dv}{1 + \frac{\Delta v}{2}\,\frac{1}{T}\left(\frac{\partial p}{\partial s}\right)_v}.$$

Since $T\left(\frac{\partial p}{\partial s}\right)_v = \frac{T}{v}\,G$,

$$\boxed{\frac{T\,ds}{\frac{\Delta v}{2}\left[\frac{\Delta p}{\Delta v} - \left(\frac{\partial p}{\partial v}\right)_s\right]} = \frac{dv}{1 + \frac{\Delta v}{2v}\,G}}$$

along H.

If we introduce a new variable η, such that

$$d\eta = \frac{T\,ds}{\frac{\Delta v}{2}\left[\frac{\Delta p}{\Delta v} - \left(\frac{\partial p}{\partial v}\right)_s\right]}$$

$$= \frac{dv}{1 + \frac{\Delta v}{2v}G}$$

it is possible to show that this is also

$$= \frac{-\,de}{\bar{p} + \frac{\Delta v}{2}\left(\frac{\partial p}{\partial v}\right)_e}$$

$$= \left(\frac{\partial v}{\partial p}\right)_s \frac{dp}{1 - \frac{\Delta p}{2}\left(\frac{\partial v}{\partial h}\right)_p}$$

$$= \left(\frac{\partial v}{\partial p}\right)_s \frac{dh}{\bar{v} + \frac{\Delta p}{2}\left(\frac{\partial v}{\partial p}\right)_h}$$

Now note that $d\eta$ cannot be equal to zero anywhere, because, if any one of ds, dv, de, dp and dh is nonzero, then $d\eta \neq 0$. Since the zeros of these differentials occur at different points on H, η does not have a stationary point anywhere. Therefore, at any point where the numerator of one of them changes sign, so also must the denominator. This may be used to obtain the following sufficient inequality conditions:

I If $\Gamma > 0$ there will be no expansion shocks

II-weak If $G > -2$ there will be no extremum of v on the Hugoniot in an expansion wave

II-strong If $G > -1$ there will be no extremum of h (min) on the Hugoniot in an expansion wave

III-weak If $G < 2\frac{\rho a^2}{p}$ there will be no extremum of pressure (max or min) on H in a compression wave

III strong If $G < \frac{\rho a^2}{p}$ there will be no e_{max} on H in a compression wave

II strong includes II weak and III strong includes III weak.

Thus we see that, depending on the

value of G, the Hugoniot becomes less pathological ~~th~~ than the figures shown on pages 24 and 26. For example, III weak is enough to prevent horizontal tangents

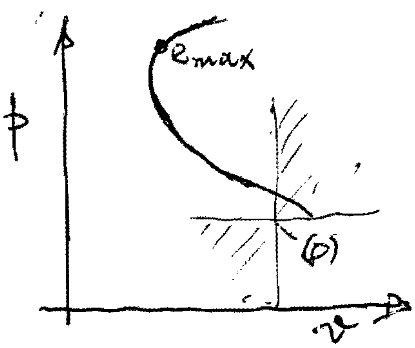

of H in compression waves and III strong further limits the positive slope of H to stay above that at e_{max}.

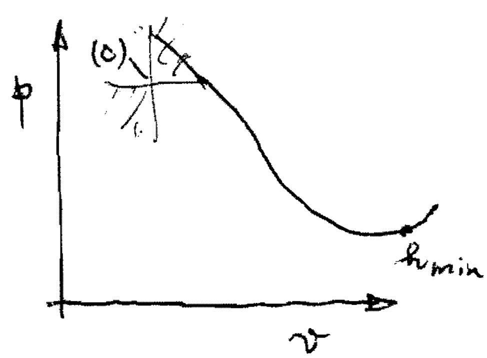

Also, in the case of an expansion wave, II weak prevents vertical tangents on H., and II-strong makes sure that the positive slope of H stops short of that at h_{min}.

Curvature of H at the CJ points

Starting from $T ds = \frac{\Delta p}{2} dv - \frac{\Delta v}{2} dp$

solve for $\frac{\Delta v}{2} dp = \frac{\Delta p}{2} dv - T ds$

replace $T ds$ from bottom of p 27

$$\frac{\Delta v}{2} dp = \left[\frac{\Delta p}{2} - \frac{\frac{\Delta v}{2}\left\{ \frac{\Delta p}{\Delta v} - \left(\frac{\partial p}{\partial v}\right)_s \right\}}{1 + \frac{1}{2}\frac{\Delta v}{v} G} \right] dv$$

So that $$\frac{dp}{dv} = \frac{\Delta p}{\Delta v} - \frac{\frac{\Delta p}{\Delta v} - \left(\frac{\partial p}{\partial v}\right)_s}{1 + \frac{\Delta v}{v} G}$$

or $$\boxed{\frac{dp}{dv} = -m^2 + \frac{m^2 - \rho^2 a^2}{1 + \frac{\Delta v}{v} G}}$$

Now differentiate this at the CJ-point, where $dm = 0$ and $m^2 = \rho^2 a^2$:

$$\left(\frac{d^2 p}{dv^2}\right)_{CJ} = 0 + \frac{0 - 2\rho a \left(\frac{\partial \rho a}{\partial v}\right)_s}{1 + \frac{\Delta v}{v} G} - \frac{m^2 - \rho^2 a^2}{\left[1 + \frac{\Delta v}{v} G\right]^2} \frac{\partial\left(\frac{\Delta v}{v} G\right)}{\partial v}$$

Now $\Gamma = \frac{1}{a}\left(\frac{\partial \rho a}{\partial \rho}\right)_s = \frac{1}{a}\left(\frac{\partial \rho a}{\partial v}\right)_s \frac{dv}{d\rho} = -\frac{1}{\rho^2 a}\left(\frac{\partial \rho a}{\partial v}\right)_s$

So $$\boxed{\left(\frac{d^2 p}{dv^2}\right)_{CJ} = \frac{2\Gamma \frac{a^2}{v^3}}{1 + \frac{\Delta v}{v} G}}$$

Now consider the two CJ points that occur in a compression and expansion discontinuity, B and E.

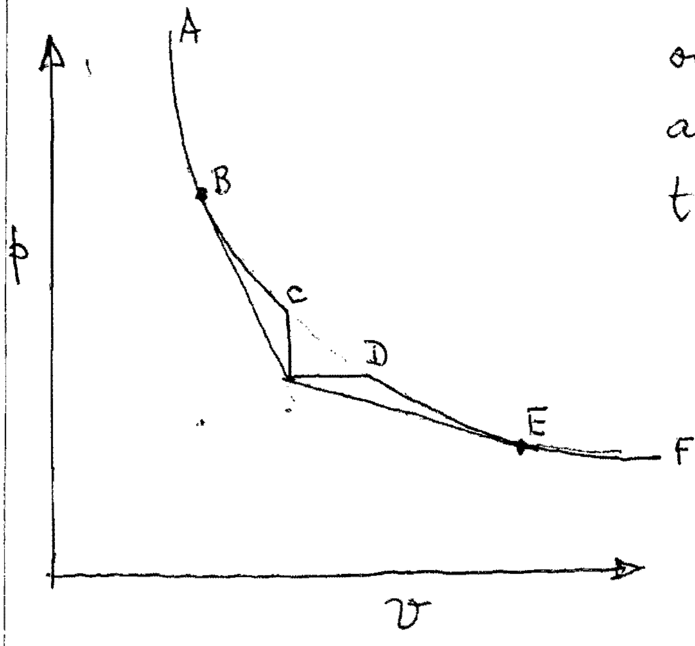

Assume $\Gamma > 0$ and III strong

On the Hugoniot

Start from

$$T\frac{ds}{dv} = \frac{1}{2}\Delta p - \frac{\Delta v}{2}\frac{dp}{dv}$$

differentiate this along the Hugoniot at CJ

$$T\frac{d^2s}{dv^2} = -\frac{\Delta v}{2}\frac{d^2p}{dv^2} \cancel{- \frac{1}{2}\frac{dp}{dv}} + \cancel{\frac{1}{2}\frac{dp}{dv}},$$

where we have used the fact that $\frac{ds}{dv} = 0$ at CJ

Therefore, $\boxed{\frac{d^2s}{dv^2} \geqslant 0 \quad \text{at B}}$ $\quad (\Delta v < 0)$

and $\boxed{\frac{d^2s}{dv^2} \leqslant 0 \quad \text{at E}}$ $\quad (\Delta v > 0)$.

We may exclude the equal sign in these as follows:

Consider $\quad p = p(v, s)\quad$ along H at CJ pt

$$\frac{dp}{dv} = \left(\frac{\partial p}{\partial v}\right)_s + \left(\frac{\partial p}{\partial s}\right)_v \frac{ds}{dv}$$

$$\frac{d^2p}{dv^2} = \left(\frac{\partial^2 p}{\partial v^2}\right)_s + \left(\frac{\partial p}{\partial s}\right)_v \frac{d^2s}{dv^2} \qquad \text{recall, } \frac{ds}{dv} = 0 \text{ at CJ}$$

Condition I: $\Gamma > 0$ or $\left(\frac{\partial^2 p}{\partial v^2}\right)_s > 0$ i.e, $\neq 0$

It follows that $\frac{d^2p}{dv^2}$ and $\frac{d^2s}{dv^2}$ can not both be zero at the CJ-point. The expression on the previous page:

$$T\frac{d^2s}{dv^2} = -\frac{\Delta v}{2}\frac{d^2p}{dv^2}$$

then shows that neither $\frac{d^2p}{dv^2}$ nor $\frac{d^2s}{dv^2}$ can be zero at the CJ point.

Hence
$$\boxed{\begin{array}{ll} \frac{d^2s}{dv^2} > 0 & \text{at } B \\ \frac{d^2s}{dv^2} < 0 & \text{at } E \end{array}}$$

with $\frac{ds}{dv} = 0$ these are the conditions for s to have a <u>minimum at B</u> and a <u>maximum at E</u>.

Similarly, by using

$$c^2 = -v_0^2\frac{\Delta p}{\Delta v}$$

get

$$dc^2 = -\frac{v_0^2}{(\Delta v)^2}\left[\Delta v\, dp - \Delta p\, dv\right] = 0 \text{ at CJ}$$

and

$$\frac{d^2c^2}{dv^2} = -\frac{v_0^2}{\Delta v}\frac{d^2p}{dv^2}$$

Thus $\boxed{\frac{d^2c^2}{dv^2} > 0 \text{ at } B \quad \text{and} \quad \frac{d^2c^2}{dv^2} < 0 \text{ at } E}$

giving that c^2 has a minimum at B and a maximum at E.

Consequences of these results:

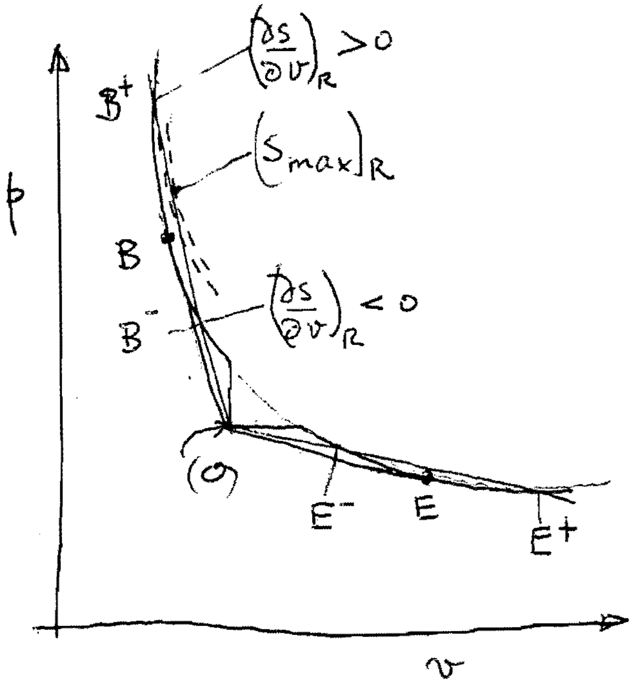

Consider two Rayleigh lines slightly off the CJ conditions. The first, a compression wave intersects the Hugoniot at B^- and B^+ on either side of the CJ-point. Similarly E^- and E^+ for expansion.

Now let B^+ and B^- approach B, noting first that

at B^+ and E^-, $\left(\frac{\partial s}{\partial v}\right)_R > 0$

and at B^- and E^+, $\left(\frac{ds}{dv}\right)_R < 0$ if $\Gamma > 0$, $G > 0$

We can write

$$\left(\frac{\partial s}{\partial v}\right)_R = \left(\frac{\partial s}{\partial v}\right)_p + \left(\frac{\partial s}{\partial p}\right)_v \left(\frac{dp}{dv}\right)_R$$

$$= \left[\left(\frac{\partial s}{\partial v}\right)_p \Big/ \left(\frac{\partial s}{\partial p}\right)_v + \frac{\Delta p}{\Delta v}\right]\left(\frac{\partial s}{\partial p}\right)_v$$

$$= \left[\rho^2 a^2 - \rho^2 (c - u_p)^2\right]\left(\frac{\partial s}{\partial p}\right)_v$$

Now $\left(\frac{\partial s}{\partial p}\right)_v$ has the same sign as G, so for $G>0$, the flow relative to the wave front is

$$\boxed{\begin{array}{l} \text{subsonic downstream, } a > |c-u_p| \text{ if } \left(\frac{\partial s}{\partial v}\right)_R > 0 \quad [B^+, E^-] \\ \text{supersonic downstream, } a < |c-u_p| \text{ if } \left(\frac{\partial s}{\partial v}\right)_R < 0 \quad [B^-, E^+] \end{array}}$$

The latter violates causality.

Now divide the Hugoniot up into regions:

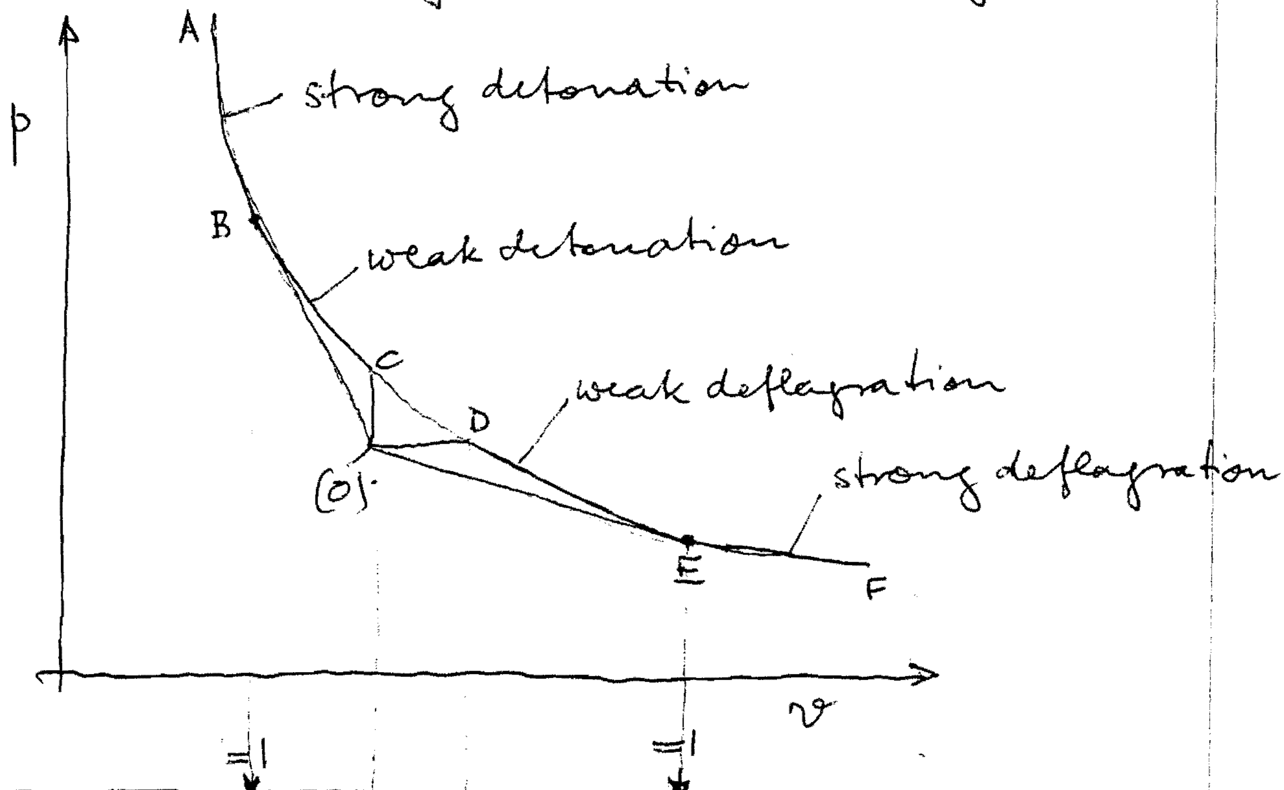

Value of M	<1	>1	<1	>1
Value of M_0	>1	>1	<1	<1

min max

According to the causality condition, weak detonations and strong deflagrations are therefore disallowed.

It is sometimes useful to see this in a plot of $|c-u_p|$ vs c shown here.

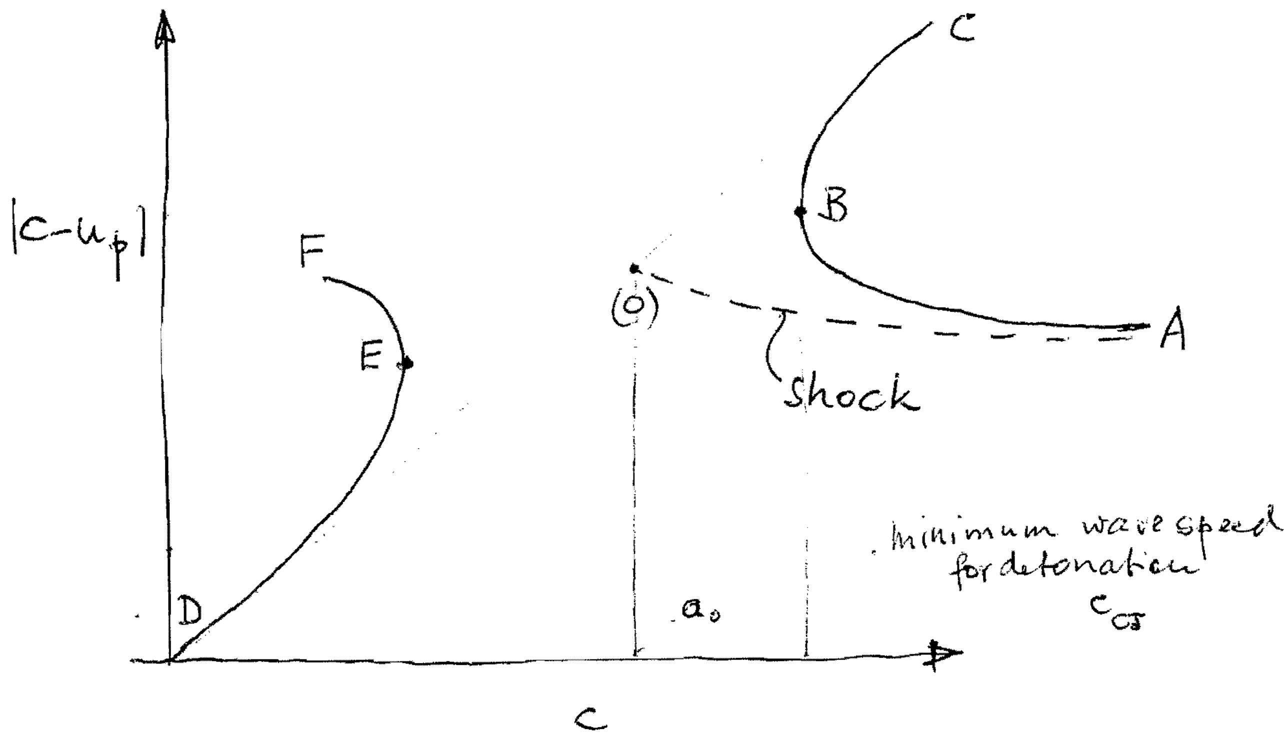

Now consider the consequences for the up-stream condition. To do this, ask the question: What is the locus of the upstream condition that produces a given down-stream condition?

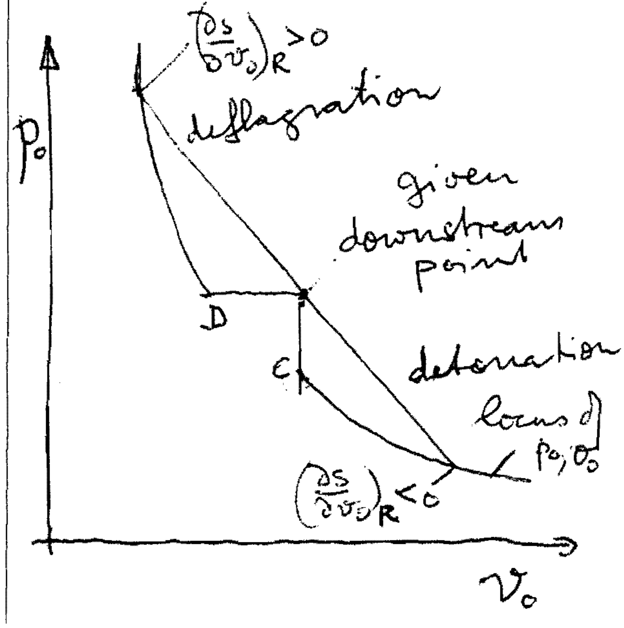

$(G>0)$

At an intersection of the Rayleigh line with the locus of p_o, v_o on the detonation branch,

$$\left(\frac{\partial s}{\partial v_o}\right)_R < 0 \quad \text{so } c^2 > a_o^2$$

Conversely at a deflagration point,

$$\left(\frac{\partial s}{\partial v}\right)_R > 0 \quad , \text{ so } \quad c^2 < a_0^2$$

Thus, the flow relative to the wave front is supersonic upstream of a detonation and subsonic upstream of a deflagration.

The results obtained here are called <u>Jouguet's rule</u>, which in summary says that the flow of the gas relative to the wave front is

Supersonic upstream of a detonation
supersonic downstream of a weak detonation
subsonic downstream of a strong detonation
subsonic upstream of a deflagration
subsonic downstream of a weak deflagration
supersonic downstream of a strong deflagration

Reference: Courant & Friedrichs "Supersonic Flow and Shock Waves" Springer 1948

Strong and weak detonations

Consider the piston problem with a detonable mixture that is initially at rest. Suppose that the detonation propagating at c brings the gas to a speed u_p of the piston.

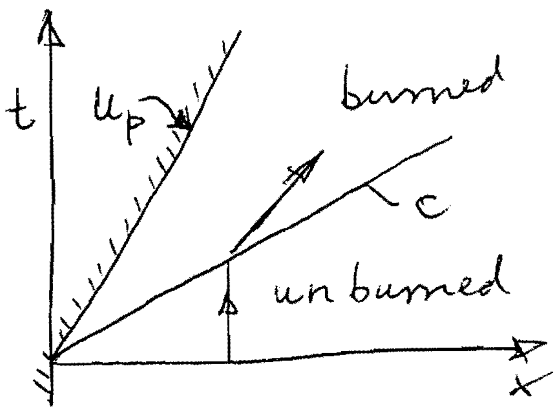

If the detonation is at the CJ condition, so that

$$c - u_p = a$$

or

$$u_p = c - a$$

then let that particular piston speed be called u_B.

If $u_p > u_B$: In this case, with conditions between the wave and the piston uniform, we get the strong detonation as the only solution, since the piston speed will produce a stronger detonation than the CJ-detonation.

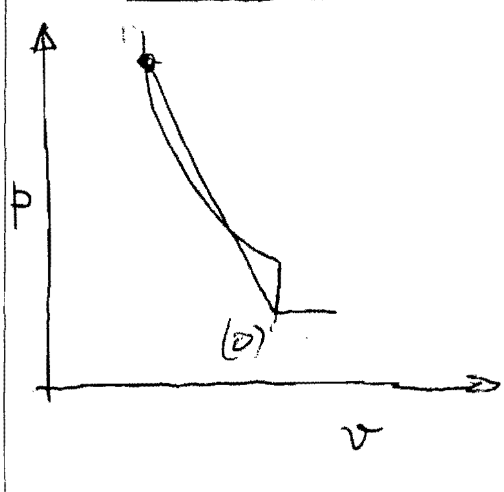

If $u_p \leq u_B$: In this case a CJ-detonation is a possible solution. Since the flow

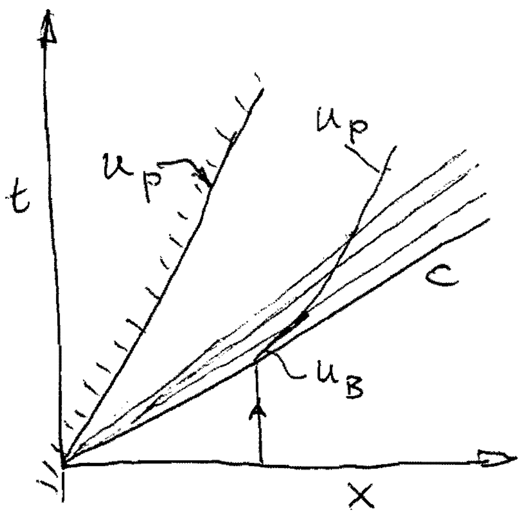

relative to the wave on the downstream side is then sonic, the speed in the lab frame is $c-a=u_B$. However, this is faster than u_p, so that an adjustment of the speed from u_B to u_p is necessary. This adjustment occurs across a centered expansion wave which follows immediately after the CJ detonation. The strength of the expansion obviously goes like u_B-u_p and it disappears when $u_p=u_B$. Since the

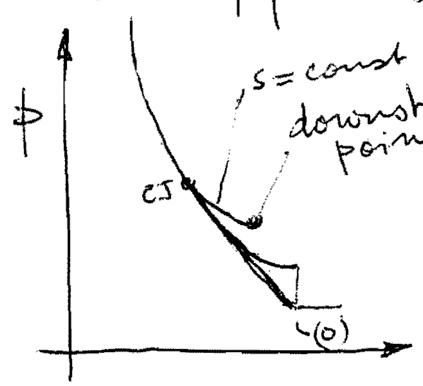

expansion is dispersed, it is isentropic.

If $u_p=0$ or $u_p<0$:

In this case the same mechanism applies, the strength of the expansion just has to be greater.

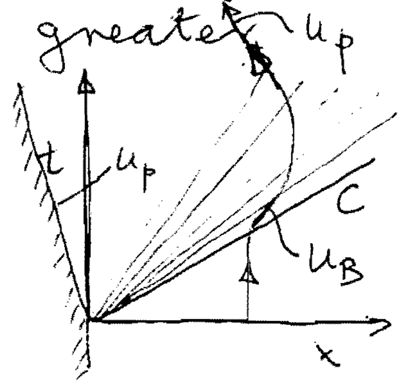

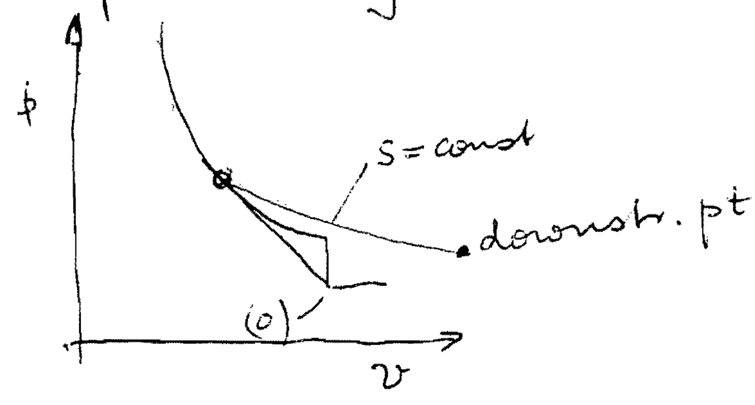

Weak detonation

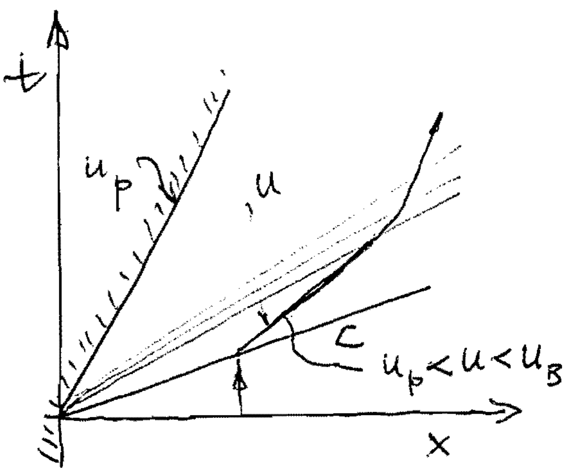

If the velocity of the flow immediately following the front is between u_p and u_B we get a centered expansion again. However, it would lag behind the front because $M > 1$. This violates causality.

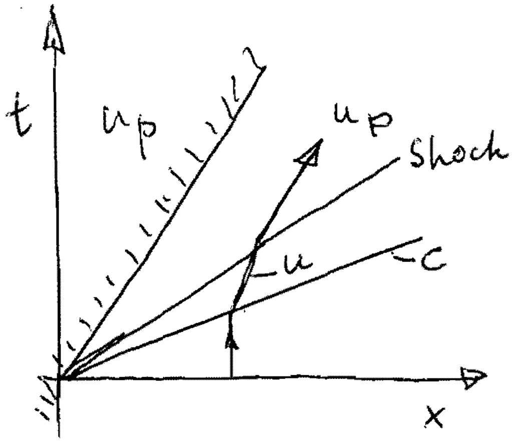

If $u < u_p$, the adjustment could be effected by a shock that lags ~~the~~ behind the detonation. When $u = u_*$ where u_* is a critical value such that $u < u_* < u_p$, the shock and the detonation coalesce and a strong detonation results. Until this condition is reached this mechanism also violates causality.

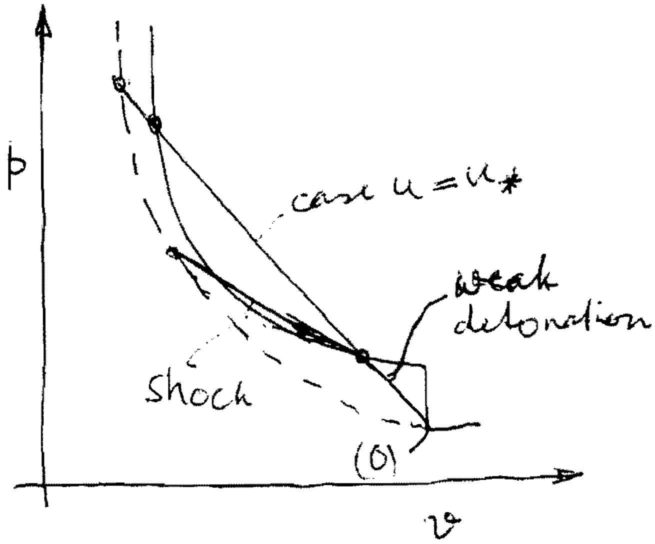

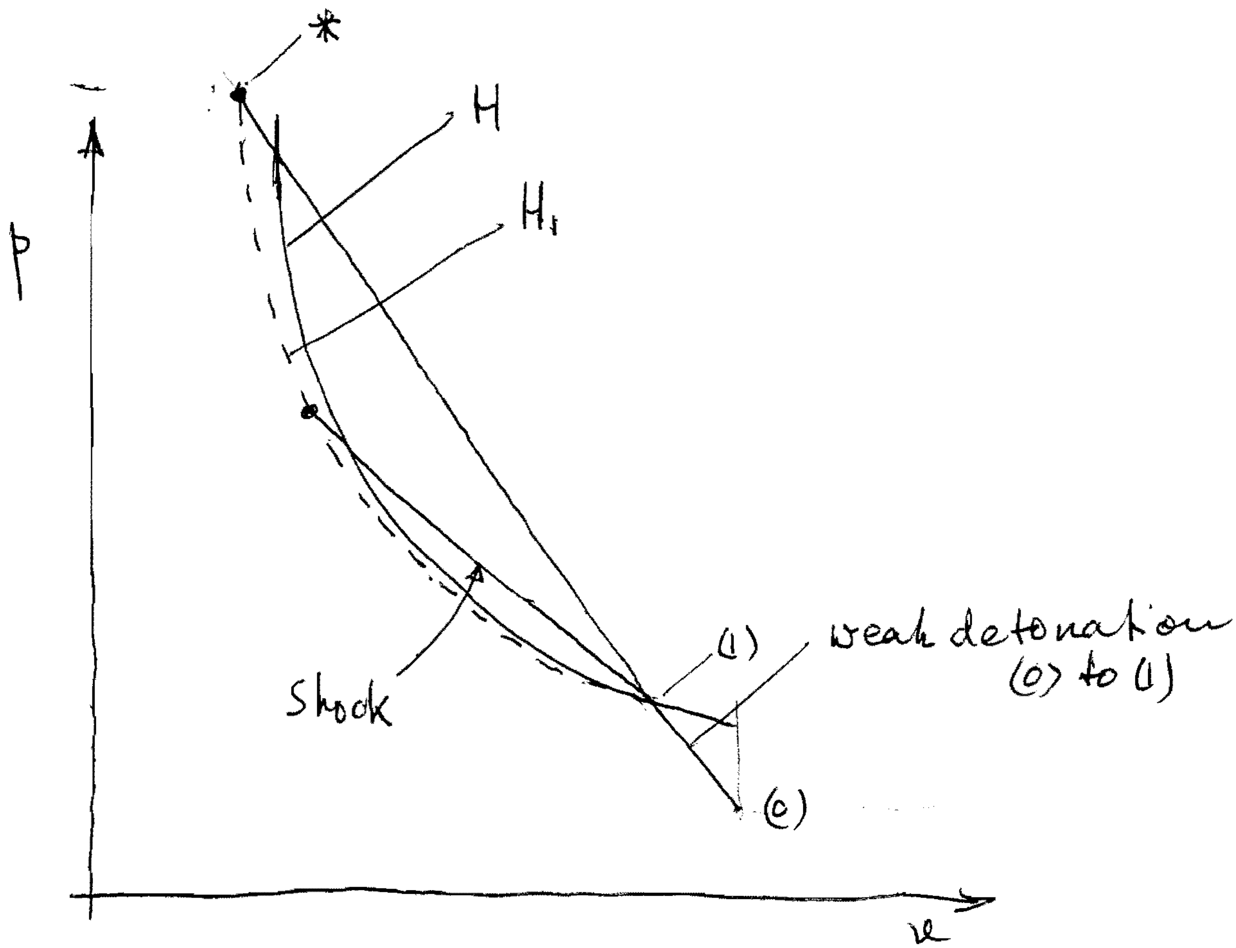
*
H
H_1
p
Shock
(1)
weak detonation
(0) to (1)
(0)
v

Deflagrations

If a tube is filled with combustible gas at rest and a deflagration is initiated at the piston a flame front propagates to the right, away from the piston. This lowers the density, so Δv is positive and u_p has to be negative, i.e., the piston has to be moved to the left. If it is not, a shock is generated at the piston which will overtake the deflagration so that the xt-diagram looks as shown.

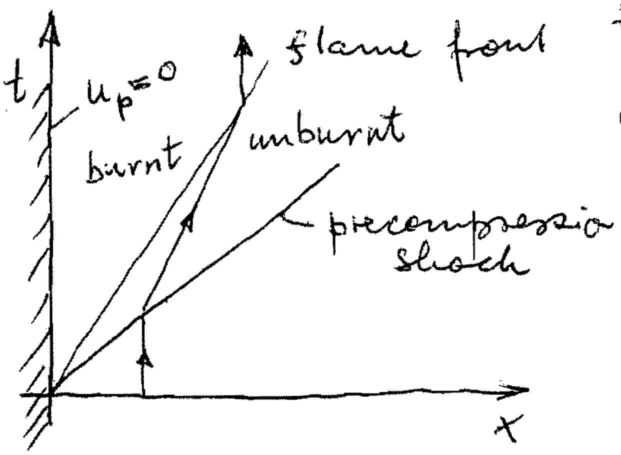

If $u_p \neq 0$, the flame front and shock adjust to produce the right u_p

To produce a deflagration without a precompression shock u_p must be negative and have just the right value.

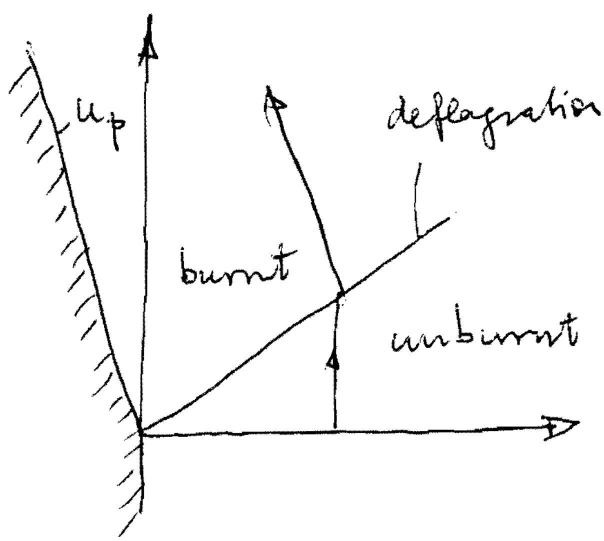

Now consider the case with a pre compression shock of just the right strength so that

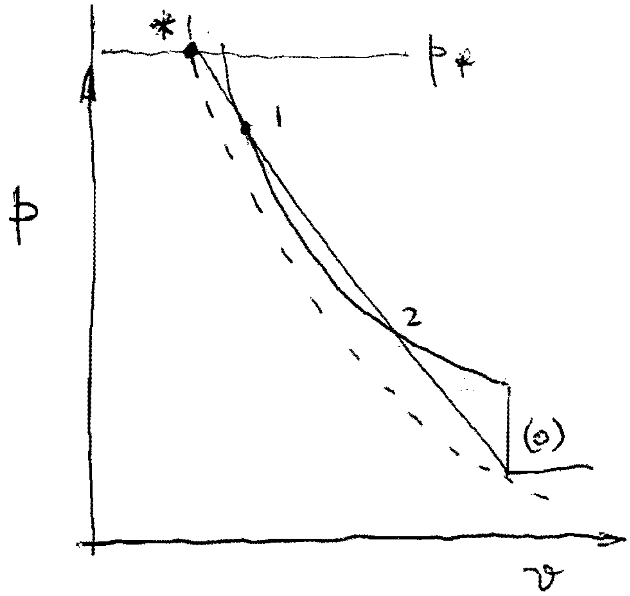

$$\frac{\Delta p}{\Delta v} = \frac{p_1 - p_*}{v_1 - v_*} = \frac{p_1 - p_0}{v_1 - v_0} = -m^2$$

i.e. the transition from (0) to (1) can be viewed as a shock wave (0) to (*) followed by a weak deflagration (*) to (1) where both waves have the same value of m. Thus we see that a strong detonation is the same as a shock wave followed by a weak deflagration.

If the shock were to be followed by a strong deflagration (violates causality) so that the weak detonation point (2) would be the final state, we would violate causality there too.

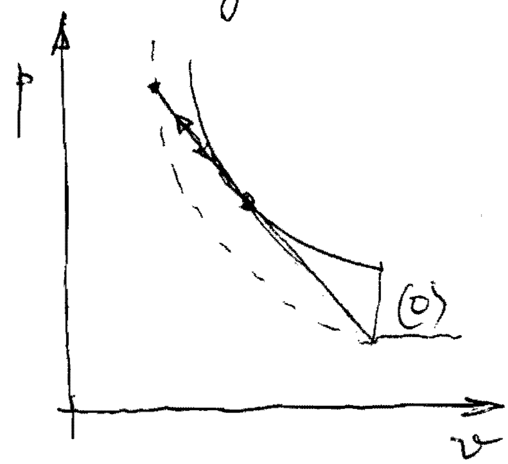

Of course a CJ-detonation can be viewed as a shock of the right strength followed by a CJ deflagration. (same m)

Impossibility of strong deflagration

Consider a deflagration to occur over a finite thickness and think of Hugoniot

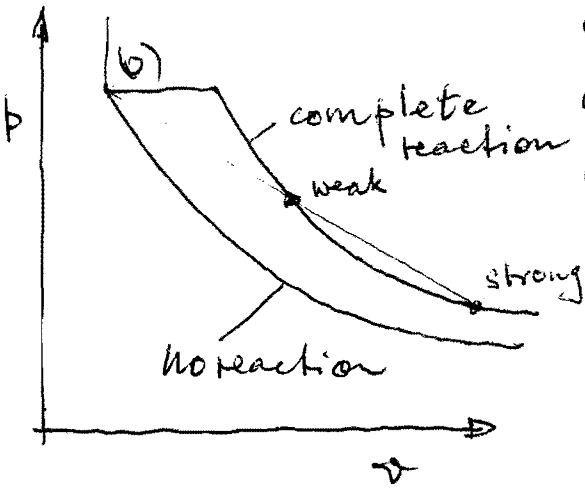

curves for various degrees of completion of the chemical reaction. The strong detonation would take the composition of the gas to points beyond the complete reaction (Rayleigh line). [Note compression case]

Alternatively one might imagine the Hugoniot curves for no reaction and for

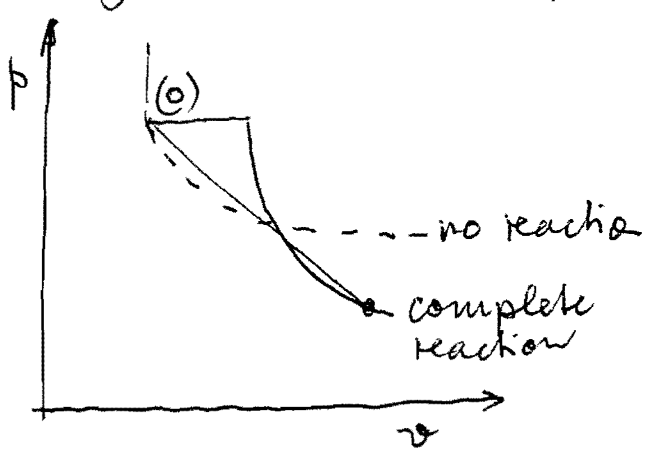

complete reaction to cross.

Difficulties are associated with both of these, so that we exclude strong deflagrations

Endothermic compression wave

An example of such a wave is a strong shock in a ~~di~~ molecular gas followed by dissociation of the gas. In this case, the

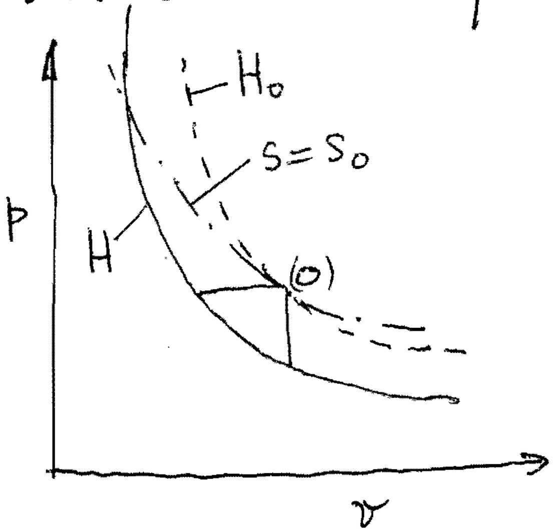

Hugoniot lies below the frozen Hugoniot. Now we have a serious problem, however. The downstream state must have a higher entropy than s_0, so that, for $G>0$, the branch of H below the isentrope $s=s_0$ is forbidden. Thus we see that this kind

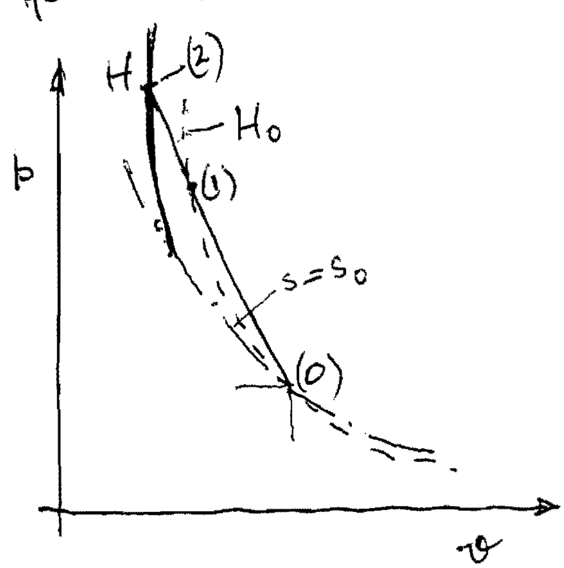

of shock can be thought of as the transition $0 \rightarrow 1$ through a non-reacting shock followed by a transition through the dissociation $1-2$ with the same value of m. A profile through such a wave would look as shown.

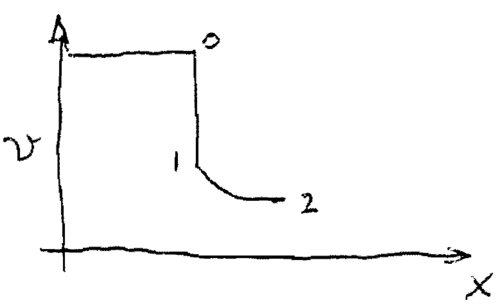

In a real situation the endothermic compression wave can be more complicated. If a high speed flow is generated by a nozzle expansion from a very hot reservoir, the reservoir state is generally significantly dissociated. As the gas expands, the atoms recombine to form molecules, but the collision frequency also decreases. There comes a point when the recombination rate is too small to cause further recombination and the composition freezes at a dissociation fraction that is higher than the equilibrium value.

A situation can therefore arise such that, for a sufficiently weak shock (in this flow) that just suffices to make the recombination occur, but is too weak to raise the equilibrium dissociation fraction to a value below the free stream value, an exothermic wave occurs. On the other hand, when the shock is strong, the gas needs to dissociate to reach equilibrium and the flow is endothermic. In that case the frozen and equilibrium Hugoniots actually do cross.

$K_1 = 0.70 \quad P_1 = 0.010$

$\alpha_1 = 0.10 \quad \rho_d/\rho_1 = 1.0E+07$

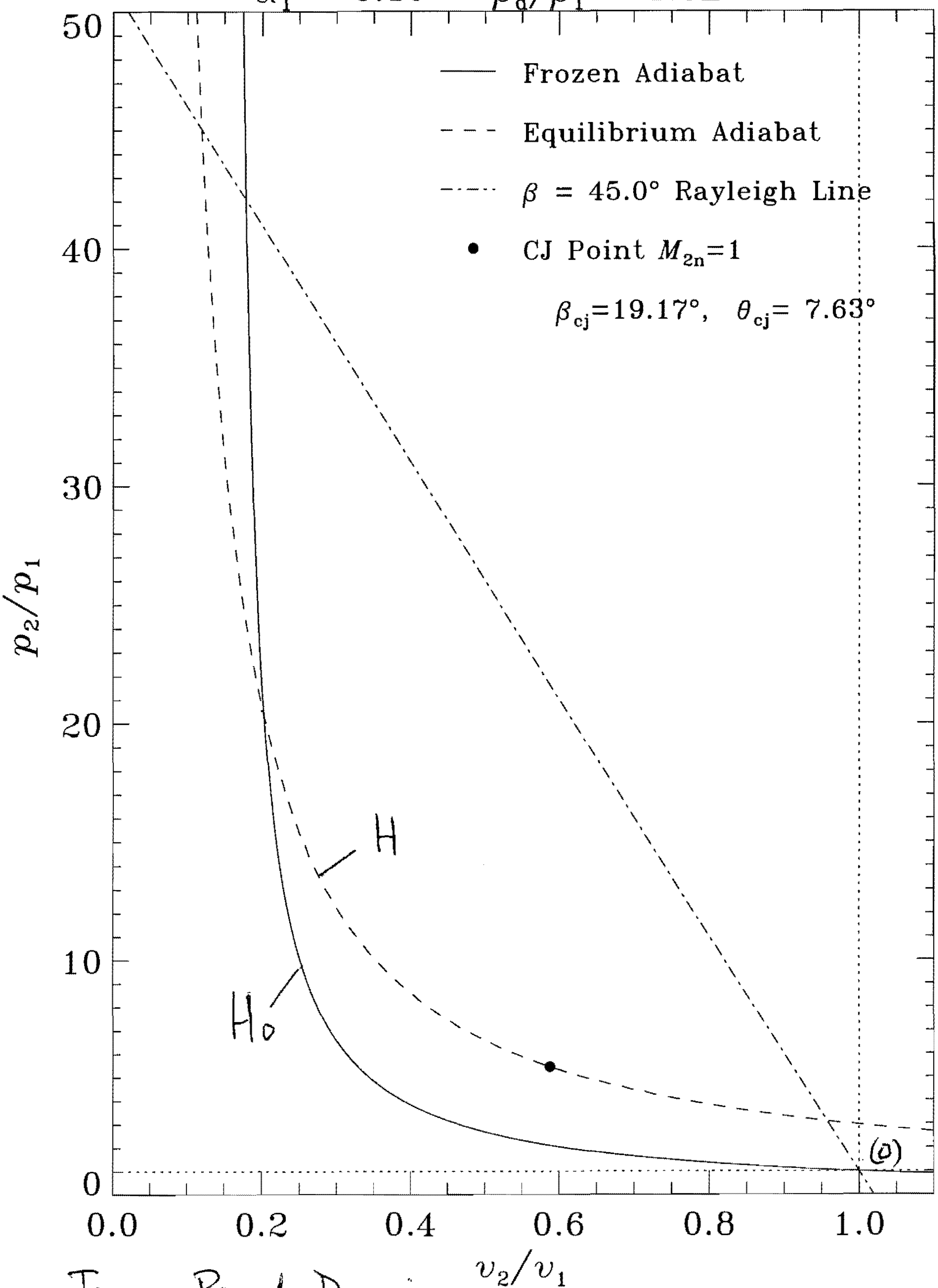

Jean-Paul Davis
Ideal Dissociating Gas.

Phase transitions

The equation of state of a substance may be represented as a surface in pvT-space. In the region where phase transitions occur, the surface may be quite complex. For example, the equation of state of water looks approx. as shown.

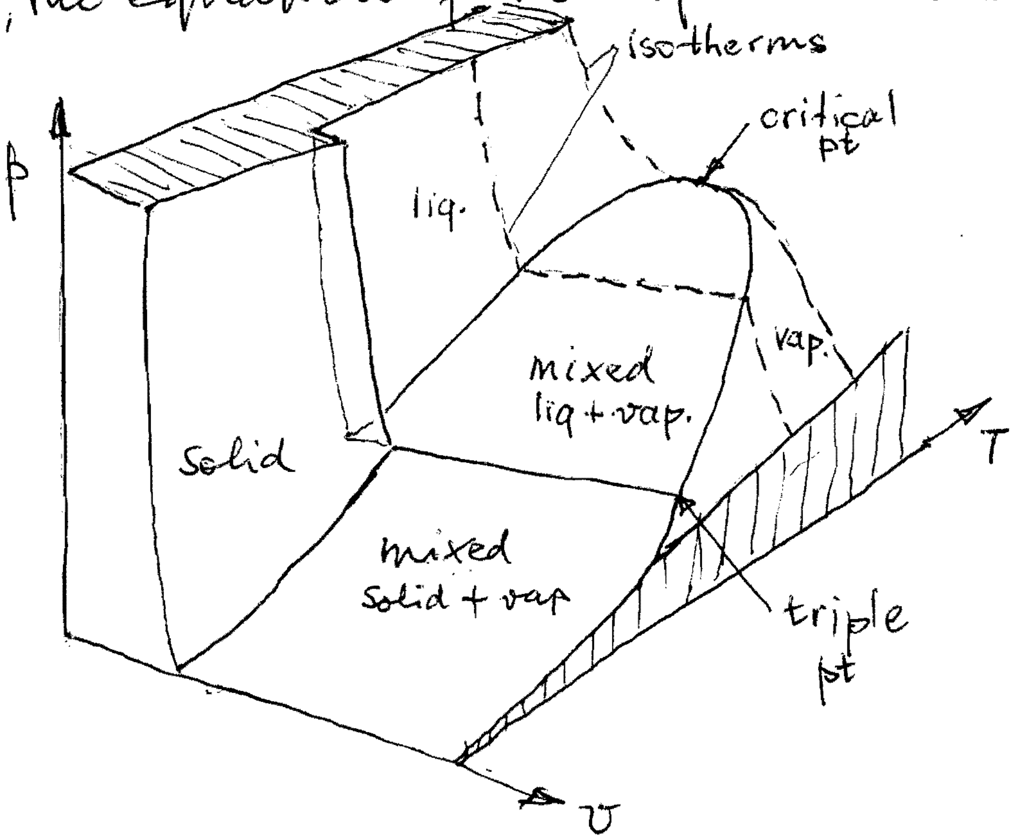

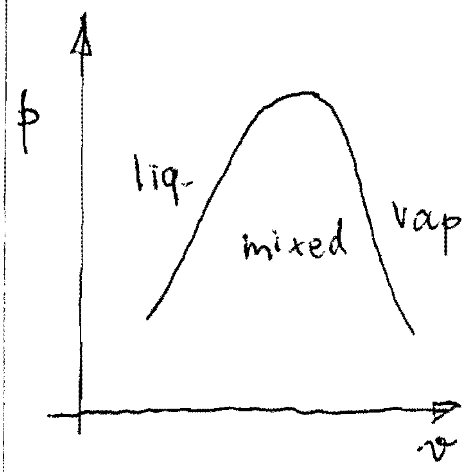

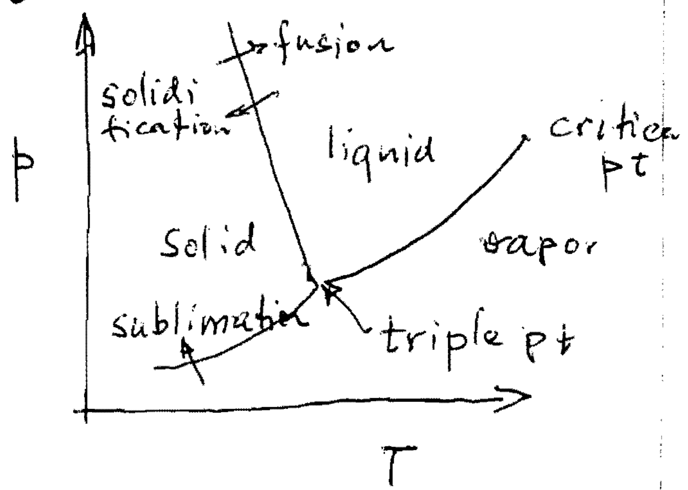

We focus our interest on the vapor - liquid boundary of various substances.

For discontinuous waves, we have seen the importance of slopes of various curves in vp-space. Consider such slopes at the boundary between vapor and mixed liquid and vapor phase. As we will show later,

$$a^2 = -v^2\left(\frac{\partial p}{\partial v}\right)_s$$

is always larger in the vapor phase than in the mixed phase and is discontinuous across the boundary.

Note that this is not so difficult to imagine, since the mixed phase has approximately the same compressibility as the vapor phase and greater density.

Fluids may be classed into two types, depending on their behavior in the region of the saturated vapor phase boundary.

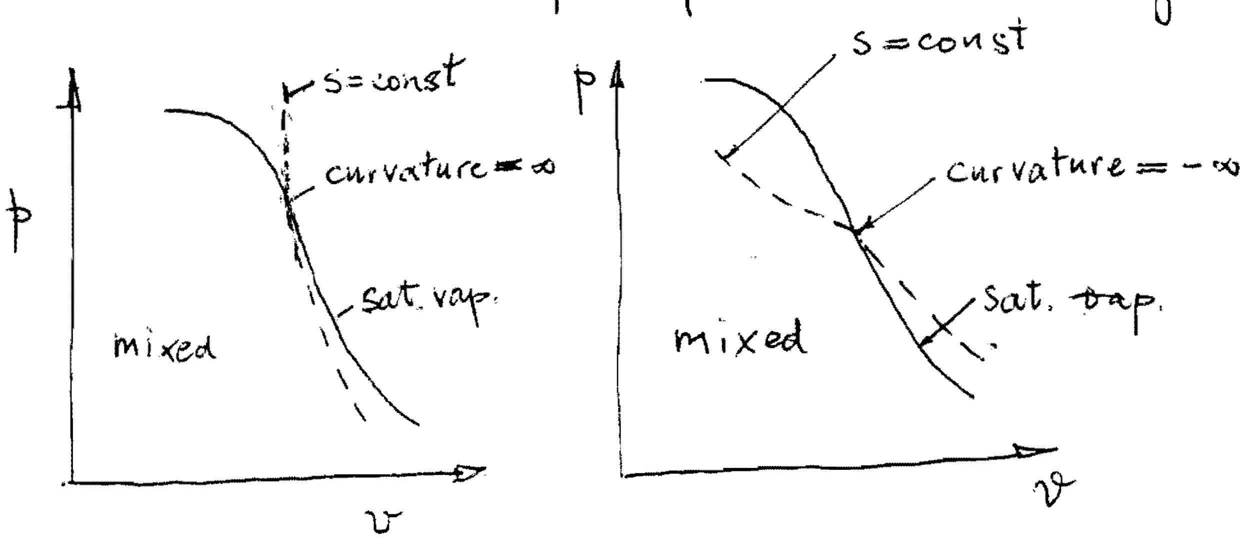

Normal Retrograde

This may also be illustrated in the sT-space

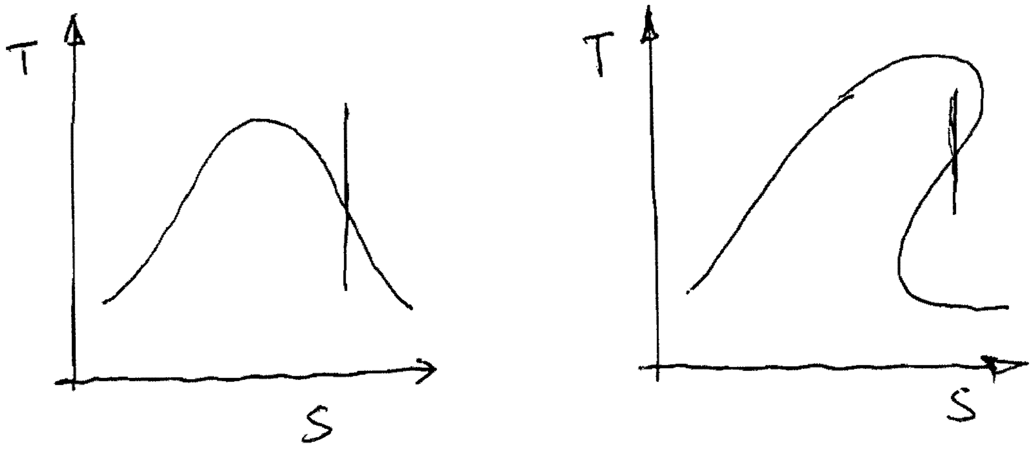

Normal Retrograde

In order to study the slopes of various curves in vp-space, consider $v(p,T)$.

$$dv = \left(\frac{\partial v}{\partial p}\right)_T dp + \left(\frac{\partial v}{\partial T}\right)_p dT.$$

for any specified value of dT/dp,

$$\frac{dv}{dp} = \left(\frac{\partial v}{\partial p}\right)_T + \left(\frac{\partial v}{\partial T}\right)_p \frac{dT}{dp}.$$

In particular, for an isentrope,

$$\left(\frac{\partial v}{\partial p}\right)_s = \left(\frac{\partial v}{\partial p}\right)_T + \left(\frac{\partial v}{\partial T}\right)_p \left(\frac{\partial T}{\partial p}\right)_s .$$

Use $\left(\frac{\partial T}{\partial p}\right)_s = -\left(\frac{\partial T}{\partial s}\right)_p \left(\frac{\partial s}{\partial p}\right)_T$

Integrability of $dg = v\,dp - s\,dT \Rightarrow \left(\frac{\partial v}{\partial T}\right)_p = -\left(\frac{\partial s}{\partial p}\right)_T$

so $\left(\frac{\partial T}{\partial p}\right)_s = \frac{T}{c_{pv}}\left(\frac{\partial v}{\partial T}\right)_p ,$

and $$\left(\frac{\partial v}{\partial p}\right)_s = \left(\frac{\partial v}{\partial p}\right)_T + \frac{T}{C_{pv}}\left(\frac{\partial v}{\partial T}\right)_p^2$$

where we have taken the vapor side of the phase boundary by writing $\left(\frac{\partial T}{\partial s}\right)_p = \frac{T}{C_{pv}}$.

However, on the phase boundary (ordinary differentials)

$$\left.\frac{dv}{dp}\right|_b = \left(\frac{\partial v}{\partial p}\right)_T + \left(\frac{\partial v}{\partial T}\right)_p \left.\frac{dT}{dp}\right|_b \quad \text{phase bdy},$$

Comparing the last two equations and recalling that

$$\left(\frac{\partial v}{\partial p}\right)_s > \left.\frac{dv}{dp}\right|_b \quad \text{for \underline{Normal Fluids}}$$

get
$$\boxed{\frac{T}{C_{pv}}\left(\frac{\partial v}{\partial T}\right)_p > \left.\frac{dT}{dp}\right|_b} \quad \text{\underline{Normal Fluid}}$$

For processes that take a substance across a phase boundary, or in the presence of more than one phase the Gibbs potential has to be extended to

$$dG = v\,dp - s\,dT + \sum_{i=1}^{N} \mu_i\, dN_i$$

where μ_i is the chemical potential of the ith phase and n_i is the number of moles of it that are present.

At phase equilibrium it is possible to show that G has a minimum. Therefore, at fixed T and p,

$$dG = \sum_{i=1}^{N} \mu_i dn_i = 0.$$

The chemical potential is the molar Gibbs potential g, so, for two phases,

$$g_1 dn_1 + g_2 dn_2 = 0$$

at the phase boundary. Since $dn_1 = -dn_2$, $g_1 = g_2$ at the phase boundary. Now

$$g = v\,dp - s\,dT,$$

so, for two points (p,T) and $(p+dp, T+dT)$ on the phase boundary,

$$d\Delta g = \frac{\partial \Delta g}{\partial T} dT + \frac{\partial \Delta g}{\partial p} dp = 0.$$

since $\Delta g = 0$ at both points. Here Δg is the change in g across the phase boundary.

$$\therefore \; d\Delta g = -\Delta s\,dT + \Delta v\,dp = 0$$

It follows that $\left.\dfrac{dp}{dT}\right|_b = \dfrac{\Delta s}{\Delta v}$

Define the latent heat of the phase transition

as $\lambda \equiv T\Delta s$

So $\boxed{\left.\dfrac{dp}{dT}\right|_b = \dfrac{\lambda}{T\Delta v}}$ Clausius Clapeyron equation

For first-order phase transitions:

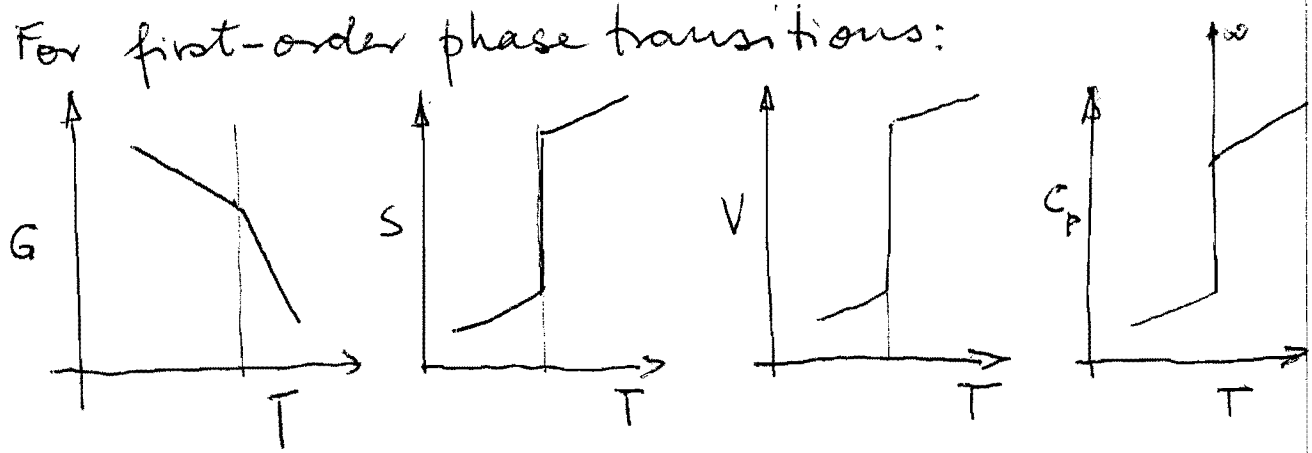

Now return to (for Normal fluids)

$$\frac{T}{C_p}\left(\frac{\partial v}{\partial T}\right)_p > \left.\frac{dT}{dp}\right|_b = \frac{\Delta v}{\Delta S} = \frac{v_v - v_\ell}{s_v - s_\ell}$$

So

$$\frac{T}{C_p}\left(\frac{\partial v}{\partial T}\right)_p > \frac{\Delta v}{\Delta S}$$

and

$$\left(\frac{\partial v}{\partial T}\right)_p > \frac{C_p \Delta v}{\lambda}.$$

If the vapor is a perfect gas, $\left(\frac{\partial v}{\partial T}\right)_p = \frac{v_v}{T}$

and, with $v_v \gg v_\ell$, $\Delta v \doteqdot v_v$

$$\frac{v_v}{T} > \frac{C_p v_v}{\lambda} = \frac{C_p v_v}{T \Delta S}$$

$\boxed{\lambda > C_p T}$ Normal fluid

At suitably chosen points on the boundary,

	MJ/kg	
	λ	$C_p T$
Normal: water	2.4	0.6
Retrograde: Refrigerant 113	0.15	0.2

As before with $\left(\frac{\partial v}{\partial p}\right)_s$, see p. 49-50, derive

$$\left(\frac{\partial p}{\partial v}\right)_s = \left(\frac{\partial p}{\partial v}\right)_T - \frac{T}{C_v}\left(\frac{\partial p}{\partial T}\right)_v^2$$

So, for the boundary between the mixed and vapor phases, we have

vapor side $\left(\frac{\partial p}{\partial v}\right)_{s_v} = \left(\frac{\partial p}{\partial v}\right)_{T_v} - \frac{T}{C_v}\left(\frac{\partial p}{\partial T}\right)_{v_v}^2$

mixed side $\left(\frac{\partial p}{\partial v}\right)_{s_m} = 0 - \frac{T}{C_{v_m}}\left(\frac{dp}{dT}\right)_m^2.$

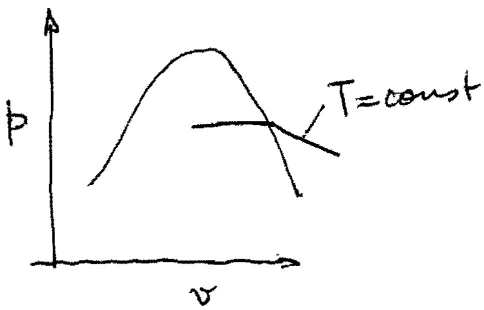

The last form is justified by the behavior of the isotherm in the mixed phase.

Subtract these two results from each other

$$\boxed{\left(\frac{\partial p}{\partial v}\right)_{s_m} - \left(\frac{\partial p}{\partial v}\right)_{s_v} = -\left(\frac{\partial p}{\partial v}\right)_{T_v} - \frac{T}{C_{v_m}}\left(\frac{dp}{dT}\right)_m^2 + \frac{T}{C_{v_v}}\left(\frac{\partial p}{\partial T}\right)_{v_v}^2} \quad \text{(A)}$$

In the following we use a lengthy argument, starting from this result, to derive the relative magnitudes of the speeds of sound in the mixed and vapor phases.

Speeds of sound in mixed and vapor phase

First, obtain C_{v_m}

Let x = mass fraction of liquid

$1-x$ = mass fraction of vapor

Then $$e_m = x e_\ell + (1-x) e_v = e_v + x \Delta e$$

$$v_m = x v_\ell + (1-x) v_v = v_v + x \Delta v$$

In the mixed phase, therefore ($v_m = v_m(T)$)

$$\left(\frac{dv}{dT}\right)_m = \left(\frac{dv_v}{dT}\right)_m + x \frac{d\Delta v}{dT} + \Delta v \frac{dx}{dT}$$

Near the saturation line, x is small. Neglecting it, a constant volume process means that

$$\left(\frac{dv}{dT}\right)_m = \left(\frac{dv_v}{dT}\right)_m + \Delta v \left(\frac{dx}{dT}\right)_m = 0$$

Also, $$C_{v_m} = \left.\frac{de_v}{dT}\right|_b + \Delta e \left(\frac{dx}{dT}\right)_m$$

$$= \left.\frac{de_v}{dT}\right|_b - \frac{\Delta e}{\Delta v} \left.\frac{dv_v}{dT}\right|_b$$

In the vapor phase, along the saturation line,

$$\left.\frac{de_v}{dT}\right|_b = \left(\frac{\partial e}{\partial v}\right)_{T_v} \left.\frac{dv_v}{dT}\right|_b + \left(\frac{\partial e_v}{\partial T}\right)_{v_v}$$

Rewrite $$\left(\frac{\partial e}{\partial v}\right)_{T_v} = \left(\frac{\partial e}{\partial v}\right)_{s_v} + \left(\frac{\partial e}{\partial s}\right)_{v_v} \left(\frac{\partial s}{\partial v}\right)_{T_v}$$

$de = T ds - p dv$

$df = -s dT - p dv$

$$= -p + T \left(\frac{\partial p}{\partial T}\right)_{v_v}$$

So that

$$\left.\frac{de_v}{dT}\right|_b = \left[T\left(\frac{\partial p}{\partial T}\right)_{v_v} - p\right]\left.\frac{dv_v}{dT}\right|_b + C_{v_v}$$

Substitute this back:

$$C_{v_m} = C_{v_v} + \left[T\left(\frac{\partial p}{\partial T}\right)_{v_v} - p - \frac{\Delta e}{\Delta v}\right]\left.\frac{dv_v}{dT}\right|_b$$

At a point on a phase boundary

$$T\Delta s = \Delta e + p\Delta v$$

$$\therefore \frac{\Delta e}{\Delta v} = T\frac{\Delta s}{\Delta v} - p$$

For a process in the mixed phase,

$$\left.\frac{dp}{dT}\right|_b = \frac{\Delta s}{\Delta v} \quad \text{so} \quad \frac{\Delta e}{\Delta v} = T\left.\frac{dp}{dT}\right|_b - p$$

Hence $$C_{v_m} = C_{v_v} + T\left[\left(\frac{\partial p}{\partial T}\right)_{v_v} - \left.\frac{dp}{dT}\right|_b\right]\left.\frac{dv_v}{dT}\right|_b$$

But, $$\left.\frac{dp}{dT}\right|_b = \left(\frac{\partial p}{\partial T}\right)_{v_v} + \left(\frac{\partial p}{\partial v}\right)_{T_v}\left.\frac{dv_v}{dT}\right|_b$$

Solve this for $dv_v/dT|_b$ and substitute above

$$\boxed{C_{v_m} = C_{v_v} - \frac{T}{\left(\frac{\partial p}{\partial v}\right)_{T_v}}\left[\left(\frac{\partial p}{\partial T}\right)_{v_v} - \left.\frac{dp}{dT}\right|_b\right]^2}$$

Consequently $$\boxed{C_{v_m} > C_{v_v}}$$

Now rewrite

$$C_{v_m} = C_{v_v} - T\left(\frac{\partial p}{\partial v}\right)_{T_v}\left(\left.\frac{dv_v}{dT}\right|_b\right)^2$$

and return to Ⓐ on page 53: Multiply Ⓐ by C_{v_m}:

$$C_{v_m}\left[\left(\frac{\partial p}{\partial v}\right)_{s_m}-\left(\frac{\partial p}{\partial v}\right)_{s_v}\right] = -T\left(\frac{dp}{dT}\Big|_b\right)^2 - C_{v_m}\left(\frac{\partial p}{\partial v}\right)_{T_v} + \frac{C_{v_m}}{C_{v_v}}T\left(\frac{\partial p}{\partial T}\right)_{v_v}^2 .$$

Substitute for C_{v_m} on R.H.S.

$$= -T\left(\frac{dp}{dT}\Big|_b\right)^2 - \left(\frac{\partial p}{\partial v}\right)_{T_v}\left[C_{v_v} - T\left(\frac{\partial p}{\partial v}\right)_{T_v}\left(\frac{dv_v}{dT}\Big|_b\right)^2\right]$$

$$+ T\left(\frac{\partial p}{\partial T}\right)_{v_v}^2\left[1-\frac{T}{C_{v_v}}\left(\frac{\partial p}{\partial v}\right)_{T_v}\left(\frac{dv_v}{dT}\Big|_b\right)^2\right]$$

$$= -C_v\left(\frac{\partial p}{\partial v}\right)_{T_v} + T\left[\left(\frac{\partial p}{\partial T}\right)_{v_v}^2 - \left(\frac{dp}{dT}\Big|_b\right)^2\right] + T\left(\frac{\partial p}{\partial v}\right)_{T_v}^2\left(\frac{dv_v}{dT}\Big|_b\right)^2$$

$$- \frac{T^2}{C_v}\left(\frac{\partial p}{\partial v}\right)_{T_v}\left(\frac{\partial p}{\partial T}\right)_{v_v}^2\left(\frac{dv_v}{dT}\Big|_b\right)^2$$

Now use $\left(\frac{dp}{dT}\Big|_b\right)^2 = \left[\left(\frac{\partial p}{\partial T}\right)_{v_v} + \left(\frac{\partial p}{\partial v}\right)_{T_v}\frac{dv_v}{dT}\Big|_b\right]^2$

to obtain $\left(\frac{\partial p}{\partial T}\right)_{v_v}^2 - \left(\frac{dp}{dT}\Big|_b\right)^2 = 2\left(\frac{\partial p}{\partial v}\right)_{T_v}\left(\frac{\partial p}{\partial T}\right)_{v_v}\frac{dv_v}{dT}\Big|_b - \left(\frac{\partial p}{\partial v}\right)_{T_v}^2\left(\frac{dv_v}{dT}\Big|_b\right)^2$

so that the above

$$= -C_v\left(\frac{\partial p}{\partial v}\right)_{T_v} - 2T\left(\frac{\partial p}{\partial v}\right)_{T_v}\left(\frac{\partial p}{\partial T}\right)_{v_v}\frac{dv_v}{dT}\Big|_b - \frac{T^2}{C_v}\left(\frac{\partial p}{\partial v}\right)_{T_v}\left(\frac{\partial p}{\partial T}\right)_{v_v}^2\left(\frac{dv_v}{dT}\Big|_b\right)^2$$

$$= -C_v\left(\frac{\partial p}{\partial v}\right)_{T_v}\left[1 + \frac{2T}{C_{v_v}}\left(\frac{\partial p}{\partial T}\right)_{v_v}\frac{dv_v}{dT}\Big|_b + \left\{\frac{T}{C_{v_v}}\left(\frac{\partial p}{\partial T}\right)_{v_v}\frac{dv_v}{dT}\Big|_b\right\}^2\right]$$

$$= -C_{v_v}\left(\frac{\partial p}{\partial v}\right)_{T_v}\left[1+\frac{T}{C_{v_v}}\left(\frac{\partial p}{\partial T}\right)_{v_v}\left.\frac{dv_v}{dT}\right|_b\right]^2$$

So that

$$\boxed{\left(\frac{\partial p}{\partial v}\right)_{s_m}-\left(\frac{\partial p}{\partial v}\right)_{s_v} = -\frac{C_{v_v}}{C_{v_m}}\left(\frac{\partial p}{\partial v}\right)_{T_v}\left[1+\frac{T}{C_{v_v}}\left(\frac{\partial p}{\partial T}\right)_{v_v}\left.\frac{dv_v}{dT}\right|_b\right]^2}$$

The R.H.S. of this equation is always >0

It follows that

$$\boxed{\begin{gathered}\left(\frac{\partial p}{\partial v}\right)_{s_m} > \left(\frac{\partial p}{\partial v}\right)_{s_v} \\ \text{or} \quad a_m < a_v\end{gathered}}$$

The speed of sound is lower in the mixed phase than in either of the pure phases.

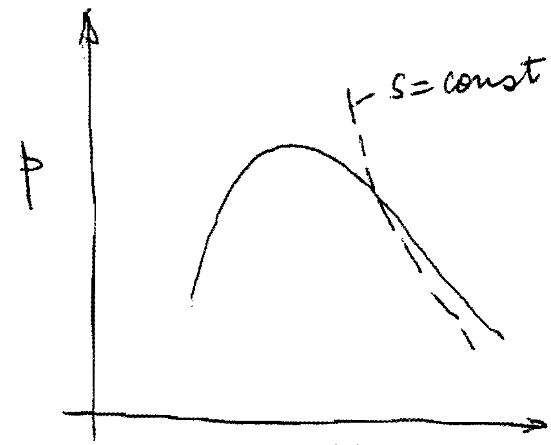

Normal

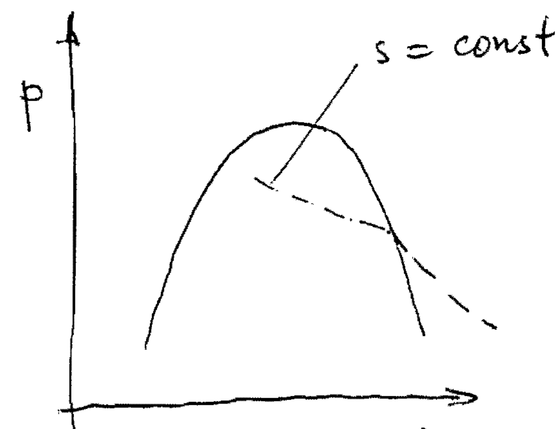

Retrograde

Note that this is true for both normal and retrograde fluids.

The Hugoniot for <u>normal fluids</u> is concave everywhere. Therefore, with $\Gamma > 0$, $G > 0$, compression waves steepen and expansion waves disperse.

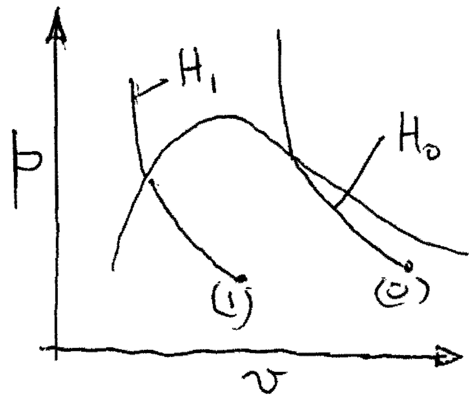

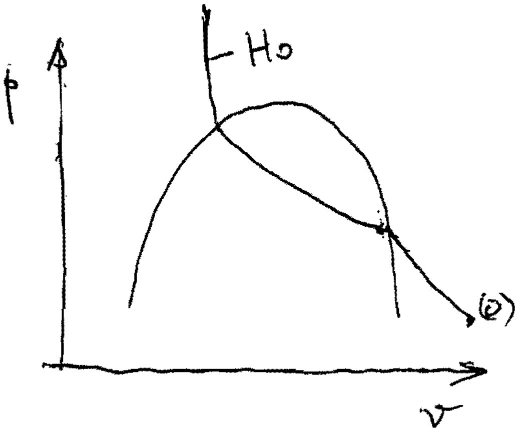

Retrograde fluids are more interesting. The Hugoniot now has a convex kink at the saturated vapor boundary. We now explore some of the possibilities in this case. In the following, assume that we are dealing with relatively weak shocks so that the Hugoniot is qualitatively similar to and nearly coincident with an isentrope. Consider the case sketched

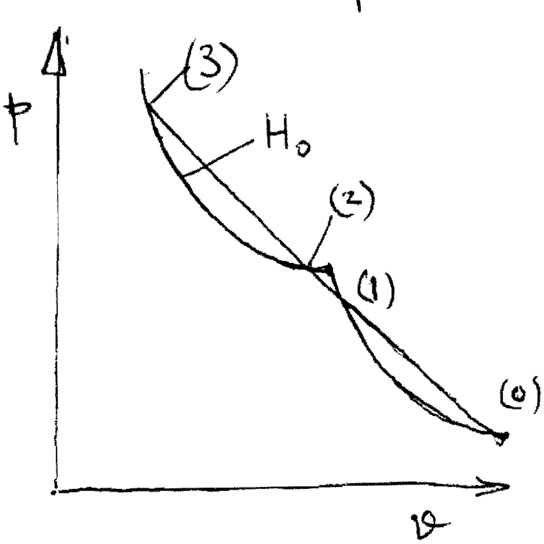

in which the Rayleigh line can intersect H_0 in 3 places. A compression shock from (0) to (1) is possible, but a shock from (0) to (2) is not permitted, because, at (2)

$$\frac{dp}{dv} > \frac{\Delta p}{\Delta v}$$

which (with our assumption that the Hugoniot is almost coincident to an isentrope) violates causality:

$$-\rho^2 a^2 > -\rho^2 (c-u_p)^2$$

$$\text{or } c-u_p > a$$

A shock from (0) to (3) is possible, provided that p_3 is imposed by piston motion at the right speed. However, a faster wave with a smaller pressure jump can precede the wave. This actually happens. The wave splits into two shocks.

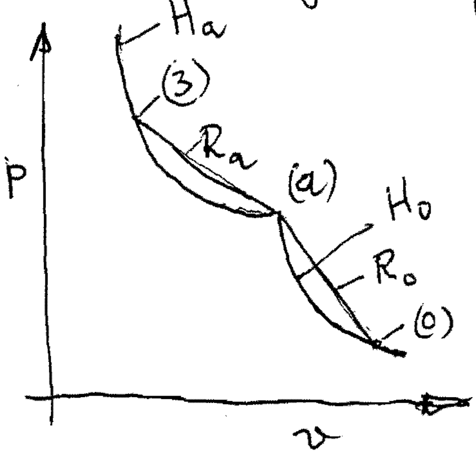

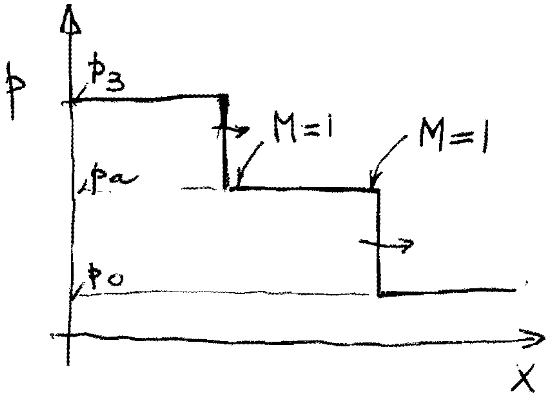

The downstream point of the shock (0)→(a) will be sonic relative to the shock since R_0 is "tangent" to H_0 there. Similarly, the upstream point of the shock (a)→(3) is sonic for the same reason.

In fact, if one imagines the kink to be locally smoothed out, so that the ~~Rayleigh~~ line from (0) to (b) makes a CJ point at (b) and that from (c) to (3) makes a CJ point at (c), we get a wave consisting of a dispersed compression wave embedded in two shocks. In an xt-diagram this appears as shown.

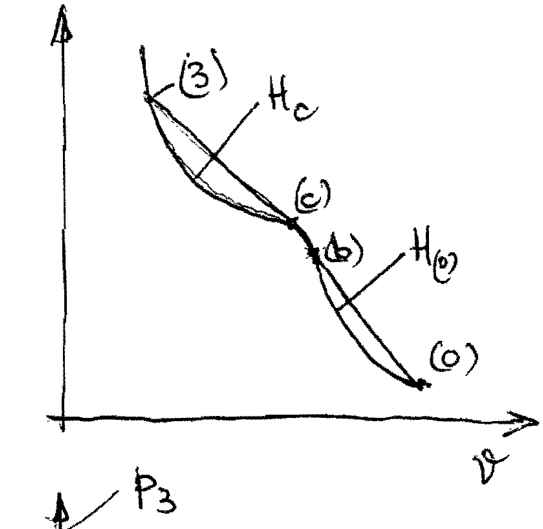

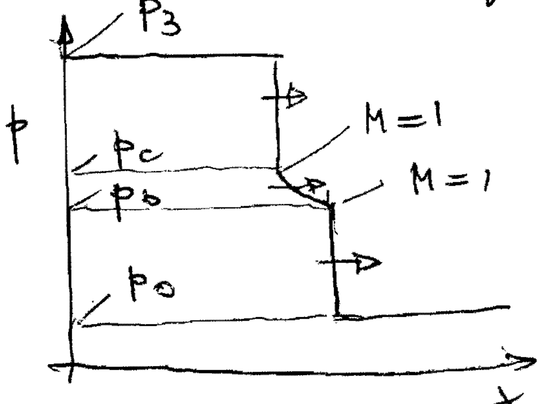

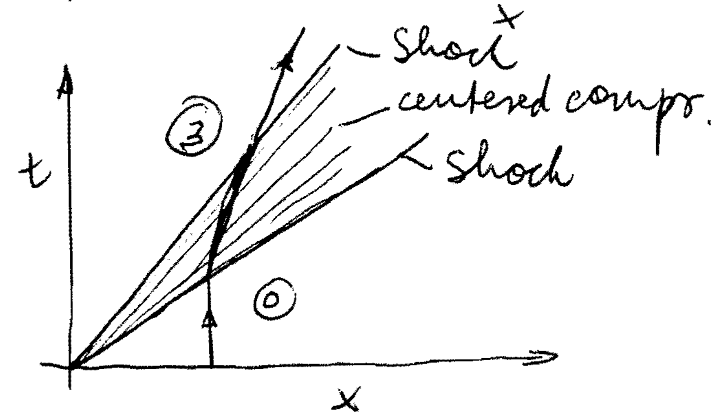

Thus the kink behaves similarly as two CJ points at which the flow relative to the wave is sonic. At each of the shocks the entropy has to increase, of course, which, with our simplification we can not show; however, ~~its~~ the solutions shown, this condition is satisfied.

The solution will always evolve until the sonic condition is reached, because it is not possible to go beyond that point, without the flow losing touch with the wave.

Now consider expansion waves in the presence of a convex kink. With an upstream

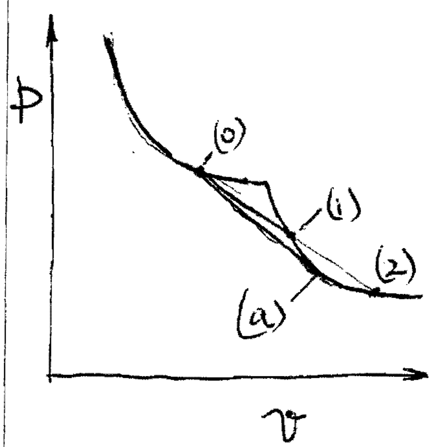

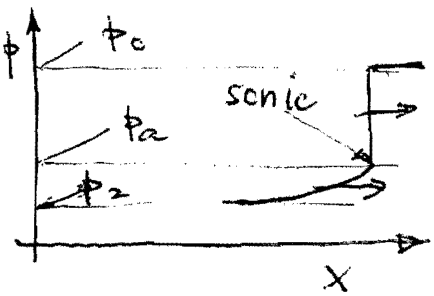

point at (0) an expansion shock (0) → (1) is allowed. However, a transition from (0) to (2) will split into a CJ expansion shock from (0) to (a) followed by a centered expansion from (a) to (2).

Even more interesting is the case when the Rayleigh line misses the kink. In this case the centered expansion (0) to (a) is faster than the expansion shock (0) → (3) so

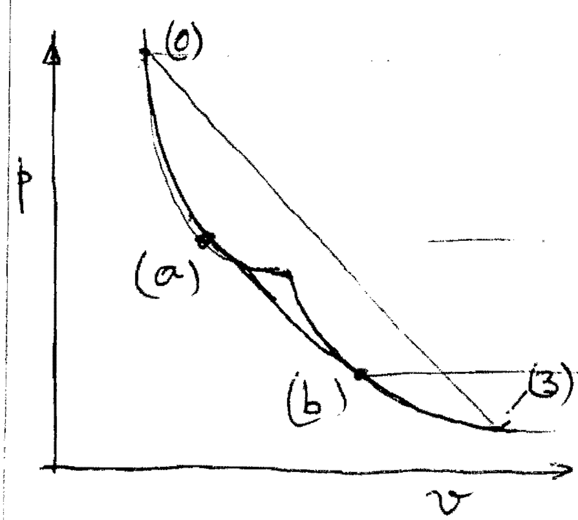

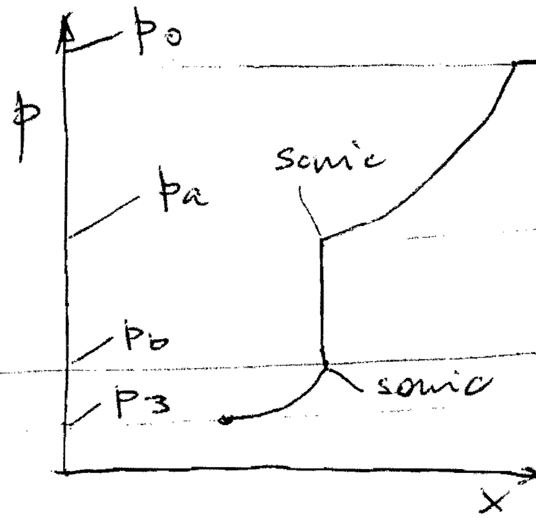

that the wave splits into an expansion shock (sonic both sides) embedded in two centered expansions.

Evolution of a pressure hump

If a pressure hump propagates in one direction in a normal fluid, the speed

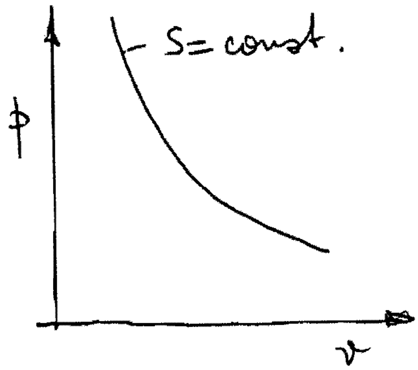

of sound increases with increasing pressure, so that an xt-diagram of a pressure hump propagating to the right looks as shown.

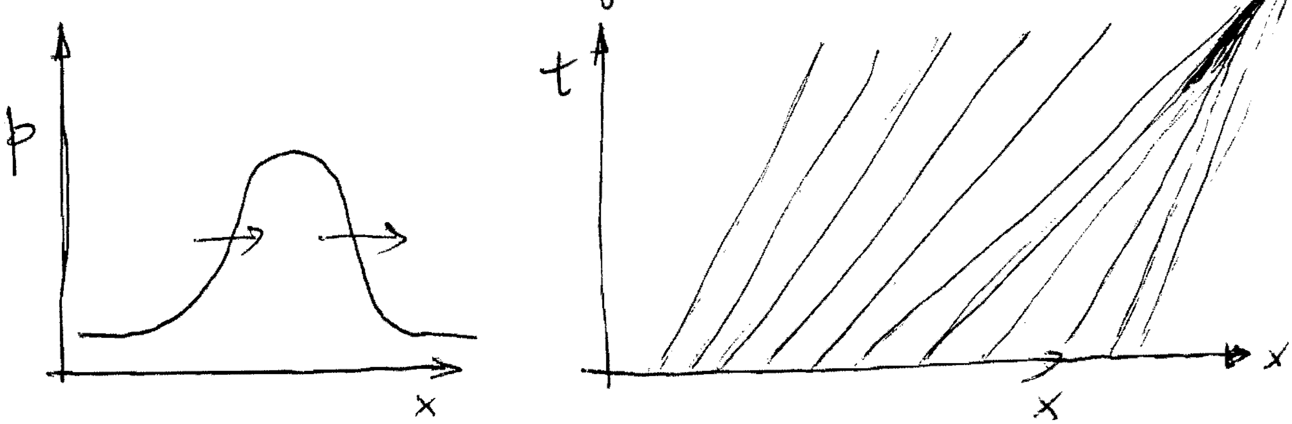

Acoustic waves on the right of the hump coalesce and on the left disperse. The pressure rise on the right focusses into a shock wave and the drop on the left

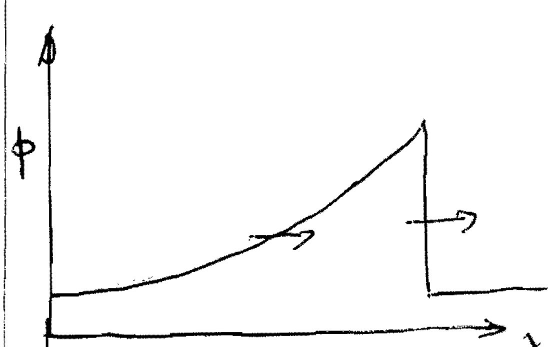

becomes a dispersed expansion wave, so that eventually the wave looks as shown here.

In the case of a retrograde fluid the situation can be extremely complex.

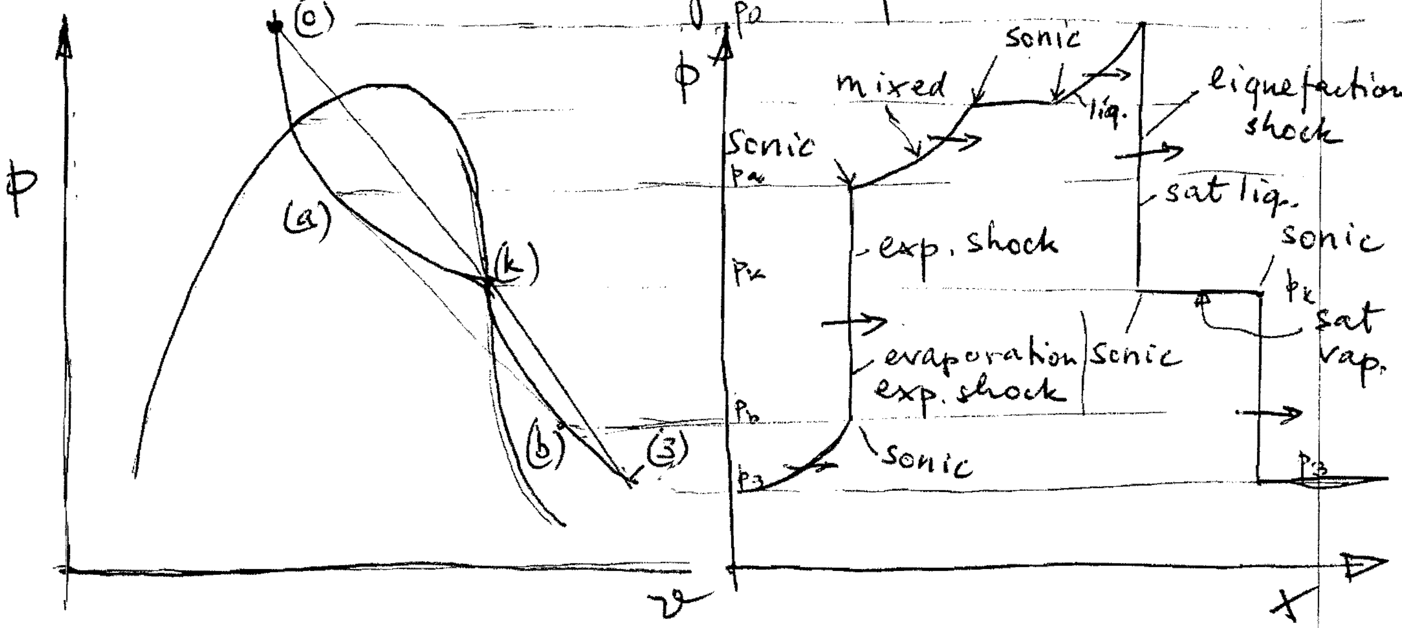

Each element of the wave evolves until sonic conditions are reached. On the right, the upstream point is (3) and we get a Rayleigh line to the kink (k) corresponding to a compression shock. This is followed by a slower compress. shock (k) to (c) that liquefies the fluid.

On the expansion side we have a fast isentropic dispersed expansion to the saturated liquid point followed by a slower isentropic dispersed expansion to the CJ-point (a). From there an expansion shock that is sonic on each side takes us to the CJ-point at (b). An isentropic expansion wave finally reaches the point (3) on the downstream side.

(The causality condition is sometimes called Information Condition)

Conditions near a critical point

The equilibrium isotherm in the region where vapor and liquid coexist is a constant pressure line. However, if the specific volume of a liquid is rapidly increased, the path $S_1 \to A$ is experimentally achievable. Also the path $S_2 \to B$ is experimentally achievable. However, since $\left(\frac{\partial p}{\partial v}\right)_T > 0$ between A and B, the material stability requirement forbids the existence of $A \to B$. A and B are called "spinodal points"

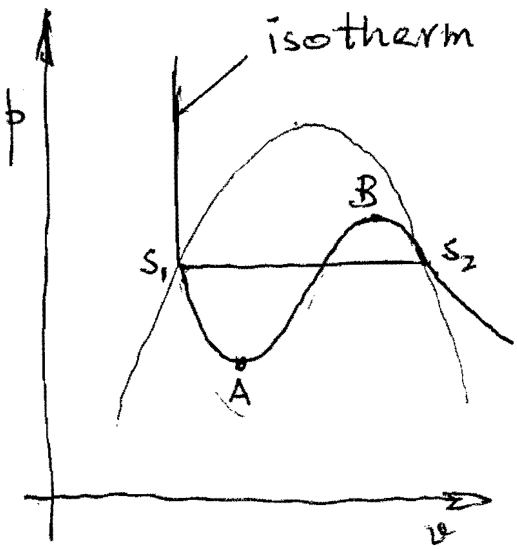

As we increase the temperature of the isotherm to just below the critical point, $\left(\frac{\partial p}{\partial v}\right)_T$ is still zero. As we cross the critical point, the slope discontinuities of the isotherm disappear, it becomes smooth and acquires a point of inflection. Right at the critical pt. $\left(\frac{\partial p}{\partial v}\right)_T = 0 = \left(\frac{\partial^2 p}{\partial v^2}\right)_T$.

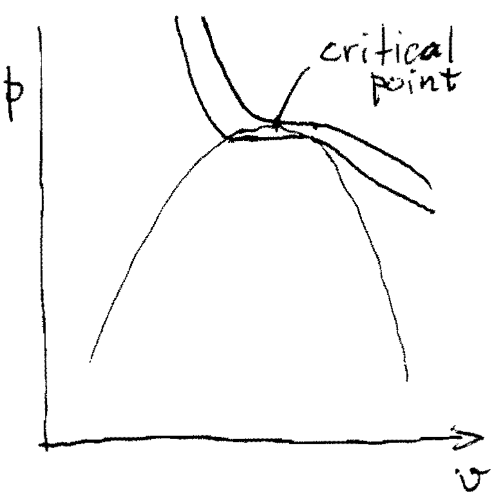

If we expand $p(v)$ along the isotherm for a small region near the critical point

$$p - p_c = \left(\frac{\partial p}{\partial v}\right)_{T_c}(v - v_c) + \left(\frac{\partial^2 p}{\partial v^2}\right)_{T_c}\frac{(v-v_c)^2}{2} + \left(\frac{\partial^3 p}{\partial v^3}\right)_{T_c}\frac{(v-v_c)^3}{6} + \ldots$$

and put $\left(\frac{\partial p}{\partial v}\right)_{T_c} = \left(\frac{\partial^2 p}{\partial v^2}\right)_{T_c} = 0$, we see that, for $\frac{p - p_c}{v - v_c} < 0$, as required by material stability, $\left(\frac{\partial^3 p}{\partial v^3}\right)_{T_c} < 0$ must hold.

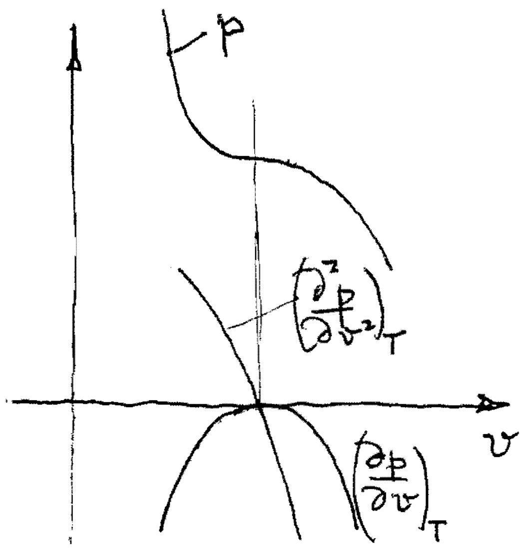

The pressure, first and second derivative along the isotherm through the critical point must therefore behave as shown.

These conditions may be used to find the constants in the van der Waals equation of state in terms of the coordinates of the triple point $(p, v, T) = (p_c, v_c, T_c)$

By writing

$$p^* = \frac{p}{p_c}, \quad v^* = \frac{v}{v_c}, \quad T^* = \frac{T}{T_c},$$

$$\left(p + \frac{a}{v^2}\right)(v - b) = RT$$

and $$e = c_v T - \frac{a}{v}$$

become
$$\boxed{\begin{aligned} \left(p^* + \frac{3}{v^{*2}}\right)(3v^* - 1) &= 8T^* \\ e^* &= \frac{c_v}{R} T^* - \frac{9}{8v^*} \end{aligned}}$$

with $$a = \frac{9RT_c v_c}{8}, \quad b = \frac{v_c}{3}, \quad e^* = \frac{e}{RT_c}$$

This is an example of a so-called "Law of corresponding states." It allows us to write down a real-gas equation of state in terms of critical point coordinates.

Using van der Waals' equation of state it is possible to show that for such a substance there exists a region in which $\Gamma < 0$. Below the curve A, $\left(\frac{\partial^2 p}{\partial v^2}\right)_s < 0$. This region lies near the R.H. branch of the saturated vapor boundary.

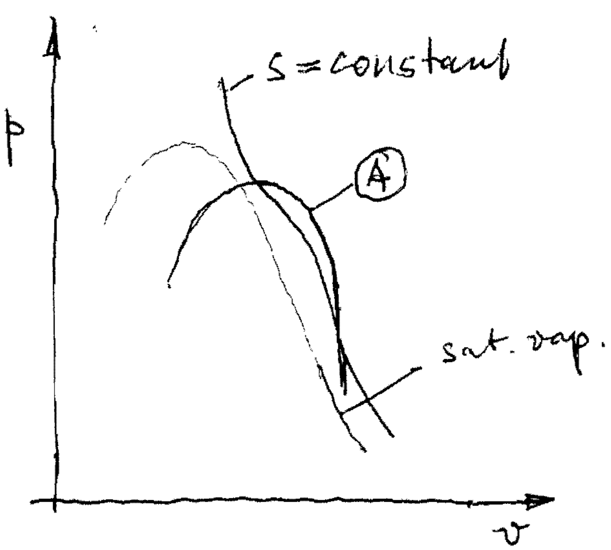

Entropy and speed of sound in van der Waals gas

Write $\quad Tds = de + pdv$

If $c_v = \text{const.}$, $\quad = c_v dT + \frac{a}{v^2}dv + pdv$

$$ds = c_v \frac{dT}{T} + \frac{p + \frac{a}{v^2}}{T}dv$$

$$ds = c_v \frac{dT}{T} + R\frac{dv}{v-b}$$

$$\boxed{\frac{s - s_0}{R} = \frac{c_v}{R}\ln\frac{T}{T_0} + \ln\frac{v-b}{v_0-b}}$$

Now take $\left(\frac{\partial p}{\partial v}\right)_s = \left(\frac{\partial p}{\partial v}\right)_T + \left(\frac{\partial p}{\partial T}\right)_v\left(\frac{\partial T}{\partial v}\right)_s$

Since $\quad p = \frac{RT}{v-b} - \frac{a}{v^2}$

$$\left(\frac{\partial p}{\partial v}\right)_T = -\frac{RT}{(v-b)^2} + \frac{2a}{v^3}$$

Also $\quad \left(\frac{\partial p}{\partial T}\right)_v = \frac{R}{v-b}$

and $\quad \left(\frac{\partial T}{\partial v}\right)_s = -\frac{R}{c_v}\frac{T}{v-b}.$

Substitute these: $\quad \left(\frac{\partial p}{\partial v}\right)_s = \frac{2a}{v^3} - \frac{RT}{(v-b)^2} - \frac{R}{c_v}\cdot\frac{RT}{(v-b)^2}$

$$\boxed{a_s^2 = -v^2\left(\frac{\partial p}{\partial v}\right)_s = -\frac{2a}{v} + \frac{v^2 RT}{(v-b)^2}\left(1 + \frac{R}{c_v}\right)}$$

It is easy to see that in the perfect-gas limit, this goes to $a_s^2 = \gamma RT$. $(a=b=0)$

<u>Value of Γ for van der Waals gas</u>

$$\left(\frac{\partial p}{\partial v}\right)_s = \frac{2a}{v^3} - \frac{\gamma RT}{(v-b)^2} = -\frac{\gamma\left(p+\frac{a}{v^2}\right)}{v-b} + \frac{2a}{v^3}$$

$$\left(\frac{\partial^2 p}{\partial v^2}\right)_s = -\frac{6a}{v^4} + \frac{\gamma\left(p+\frac{a}{v^2}\right)}{(v-b)^2} - \frac{\gamma}{v-b}\left(\left(\frac{\partial p}{\partial v}\right)_s - \frac{2a}{v^3}\right)$$

$$= -\frac{6a}{v^4} + \frac{\gamma\left(p+\frac{a}{v^2}\right)}{(v-b)^2} - \frac{\gamma}{v-b}\left[-\frac{\gamma\left(p+\frac{a}{v^2}\right)}{v-b}\right]$$

$$= -\frac{6a}{v^4} + \gamma(\gamma+1)\frac{p+\frac{a}{v^2}}{(v-b)^2}$$

$$\Gamma = \frac{v^3}{2a_s^2}\left(\frac{\partial^2 p}{\partial v^2}\right)_s = \frac{-\frac{6a}{v} + \gamma(\gamma+1)\left(p+\frac{a}{v^2}\right)\frac{v^3}{(v-b)^2}}{2\left[-\frac{2a}{v} + \frac{\gamma v^2 RT}{(v-b)^2}\right]}$$

$$\boxed{\Gamma = \frac{\gamma(\gamma+1)\frac{v^3}{(v-b)^3}RT - \frac{6a}{v}}{2\left[\gamma RT\frac{v^2}{(v-b)^2} - \frac{2a}{v}\right]}}$$

In the perfect-gas limit, this goes to $\frac{\gamma+1}{2}$ as it should.

Γ changes sign when

$$\frac{\gamma(\gamma+1)}{6}\left(p+\frac{a}{v^2}\right) = \frac{a(v-b)^2}{v^4}$$

or when
$$\boxed{p = \frac{6a}{\gamma(\gamma+1)}\frac{(v-b)^2}{v^4} - \frac{a}{v^2}}$$

This is the curve A on p 66.

<u>Speed of sound near critical point.</u>

With
$$a_s^2 = \gamma RT\frac{v^2}{(v-b)^2} - \frac{2a}{v}$$

write in terms of critical-point coordinates

$$\frac{a_s^2}{RT_c} = \frac{\gamma T^*}{\left(1-\frac{1}{3v^*}\right)^2} - \frac{9}{4v^*}$$

At the critical point, the starred quantities are all equal to one.

$$\boxed{\frac{a_s^2}{RT_c} = \frac{9}{4}(\gamma-1)} \quad \text{at critical pt.}$$

For gases with γ close to 1, this can be much smaller than γ, so that the speed of sound can be quite small.

Ae/APh 237 Assignment No. 3, January 23, due January 30, 2003

PROBLEM 1.

Consider a general Hugoniot curve. Show that if a piston–velocity minimum exists, it must lie between the specific–volume minimum and the entropy minimum.

PROBLEM 2.

Determine an equation for the Hugoniot curve for a solid with the following equations of state:

$$e = e_c(v) + c_v T$$

$$p = p_c(v) + c_v G T / v.$$

Simplify the Hugoniot for moderately strong shocks, $p_0 \ll p$, $p_0 \ll p_c$, $e_0 \ll e_c$. Sketch the curve.

PROBLEM 3.

Use the peculiarities of the isotherm at the critical point in order to determine a "law of corresponding states" for a van der Waals gas, expressing these two equations with variables normalized with their values at the critical point. Determine the boundary of the region in vp-space where the fundamental derivative of gasdynamics Γ is negative. Make a quantitative diagram showing this boundary and the saturated vapor boundary.

PROBLEM 4.

Consider waves in a retrograde fluid. Explain the cases that may arise when a piston in a tube filled with this fluid is first withdrawn (brought suddenly to a speed moving away from the fluid) and then suddenly stopped. Draw appropriate Rayleigh lines, xp-diagrams and xt-diagrams.

Weak Shock Theory

Whitham Ch. 2, 6

In the waves we have dealt with so far, it was necessary to consider the thermodynamic behavior of the medium because entropy changes were generally not negligible, so that any variable was always dependent on two state variables, e.g., $p = p(v, s)$. However, since entropy changes across a shock appear only in the third order of Δv, we can deal with nonlinear waves without introducing thermodynamics if we cut expansions off at the second order. for sufficiently weak waves. This means that we can consider p to be $p(v)$ or $p(\rho)$, i.e. a function of only a single variable for such waves.

Consider one-dimensional motion. The variables of the problem are

$$\rho, \; p(\rho), \; u(\rho), \; q \equiv \rho u = Q(\rho)$$

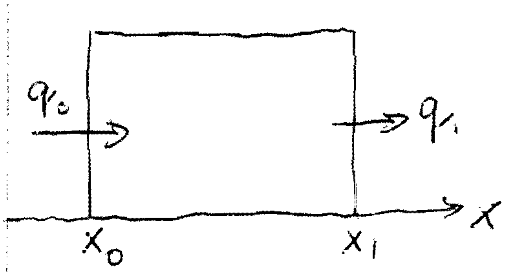

Consider a fixed control volume between x_0 and x_1:

$$\frac{d}{dt} \int_{x_0}^{x_1} \rho \, dx = q_0 - q_1$$

is tantamount to the statement that the change in mass contained in the control volume is equal to the mass flowing in minus the mass flowing out. If derivatives of ρ are continuous in the interval $x_0 \to x_1$ differentiation gives

$$\frac{\partial \rho(x,t)}{\partial t} + \frac{\partial q(x,t)}{\partial x} = 0 .$$

If, on the other hand, the control volume contains a discontinuity at $x = s(t)$,

$$\frac{d}{dt}\int_{x_0}^{s_-(t)} \rho\, dx + \frac{d}{dt}\int_{s_+(t)}^{x_1} \rho\, dx = q_0 - q_1 .$$

We can rewrite this using Leibniz' Rule:

$$\int_{x_0}^{s_-(t)} \frac{\partial \rho}{\partial t}\, dx + \rho(s_-(t),t)\frac{ds}{dt} + \int_{s_+(t)}^{x_1} \frac{\partial \rho}{\partial t}\, dx - \rho(s_+(t),t)\frac{ds}{dt} = q_0 - q_1$$

If the conditions are uniform between x_0 and s_- and uniform between s_+ and x_1, or if $x_1 - x_0 \to 0$, $\frac{\partial \rho}{\partial t} = 0$ in the integrals, so that they do not contribute. It follows that

$$(\rho_+ - \rho_-)\frac{ds}{dt} = q_1 - q_0$$

Now $\frac{ds}{dt} = c$ is the wave speed, so we see that

$$\boxed{c\,\Delta\rho = \Delta q}$$

shock jump condition

However, we have seen on p. 70 that $q = Q(\rho)$.

Therefore,
$$\frac{\partial q}{\partial x} = \frac{dQ}{d\rho}\frac{\partial \rho}{\partial x} = Q'\frac{\partial \rho}{\partial x}$$

Substitute this into the equation for continuous derivatives of q on p. 71:

$$\frac{\partial \rho}{\partial t} + Q'\frac{\partial \rho}{\partial x} = 0 .$$

Now seek a path along which $d\rho = 0$

$$d\rho = \frac{\partial \rho}{\partial t}dt + \frac{\partial \rho}{\partial x}dx = 0$$

$$\text{or } \frac{dx}{dt} = -\frac{\partial \rho/\partial t}{\partial \rho/\partial x} = Q' .$$

This means that Q' is the propagation speed of disturbances, and we may write

$$\boxed{\frac{\partial \rho}{\partial t} + a(\rho)\frac{\partial \rho}{\partial x} = 0. \qquad \Delta Q = c\,\Delta\rho}$$

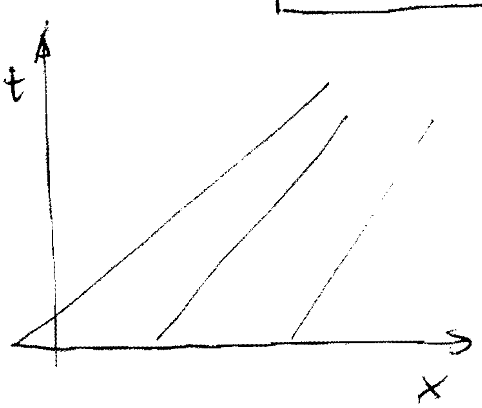

slopes of characteristics in xt-space depend on ρ, so that steepening and dispersion of waves can occur.

<u>Initial Value Problem</u> given $\rho = f(x)$ at $t=0$

Let one of the characteristics intersect the x-axis at $x = \xi$. Then the value ξ identifies the characteristic in terms of the place where it came from at $t=0$. Then $\rho = f(\xi)$ anywhere, since ρ = constant along characteristics. The slope of the characteristics is
$$\frac{dx}{dt} = a(\rho) = a(f(\xi)) = A(\xi) \text{ say}$$
Therefore the equation of the characteristic is
$$x = \xi + A(\xi)t$$
Hence the solution of the initial value problem is
$$\boxed{\begin{aligned} &\rho = f(\xi), \quad a = A(\xi) = a(f(\xi)) \\ &\text{on } x = \xi + A(\xi)t. \end{aligned}}$$

Since steepening occurs when characteristics converge, this may lead to intersection of characteristics and consequent multivaluedness. We therefore need to permit weak discontinuous waves to occur. To examine this write
$$Q = Q_0 + C_1\rho + C_2\rho^2 + \dots$$
neglecting cubic and higher terms as stated at the start.

Then
$$a(\rho) = Q' = c_1 + 2c_2\rho \qquad \underline{\underline{\text{Linear!}}}$$

Now c (the wave speed of the discontinuity)
$$c = \frac{\Delta Q}{\Delta \rho} = \frac{Q_0 + c_1\rho_1 + c_2\rho_1^2 - Q_0 - c_1\rho_0 - c_2\rho_0^2}{\rho_1 - \rho_0}$$
for a discontinuous wave with upstream state (0) and downstream state (1).
$$c = c_1 + c_2(\rho_1+\rho_0)(\rho_1-\rho_0)/\rho_1-\rho_0$$
$$= c_1 + c_2(\rho_1+\rho_0)$$

But
$$\frac{a_0+a_1}{2} = \frac{c_1 + 2c_2\rho_0 + c_1 + 2c_2\rho_1}{2}$$
$$= c_1 + c_2(\rho_1+\rho_0)$$

Therefore,
$$\boxed{c = \frac{a_0+a_1}{2} = \frac{1}{2}\left[A(\xi_0) + A(\xi_1)\right]}$$

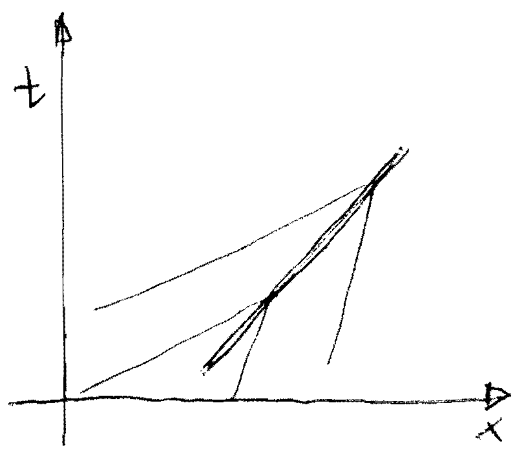

The slope of the shock is the average of the slopes of the converging characteristics in xt-space

Since a and ρ are linearly related, conservation of ρ implies conservation of a.

To show this, multiply

$$\frac{\partial \rho}{\partial t} + a \frac{\partial \rho}{\partial x} = 0$$

by $\frac{da}{d\rho} = a'$:

$$a' \frac{\partial \rho}{\partial t} + a' a \frac{\partial \rho}{\partial x} = 0$$

or

$$\boxed{\frac{\partial a}{\partial t} + a \frac{\partial a}{\partial x} = 0}$$

[Note: This equation is independent of the sign of $a' = da/d\rho$.]

If a is conserved, this means that

$$\int a\,dx = \text{const.}$$

It follows that the evolution of a hump in a from

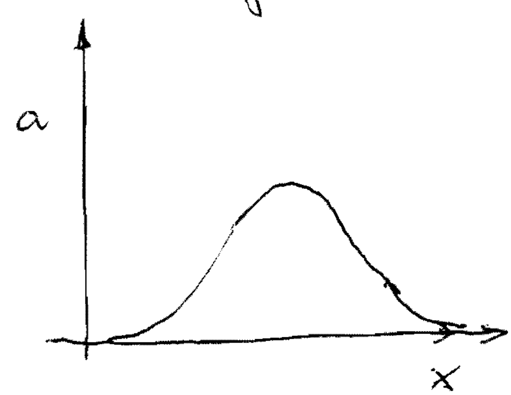

to

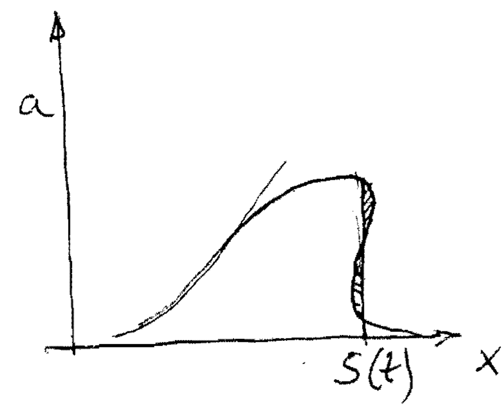

requires that the piece that is cut by the discontinuous wave at $x = s(t)$ makes the areas of the two hatched parts equal.

Areas are preserved in a mapping from a to $A(\xi)$. This means that the area rule also applies to $A(\xi)$

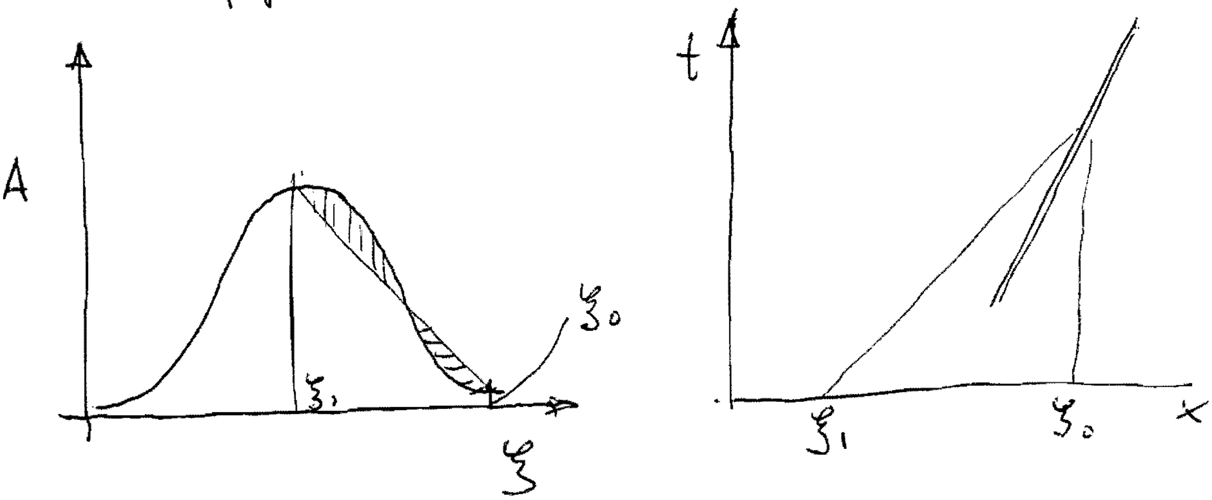

~~To show this~~, Analytically write this as

$$\frac{1}{2}\left[A(\xi_1)+A(\xi_0)\right](\xi_0-\xi_1) = \int_{\xi_1}^{\xi_0} A(\xi)\,d\xi .$$

Let the shock be at $x = s(t)$ so that

$$s(t) = \xi_0 + A(\xi_0)t$$

and $s(t) = \xi_1 + A(\xi_1)t$

Solve for t
$$t = \frac{\xi_0 - \xi_1}{A(\xi_1) - A(\xi_0)}$$

From these equations we can determine $s(t)$, $\xi_1(t)$ and $\xi_0(t)$ along the shock.

Behavior of shock at large times

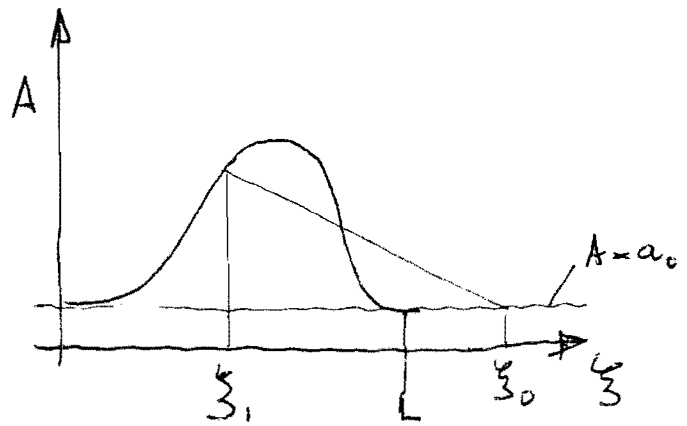

If the upstream value of ξ, i.e. ξ_0 is larger than L, the value beyond the point where A varies, so that $A = a_0$ for $\xi > L$ then subtract

$$a_0(\xi_0 - \xi_1) = \int_{\xi_1}^{\xi_0} a_0\, d\xi$$

from the equal area equation:

$$\frac{1}{2}\left[A(\xi_1) + \overset{a_0}{A(\xi_0)} - 2a_0\right](\xi_0 - \xi_1) = \int_{\xi_1}^{\xi_0} \left[A(\xi) - a_0\right] d\xi$$

At large times $A(\xi_0) = a_0$.

Thus,
$$\frac{1}{2}\left[A(\xi_1) - a_0\right](\xi_0 - \xi_1) = \int_{\xi_1}^{L} \left[A(\xi) - a_0\right] d\xi$$

also
$$t = \frac{\xi_0 - \xi_1}{A(\xi_1) - a_0}.$$

Therefore,
$$\frac{1}{2}\left[A(\xi_1) - a_0\right]^2 t = \int_{\xi_1}^{L} \left[A(\xi) - a_0\right] d\xi \quad \text{— (A)}$$

Also,
$$s(t) = \xi_1 + A(\xi_1)\,t$$
and
$$a = A(\xi_1)$$

where ξ_1 has to satisfy (A)

As $t \to \infty$, $\xi_1 \to 0$ and $A(\xi_1) \to a_0$. Then (A) gives

$$\frac{1}{2}\left[A(\xi_1) - a_0\right]^2 t \doteq \int_0^L \left[A(\xi) - a_0\right] d\xi = B, \text{ say.}$$

B is the area of the hump above $A = a_0$

$$\boxed{\begin{aligned} \lim_{\xi_1 \to 0} A(\xi_1) &= a_0 + \sqrt{\frac{2B}{t}} \\ \lim_{\xi_1 \to 0} s &= a_0 t + \sqrt{2Bt} \\ \lim_{\xi_1 \to 0} \quad &= a_0 + \sqrt{\frac{2B}{t}} \end{aligned}}$$

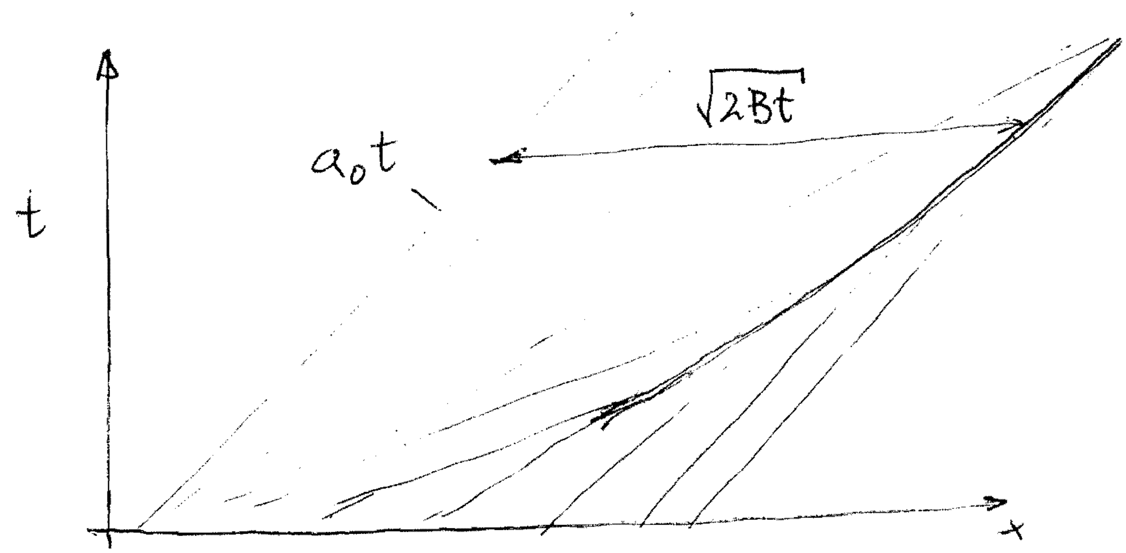

Strength of shock $\dfrac{a - a_0}{a_0} \sim \dfrac{1}{\sqrt{t}}$

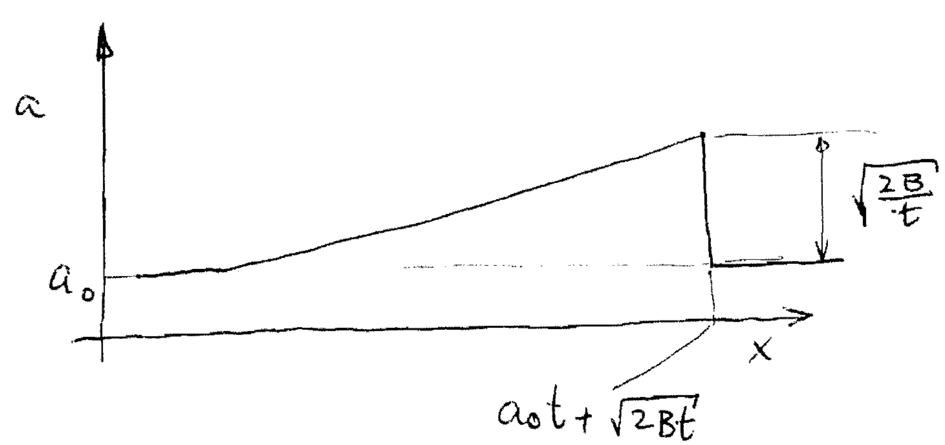

Waves in traffic.

A good example of where weak wave theory works well is that of traffic flow. Let the velocity of the cars be u, the traffic density (cars per unit length of road) ρ, traffic flux (cars passing a fixed point per unit time) $\rho u = Q(\rho)$.

The speed $u = \frac{Q(\rho)}{\rho}$ has a finite maximum value when there are no cars, i.e. at zero density. For law-abiding drivers this may be thought of as the speed limit, ~~for~~ otherwise the limit of the capability of the car. So $Q'(0) = u_{max}$. Also at $\rho = 0$, $Q = 0$, so $Q(0) = 0$. The flux is again equal to zero when the cars are bumper to bumper. Let the density be ρ_j at that condition. $Q(\rho_j) = 0$

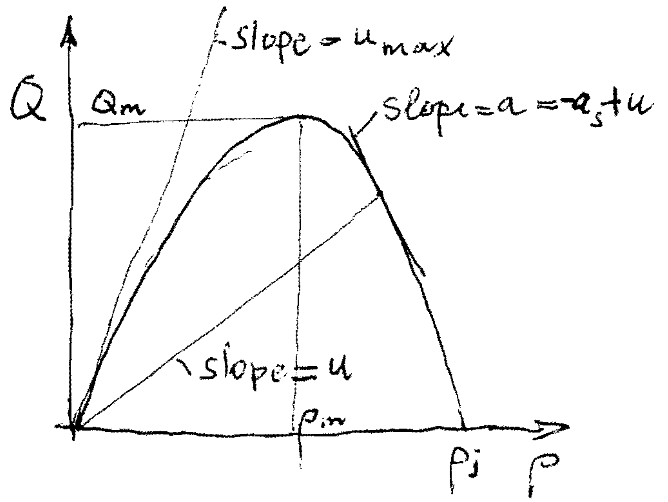

It follows that Q has a maximum value in the range $0 < \rho < \rho_j$. $u = Q/\rho$ is the slope of the straight line from the origin.

$$a = Q'(\rho) = u(\rho) + \rho u'(\rho)$$

$$Q = C_1\rho + C_2\rho^2$$

$$Q' = C_1 + 2C_2\rho$$

at $\rho = 0$, $Q' = C_1 = u_m$

at $\rho = \rho_m$, $Q' = 0$, so $2C_2 = -\frac{C_1}{\rho_m}$

$$C_2 = -\frac{u_m}{2\rho_m}$$

$$Q = u_m\rho - \frac{u_m\rho^2}{2\rho_m}$$

Since $u' < 0$ (u decreases with increasing ρ, see diagram) this says that $u > a$. In other words, waves propagate backward relative to the cars. This is not surprising since the drivers take their cues from ahead of their cars, so information travels from front to back.

The slope of the curve $Q(\rho)$ is a, so

$$u' = \frac{a-u}{\rho}$$

To the right of $\rho = \rho_m$, the flow is therefore subsonic, to the left supersonic and at maximum traffic flux it is sonic. The value of u at $\rho = \rho_m$ is approximately 25 mph. Waves propagate backward relative to the road when $\rho < \rho_m$ and vice versa

The slope at $\rho = \rho_j$ is related to the reaction time τ of the drivers. The safe distance between cars is $u\tau$, so, with a car length L, a distance between cars h, near $\rho = \rho_j$,

$$h - L = u\tau$$

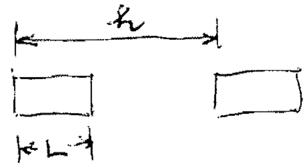

Now $h = \frac{1}{\rho}$ and $L = 1/\rho_j$

So $$u = \frac{1/\rho - 1/\rho_j}{\tau} = \frac{1}{\tau\rho_j}\left(\frac{\rho_j}{\rho} - 1\right) = \frac{L}{\tau}\left(\frac{\rho_j}{\rho} - 1\right)$$

$$Q(\rho) = a\rho \log \frac{\rho_j}{\rho}$$

$$Q' = a \log \left(\frac{\rho_j}{\rho}\right) + \frac{a\cancel{\rho}\cancel{\rho}}{\rho} = 0$$

when $\log \frac{\rho_j}{\rho} = \cancel{\rho}\frac{\rho_j}{\rho}$

$\cancel{\rho =}$

$$\frac{1}{\left(\frac{1}{\rho}\right)} d\frac{1}{\rho} = -\frac{\cancel{\rho}\rho_j}{\rho^{\cancel{2}}}$$

$\cancel{a}$ a

$$Q = \rho u_m \left(1 - \frac{\rho}{2\rho_m}\right)$$

$$= \rho u_m \left(1 - \frac{\rho}{\rho_j}\right)$$

$$\rho_j = \frac{1}{L}$$

$$\boxed{Q = \rho u_m (1 - \rho L)}$$

~~car length~~ $Q_m = \rho_m u_m \left(1 - \frac{\rho_m}{\rho_j}\right)$

u_m

$$u^* = \frac{Q}{\rho} = \frac{u_m}{2} \quad \cancel{=}$$

Therefore $\quad Q = \frac{L}{\tau}(\rho_j - \rho) \quad$ near $\rho = \rho_j$

and, at $\rho = \rho_j$, $\quad Q' = -\frac{L}{\tau}$

The value of L/τ is approximately 14 mph

All the features of weak wave theory apply. The evolution of a bump in traffic density is to steepen into a shock at the rear and to disperse into an expansion at the front

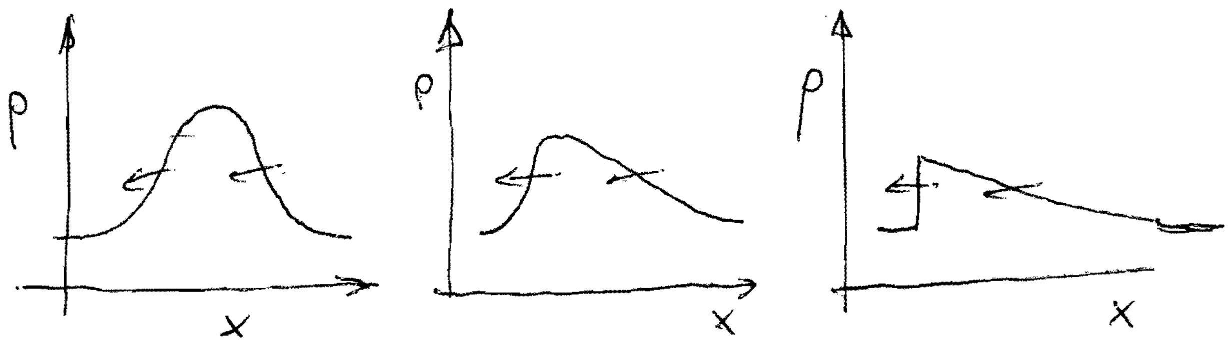

The amplitude of the shock now has a maximum $(\rho_j - \rho)$ but the behavior of

$$a - a_0 = -\sqrt{\frac{2B}{t}} \quad \text{etc.}$$

is as in weak wave theory.

<u>Waves in the vicinity of a traffic light</u>

When a traffic light turns red, a shock propagates backward into the oncoming traffic, stopping the cars. When it turns green again, an expansion wave propagates backward relative to the cars, accelerating them. At the location of the traffic light the flow is just sonic, so the expansion travels backward relative to the road On the left of the traffic light and forward on the right

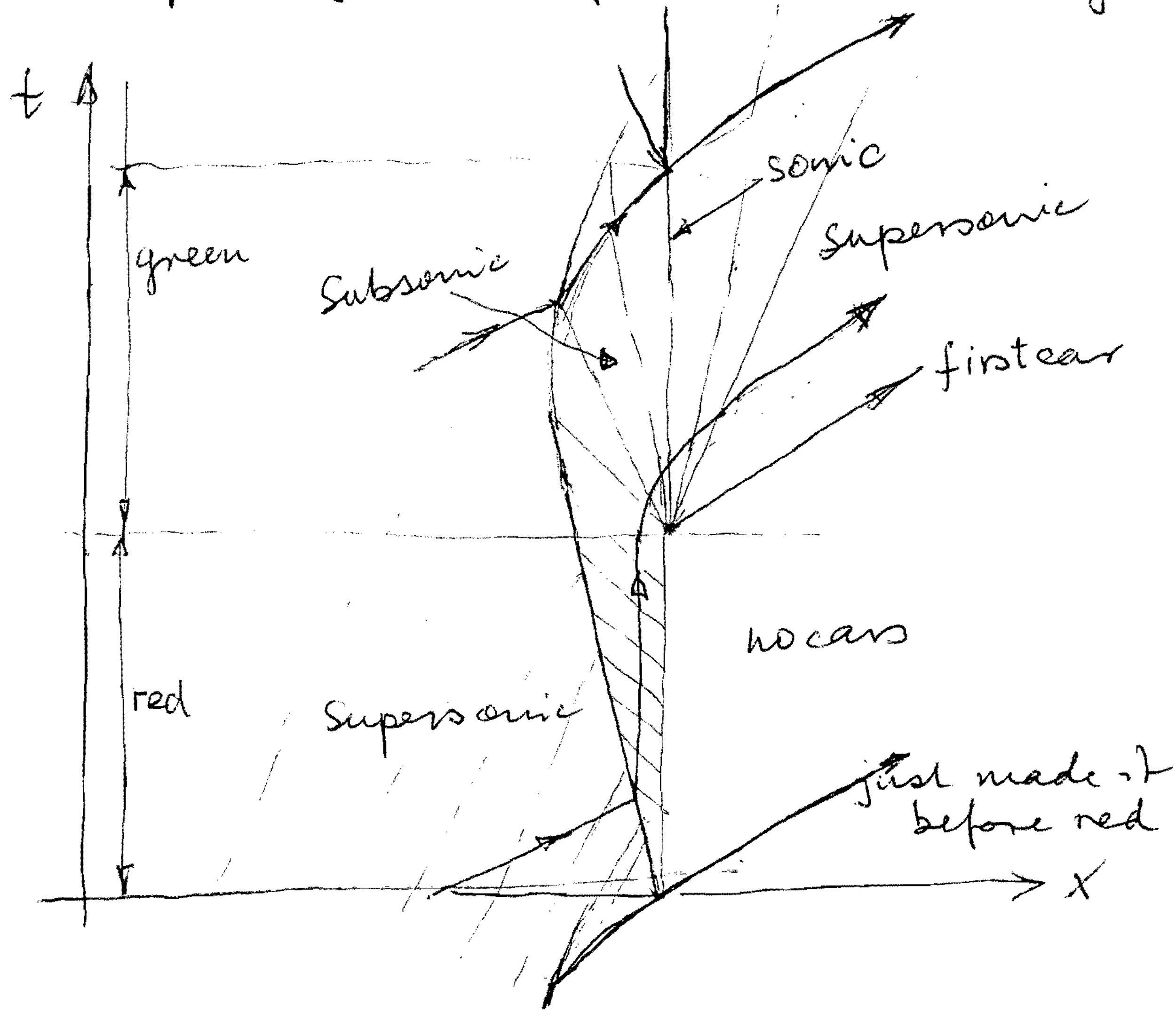

Light traffic

Each car has to stop only at most once at a given traffic light

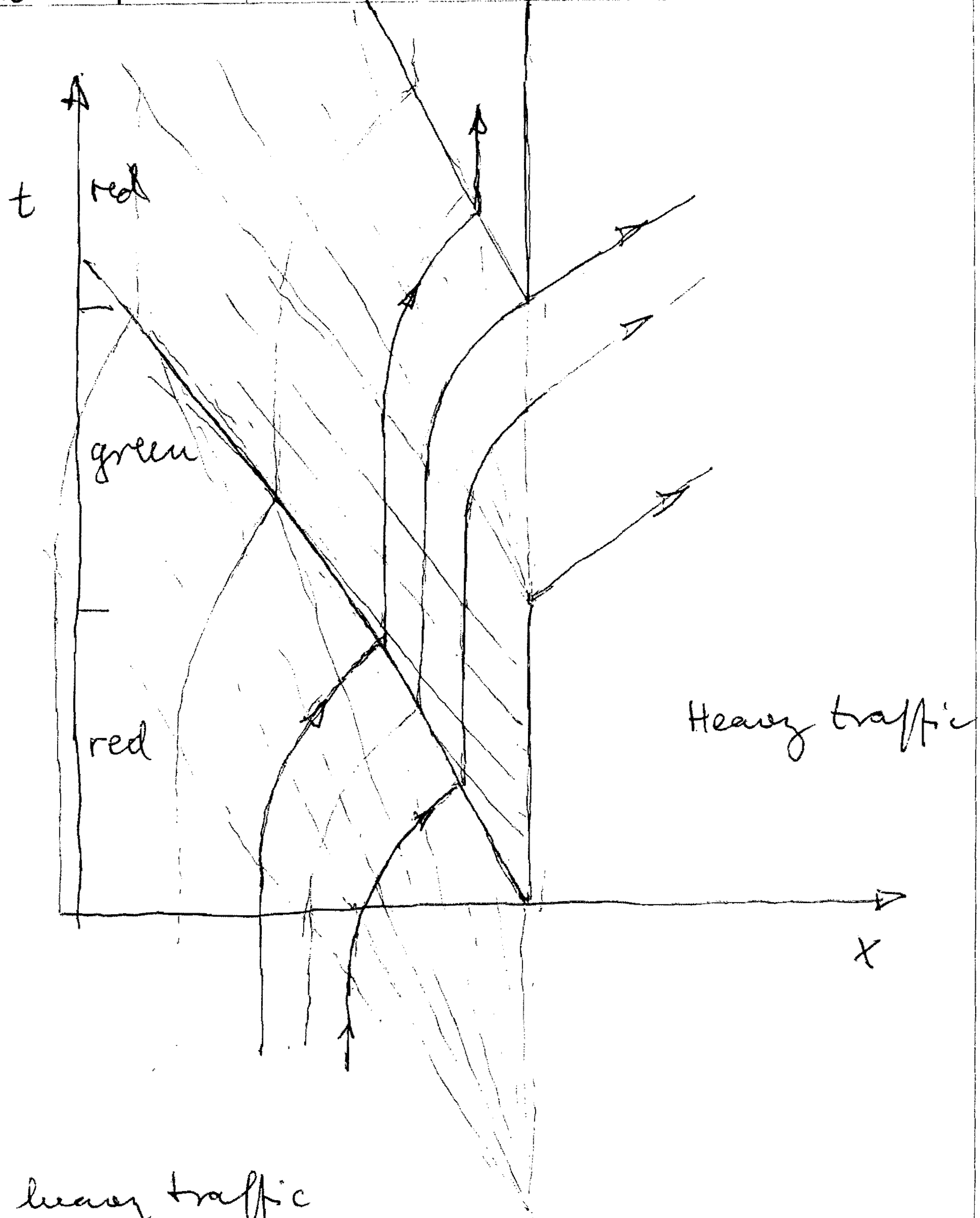

In heavy traffic
the traffic may just reach sonic speed
(or slightly supersonic) and each car
has to stop several times at the same
traffic light. The expansion wave from
the point at which the traffic light

turns green accelerates the shock relative to the ground, but weakens it relative to the cars, until it becomes a Mach wave.

Viscous dispersion, shock structure

In the case of weak shocks an analytical solution can be obtained for the structure within the shock wave. Diffusive effects such as viscosity smear out nonuniformities through contributions to the flux term that are proportional to $d\rho/dx$, so in the presence of such effects, we could write

$$q = Q(\rho) - \nu \frac{\partial \rho}{\partial x}$$

with a kinematic viscosity ν, in

$$\frac{\partial \rho}{\partial t} + \frac{\partial q}{\partial x} = 0 .$$

Thus,

$$\frac{\partial \rho}{\partial t} + a(\rho)\frac{\partial \rho}{\partial x} = \nu \frac{\partial^2 \rho}{\partial x^2} .$$

We seek a steady solution to this equation, i.e. one in which diffusion and steepening have reached a balance. We expect the

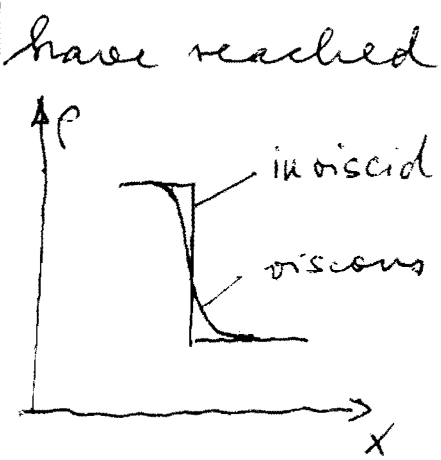

flow to be steady in the space coordinate of the shock, say

$$\xi = x - ct$$

Note

$$\rho \frac{d\rho}{d\xi} = C_2(\rho - \rho_1)(\rho - \rho_0)$$

constants must satisfy this since

$$\frac{d\rho}{d\xi} = 0 \quad \text{at } \rho = \rho_1 \quad \text{and at } \rho = \rho_0$$

So $K - K_1 = 0$

Now $\quad \dfrac{\partial \rho}{\partial t} = \dfrac{d\rho}{d\xi}\dfrac{\partial \xi}{\partial t} = -c\dfrac{d\rho}{d\xi}$

so

$$-c\frac{d\rho}{d\xi} + a\frac{d\rho}{d\xi} = \nu\frac{d^2\rho}{d\xi^2}$$

Integrate this once with $Q' = a$

$$-c\rho + Q + K = \nu\frac{d\rho}{d\xi}, \qquad \text{(A)}$$

where K is a constant of integration.

Now recall

$$c = \frac{\Delta Q}{\Delta \rho} = \frac{Q_1 - Q_0}{\rho_1 - \rho_0}$$

$$= c_1 + c_2(\rho_1 + \rho_0)$$

and use this to express

$$Q - c\rho = c_0 + c_1\rho + c_2\rho^2 - c_1\rho - c_2\rho(\rho_1 + \rho_0)$$

$$= c_0 + c_2(\rho^2 - \rho\rho_1 - \rho\rho_0)$$

$$= c_0 + c_2(\rho - \rho_1)(\rho - \rho_0) - c_2\rho_1\rho_0$$

$$= \underbrace{(c_0 - c_2\rho_1\rho_0)}_{\text{const.}} + c_2(\rho - \rho_1)(\rho - \rho_0)$$

$\therefore$ L.H.S. of (A) (with a new constant K_1)

$$Q - c\rho + K_1 = c_2(\rho - \rho_1)(\rho - \rho_0)$$

Introduce
$$r = \frac{\rho - \rho_0}{\rho_1 - \rho_0}$$
$$dr = \frac{d\rho}{\rho_1 - \rho_0}$$

$$\frac{c_2 d\xi}{\nu} = \frac{(\rho-\rho_1)\,d\rho}{(\rho-\rho_0)^2(\rho-\rho_1)}$$
$$= -\frac{(\rho_1-\rho_0)\,dr}{\frac{\rho-\rho_0}{\rho_1-\rho_0}\cdot\frac{\rho_1-\rho_0-(\rho-\rho_0)}{\rho_1-\rho_0}(\rho_1-\rho_0)^2}$$
$$= \frac{-1}{\rho_1-\rho_0}\cdot\frac{dr}{r(1-r)}$$

$$\boxed{\frac{c_2 \xi}{\nu} = -\frac{1}{\rho_1-\rho_0}\ln\frac{1-r}{r}}$$

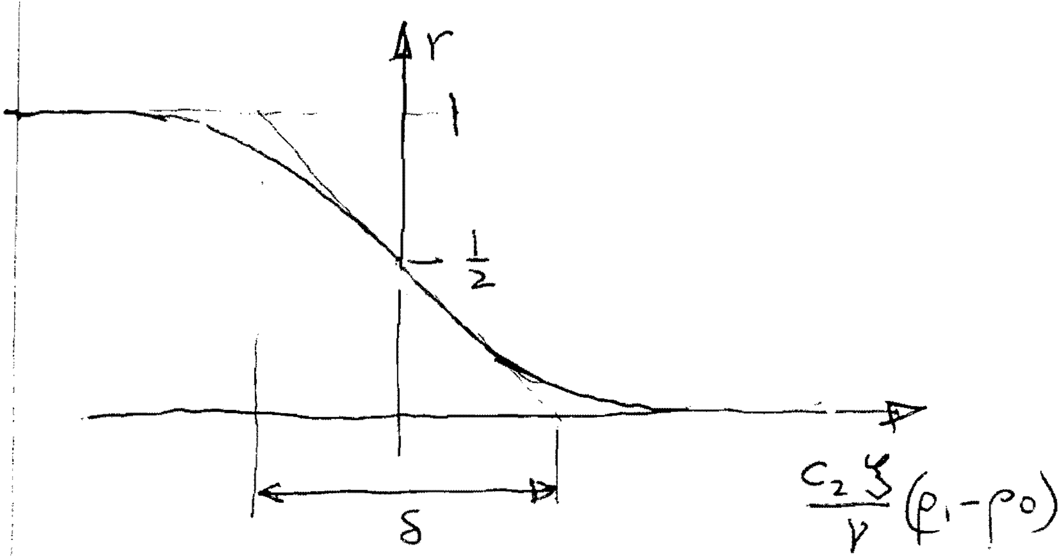

$\rho u = \text{const}$

$\rho \Delta u = -u \Delta \rho$

$\Delta u = -\frac{u}{\rho} \Delta \rho$

$\delta = \frac{32\gamma}{3(\gamma+1)} \frac{P_0}{\Delta p} \not{p}$

$Q = 0$

$c_1 \rho_j + C_2 \rho_j^2 = 0$

$C_2 = \frac{C_1}{\rho_j}$

perfect gas:

$u_{max} = \frac{2}{\gamma-1} a_0$

$\rho_{max} = \left(\frac{2}{\gamma+1}\right)^{2/\gamma-1} \rho_0$

$c_2 = -\frac{a_0 / \rho_0}{\gamma-1} \left(\frac{\gamma+1}{2}\right)^{\frac{2}{\gamma-1}}$

The shock thickness δ may be defined by the amplitude divided by the maximum slope

$$\frac{d\xi}{dr} = \frac{\nu}{c_2(\rho_1-\rho_0)}\,\frac{1}{r(1-r)} = \frac{\nu}{c_2(\rho_1-\rho_0)}\cdot\frac{1}{4} \quad \text{at } \xi=$$

The thickness is therefore

$$\boxed{\delta = \frac{\nu}{4c_2(\rho_1-\rho_0)}}$$

This is directly proportional to the viscosity and inversely proportional to the shock strength. Shocks become thick as strength decreases.

Note that the constant c_2 may be written in terms of u_{max} and ρ_m, the maximum speed and the density at maximum flux as
$$c_2 = -\frac{u_{max}}{2\rho_m}.$$

However, the approximation of a parabolic $Q(\rho)$ is not very good at $\rho = 0$, so this does not give good results. Also, in a fluid, the bulk viscosity has to be used. We therefore go into this in more detail.

Stress in viscous fluid

$$\underset{\approx}{S} = 2\mu \underset{\approx}{D} + \underbrace{\left(\mu_p - \tfrac{2}{3}\mu\right)}_{\text{bulk viscosity}} \nabla\cdot\underset{\sim}{u}\ \underset{\approx}{I}$$

~~μ_p results from~~

Shock structure in a perfect gas

For a shock propagating in the x-direction the viscous contribution to the normal stress is

$$\sigma_{xx} = \left(\tfrac{4}{3}\mu + \mu_p\right)\frac{du}{dx} = \hat{\mu}\frac{du}{dx}, \text{ say}$$

μ_p is the pressure viscosity.
Another diffusive effect is conduction of heat

$$q_x = -k\frac{dT}{dx}$$

where q is now heat flux, and k is the thermal diffusivity. In shock-fixed coordinates (u is speed relative to shock).

Continuity $$\frac{d\rho u}{dx} = 0$$

Momentum $$\rho u\frac{du}{dx} = -\frac{dp}{dx} + \frac{d}{dx}\left(\hat{\mu}\frac{du}{dx}\right)$$

rewrite $$\frac{d}{dx}\left(\rho u^2 + p - \hat{\mu}\frac{du}{dx}\right) = 0$$

Energy $$\rho u\frac{d}{dx}\left(\tfrac{u^2}{2} + h\right) = \frac{d}{dx}\left(\hat{\mu}u\frac{du}{dx} + k\frac{dT}{dx}\right)$$

Integrate each of these once:

$$\rho u = Q_0 = \rho_1 u_1 \qquad \text{— (C)}$$

$$\rho u^2 + p - \hat{\mu}\frac{du}{dx} = p_0 = \rho_1 u_1^2 + p_1 \qquad \text{— (M)}$$

$$\frac{u^2}{2} + h - \frac{\hat{\mu}}{\rho}\frac{du}{dx} - \frac{k}{\rho u}\frac{dT}{dx} = h_0 = h_1 + \frac{u_1^2}{2} \qquad \text{— (E)}$$

where the subscript 1 denotes the upstream state and the subscript o denotes integration constants. The continuity equation allows us to write $\rho = Q_0/u$, so that T and u may be used as independent state variables for thermodynamic equilibrium considerations in place of T and ρ. Rewrite M and E

$$\hat{\mu}\frac{du}{dx} = p - p_0 + Q_0 u \qquad \text{— (A)}$$

$$\frac{k}{Q_0}\frac{dT}{dx} = h - h_0 - \frac{u^2}{2} + \frac{p_0 - p}{Q_0}u \qquad \text{— (B)}$$

If we know $p = p(T,\rho)$, $h = h(T,\rho)$ from the thermal and caloric equations of state and $\hat{\mu}(T,\rho)$ and $k(T,\rho)$ from the constitutive equations of the medium, we can express the R.H.S.'s and the coefficients on the left in terms of T and u so that the problem may be solved at least numerically.

<u>Special case</u> (A) Assume

(1) Thermally perfect gas: $h = h(T)$, $dh = c_p(T)dT$

$$E \Rightarrow \quad \frac{u^2}{2} + h - h_0 = \frac{\hat{\mu}}{\rho u}\left(\frac{d}{dx}\left(\frac{u^2}{2}\right) + \frac{k}{c_p\hat{\mu}}\frac{dh}{dx}\right)$$

Put $\frac{\hat{\mu}c_p}{k} \equiv \widehat{Pr}$. If $\mu_p = 0$, $\widehat{Pr} = \frac{4}{3}\frac{\mu c_p}{k} = Pr\frac{4}{3}$

(2) Assume $\frac{c_p \hat{\mu}}{k} = \hat{P}_r = 1$ (i.e. $Pr = \frac{3}{4}$)

The last equation then becomes

$$\frac{u^2}{2} + h - h_0 = \frac{\hat{\mu}}{\rho u} \frac{d}{dx}\left(\frac{u^2}{2} + h - h_0\right)$$

For $x \to \pm\infty$ $u^2/2 + h - h_0 = 0$. The only solution of this equation is therefore

$$\frac{u^2}{2} + h = h_0$$

throughout the shock.

(3.) Assume calorically perfect gas; $c_p = $ const.

$$h = c_p T = \frac{c_p}{R} \frac{p}{\rho} = \frac{\gamma}{\gamma - 1} \frac{p}{\rho}$$

So $p = \frac{\gamma - 1}{\gamma} h\rho = \frac{\gamma - 1}{\gamma}\left(h_0 - \frac{u^2}{2}\right)\rho$

Substitute in (A) and rewrite

$$\frac{2\gamma}{\gamma+1} \frac{\hat{\mu}}{Q_0} \frac{du}{dx} = \frac{1}{u}\left[u^2 - \frac{2\gamma}{\gamma+1} \frac{p_0}{Q_0} u + \frac{2(\gamma-1)}{\gamma+1} h_0\right]$$

The quadratic in square brackets on the right has two roots $u = u_1$ and $u = u_2$. For each of these values of u, $du/dx = 0$, so that they are recognized as the upstream and downstream values of u. We can therefore write

$$\frac{2\gamma}{\gamma+1} \frac{\hat{\mu}}{Q_0} \frac{du}{dx} = \frac{(u - u_1)(u - u_2)}{u}$$

④ Assume $\hat{\mu} \propto T^{\omega}$

Since total enthalpy is constant through the shock $T = \dfrac{h_0 - \frac{u^2}{2}}{c_p}$.

Putting $l_1 = \dfrac{2\gamma}{\gamma+1} \dfrac{\hat{\mu}_0}{Q_0}$, the equation at the bottom of p. 91 becomes

$$l_1 \frac{du}{dx} = \left(\frac{h_0}{h_0 - \frac{u^2}{2}} \right)^{\omega} \frac{(u-u_1)(u-u_2)}{u}$$

The simplest case is $\omega = 0$, i.e. viscosity independent of temperature.

$$l_1 \frac{du}{dx} = \frac{(u-u_1)(u-u_2)}{u}$$

$$\boxed{\frac{x}{l_1} = \frac{u_1 \ln\left(1 - \frac{u}{u_1}\right) - u_2 \ln\left(\frac{u}{u_2} - 1\right)}{u_1 - u_2}}$$

The equation can also be integrated in closed form when $\omega = 1$.

<u>Special case ⓑ</u> Perfect gas, $k = 0$, i.e. $\hat{P}_r = \infty$

leads to $\dfrac{\hat{\mu}}{Q_0} \dfrac{2}{\gamma+1} \dfrac{du}{dx} = \dfrac{(u-u_1)(u-u_2)}{u}$

or $l_2 \dfrac{du}{dx} = \dfrac{(u-u_1)(u-u_2)}{u}$

$l_2 = l_1/\gamma$ so profile is steeper by the factor γ

$$Q_0 = \rho_1 u_1$$

$$2\rho_2 u_2^2 > p_0 = p_1 + \rho_1 u_1^2$$

$$\rho_2 u_2^2 - \rho_1 u_1^2 > p_1 - \rho_2 u_2^2$$

$$u_2 - u_1 > \frac{p_1 - \rho_2 u_2^2}{Q_0} > \frac{p_1}{Q_0} - u_2$$

$$2u_2 > \frac{p_1 + \rho_1 u_1^2}{Q_0} > \frac{p_1}{Q_0} + u_1$$

$$\cancel{u_2 - (u_1 - u_2) >}$$

$$2u_2 - u_1 > \frac{p_1}{Q_0}$$

put $u_1 = u_2 + \Delta u$ $\qquad\qquad$ $\Delta u = u_1 - u_2$

$$u_2 - \Delta u > \frac{p_1}{Q_0}$$

$$\Delta u < u_2 - \frac{p_1}{Q_0}$$

Special case (C) $\hat{\mu} = 0$, $k \neq 0$, i.e. $\hat{Pr} = 0$

This leads to

$$\underbrace{\frac{2(\gamma-1)}{\gamma+1}\frac{k}{RQ_0}}_{\ell_3}\frac{du}{dx} = \frac{(u-u_1)(u-u_2)}{2u - \frac{p_0}{Q_0}}$$

$$\boxed{\frac{x}{\ell_3} = \frac{\left(2u_1 - \frac{p_0}{Q_0}\right)\ln\left(1-\frac{u}{u_1}\right) - \left(2u_2 - \frac{p_0}{Q_0}\right)\ln\left(\frac{u}{u_2}-1\right)}{u_1 - u_2}}$$

This gives a smooth structure only when $2u_2 > p_0/Q_0$, i.e. when the shock is sufficiently weak (Note $2u_1 > p_0/Q_0$ is always true). If $2u_2 < p_0/Q_0$, we get the behavior shown in the sketch.

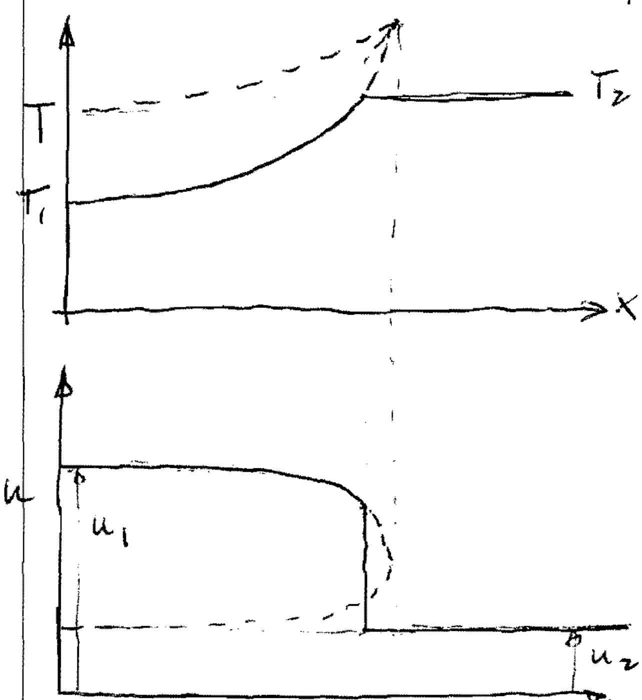

The equation gives the smooth double valued u curve — ··· and the corresponding T curve. A discontinuous shock occurs at the point where the curve coming from T_1 intersect T_2.

Special case: Weak shock

$$\Delta u = u_1 - u_2 \ll \sqrt{u_1 u_2} \equiv a^*,$$ speed of sound at $x=0$

$$\frac{\Delta u}{\alpha} = -\frac{2}{\gamma+1}\left(M_1^2-1\right)$$

$M_1 = 0.1$ say

$\frac{2}{\gamma+1} \times 0.1$

$= 0.14$

$7 \times 3 = 21$

if $M_1 = 0.01$

$\rightarrow 210$ ...

In this case we get

$$\boxed{\frac{x\,\Delta u}{a^{*}\,l_1} = \ln\left(\frac{u_1 - u}{u - u_1}\right)}$$

which corresponds to the result on p. 87

With $\mu_p = 0$, $\hat{P}r = 1$, $\hat{\mu} = \frac{4}{3}\mu$ and the shock thickness becomes

$$\boxed{l = \frac{32}{3(\gamma+1)}\,\frac{\mu_*}{\rho_*\,\Delta u}}$$

Where the starred quantities are evaluated at the point where $u = a^*$.

This may be expressed in terms of the mean free path λ $\left[\lambda \doteq \frac{\mu}{\rho a}\right]$ speed of sound

$$\boxed{l \doteq 3\,\frac{a^*}{\Delta u}\,\lambda}$$

<u>Note</u>: In a shock wave, the entropy actually has a maximum value.

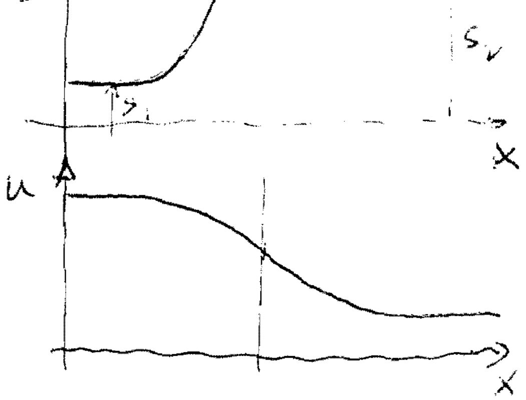

For details about this, further reading in Landau + Lifshitz.

Ae/APh 237 Assignment No. 4, January 30, due February 6, 2003

PROBLEM 1.

In the relation

$$Q = c_0 + c_1\rho + c_2\rho^2$$

find the condition that determines whether expansions or compressions steepen. Obtain the coefficients c_0, c_1, c_2 for the traffic flow problem in terms of the speed limit, V_m, the average vehicle length, L, and the reaction time of the driver–vehicle system, τ. Hence show that, for this flow, compression waves steepen. Obtain expressions for the density and vehicle speed at the maximum flux density. What can be done to increase the maximum value of Q? Which of these measures would drivers like best? Explain.

PROBLEM 2.

The unimpeded flux density, Q_u in traffic flow may be larger than the corresponding time–averaged flux density, Q_a for cases in which shock waves occur. Consider the case of traffic flow with a traffic light of period T_l, equally divided between green and red. Use the relations derived in Problem 1 to find the maximum value of Q_a for which the traffic light just does not reduce the flux density. Also find the maximum delay imposed on an individual vehicle by the traffic light at that condition. Make suitable approximations as you need them.

PROBLEM 3.

Make and discuss a gas-dynamical analogy of the traffic–light problem.

PROBLEM 4.

The density distribution of a one–dimensional, right–travelling wave is given at a particular time by a triangular excursion from a constant value ρ_0. Take the amplitude and length of the excursion to be ρ_a and λ. Determine the evolution of the density as a function of time and space.

Simple waves in one-dimensional flow

Inviscid, isentropic.

Euler equations

$$\frac{\partial \rho}{\partial t} + \frac{\partial \rho u}{\partial x} = 0 \qquad C$$

$$\frac{\partial \rho u}{\partial t} + \frac{\partial \rho u^2}{\partial x} = -\frac{\partial p}{\partial x} \qquad M$$

$$\frac{\partial s}{\partial t} + u\frac{\partial s}{\partial x} = \frac{Ds}{Dt} = 0 \qquad E$$

We distinguish between the concepts of isentropic flow ($ds=0$ along particle path) homentropic ($ds=0$ along any path, $s=s_0$)

$$dp = \left(\frac{\partial p}{\partial s}\right)_\rho ds + \left(\frac{\partial p}{\partial \rho}\right)_s d\rho .$$ Along particle path, $ds=0$ $\therefore$

$$\frac{Dp}{D\rho} = \left(\frac{\partial p}{\partial \rho}\right)_s = a^2$$

Rewrite C:

$$\frac{\partial \rho}{\partial t} + u\frac{\partial \rho}{\partial x} + \rho\frac{\partial u}{\partial x} = 0$$

or

$$\frac{D\rho}{Dt} + \rho\frac{\partial u}{\partial x} = 0$$

or

$$\frac{D\rho}{Dp}\frac{Dp}{Dt} + \rho\frac{\partial u}{\partial x} = 0$$

i.e.

$$\frac{1}{a^2}\frac{\partial p}{\partial t} + \frac{u}{a^2}\frac{\partial p}{\partial x} + \rho\frac{\partial u}{\partial x} = 0$$

$$\frac{\partial p}{\partial t} + u\frac{\partial p}{\partial x} + \rho a^2\frac{\partial u}{\partial x} = 0 \qquad \text{— (1)}$$

Rewrite M

$$\rho\frac{\partial u}{\partial t} + \rho u\frac{\partial u}{\partial x} + \frac{\partial p}{\partial x} = 0 \quad \text{——} (2)$$

Write $a \times (2) + (1)$:

$$\boxed{\frac{\partial p}{\partial t} + (u+a)\frac{\partial p}{\partial x} + \rho a\left[\frac{\partial u}{\partial t} + (u+a)\frac{\partial u}{\partial x}\right] = 0} \quad \text{——} (3)$$

and $(1) - a \times (2)$

$$\boxed{\frac{\partial p}{\partial t} + (u-a)\frac{\partial p}{\partial x} - \rho a\left[\frac{\partial u}{\partial t} + (u-a)\frac{\partial u}{\partial x}\right] = 0} \quad \text{——} (4)$$

If we choose a path such that $\frac{dx}{dt} = u+a$ and define the length element along that path to be $d\eta$, then

$$\frac{\partial p}{\partial t} + (u+a)\frac{\partial p}{\partial x} = \frac{dp}{d\eta} \quad \text{etc.}$$

Therefore the above equation (3) becomes

$$\boxed{\begin{array}{ll} dp + \rho a\, du = 0 & \text{along } \frac{dx}{dt} = u+a \\ dp - \rho a\, du = 0 & \text{along } \frac{dx}{dt} = u-a \end{array}}$$

and (4) →

These are thus three special paths in xt-space along which the partial d.e. becomes an ordinary d.e.

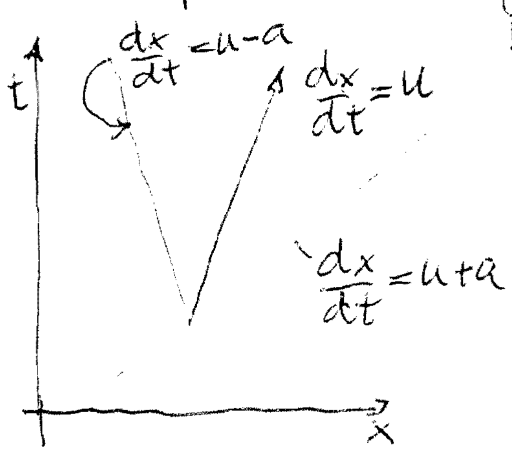

Integrate these equations:

$$\boxed{\int \frac{dp}{\rho a} \pm u = \begin{matrix} P \\ Q \end{matrix} \quad \text{along } \frac{dx}{dt} = u \pm a}$$

where P and Q are constants

Special case homentropic flow, $s = s_0$

In this case eliminate p:

$$\frac{dp}{\rho a} = \left(\frac{\partial p}{\partial a}\right)_s \frac{da}{\rho a} = \left(\frac{\partial p}{\partial \rho}\right)_s \left(\frac{\partial \rho}{\partial a}\right)_s \frac{da}{\rho a}$$

$$= \frac{a\,da}{\rho\left(\frac{\partial a}{\partial \rho}\right)_s} = \frac{da}{\frac{1}{a}\left(\frac{\partial \rho a}{\partial \rho}\right)_s - 1}$$

$$\frac{dp}{\rho a} = \frac{da}{\Gamma - 1}$$

Hence,

$$\boxed{\int \frac{da}{\Gamma(a) - 1} \pm u = \begin{matrix} P \\ Q \end{matrix} \quad \text{along } \frac{dx}{dt} = u \pm a}$$

Homentropic flow

A simple wave is one that is bordered on one side in xt-space by uniform flow.

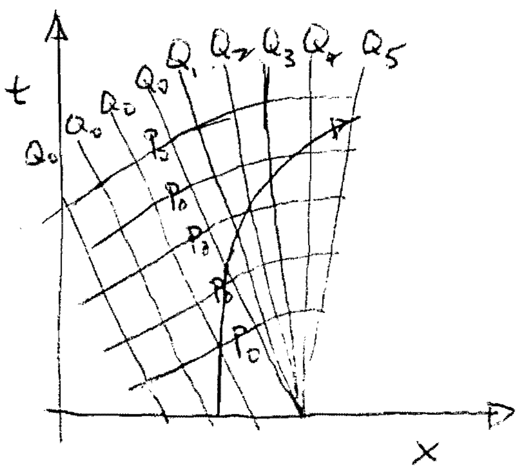

Eg. on the left:

$$\int \frac{da}{\Gamma - 1} + u = P_0 \,, \quad \text{uniform}$$

In the centered simple wave,

$$\int \frac{da}{\Gamma - 1} - u = Q \quad \text{along } \frac{dx}{dt} = u - a$$

add these,

$$\int \frac{da}{\Gamma - 1} = \frac{P_0 + Q}{2} = \text{const. on } \frac{dx}{dt} = u - a$$

subtract

$$u = \frac{P_0 - Q}{2} = \text{const. along } \frac{dx}{dt} = u - a$$

It follows that u and a are separately constant along $\frac{dx}{dt} = u - a$

Therefore, the Q characteristics are straight.

If the simple wave is bordered by a uniform region on the right, the P characteristics are straight in the simple wave.

Now investigate the behavior of simple waves in relation to the signs of Γ and $\Gamma-1$

Consider a <u>left-facing simple wave</u>, so that

$$\frac{da}{\Gamma-1} + du = 0 \qquad \text{everywhere.}$$

$$\boxed{du = -\frac{da}{\Gamma-1}}$$

The slope of the Q characteristics in the simple wave (the straight ones) is

$$\frac{dx}{dt} = u - a$$

$$d\left(\frac{dx}{dt}\right) = du - da = -\frac{da}{\Gamma-1} - da = -\frac{da\,\Gamma}{\Gamma-1}$$

Think of these differentials as changes along ~~the particle path~~ P characteristics. First, note the behavior of $\frac{\Gamma}{\Gamma-1}$. It is negative for $0 < \Gamma < 1$ and positive everywhere else.

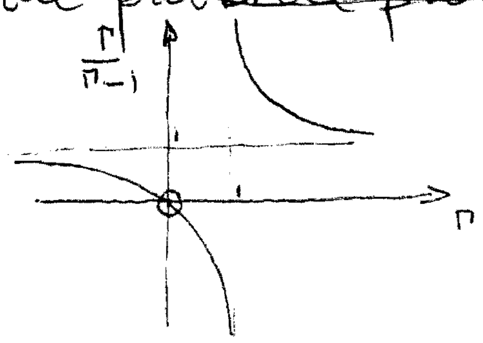

Case distinctions for Left facing wave

$$\boxed{du = -\frac{da}{\Gamma-1}\ ;\ d\left(\frac{dx}{dt}\right) = -\frac{\Gamma}{\Gamma-1}\,da}$$

$\boxed{\text{Note: } \frac{\rho}{a}\frac{d\rho}{da} = \Gamma-1}$

$\boxed{\Gamma > 1 \quad \frac{d\rho}{da} > 0}$

a) If $da < 0$, then $\boxed{d\rho < 0 \quad dp < 0}$

$\therefore du > 0$

and $d\left(\frac{dx}{dt}\right) > 0$

particle accelerates

characteristics diverge

<u>Expansion fan</u>

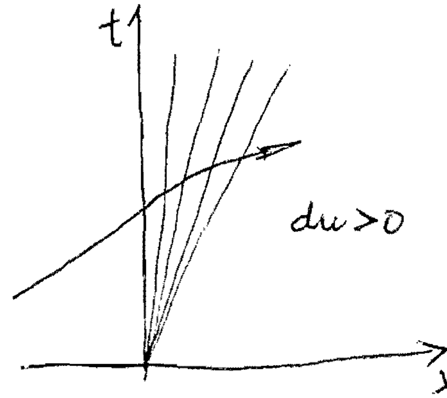

b) $da > 0 \Rightarrow \boxed{d\rho > 0 \quad dp > 0}$ $\therefore du < 0$, $d\left(\frac{dx}{dt}\right) < 0$

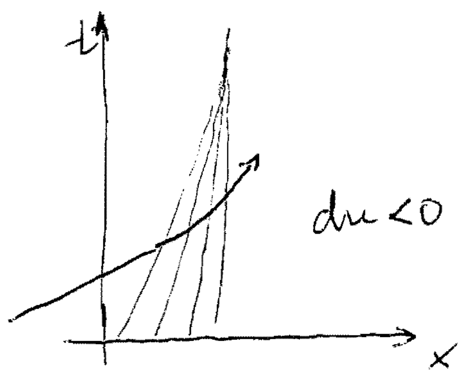

<u>Compression shock</u>

$\boxed{0 < \Gamma < 1 \quad \frac{da}{d\rho} < 0}$

a) $da < 0 \Rightarrow \boxed{d\rho > 0 \quad dp > 0}$ $\therefore du < 0$, $d\left(\frac{dx}{dt}\right) < 0$

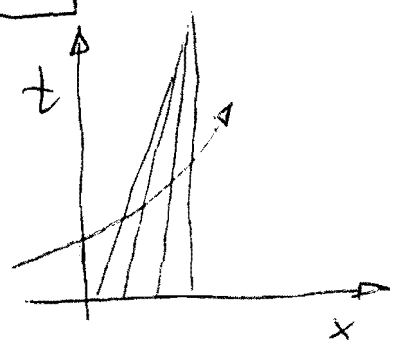

particle decelerates

characteristics converge

<u>Compression shock</u>

b) $da > 0 \Rightarrow \boxed{\begin{matrix} d\rho < 0 \\ dp < 0 \end{matrix}}$ $du > 0$, $d\left(\frac{dx}{dt}\right) > 0$

particle accelerates
characteristics diverge
<u>Expansion fan</u>

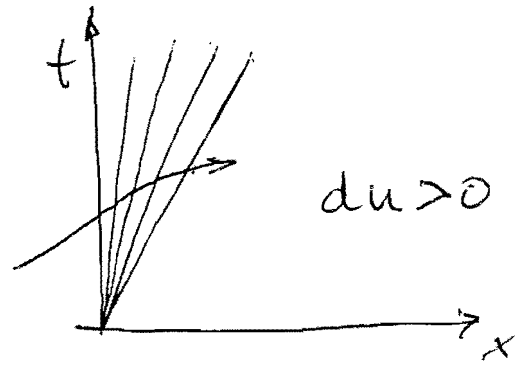

$du > 0$

$\boxed{\begin{matrix} \Gamma < 0 \\ \frac{da}{d\rho} < 0 \end{matrix}}$ $\left(\frac{\Gamma}{\Gamma - 1} > 0\right)$

a) $da < 0 \Rightarrow \boxed{\begin{matrix} d\rho > 0 \\ dp > 0 \end{matrix}}$ $du < 0$, $d\left(\frac{dx}{dt}\right) > 0$

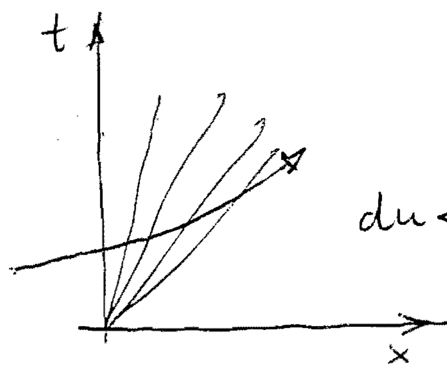

$du < 0$

particles decelerate,
characteristics diverge
<u>compression fan</u>

b) $da > 0 \Rightarrow \boxed{\begin{matrix} d\rho < 0 \\ dp < 0 \end{matrix}}$ $du > 0$, $d\left(\frac{dx}{dt}\right) < 0$

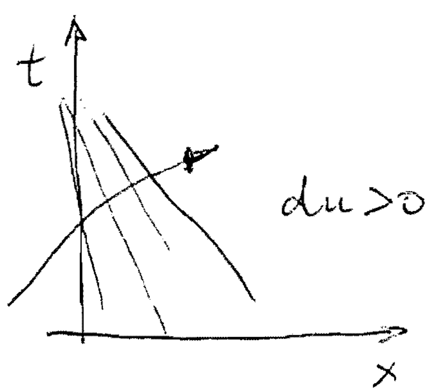

$du > 0$

particles accelerate
characteristics converge
<u>expansion shock</u>

Again observe that along $x=0$ the flow is sonic for all t, since

$$M = \frac{2}{\gamma-1}\left(\frac{a_0}{a}-1\right)$$

$$= \frac{2}{\gamma-1}\left[\frac{\gamma+1}{2}\frac{1}{1-\frac{\gamma-1}{2}\frac{x}{a_0 t}}-1\right]$$

$$= 1 \text{ when } x=0.$$

Now recall the steady expansion of a gas from a reservoir at rest and compare with the unsteady expansion above.

Steady: $\dfrac{T_t}{T} = 1+\dfrac{\gamma-1}{2}M^2$

Where T_t is the temperature in the reservoir.

Unsteady $\dfrac{T_0}{T} = \left(1+\dfrac{\gamma-1}{2}M\right)^2$

Now ask for the ratio of the rest temperatures required for the same T and M to result in steady and unsteady flow. Get

$$\frac{T_t}{T_0} = \frac{1+\frac{\gamma-1}{2}M^2}{\left(1+\frac{\gamma-1}{2}M\right)^2}$$

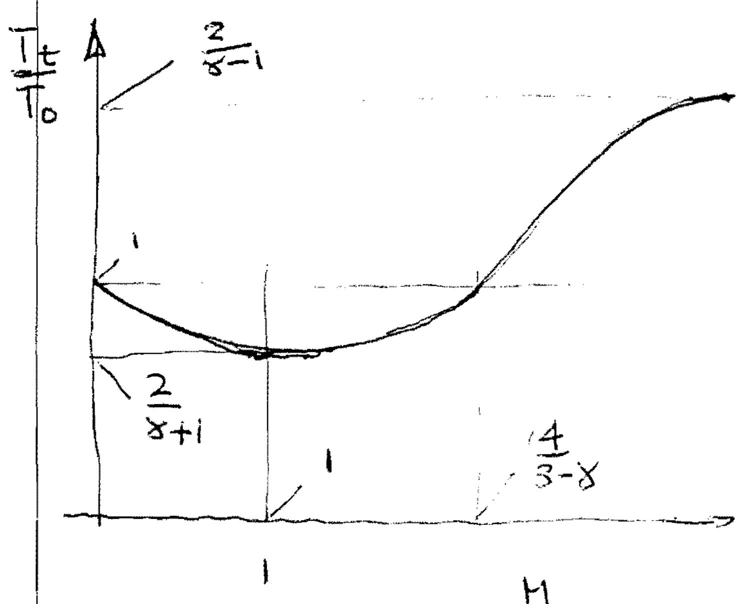

Thus, it seems that

an unsteady expansion can produce high Mach numbers from a colder rest temperature than a steady one.

This may be explained in terms of the energy equation:

$$\frac{Ds}{Dt} = 0 \quad \text{or} \quad \frac{Dh}{Dt} - \frac{1}{\rho}\frac{Dp}{Dt} = 0$$

$h = h_t - \frac{u^2}{2}$

$$\frac{Dh_t}{Dt} - \frac{1}{2}\frac{Du^2}{Dt} - \frac{1}{\rho}\frac{\partial p}{\partial t} - \frac{u}{\rho}\frac{\partial p}{\partial x} = 0$$

$$\frac{Dh_t}{Dt} - \frac{1}{\rho}\frac{\partial p}{\partial t} = u\frac{Du}{Dt} + \frac{u}{\rho}\frac{\partial p}{\partial x} = 0 \text{ from M}$$

$$\therefore \quad \frac{Dh_t}{Dt} = \frac{1}{\rho}\frac{\partial p}{\partial t}$$

The r.h.s. is zero in steady flow, but not in unsteady flow.

Maximum velocities are therefore also different

non steady $\quad u_{max} = \frac{2}{\gamma-1} a_0$

steady $\quad u_{max} = \sqrt{\frac{2}{\gamma-1}}\, a_t$

Total Temperature Variation in Nonsteady Isentropic Flow
Ae237

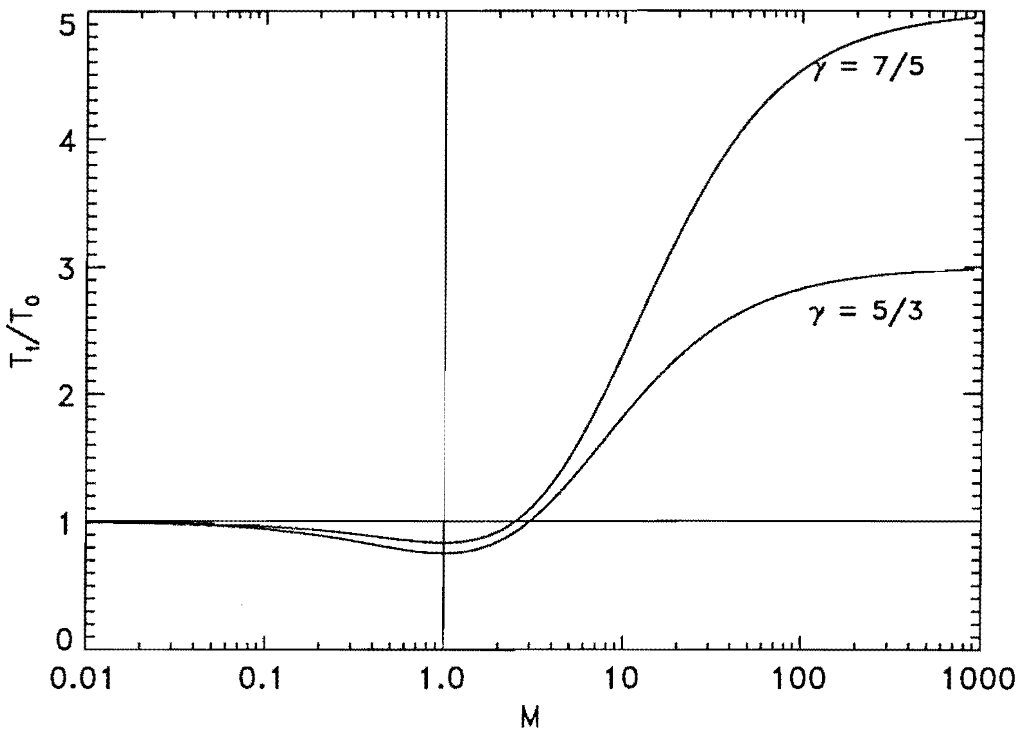

Rest temperature required to expand from rest to M with a steady expansion (T_t) and with unsteady expansion (T_0)

6 February 1993

Wave interactions in one-d. steady and non steady flow.

To illustrate, consider the shock tube problem. A tube is filled to the left of a diaphragm with high-pressure gas, p_4, and with low pressure, p_1, on the right. At $t=0$ the diaphragm bursts so that an expansion wave propagates to the left into the high-pressure gas and a shock propagates to the right into the low-pressure gas.

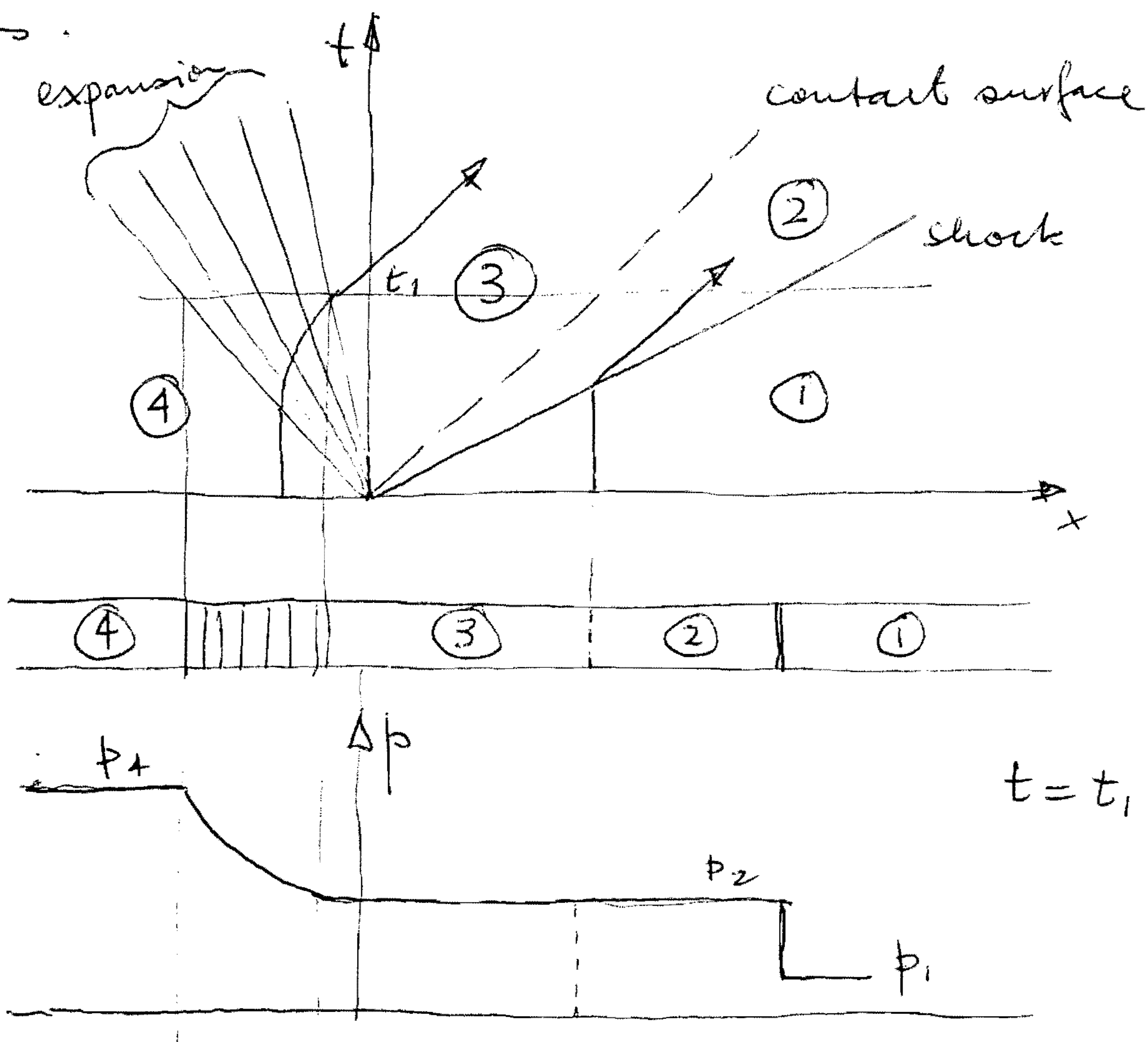

The shock changes u from zero to u_2. The expansion changes u from zero to u_3.

Since $u_2 = u_3$ and also $p_2 = p_3$ (interface is not accelerated) a convenient way to solve the problem of what shock speed will result is to consider the up-plane. The conditions achievable from state ① via a shock wave lie on a unique curve (derivable from Hugoniot) in up-space. Similarly, the conditions achievable from state ④ via an expansion wave lie on a unique curve. The solution for states ②,③ with equal p and equal u is therefore at the intersection of the two curves.

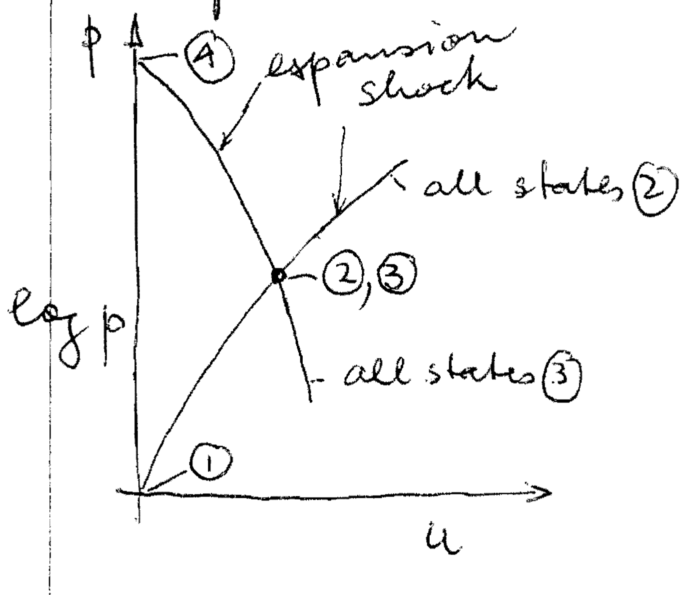

The up-diagram is a powerful tool for solution of many gas-dynamical problems.

Velocity pressure curves

Comparison of steady and non-steady waves

Non-steady simple wave adjacent to p_0, a_0

Expansion $\quad \dfrac{a}{a_0} = 1 - \dfrac{\gamma-1}{2}\dfrac{\Delta u}{a_0}$

$$\boxed{\frac{p}{p_0} = \left(1 - \frac{\gamma-1}{2}\frac{\Delta u}{a_0}\right)^{\frac{2\gamma}{\gamma-1}}}$$

Steady Expansion

$$a^2 + \frac{\gamma-1}{2} u^2 = a_0^2 + \frac{\gamma-1}{2} u_0^2$$

$$\frac{a^2}{a_0^2} = 1 - \frac{\gamma-1}{2} \frac{u^2 - u_0^2}{a_0^2}$$

But $u^2 - u_0^2 = (\Delta u)^2 + 2 u_0 \Delta u$

$$\therefore \quad \frac{a^2}{a_0^2} = 1 - \frac{\gamma-1}{2}\left[\left(\frac{\Delta u}{a_0}\right)^2 + 2\frac{\Delta u}{a_0} M_0\right]$$

$\left(M_0 = \frac{u_0}{a_0}\right)$

$$\boxed{\frac{p}{p_0} = \left\{1 - \frac{\gamma-1}{2}\left[\left(\frac{\Delta u}{a_0}\right)^2 + 2\frac{\Delta u}{a_0} M_0\right]\right\}^{\frac{\gamma}{\gamma-1}}}$$

Note: in nonsteady flow, a is linear in u so that $p = p\left(\frac{\Delta u}{a_0}\right)$

In steady flow, a is quadratic in u. This has the consequence that M_0 is a parameter and $p = p\left(\frac{\Delta u}{a_0}, M_0\right)$

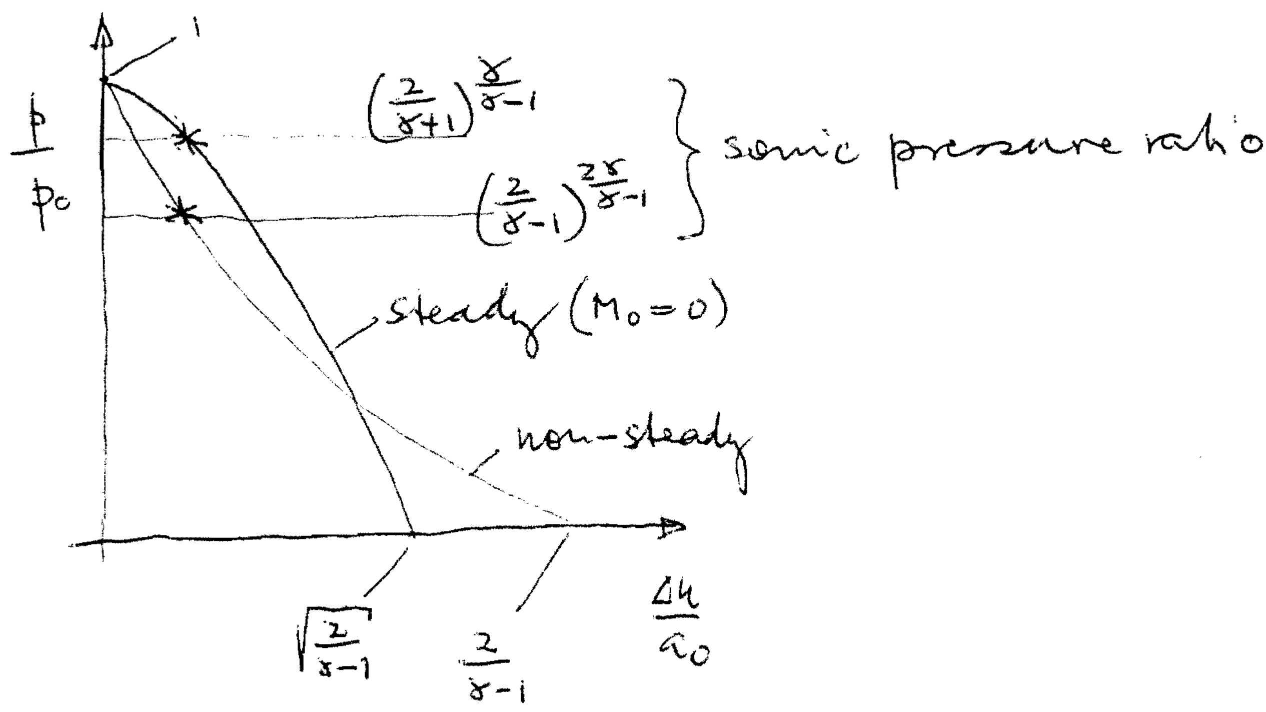

<u>Shock wave</u>

$$p - p_0 = \rho_0 c \Delta u$$

where c is the shock speed relative to the upstream gas. $M_s \equiv \frac{c}{a_0}$.

$$\frac{p}{p_0} = 1 + \frac{\rho_0 a_0^2}{p_0} M_s \frac{\Delta u}{a_0}$$

γ

But $\frac{p}{p_0} = 1 + \frac{2\gamma}{\gamma+1}(M_s^2 - 1)$ (shock jump)

Solve for $M_s = \sqrt{\left(\frac{p}{p_0} - 1\right)\frac{\gamma+1}{\gamma} + 1}$

and substitute this above to get

$$\boxed{\frac{\Delta u}{a_0} = \frac{\frac{1}{\gamma}\frac{\Delta p}{p_0}}{\sqrt{1 + \frac{\gamma+1}{2}\frac{\Delta p}{p_0}}}}$$

or

$$\boxed{\frac{p}{p_0} = 1 + \gamma\frac{\Delta u}{a_0}\left[\frac{\gamma+1}{4}\frac{\Delta u}{a_0} + \sqrt{1 + \frac{\gamma+1}{4}\left(\frac{\Delta u}{a_0}\right)^2}\right]}$$

It is interesting to compare the shock curve slope with ρa and $\rho_0 a_0$.

$$\frac{dp}{du} = \rho_0 a_0 \frac{\left(1 + \frac{\gamma+1}{2\gamma}\frac{\Delta p}{p_0}\right)^{3/2}}{1 + \frac{\gamma+1}{4\gamma}\frac{\Delta p}{p_0}} > \rho_0 a_0$$

It is possible to show that this is also

$$= \rho a \frac{1 + \frac{\gamma+1}{2\gamma}\frac{\Delta p}{p_0}}{1 + \frac{\gamma+1}{4\gamma}\frac{\Delta p}{p_0}} \sqrt{\frac{1 + \frac{\gamma-1}{2\gamma}\frac{\Delta p}{p_0}}{1 + \frac{\Delta p}{p_0}}}$$

For weak shocks, expand for $\frac{\Delta p}{p_0} \ll 1$ to get $\frac{dp}{du} < \rho a$.

For strong shocks neglect the 1's:

$$\frac{dp}{du} = \rho_0 a_0 \sqrt{\frac{2(\gamma+1)}{\gamma}\frac{\Delta p}{p_0}} > a_0 \rho_0$$

and $\frac{dp}{du} = \rho a \sqrt{\frac{2(\gamma-1)}{\gamma}} < \rho a$ if $1<\gamma<2$

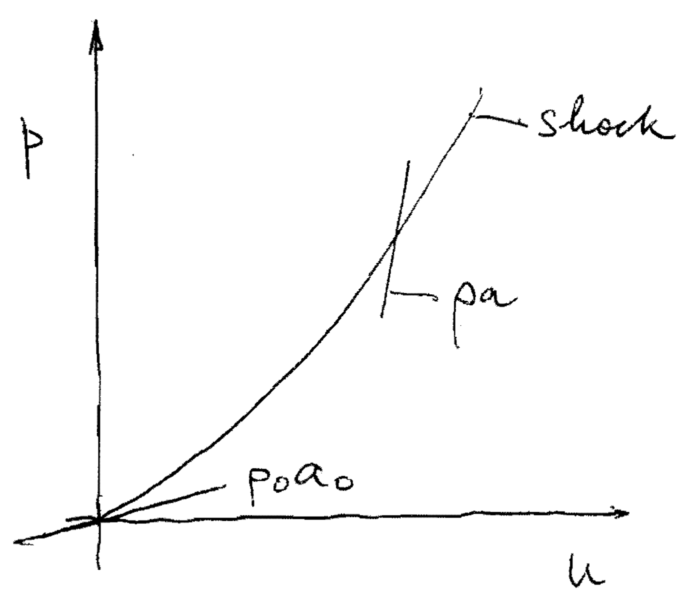

PRESSURE-VELOCITY DIAGRAM

Summary of Equations

Laboratory Coordinate System

Shock

$$\frac{p}{p_0} = 1 + \gamma \frac{\Delta u}{a_0} \left[\frac{\gamma+1}{4} \frac{\Delta u}{a_0} + \sqrt{1 + \frac{\gamma+1}{4} \left(\frac{\Delta u}{a_0} \right)^2} \right] \tag{1}$$

Non-steady Isentropic Flow

$$\frac{p}{p_0} = \left(1 - \frac{\gamma-1}{2} \frac{\Delta u}{a_0} \right)^{\frac{2\gamma}{\gamma-1}} \tag{2}$$

$$= \left(\frac{1 + \frac{\gamma-1}{2} M_0}{1 + \frac{\gamma-1}{2} M} \right)^{\frac{2\gamma}{\gamma-1}} \tag{3}$$

Steady Isentropic Flow

$$\frac{p}{p_0} = \left\{ 1 - \frac{\gamma-1}{2} \left[\left(\frac{u}{a_0} \right)^2 - {M_0}^2 \right] \right\}^{\frac{\gamma}{\gamma-1}} \tag{4}$$

$$= \left[1 - \frac{\gamma-1}{2} \frac{\Delta u}{a_0} \left(2M_0 + \frac{\Delta u}{a_0} \right) \right]^{\frac{\gamma}{\gamma-1}} \tag{5}$$

$$= \left(\frac{1 + \frac{\gamma-1}{2} M_0^2}{1 + \frac{\gamma-1}{2} M^2} \right)^{\frac{\gamma}{\gamma-1}} \tag{6}$$

$$\frac{p}{p_t} = \left[1 - \frac{\gamma-1}{2} \left(\frac{u}{a_0} \frac{a_0}{a_t} \right)^2 \right]^{\frac{\gamma}{\gamma-1}} \tag{7}$$

Pressure - Velocity Diagram
Ae237

$p/p_0 > 1$ - Shock Discontinuities
$p/p_0 < 1$ - Continuous Expansion Waves

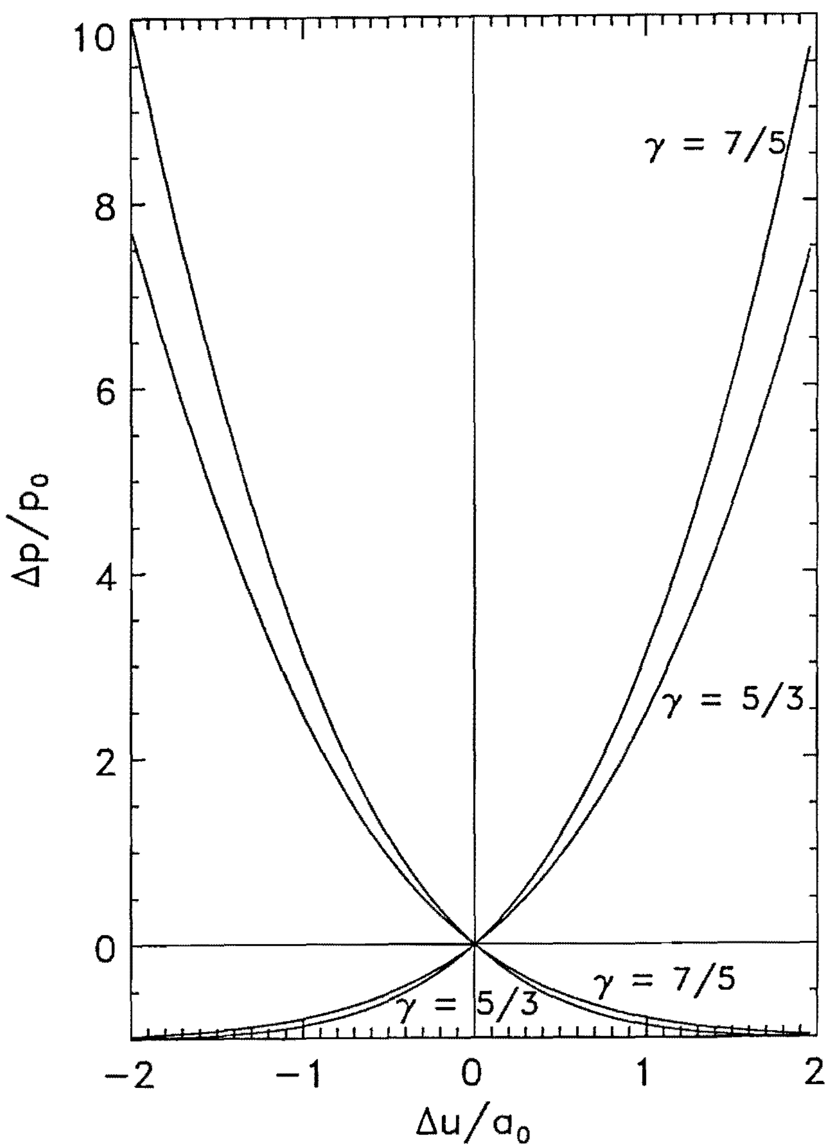

6 February 1993

Pressure - Velocity Diagram
Ae237

Note nonuniform vertical scale.

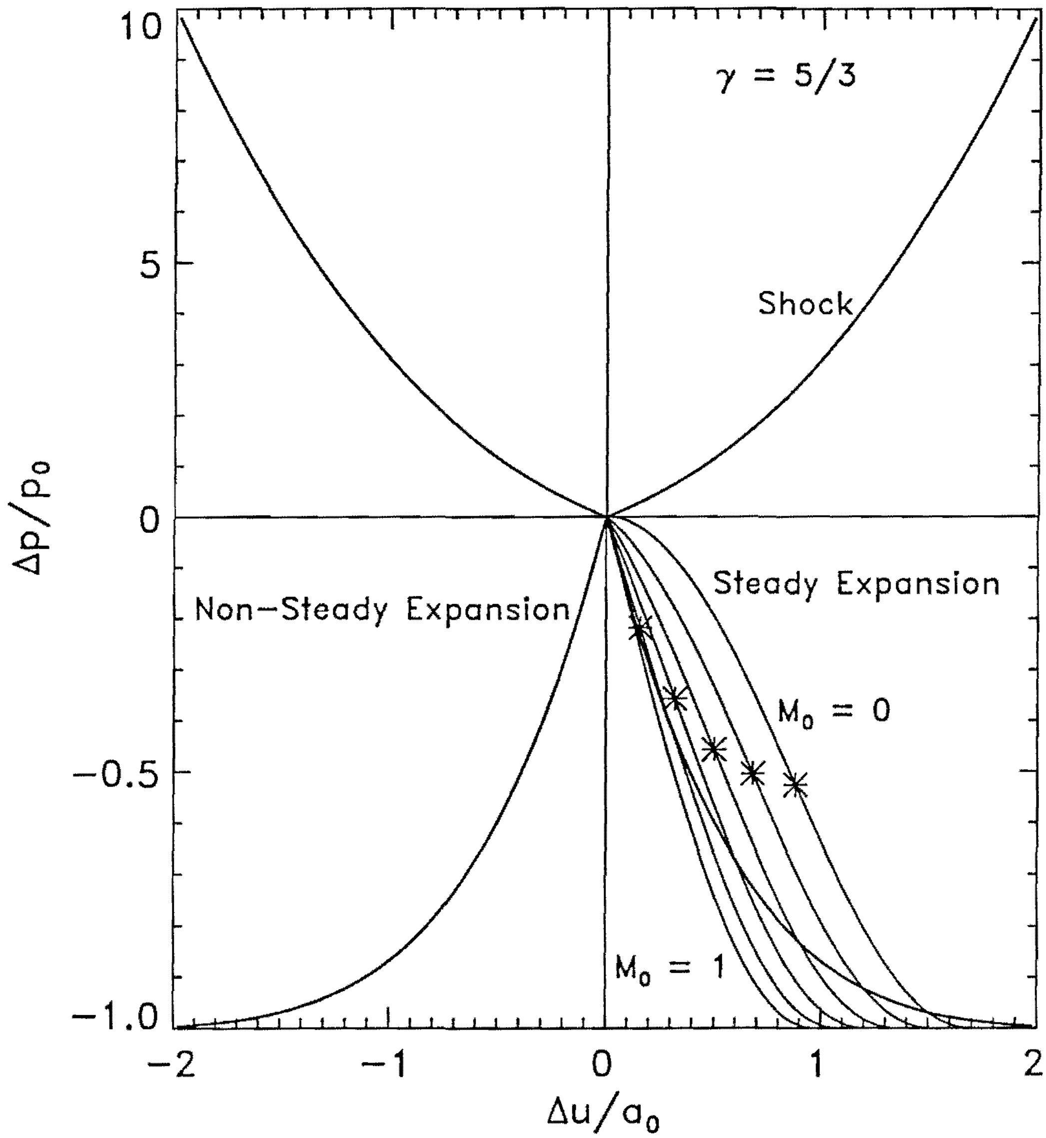

Solution of simple shock tube problem

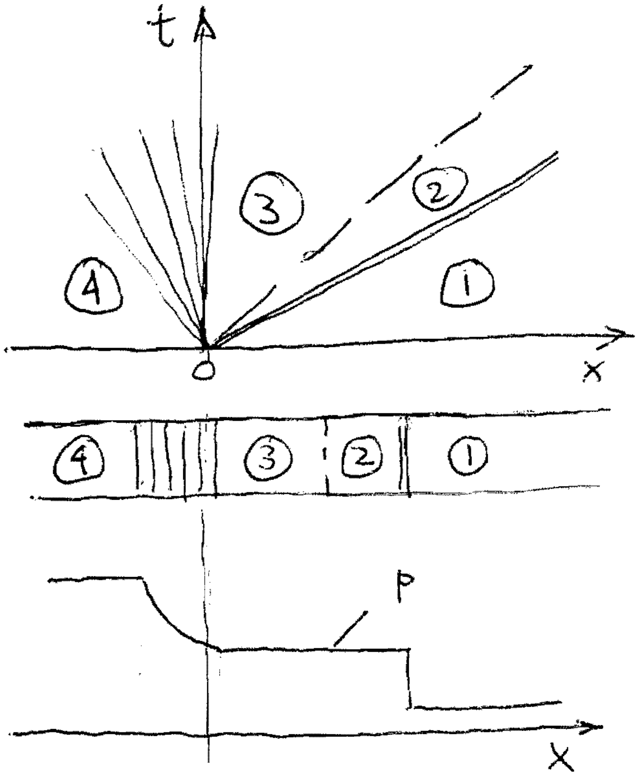

A tube initially filled with test gas at condition 1 to the right of a diaphragm and ~~to the left~~ with driver gas at condition 4 to the left is started by rupturing the diaphragm at $t=0$. If the diaphragm breaks in zero time, a shock wave is formed immediately that propagates to the right into the test gas and an expansion propagates to the left into the driver gas. We solve this by requiring $p_3 = p_2$, $u_3 = u_2$

$$\frac{p_4}{p_1} = \underbrace{\left(\frac{p_4}{p_3}\right)}_{\text{unsteady expn}} \overbrace{\left(\frac{p_3}{p_2}\right)}^{=1} \overbrace{\left(\frac{p_2}{p_1}\right)}^{\text{shock}} = \frac{p_2/p_1}{\left(1 - \frac{\gamma_4 - 1}{2}\frac{a_1}{a_4}\frac{u_3}{a_1}\right)^{\frac{2\gamma_4}{\gamma_4 - 1}}}$$

$u_2 = u_3 \Rightarrow (u_2/a_1)$ shock

$$\frac{u_2}{a_1} = \frac{2}{\gamma_1 + 1}\frac{M_s^2 - 1}{M_s}$$

$$\boxed{\frac{p_4}{p_1} = \frac{1 + \frac{2\gamma_1}{\gamma_1 + 1}\left(M_s^2 - 1\right)}{\left(1 - \frac{\gamma_4 - 1}{\gamma_1 + 1}\frac{a_1}{a_4}\frac{M_s^2 - 1}{M_s}\right)^{\frac{2\gamma_4}{\gamma_4 - 1}}}}$$

For weak shocks   put $M_s = 1+\varepsilon$

$$\frac{p_4}{p_1} \doteq 1 + 2\varepsilon\left[\frac{2\gamma_1 + \frac{a_1}{a_4}(\gamma_4 - 1)}{\gamma_1 + 1}\right]$$

for same gases, same temperature,

$$\frac{p_4}{p_1} = 1 + 2(M_s - 1)\frac{3\gamma - 1}{\gamma + 1}$$

$$\boxed{M_s = 1 + \left(\frac{p_4}{p_1} - 1\right)\cdot\frac{\gamma+1}{2(3\gamma-1)}}$$ weak shock same gas same T

For strong shocks, the limit at $p_4/p_1 = \infty$ is only achievable if a_4/a_1 is sufficiently small. In that case

$$\boxed{\frac{M_s^2 - 1}{M_s} = \frac{a_4}{a_1}\,\frac{\gamma_1+1}{\gamma_4+1}} \quad \frac{p_4}{p_1} = \infty$$

With He/Air at the same temperature $\frac{a_4}{a_1} = 2.94$

$$M_s - \frac{1}{M_s} = 2.94 \times \frac{2.4}{0.67} = 10.8$$

$$M_s = 10.9$$

With $\frac{p_4}{p_1}$ large but finite the shock speed is scaled by the speed of sound of the driver gas.

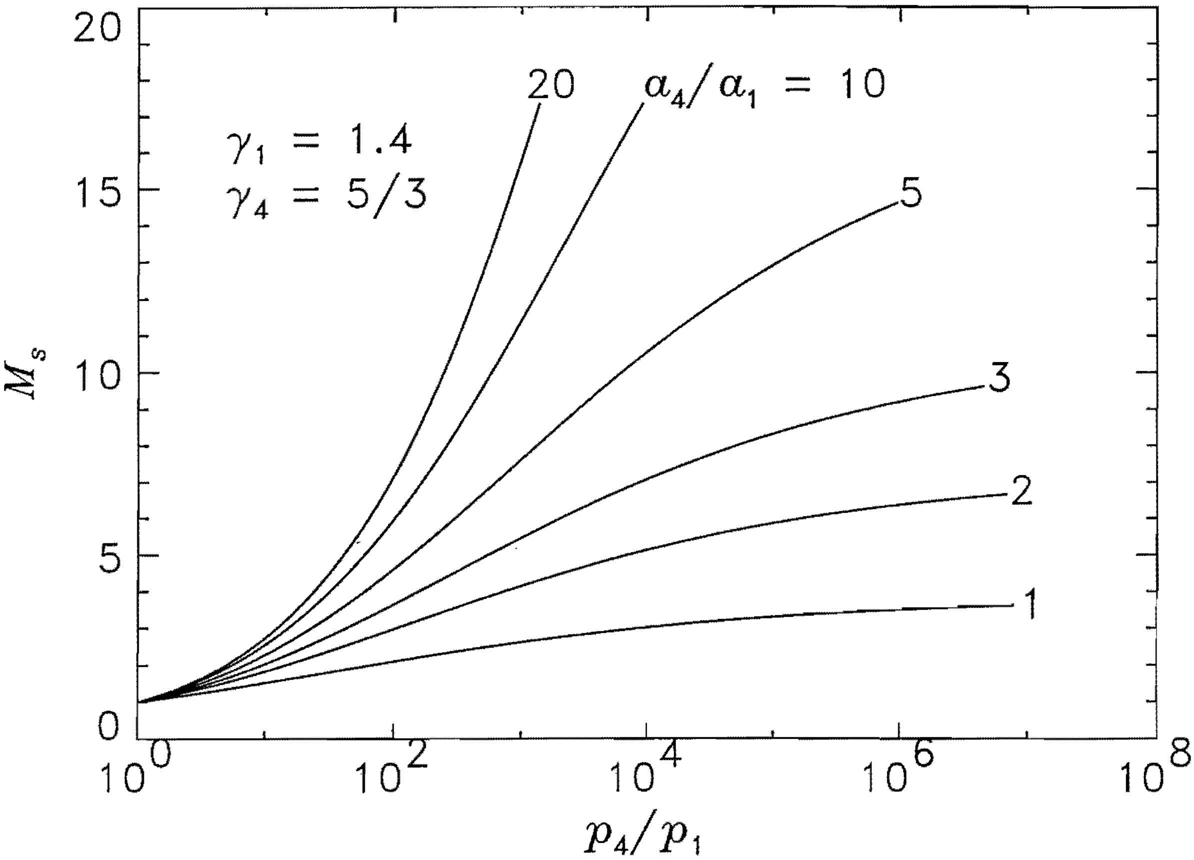

Examples of solutions of the shock tube equation for He/Air

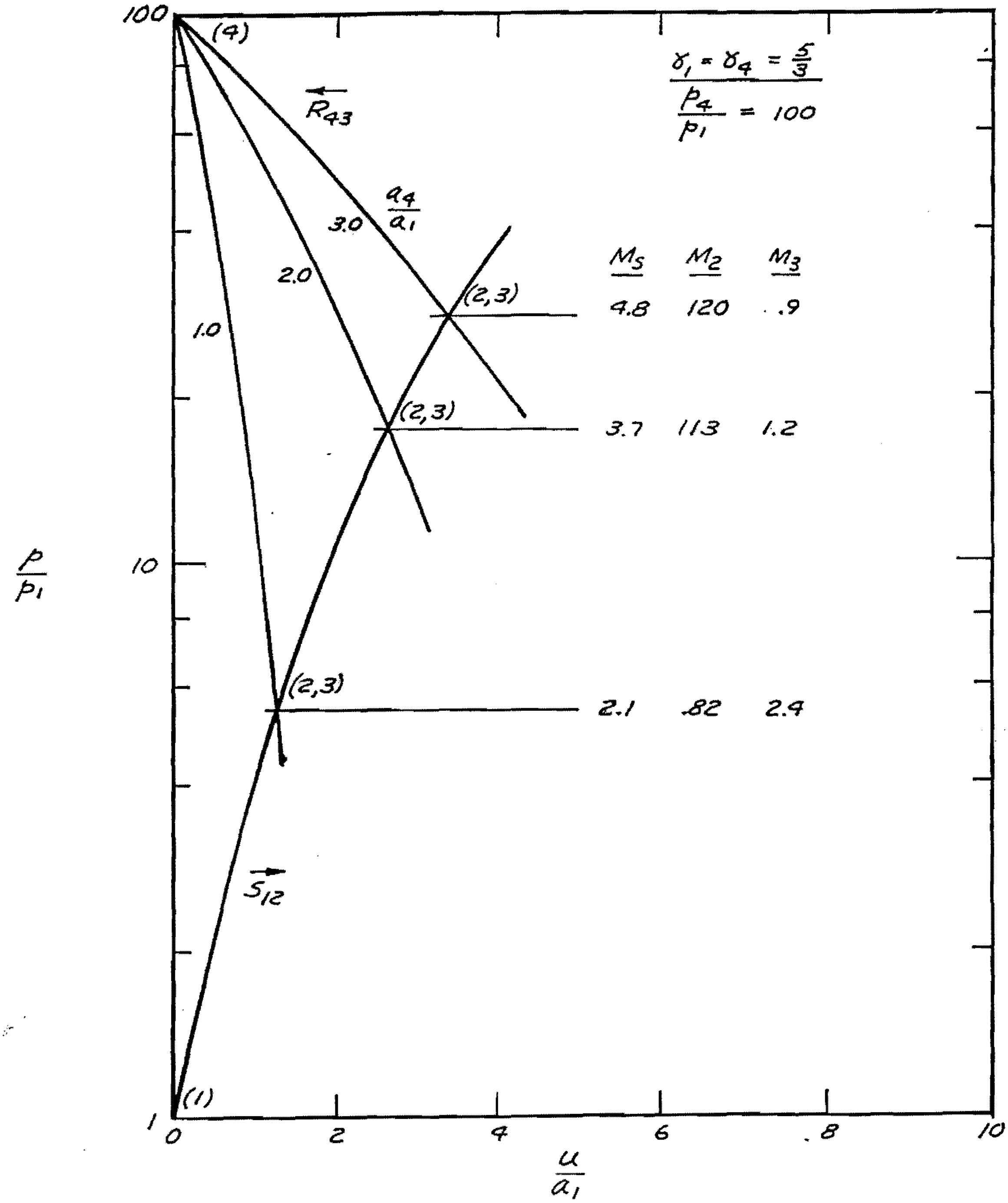

FIG. 3

Solutions of the shock tube equation in the up-diagram.

Shock reflection at the end wall

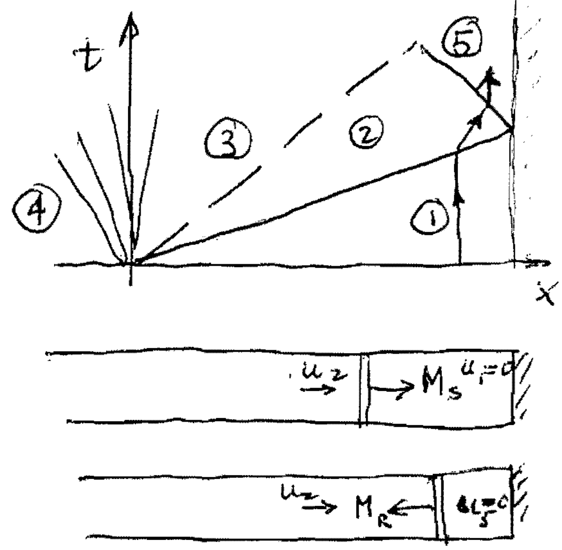

Define M_s and M_r as wave speed relative to upstream flow divided by speed of sound in upstream flow.

Thus, for the incident shock:

$$S: \quad \frac{\Delta u}{a_1} = \frac{u_2-u_1}{a_1} = \frac{u_2}{a_1} = \frac{2}{\gamma+1}\,\frac{M_s^2-1}{M_s}$$

and for the reflected shock,

$$R: \quad \frac{\Delta u}{a_2} = \frac{u_2-u_5}{a_2} = \frac{u_2}{a_2} = \frac{2}{\gamma+1}\,\frac{M_R^2-1}{M_R}$$

Therefore
$$\boxed{\frac{M_R^2-1}{M_R} = \frac{a_1}{a_2}\,\frac{M_s^2-1}{M_s}}$$

For $M_s \gg 1$, $\quad \dfrac{a_2}{a_1} = \sqrt{\dfrac{\left\{2\gamma M_s^2-(\gamma-1)\right\}\left[2+(\gamma-1)M_s^2\right]}{(\gamma+1)^2 M_s^2}} \doteq \sqrt{\dfrac{2\gamma(\gamma-1)}{(\gamma+1)^2}}\,M_s$

The r.h.s. of the box is therefore a constant in the high-M_S limit and so $M_R \to$ const.

Calculate the pressure in region 5:

$$\boxed{\frac{p_5-p_1}{p_1} = 2\,\frac{p_2-p_1}{p_1}\;\frac{1+\left(\frac{1}{2}+\frac{\gamma-1}{\gamma+1}\right)(M_s^2-1)}{1+\frac{\gamma-1}{\gamma+1}(M_s^2-1)}}$$

Using the up-diagram for the reflected shock

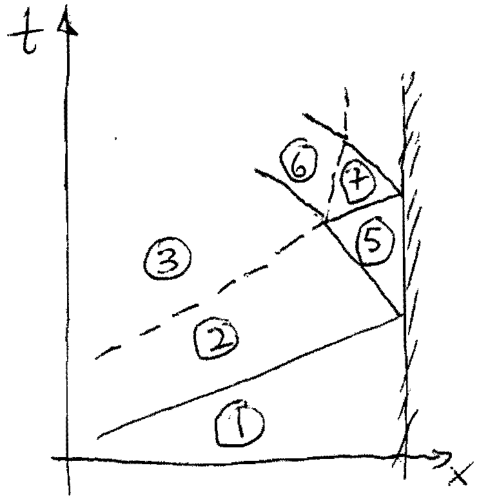

When the reflected shock impinges on the interface a shock is transmitted into region 3 and either a shock or an expansion is reflected and propagates into region 5.

The reflected shock $\overleftarrow{S}_{25}$ may intersect the p-axis above or below the point (4), depending on conditions. (see p 121 for quantitative examples)

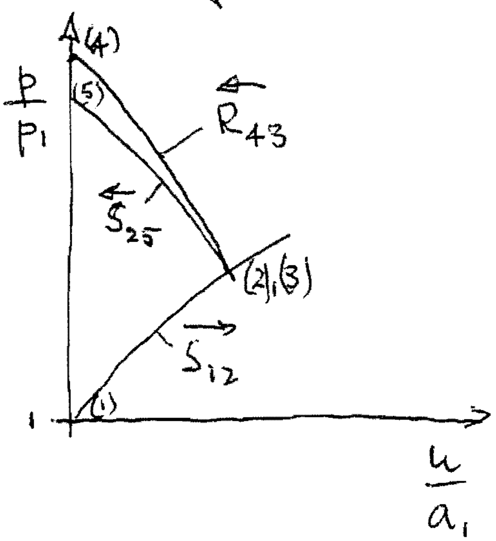

In the figure on p 122 the up-diagram shows two examples of possible maps of the waves 36 and 57. The upper one shows the case $p_5 < p_4$, and $\overleftarrow{S}_{36}$ above $\overleftarrow{S}_{25}$. In that case, 57 is a shock, and $p_6 = p_7 > p_5$, $u_6 = u_7 > 0$. This case is called "overtailored".

The other case shows $p_5 > p_4$, $\overleftarrow{S}_{36}$ below $\overleftarrow{S}_{25}$. In that case, 57 is an expansion, $p_6 = p_7 < p_5$, $u_6 = u_7 < 0$. This is called "undertailored".

The corresponding pressure-time traces

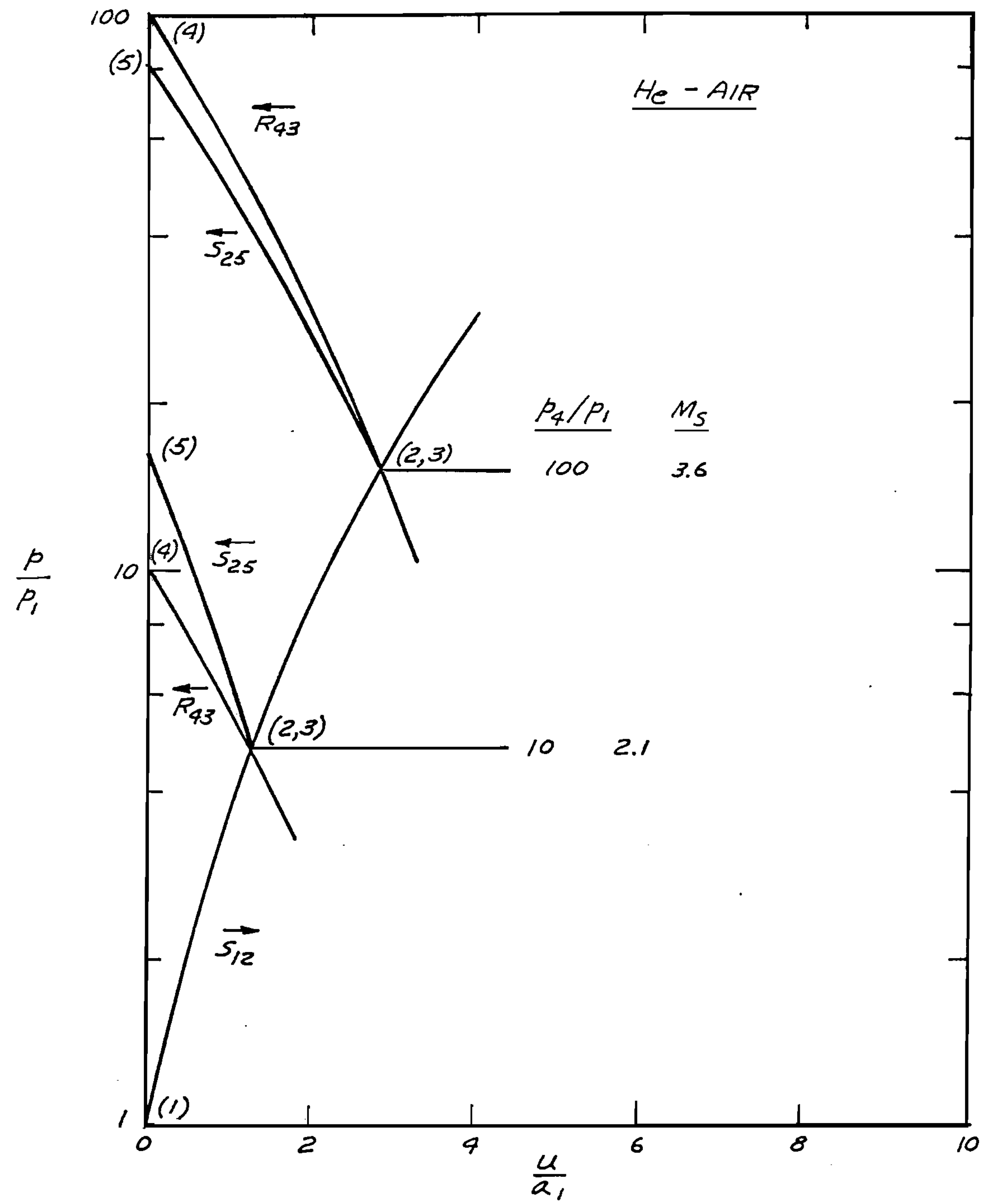

FIG. 4

Reflected shock with cases $p_5 < p_4$
and $p_5 > p_4$

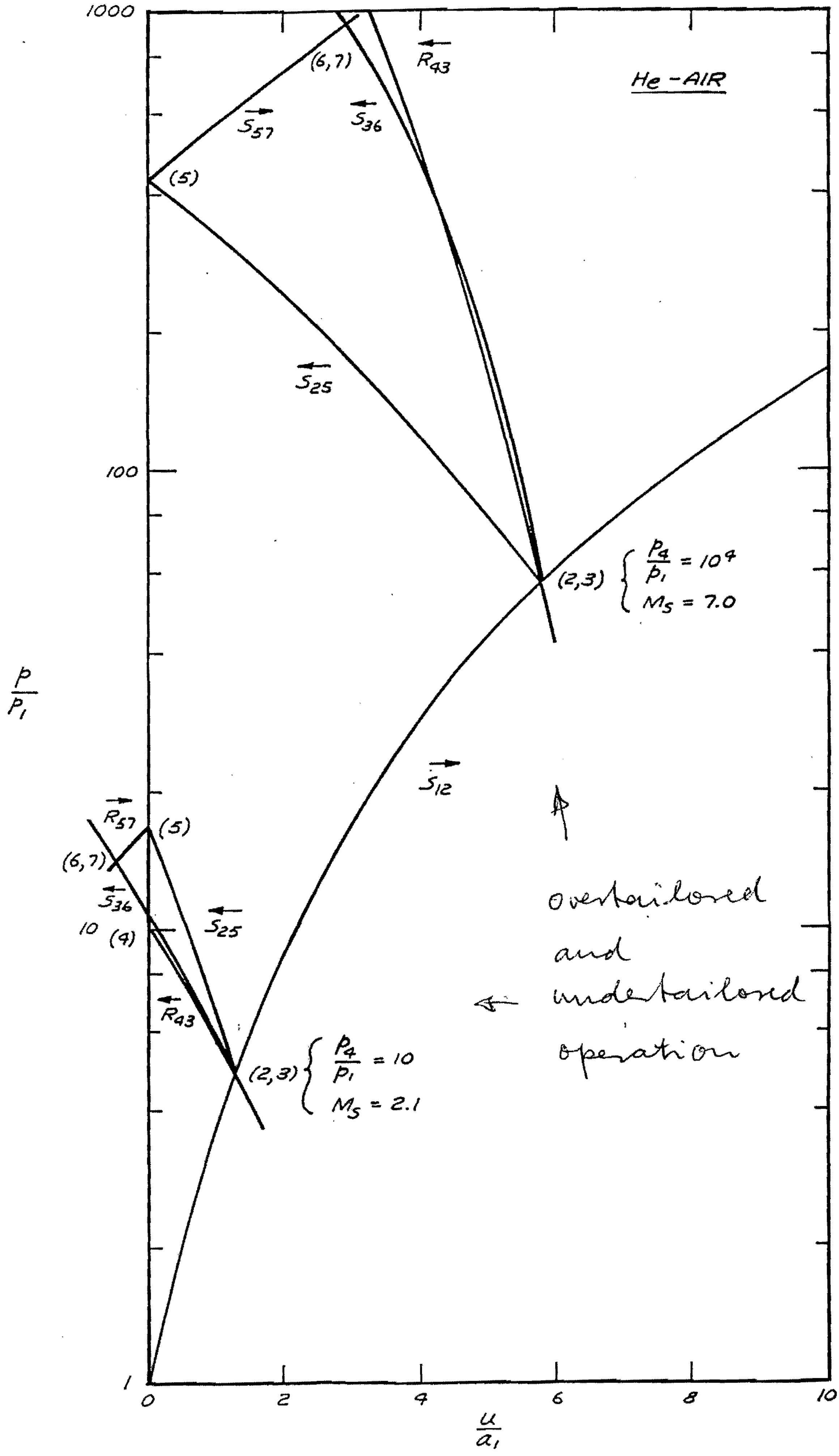
He - AIR
1000
100
10
1
0
2
4
6
8
10
p / p1
u / a1
(6,7)
R43
S57
S36
(5)
S25
(2,3)
p4/p1 = 10^4
Ms = 7.0
S12
R57
(5)
(6,7)
S36
(4)
S25
R43
(2,3)
p4/p1 = 10
Ms = 2.1
overtailored
and
undertailored
operation

FIG. 5

on the end wall look qualitatively as shown

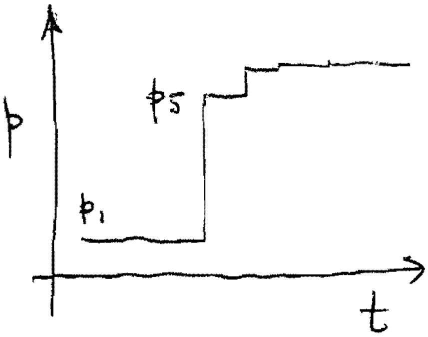

overtailored

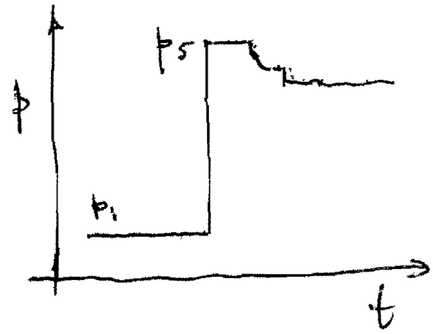

undertailored

In a reflected shock tunnel one wishes to have as long as possible a period of constant pressure at the shock tube end wall. This is achieved in the so-called tailored operation for which the up-diagram is shown on p. 124.

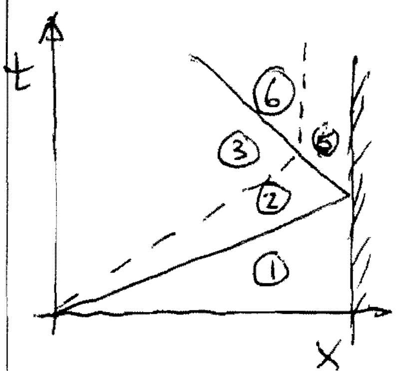

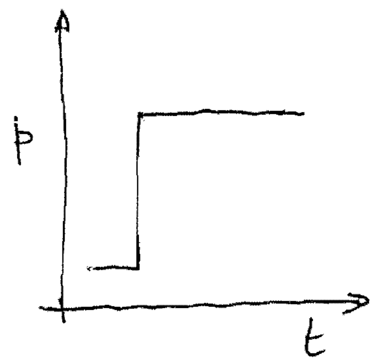

Tailored interface condition

In this case, let the speed of the transmitted shock be u_T and that of the reflected shock u_R. In the shock jump condition

$$\Delta p = \rho_0 c \, \Delta u$$

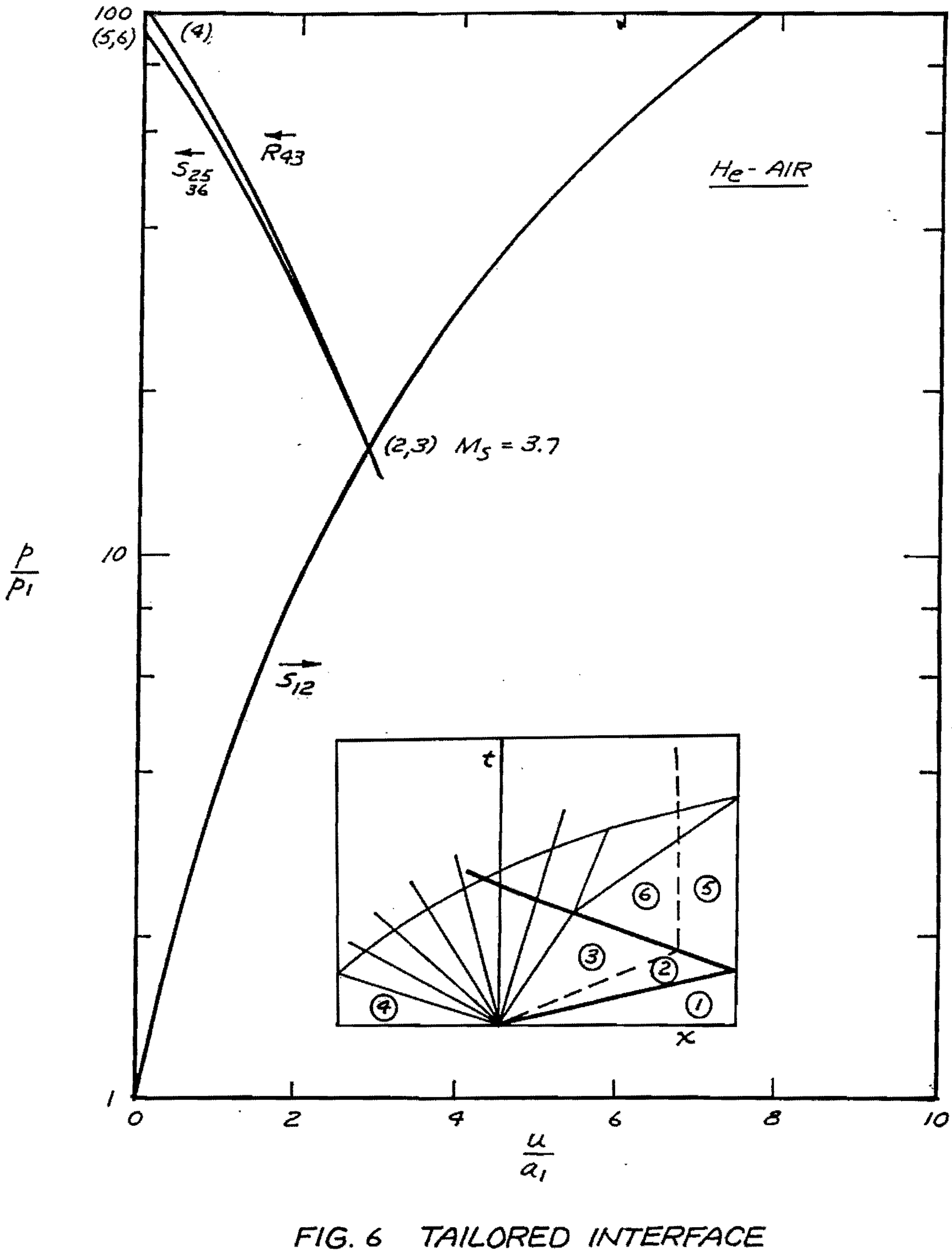

FIG. 6 TAILORED INTERFACE

the wave speed relative to the upstream flow for $\overleftarrow{S}_{25}$ is

$$c_{25} = u_2 + u_R$$

and the upstream density is ρ_2

Similarly for $\overleftarrow{S}_{36}$

$$c_{36} = u_3 + u_T = u_2 + u_T$$

and the upstream density is ρ_3

Therefore

$$\Delta p_{25} = \rho_2 (u_2 + u_R) \Delta u_{25}$$

and

$$\Delta p_{36} = \rho_3 (u_2 + u_T) \Delta u_{36}$$

The tailored interface condition is

$$\Delta p_{25} = \Delta p_{36} \quad \text{and} \quad \Delta u_{25} = \Delta u_{36}$$

It follows that, for tailored operation,

$$\boxed{\rho_2 (u_2 + u_R) = \rho_3 (u_2 + u_T)}$$

The quantity $\rho_0 c$ is sometimes called the "shock impedance" in analogy with the "acoustic impedance" ρa for very weak waves. Tailored interface operation thus demands that the shock impedances are the same in 2 and 3 for the given reflected shock speeds.

To get a quantitative result, apply

$$\frac{\Delta u}{a_0} = \frac{\frac{1}{\gamma}\frac{\Delta p}{p_0}}{\sqrt{1+\frac{\gamma+1}{2\gamma}\frac{\Delta p}{p_0}}}$$

to the reflected and transmitted shocks and equate $\Delta p_{25} = \Delta p_{36}$, $\Delta u_{25} = \Delta u_{36}$:

$\overleftarrow{S}_{25}$:
$$\frac{u_2}{a_2} = \frac{\frac{1}{\gamma_1}\frac{p_5-p_2}{p_2}}{\sqrt{1+\frac{\gamma_1+1}{2\gamma_1}\frac{p_5-p_2}{p_2}}}$$

$\overleftarrow{S}_{36}$:
$$\frac{u_3}{a_3} = \frac{\frac{1}{\gamma_4}\frac{p_6-p_3}{p_3}}{\sqrt{1+\frac{\gamma_4+1}{2\gamma_4}\frac{p_6-p_3}{p_3}}}$$

$u_3 = u_2$, $\frac{p_6-p_3}{p_3} = \frac{p_5-p_2}{p_2}$, so

$$\boxed{\frac{a_3}{a_2} = \frac{\gamma_4}{\gamma_1}\sqrt{\frac{1+\frac{\gamma_4+1}{2\gamma_4}\frac{p_5-p_2}{p_2}}{1+\frac{\gamma_1+1}{2\gamma_1}\frac{p_5-p_2}{p_2}}}}$$ Tailored interface

If $\gamma_4 = \gamma_1$, this requires $a_3 = a_2$. In that case, with $\rho \sim \frac{p}{a^2}$, since $p_2 = p_3$ this also means that $\rho_3 = \rho_2$. Note that, then,

$$\frac{T_3}{T_2} = \frac{\mathcal{M}_3}{\mathcal{M}_2} \qquad \mathcal{M} \equiv \text{molecular weight.}$$

Show movie of tailored operation

Ae/APh 237 Assignment No. 5, February 6, due February 13, 2003

PROBLEM 1.

By writing $dx/dt = u$, and expressing u in terms of x/a_0t in a left–facing centered expansion propagating into a perfect gas at rest, find the equation of a particle path in (x,t)–space.

Hint:

$$\frac{dx}{dt} - b\frac{x}{t} = t^b\frac{d(x/t^b)}{dt}.$$

Plot the result and check that it gives the correct maximum speed.

PROBLEM 2.

Go through the case distinctions for convergence or divergence of characteristics in simple compressions or expansions depending on the value of the fundamental derivative of gasdynamics, in the case when the Grüneisen parameter is negative. Make a table of the results.

PROBLEM 3.

For a certain experiment it is necessary to produce a flow at Mach number 1.5 and density 2 kg/m^3 behind a shock wave in a shock tube. The test gas is air. Determine suitable values of the diaphragm burst pressure and the initial shock tube pressure when the driver gas is air and all temperatures are initially 300 K. Repeat this for helium driver gas. Comment.

PROBLEM 4.

Consider shock reflection from the end wall of a shock tube. Let the Mach number of the flow downstream of the incident shock (in the laboratory frame) be M_2. Show that the reflected shock Mach number M_R is the reciprocal of M_2. Make a plot of M_R as a function of γ, with the shock Mach number, M_S, as a parameter. In shock tunnels, an undesirable feature is the reflected–shock–induced separation of the boundary layer generated by the incident shock. A rule of thumb for shock–induced separation is that, to avoid it, the shock Mach number has to be smaller than 1.3. Is there a realistic range of γ where we may expect that a strong shock reflecting from an end wall will not cause boundary layer separation?

Evolution of a simple compression wave into a shock

Consider a simple right-facing compression wave that is generated by a piston accelerating to the right. Let the piston path be given by

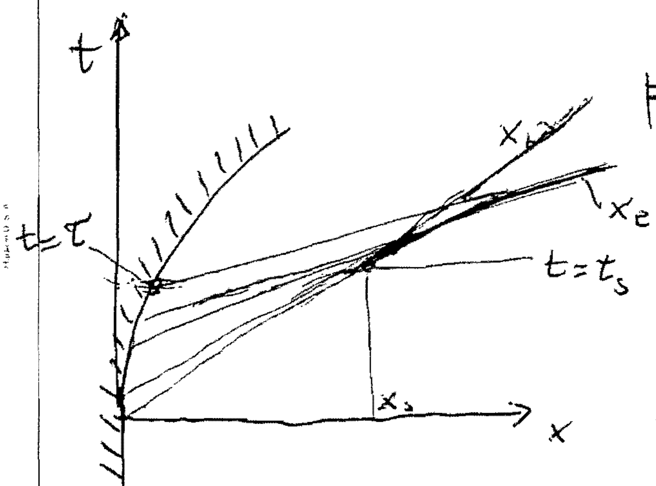

$$x_p = x_p(t)$$

$$u_p = \frac{dx_p}{dt}(t)$$

$$b_p = \frac{d^2x_p}{dt^2}(t)$$

The slope of a characteristic that starts from the piston face at $t=\tau$ is

$$\frac{dx}{dt} = u + a = u + a_0 + \frac{\gamma-1}{2}u = a_0 + \frac{\gamma+1}{2}u$$

$$= a_0 + \frac{\gamma+1}{2}u_p(\tau)$$

The equation of this characteristic is therefore

$$x = x_p(\tau) + (t-\tau)\left[a_0 + \frac{\gamma+1}{2}u_p(\tau)\right]$$

Treating τ as a parameter, this gives the equations for all the characteristics starting from the piston. For a perfect gas (implied above) the characteristics in such a wave converge, to form an envelope starting at the point (x_s, t_s). To find this point, ~~differentiate~~ observe, that, on the envelope

~~the slopes of~~ neighboring characteristics ~~are the same~~ intersect, so that

$$0 = \frac{dx}{d\tau} = u_p(\tau) + (t-\tau)\cdot\frac{\gamma+1}{2}b_p(\tau) - \left[a_0 + \frac{\gamma+1}{2}u_p(\tau)\right]$$

on the envelope. Now assume that the point (x_s, t_s) lies on the characteristic issuing from $(0,0)$ and that $u_p(0)=0$. Thus the time t_s is given by

$$t_s \frac{\gamma+1}{2} b_p(0) = a_0$$

$$\boxed{t_s = \frac{2}{\gamma+1}\frac{a_0}{b_p(0)}}$$

Substituting this into the equation for x, with $x_p(0)=0$, $u_p(0)=0$,

$$\boxed{x_s = \frac{2}{\gamma+1}\frac{a_0^2}{b_p(0)}}$$

Note that the coordinates of the point where the characteristics first overlap increase with decreasing piston acceleration, giving no overlap at $b_p(0)=0$, and at infinite $b_p(0)$, give $(x_s, t_s) = (0,0)$.

This is a very real problem in a free-piston shock tunnel like T5, where the driver-gas is heated by adiabatic piston compression

Here we don't want a shock wave to form in the compression tube because it would make the driver gas nonuniform at diaphragm burst.

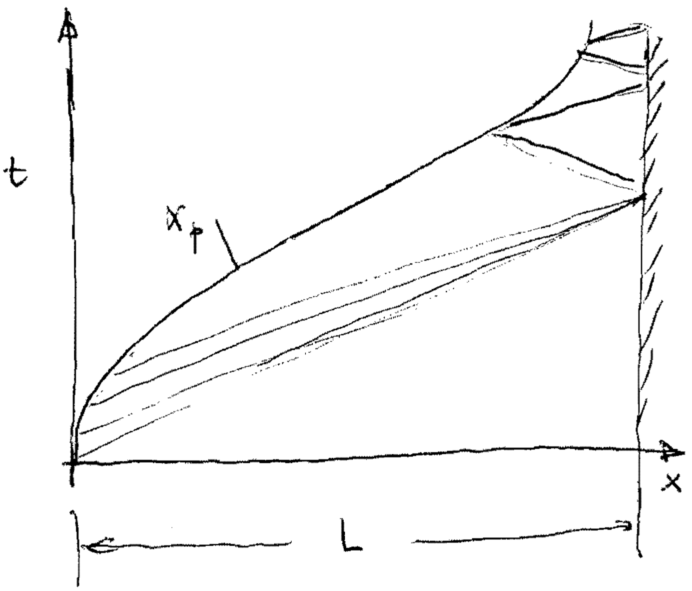

I.e. we want x_s to be much larger than L. In the case of T5, L = 30 m.

With pure helium driver gas, $a_0 = 1000$ m/s

so $$x_s = \frac{4}{3}\frac{a_0^2}{b_p(0)} \gg L$$

$$b_p(0) \ll \frac{4}{3}\frac{a_0^2}{L}$$

Now $b_p(0)$ is $p_R A/m_p$ where p_R is the pressure in the gas pushing the piston, and m_p is the piston mass, cross sectional area of tube A. Hence

$\frac{\pi D^2}{4} = \frac{\pi \times (0.3)^2}{4} = 0.07$

$$p_R \ll \frac{4}{3}\frac{a_0^2 m_p}{L A} = \frac{4 \times 10^6 \times 120}{3 \times 30 \times 0.07} = 76 \text{ MPa}$$

With Helium driver gas, this condition is hard not to satisfy, but adding argon to the helium for lower enthalpy flows we sometimes observe shock formation.

Return to the shock formation. In the cusp shaped region between x_b and x_e the characteristics overlap (p. 127). We can show this in a xu-diagram. For

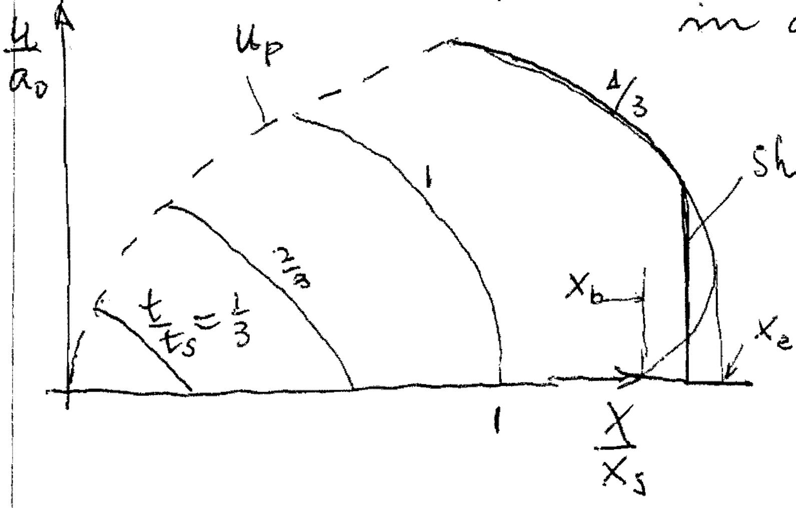

$t > t_s$ the particle speed is double-valued in $x_b < x < x_e$ and a shock wave forms instead. These velocity profiles can be calculated for the special piston path $x_p = Bt^2/2$ with B constant from the quadratic

$$\frac{\gamma(\gamma+1)}{4}\left(\frac{u}{a_0}\right)^2 + \frac{\gamma+1}{2}\left(1-\frac{t}{t_s}\right)\frac{u}{a_0} + \frac{x}{x_s} - \frac{t}{t_s} = 0.$$

Wave interactions

1. Shock impinging on density interface

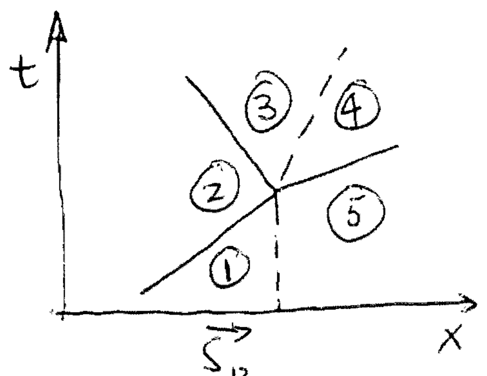

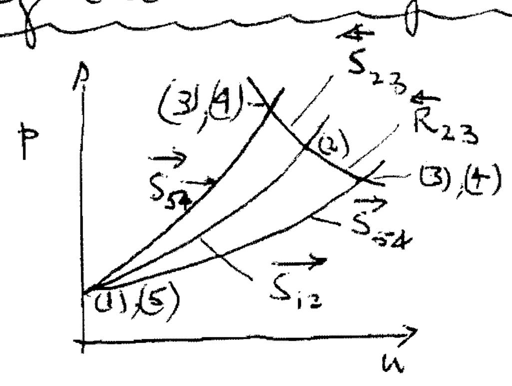

A shock impinging on a stationary density interface 15, will generate a transmitted shock $\vec{S}_{54}$ and a reflected wave 23 which may be a shock or a rarefaction, depending on conditions. If the transmitted shock $\vec{S}_{54}$ lies below $\vec{S}_{12}$ in up-space the reflected wave will be an expansion $\overleftarrow{R}_{23}$ and if $\vec{S}_{54}$ lies above $\vec{S}_{12}$ it will be a shock $\overleftarrow{S}_{23}$

② Two shocks of opposite family (facing in opposite directions)

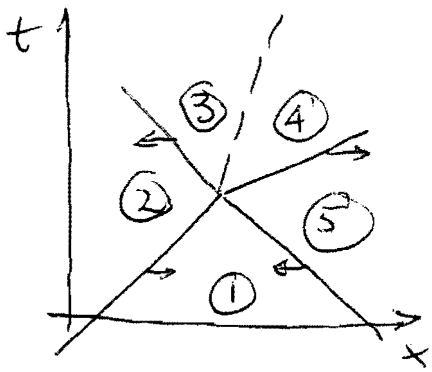

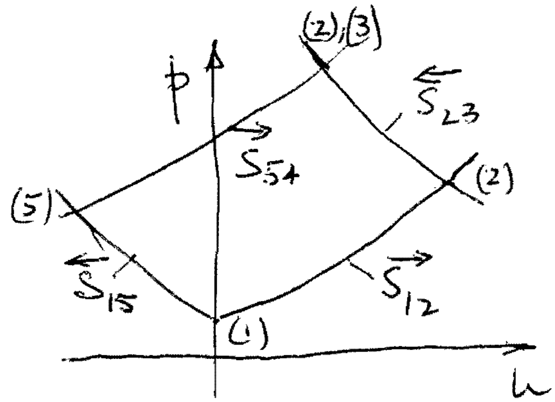

Region ① is at rest. The shock strengths of $\vec{S}_{12}$ and $\overleftarrow{S}_{15}$ are given, so (5) and (2) are known. The intersection of the right facing shock curve through (5) and the left-facing shock curve through (2) gives the speed and pressure of the resulting interface.

③ Expansion and shock of opposite family

If a shock $\vec{S}_{12}$ impinges on an expansion fan $\overleftarrow{R}_{15}$ with ① at rest the interaction no longer occurs at a single point in xt-space but along a line. The resulting interface is therefore not a line in xt-space but a broad strip.

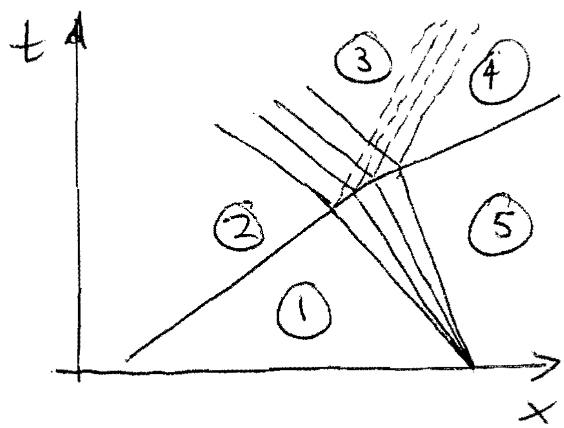

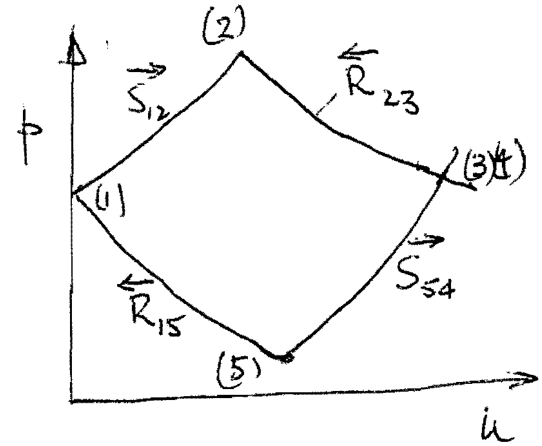

To solve this problem mathematically:

$\overleftarrow{R}_{15}$ and $\overrightarrow{S}_{12}$ are given:

$\overleftarrow{R}_{15}$ →
$$\frac{\gamma-1}{2} u_5 + a_5 = a_1$$

gives
$$\left(\frac{p_5}{p_1}\right)^{\frac{\gamma-1}{2\gamma}} = \frac{a_5}{a_1} = 1 - \frac{\gamma-1}{2}\frac{u_5}{a_1} \qquad \text{—— (1)}$$

$\overrightarrow{S}_{12}$ →
$$\frac{p_2}{p_1} = 1 + \frac{2\gamma}{\gamma+1}\left(M_S^2 - 1\right)$$

$$M_S = \sqrt{1 + \frac{\gamma+1}{2\gamma}\frac{p_2-p_1}{p_1}}$$

$$\frac{u_2}{a_1} = \frac{\frac{1}{\gamma}\frac{p_2-p_1}{p_1}}{\sqrt{1+\frac{\gamma+1}{2\gamma}\frac{p_2-p_1}{p_1}}} \qquad \text{—— (2)}$$

also get $\frac{a_2}{a_1}\left(\frac{p_2-p_1}{p_1}\right)$ from shock jump —— (3)

$\overrightarrow{S}_{54}$
$$\frac{u_3-u_5}{a_5} = \frac{\frac{1}{\gamma}\frac{p_3-p_5}{p_5}}{\sqrt{1+\frac{\gamma+1}{2\gamma}\frac{p_3-p_5}{p_5}}} \qquad \text{—— (4)}$$

$u_4 = u_3$
$p_4 = p_3$

and $\overleftarrow{R}_{23}$: $$\frac{u_3-u_2}{a_2} = \frac{2}{\gamma-1}\left[1-\left(\frac{p_3}{p_2}\right)^{\frac{\gamma-1}{2\gamma}}\right] \qquad (5)$$

Solve for $\frac{u_3}{a_1}$ from each of (4) and (5):

$$\frac{u_3}{a_1} = \frac{u_5}{a_1} + \frac{a_5}{a_1}\,\frac{\frac{1}{\gamma}\,\frac{p_3-p_5}{p_5}}{\sqrt{1+\frac{\gamma+1}{2\gamma}\,\frac{p_3-p_5}{p_5}}}$$

$$\frac{u_3}{a_1} = \frac{u_2}{a_1} + \frac{a_2}{a_1}\cdot\frac{2}{\gamma-1}\left[1-\left(\frac{p_3}{p_2}\right)^{\frac{\gamma-1}{2\gamma}}\right]$$

Substitute in these for $\frac{u_5}{a_1}$, from (1), $\frac{a_5}{a_1}$ from (1), $\frac{u_2}{a_1}$ from (2), $\frac{a_2}{a_1}$ from (3), then equate the two results. Solve by iteration. Guess p_3 to start.

(4) Two shocks of the same family

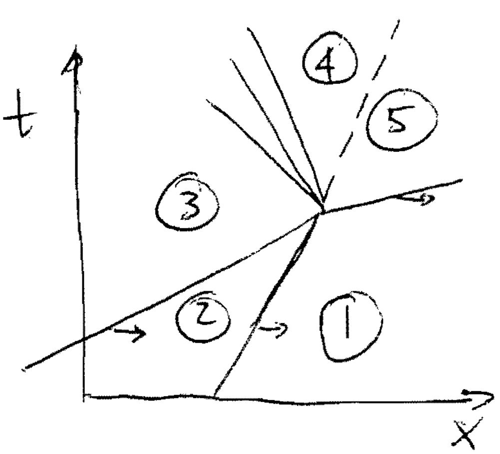

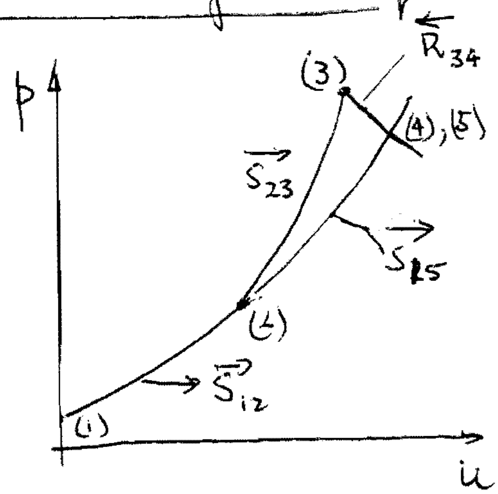

$\overrightarrow{S}_{23}$ lies above $\overrightarrow{S}_{15}$, (which follows the same curve as $\overrightarrow{S}_{12}$). The reflected wave therefore has to be an expansion.

⑤ Expansion wave catching up with shock

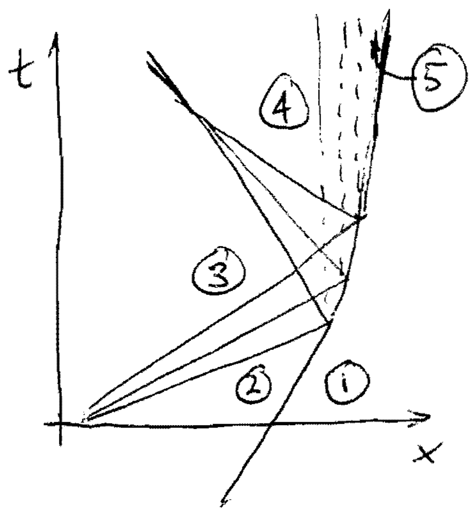

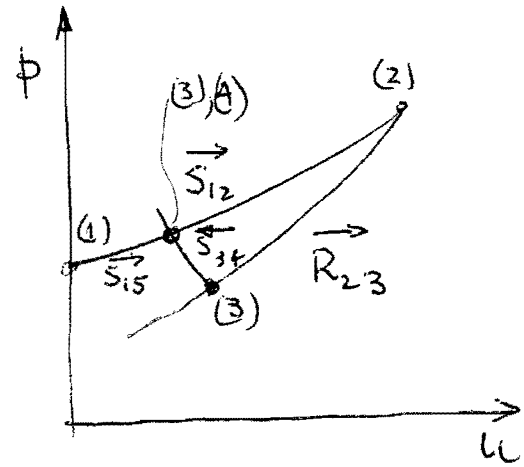

There exist several possibilities in this case. If the expansion wave is so strong that the velocity in ③ is negative, get left picture below. It is also possible that the expansion wave curve $\vec{R}_{23}$ intersects the shock curve $\vec{S}_{12}$. In that case, three possibilities exist.

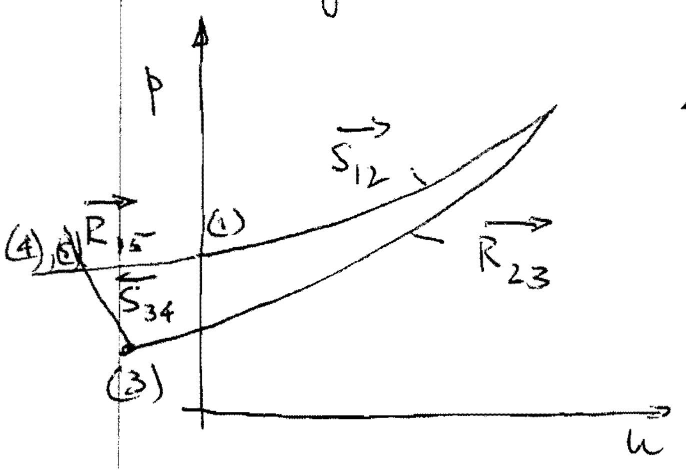

a) reflected expansion, transmitted expansion
b) reflected compression
c) no reflection.

See figure on left.

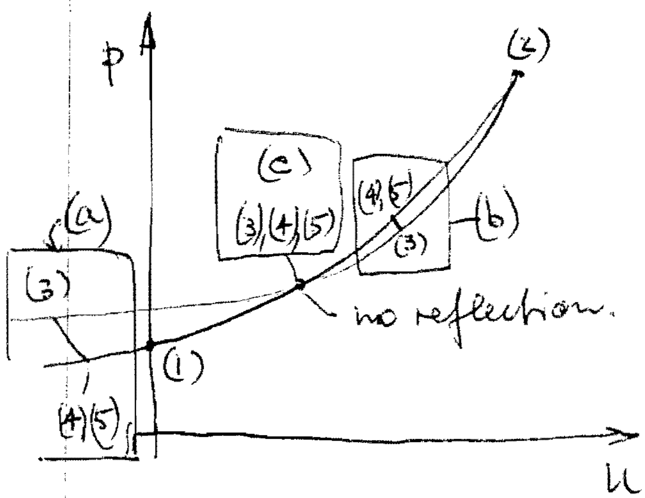

Conditions for no reflection

$\overrightarrow{R}_{23}$ $\quad \dfrac{u_2-u_3}{a_2} = \dfrac{2}{\gamma-1}\left[1-\left(\dfrac{p_3}{p_2}\right)^{\frac{\gamma-1}{2\gamma}}\right]$ —— (1)

$\overrightarrow{S}_{12}$ $\quad \dfrac{u_2}{a_1} = \dfrac{\frac{1}{\gamma}\,\frac{p_2-p_1}{p_1}}{\sqrt{1+\frac{\gamma+1}{2\gamma}\,\frac{p_2-p_1}{p_1}}}$ —— (2)

If no reflection, (3) lies on S_{12}, so

$$\frac{u_3}{a_1} = \frac{\frac{1}{\gamma}\,\frac{p_3-p_1}{p_1}}{\sqrt{1+\frac{\gamma+1}{2\gamma}\,\frac{p_3-p_1}{p_1}}} \qquad \text{—— (3)}$$

Solve (1) for $\dfrac{u_3}{a_2}$

$$\frac{u_3}{a_2} = \frac{u_2}{a_2} - \frac{2}{\gamma-1}\left[1-\left(\frac{p_3}{p_2}\right)^{\frac{\gamma-1}{2\gamma}}\right]$$

or $$\frac{u_3}{a_1} = \frac{u_2}{a_1} - \frac{2}{\gamma-1}\,\frac{a_2}{a_1}\left[1-\left(\frac{p_3}{p_2}\right)^{\frac{\gamma-1}{2\gamma}}\right]$$

Substitute for $\dfrac{u_3}{a_1}$ and $\dfrac{u_2}{a_1}$ in this from (3) and (2) to get

$$\frac{\frac{1}{\gamma}\left(\frac{p_3}{p_2}\frac{p_2}{p_1}-1\right)}{\sqrt{1+\frac{\gamma+1}{2\gamma}\left(\frac{p_3}{p_2}\frac{p_2}{p_1}-1\right)}} + \frac{2}{\gamma-1}\,\frac{a_2}{a_1}\left[1-\left(\frac{p_3}{p_2}\right)^{\frac{\gamma-1}{2\gamma}}\right] - \frac{u_2}{a_1} = 0$$

For a given shock $\overrightarrow{S}_{12}$, $\dfrac{p_2}{p_1}$, $\dfrac{a_2}{a_1}$ and $\dfrac{u_2}{u_1}$ are known so this is an equation for $\dfrac{p_3}{p_2}$ such that there will be no reflection. Solve iteratively. A special case exists such that $p_3 = p_1$, i.e. that the intersection occurs on the p axis. In that case there is no reflected and no transmitted wave, i.e. the expansion wave exactly cancels the shock. For $\gamma = 1.4$, this occurs when $\frac{p_2}{p_1} = 1.273$. The curve of $\frac{p_3}{p_2}$ vs $\frac{p_2}{p_1}$ for no reflection is shown here for $\gamma = 1.4$

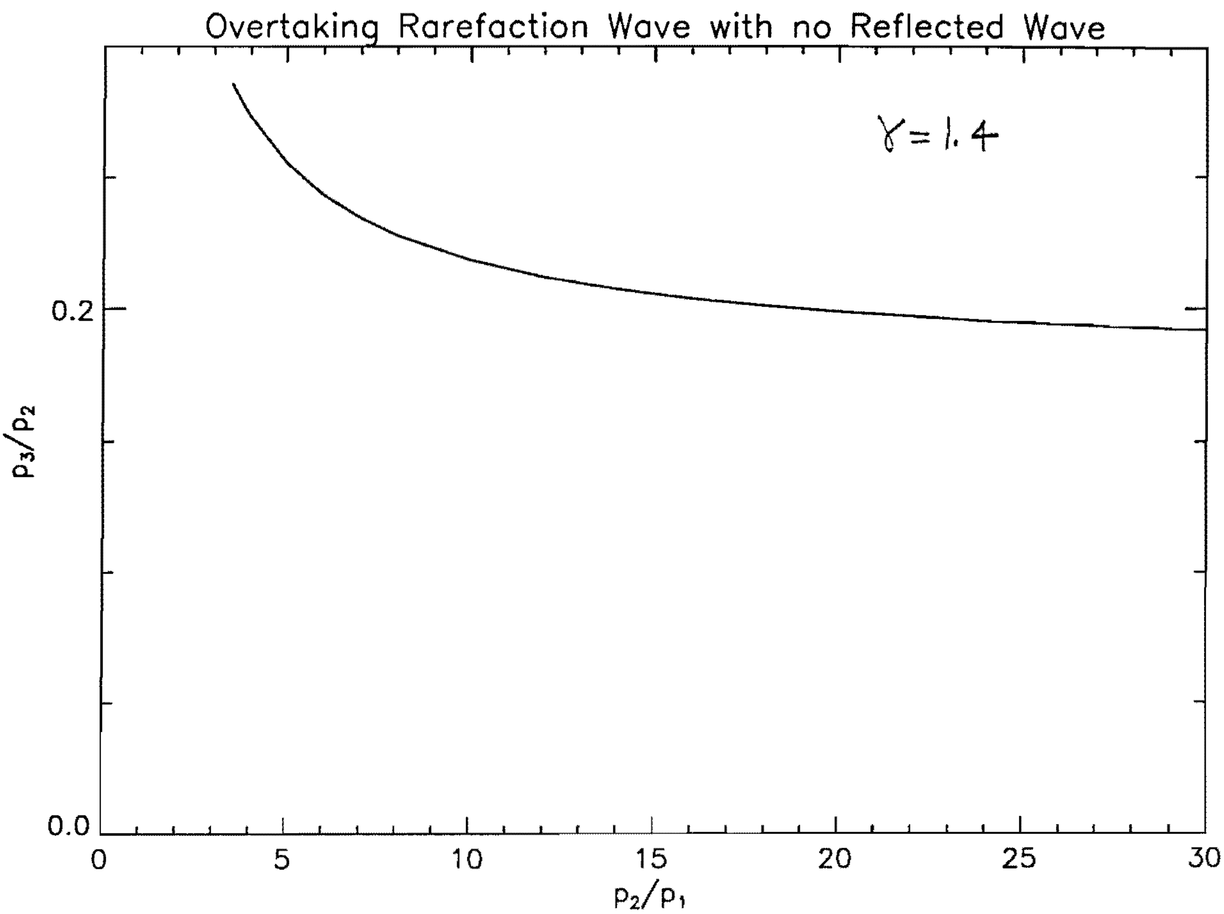

Waves interacting with area change

In situations when the area of a duct changes, ~~it~~ steady as well as unsteady expansions and compressions occur. Recall that in steady isentropic flow, the conservation equations are (quasi-one-dimensional flow)

$$\rho u A = \rho^* u^* A^*$$

$$dp + \rho u \, du = 0$$

$$a^2 + \frac{\gamma-1}{2} u^2 = a_t^2$$

With $a^2 = \frac{dp}{d\rho}$ these lead to

$$\boxed{\left(\frac{A}{A^*}\right)^2 = \frac{1}{M^2}\left[\frac{2}{\gamma+1}\left(1+\frac{\gamma-1}{2}M^2\right)\right]^{\frac{\gamma+1}{\gamma-1}}} \qquad \left(M = \frac{u}{a}\right)$$

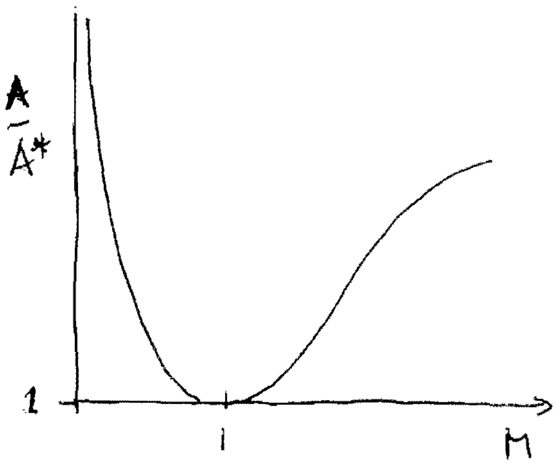

This has a minimum value of 1 at $M = 1$. In subsonic flow an area decrease causes an increase in M, and vice versa.

In the following, the area changes are treated as if they were abrupt, ~~and~~ but the flow is considered to be smooth. This is valid, provided one remembers that we are dealing with the far-field view.

<u>Piston withdrawal, area reduction.</u>

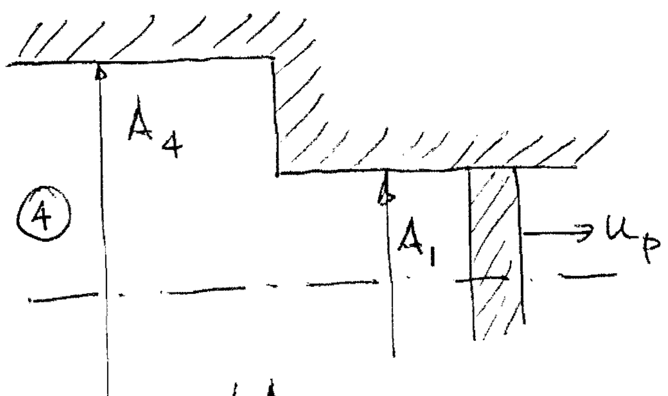

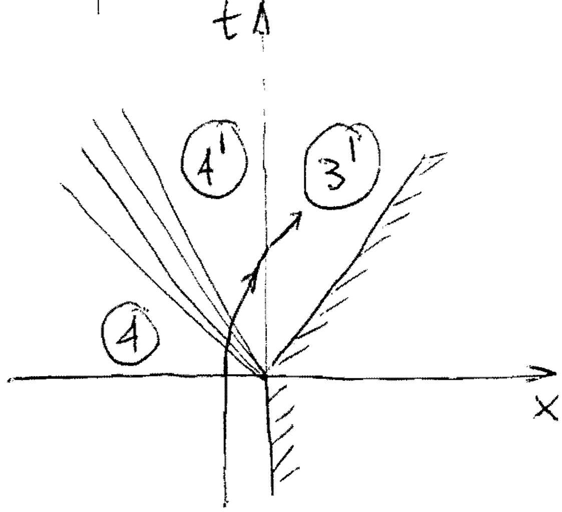

A piston is initially located at an abrupt area change from A_4 to A_1. It is then impulsively accelerated to a constant speed u_p away from the area change. This causes an unsteady expansion wave to propagate to the left, changing the initial state (4) to (4'). We now wish to know what is the state (3') near the piston. Distinguish three possibilities:

a) $u_{3'} = u_p < a_{3'}$, i.e. $M_{3'} < 1$

b) $u_{3'} = u_p = a_{3'}$, $M_{3'} = 1$

c) $u_{3'} = u_p > a_{3'}$, $M_{3'} > 1$.

If there is a change in pressure across the area change after a long time, then this will be a <u>steady</u> expansion ~~and~~ to which the equation and sketch on p. 137 apply.

a) $\underline{M_{3'} < 1}$ given. The area Mach number curve for the steady expansion from 4' to 3' connects the two Mach numbers $M_{3'}$ and $M_{4'}$ with A_4 and A_1 through a relation.

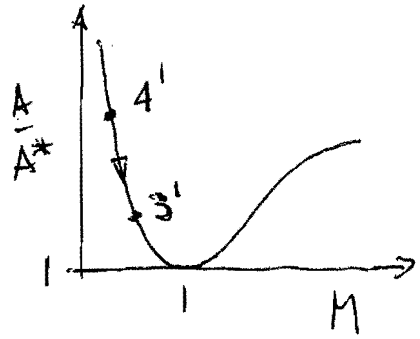

$$\frac{A_4}{A_*}(M_{4'},\gamma) \cdot \frac{1}{A_1/A_*(M_{3'},\gamma)} = \frac{A_4}{A_1}(M_{4'}, M_{3'}) \qquad (1)$$

Also, a_4 and $a_{4'}$ are connected to each other by the unsteady expansion relation, giving an equation of the form

$$\frac{a_4}{a_{4'}}(M_{4'},\gamma)$$

Further, the speed of sound in 3' is related to the reservoir speed of sound in 3' ($a_{t_{3'}}$) by a relation of the form

$$\frac{a_{t_{3'}}}{a_{3'}}(M_{3'},\gamma)$$

(steady isentropic expansion), and, since the process $4' \to 3'$ is a steady isentropic expansion, $a_{t_{4'}} = a_{t_{3'}}$.

Therefore

$$M_{3'} = \frac{u_{3'}}{a_{3'}} = \frac{\overset{\text{given}}{u_{3'}}}{\underset{\text{known}}{a_4}} \cdot \overbrace{\frac{a_4}{a_{4'}}(M_{4'},\gamma)}^{\text{unsteady expansion}} \overbrace{\frac{a_{t_{4'}}}{\cancel{a_{t_{3'}}}}}^{=1} \overbrace{\frac{a_{t_{3'}}}{a_{3'}}(M_{3'},\gamma)}^{\text{steady expansion}} \qquad (2)$$

gives a second equation connecting $M_{3'}$ and $M_{4'}$

Equations ① and ② can then be solved iteratively for $M_{3'}$ and $M_{4'}$.

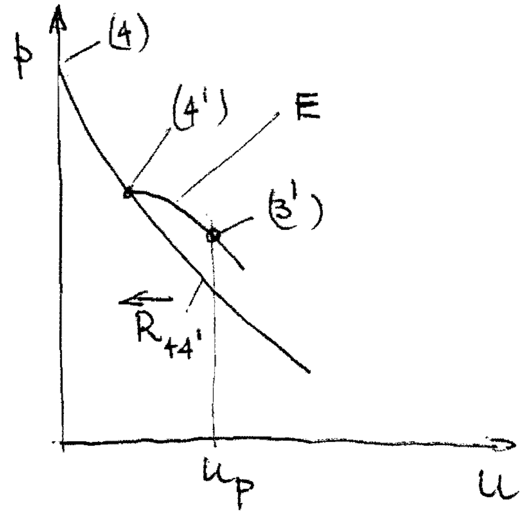

In the up-diagram, the process appears as shown, though the values have to be determined by the above iterative solution.

Case b) $M_{3'} = 1$, $A_1 = A_*$. The procedure is simpler in this case, since $\frac{A_4}{A_1} = \frac{A_4}{A^*} = f(M_{4'})$

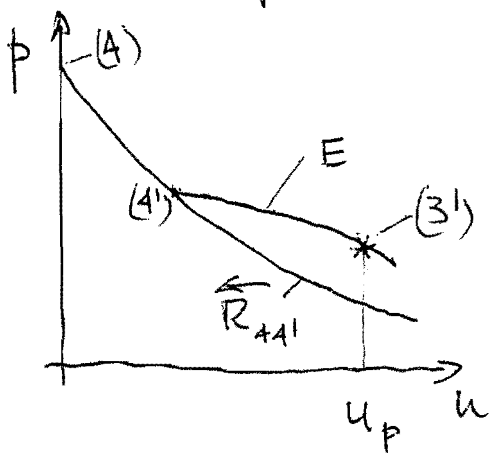

In the up-plane the steady expansion now proceeds up to the sonic condition $*$. Note that the point (4') is not the same as in case a)

Case c) $M_{3'} > 1$, $A_1 = A^*$. Now the steady expansion can accelerate the flow only to the sonic speed in 3' (area). A further unsteady expansion is therefore necessary to accelerate the flow to supersonic speed. Again construct two relations

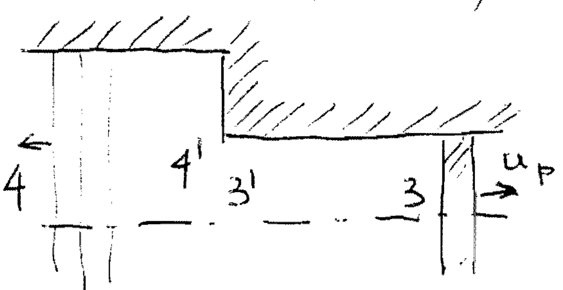

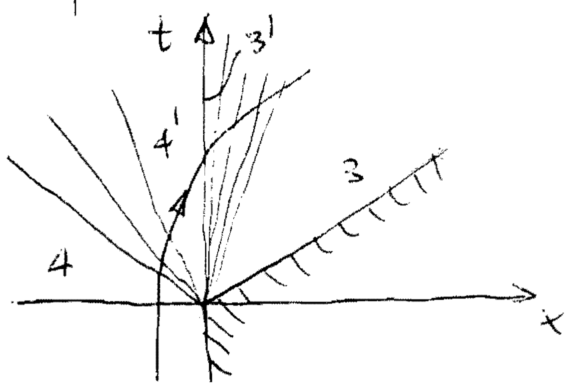

between $M_{4'}$ and $M_{3'}$ to solve iteratively.

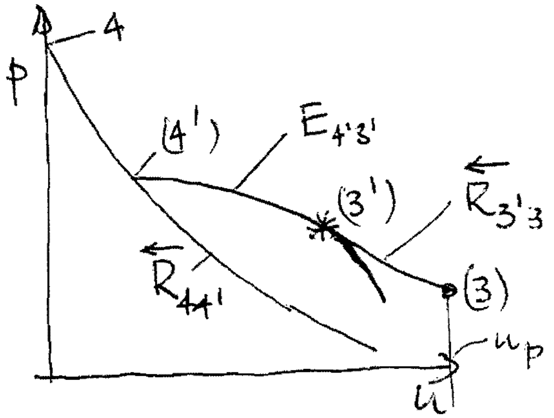

In the up-diagram, this is seen to be an unsteady expansion $\overleftarrow{R}_{44'}$ followed by a steady expansion $E_{4'3'}$ and a second unsteady expansion $\overleftarrow{R}_{3'3}$ with 3' sonic. The locus of end states in the up-diagram as u_p is increased from zero is shown as a dashed line in the figure to the left.

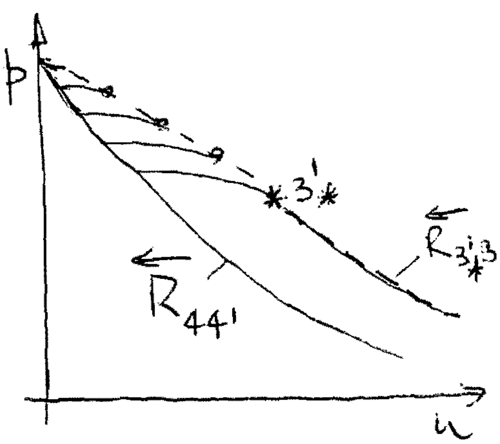

Piston withdrawal, area increase

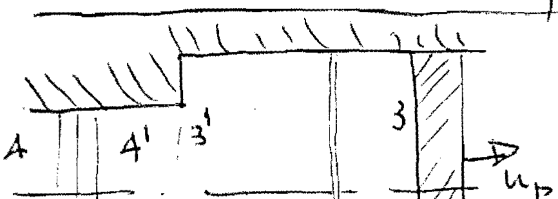

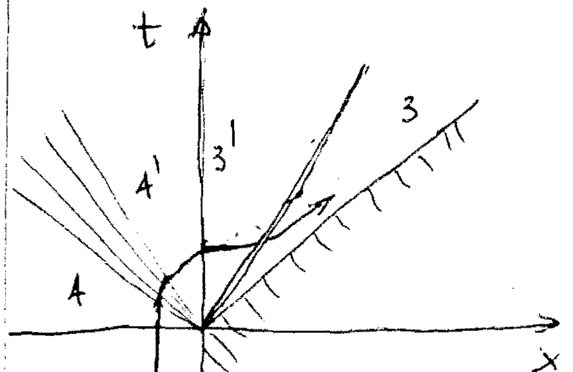

In this case the process $4' \to 3'$ is a subsonic isentropic steady compression, provided that $M_{4'} < 1$. If 4' is sonic 3' may be at even higher Mach number, and the matching to the piston speed occurs via a shock wave. This is the case shown in xt here.

The three possible cases are shown in the up-plane here.

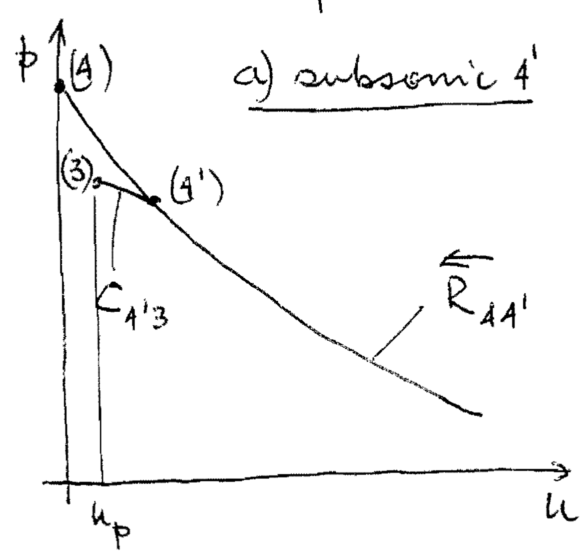

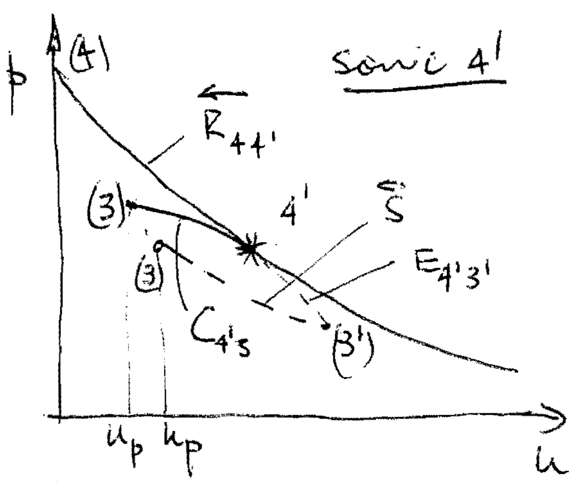

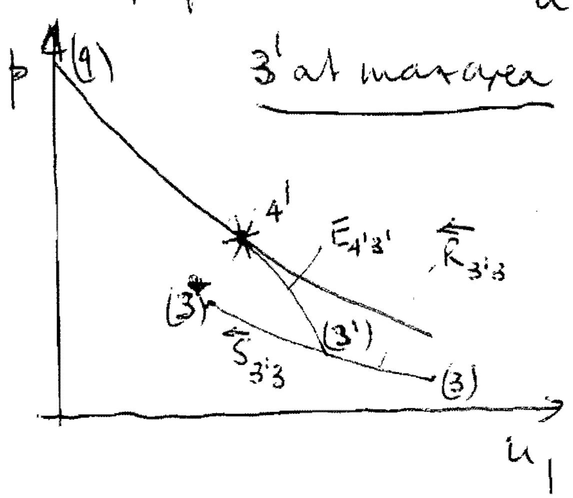

In case a) 4' is subsonic, so that an area increase is a compression. The process is the unsteady expansion $R_{44'}$ followed by the steady compression $C_{4'3}$. The same can happen when the point 4' is sonic.

If 4' is sonic, a second possibility is that the area increase causes a steady expansion to 3' ~~and~~ followed by a left facing shock $\overleftarrow{S}_{3'3}$. This solution is shown as dashed lines and corresponds to the higher u_p. With a gradual area increase, increasing u_p moves the shock wave downstream until it sits at the maximum area. Further increase of u_p then causes the shock to weaken and disappear, and finally to turn into an unsteady expansion

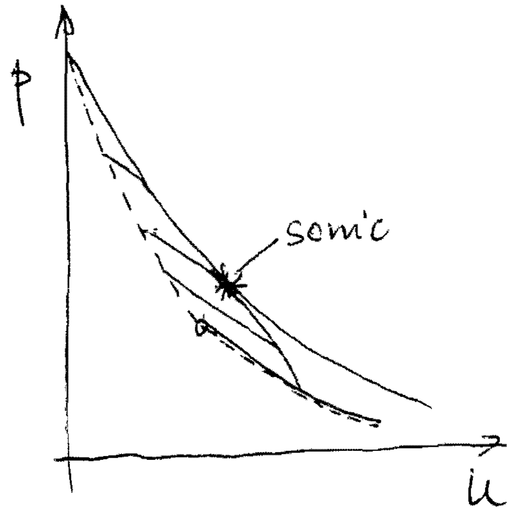

The locus of end points as u_p is increased for area increase with piston withdrawal can again be shown in the up-plane see dashed line here.

To illustrate the shock movement in the physical plane with gradual area increase, the three sketches to the left show the cases when the shock sits in the region where the area increases and the case when the wave sits at maximum area, either as a shock or as an expansion depending on the imposed speed u_3

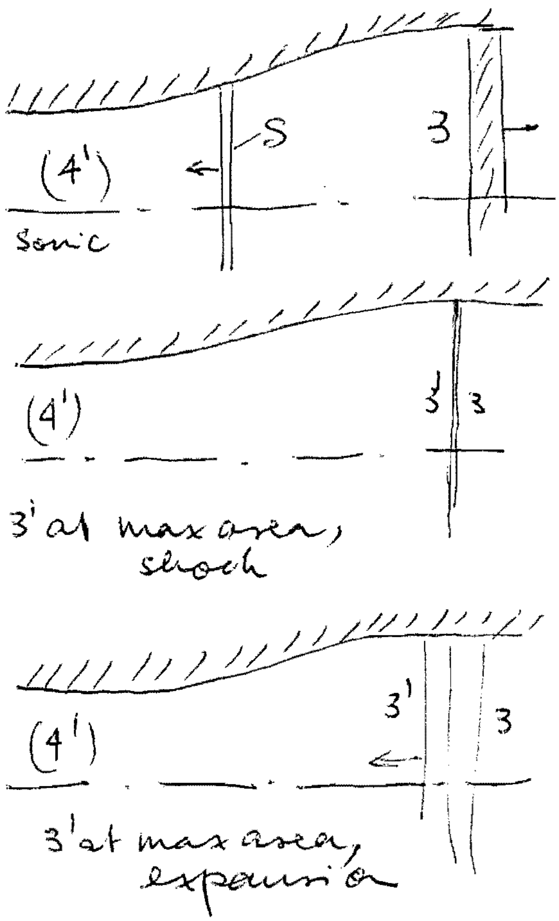

Piston withdrawal, area change with throat.

Now consider the case when a throat of Area A_* is inserted between A_4 and A_1.

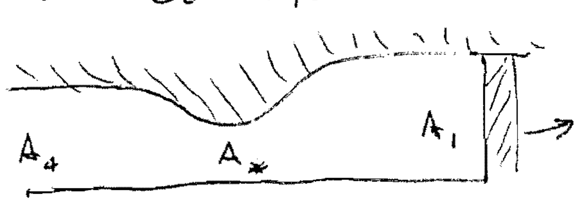

If $u_{3'}$ is smaller than a critical speed u_A,

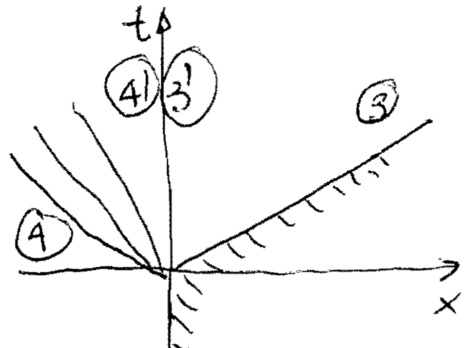

the speed at the throat does not reach sonic speed This is illustrated in the up-plane here. In that case the unsteady expansion $\overleftarrow{R}_{44'}$ is followed by the steady expansion to the throat and a steady compression back along the same path to 3'. When $u_{3'}$ exceeds u_A, the speed reaches sonic speed at the throat and expands thereafter to a supersonic speed. If there is a net area increase, the point 3' lies below $R_{44'}$, and the point 3 is reached via a shock or unsteady expansion, depending on whether $u_3 = u_p >$ or $< u_{3'}$. Similarly with net area decrease 3' lies above $\overleftarrow{R}_{44'}$

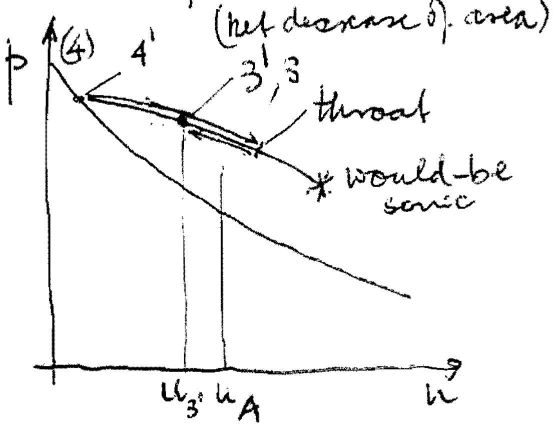

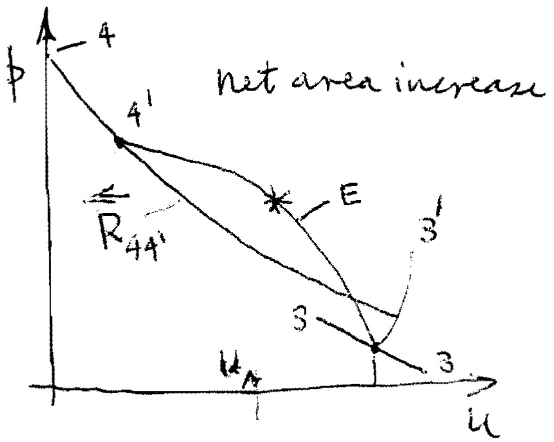

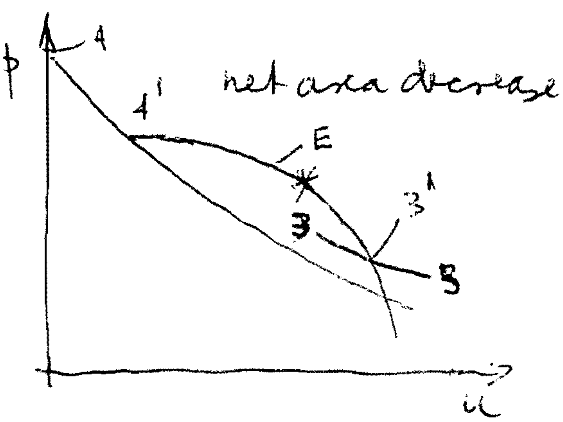

and again 3 is reached via a shock or expansion as the relative magnitude of u_3 and $u_{3'}$ changes.

However there is a difference between the cases of net area increase and decrease. In a net increase the subsonic compression takes the flow to a point to the left of $\overleftarrow{R}_{44'}$ when $u_{3'} < u_A$, and so does the shock when $u_{3'} > u_A$

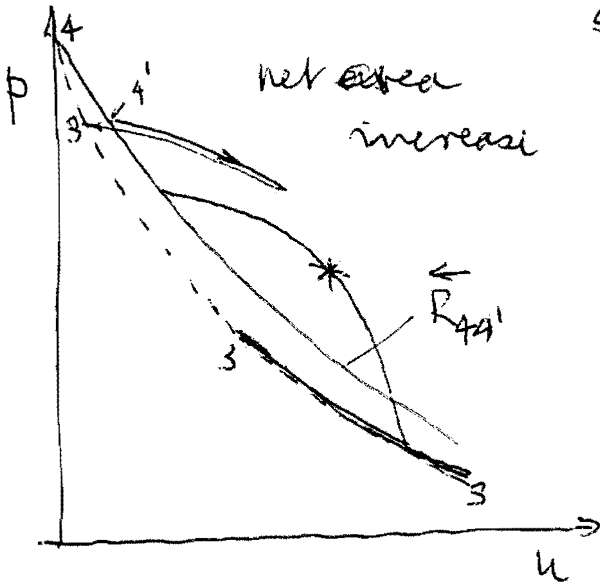

so that the locus of end points lies along the dashed curve shown here.

In contrast a net area decrease is depicted by the second sketch on p 144 and the locus of end points is illustrated by the dashed line in the bottom sketch here.

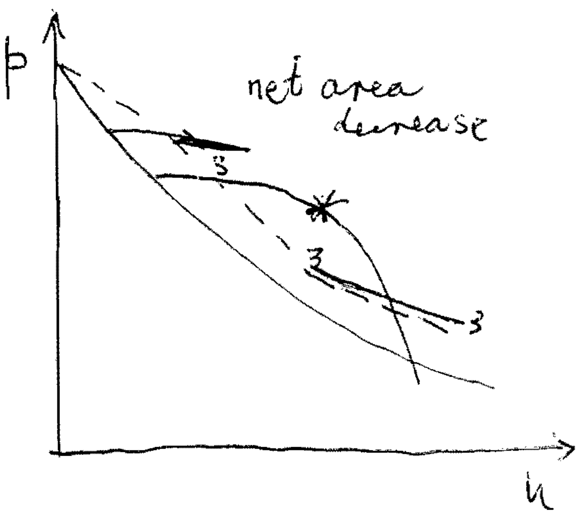

Shock tube with a throat at the diaphragm station

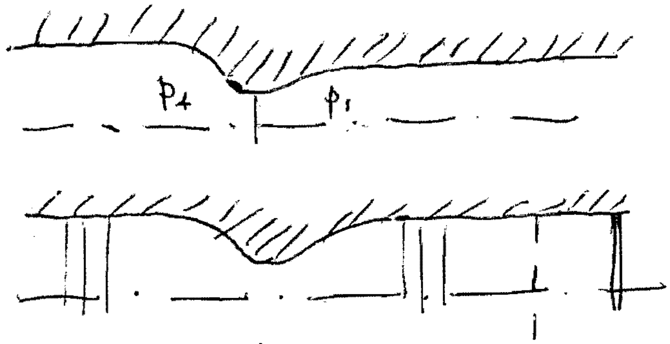

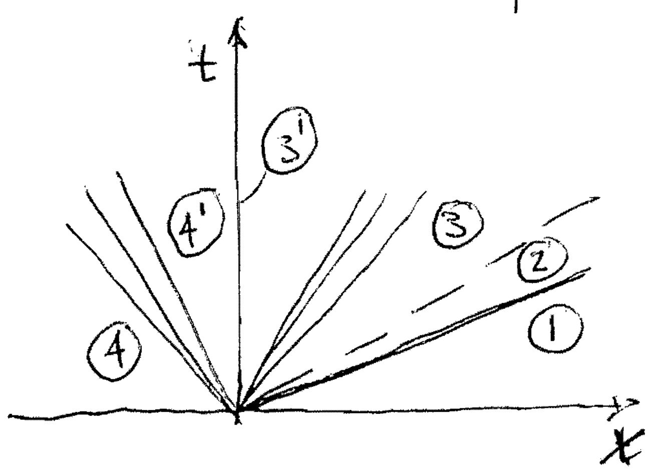

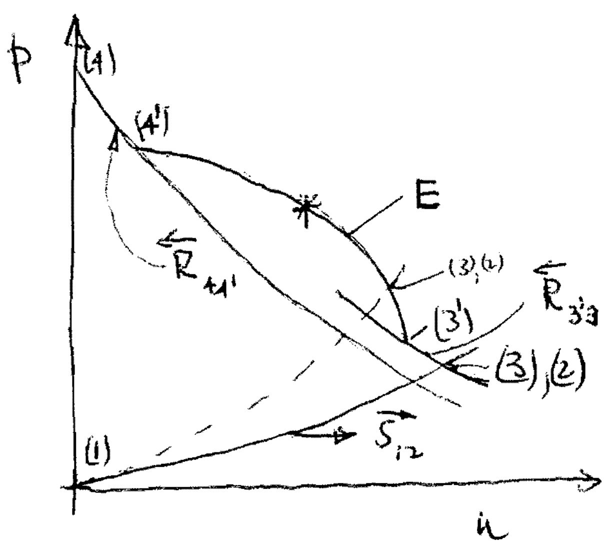

It is sometimes convenient to reduce the shock tube diameter at the diaphragm station, to be able to support the pressure difference $p_4 - p_1$ with a thinner diaphragm, that will open more quickly. This may be solved by using the up-diagram as a guide. In this case, a steady expansion occurs between two unsteady expansions, in the case when S_{12} intersects $R_{3'3}$. Alternatively (dashed S_{12}), the point 3, 2 may lie on E and the expansion $R_{3'3}$ would be eliminated, or it could be replaced by a shock. Another possibility is that $R_{44'}$ is eliminated. The equation for this shock tube may be obtained as follows.

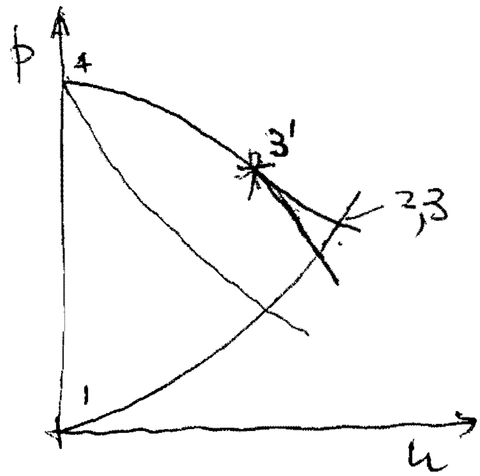

$$\frac{p_4}{p_1} = \frac{p_4}{p_{3'}}\,\frac{p_{3'}}{p_3}\,\cancel{\frac{p_3}{p_2}}^{\,=1}\,\frac{p_2}{p_1}$$

$$= \frac{p_2/p_1}{\left[\dfrac{a_{3'}}{a_4}\;\dfrac{a_3}{a_{3'}}\right]^{\frac{2\gamma}{\gamma-1}}}$$

Now $a_3 + \frac{\gamma-1}{2}u_3 = a_{3'} + \frac{\gamma-1}{2}u_{3'}$

so $$\frac{a_3}{a_{3'}} = 1 + \frac{\gamma-1}{2}M_{3'} - \frac{\gamma-1}{2}\,\frac{u_3}{a_{3'}}$$

$$= 1 + \frac{\gamma-1}{2}M_{3'} - \frac{\gamma-1}{2}\,\frac{u_2}{a_1}\,\frac{a_1}{a_4}\,\frac{a_4}{a_{3'}}$$

This leads to the solution of the shock tube equation (in the general case $4 \neq 4'$, $3' \neq *$)

$$\boxed{\frac{p_4}{p_1} = \frac{p_2/p_1}{\left[g - \frac{\gamma_4-1}{2}\,\frac{a_1}{a_4}\,\frac{u_2}{a_1}\right]^{\frac{2\gamma_4}{\gamma_4-1}}}}$$

where $$g = \sqrt{\frac{1+\frac{\gamma_4-1}{2}M_{4'}^2}{1+\frac{\gamma_4-1}{2}M_{3'}^2}}\;\frac{1+\frac{\gamma_4-1}{2}M_{3'}}{1+\frac{\gamma_4-1}{2}M_{4'}}$$

All the γ's in this are γ_4. The shock Mach number for infinite p_4/p_1 is then given by

$$\frac{M_s^2-1}{M_s} = g\left(\frac{A_4}{A^*}, \frac{A_1}{A^*}, \gamma_4\right) \frac{a_4}{a_1} \frac{\gamma_1+1}{\gamma_4-1}$$

The behavior of g is shown on the graphs p 149 ($\gamma = 5/3$) and 150 ($\gamma = 7/5$), and p 151 shows M_s as fn of $\frac{a_4}{a_1} g$

Now recall that in the ordinary shock tube, the tailored-interface reflected-shock test time τ is limited by the arrival of the reflected expansion wave. With a throat, it can be limited by the arrival (much earlier) of $\overleftarrow{R}_{33'}$ (see p. 146) Therefore the best test time is achieved by operating at a point where neither a shock $S_{33'}$ nor an expansion $R_{33'}$ occurs. This is called "steady tailoring". This condition permits us to write

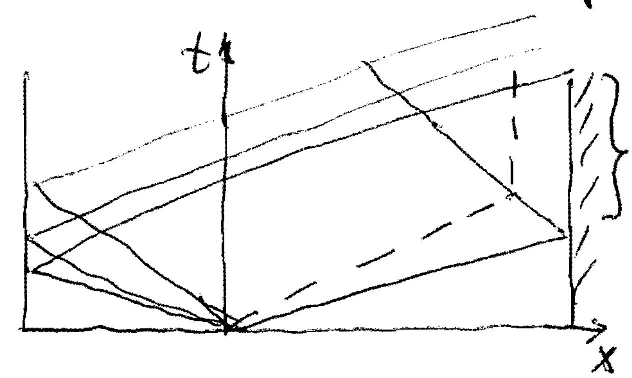

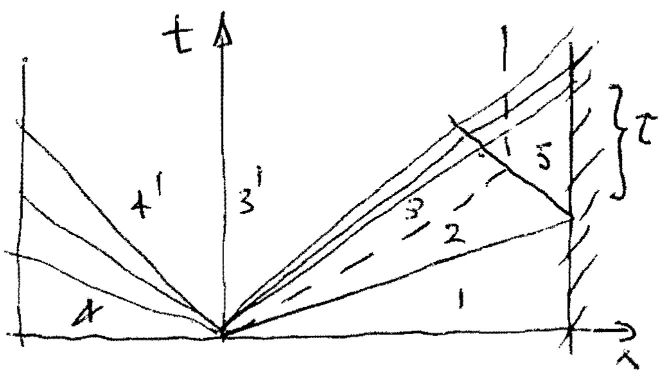

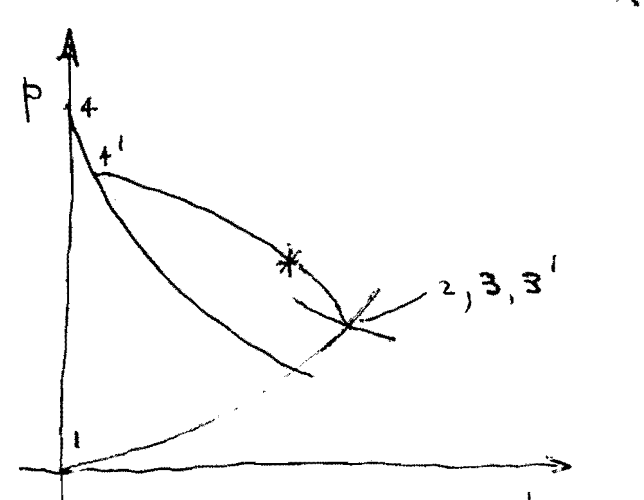

$$M_3 = M_{3'} = \frac{\frac{1}{\gamma_4} \frac{p_5 - p_2}{p_2}}{\sqrt{1 + \frac{\gamma_4+1}{2\gamma_4} \frac{p_5-p_2}{p_2}}}$$

see p 152 for condition

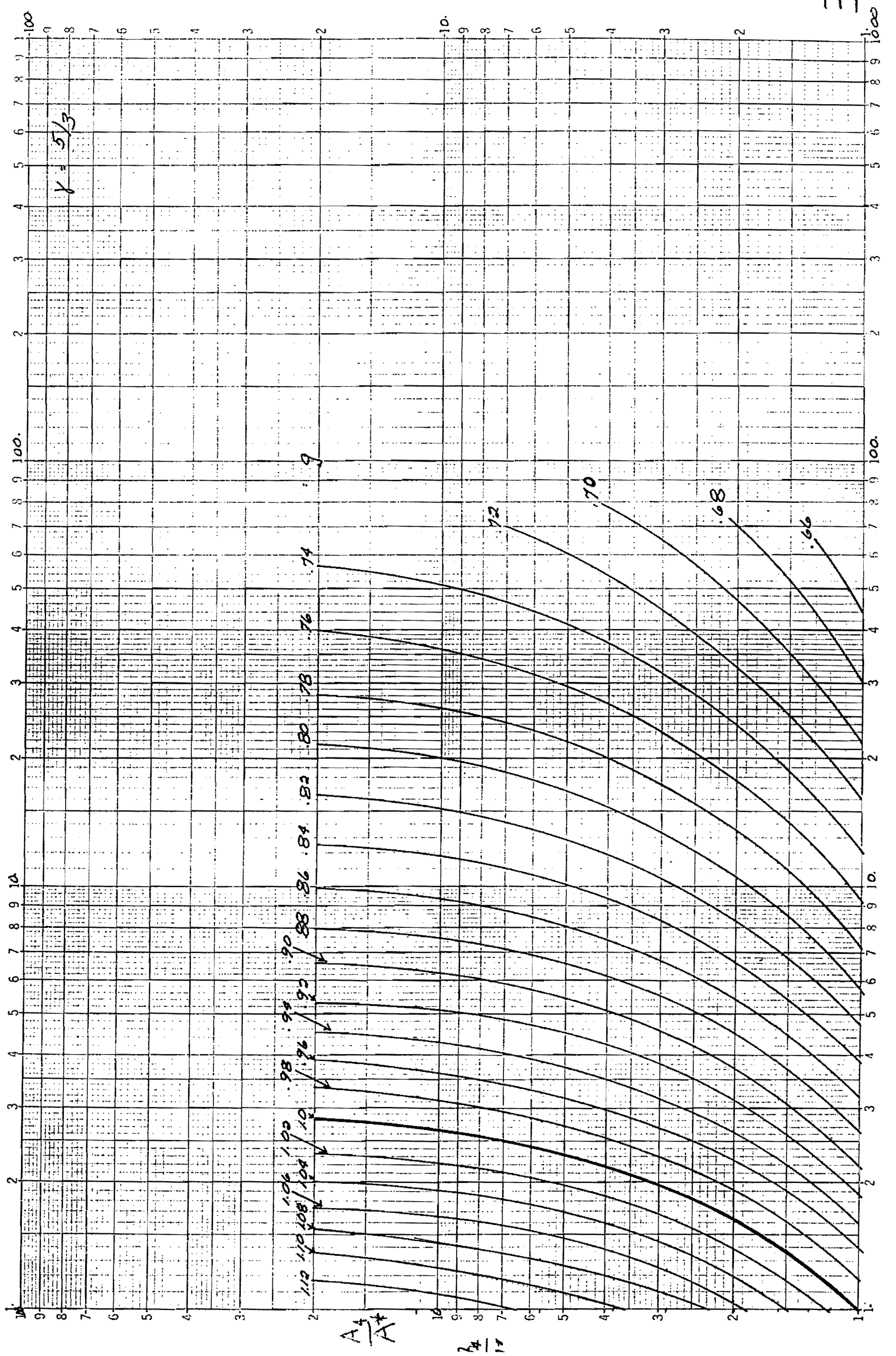
γ = 5/3
.66
.68
.70
.72
.74
.76
.78
.80
.82
.84
.86
.88
.90
.92
.94
.96
.98
1.0
1.02
1.04
1.06
1.08
1.10
1.12
A/A*

Fig. 9a

5-2-63

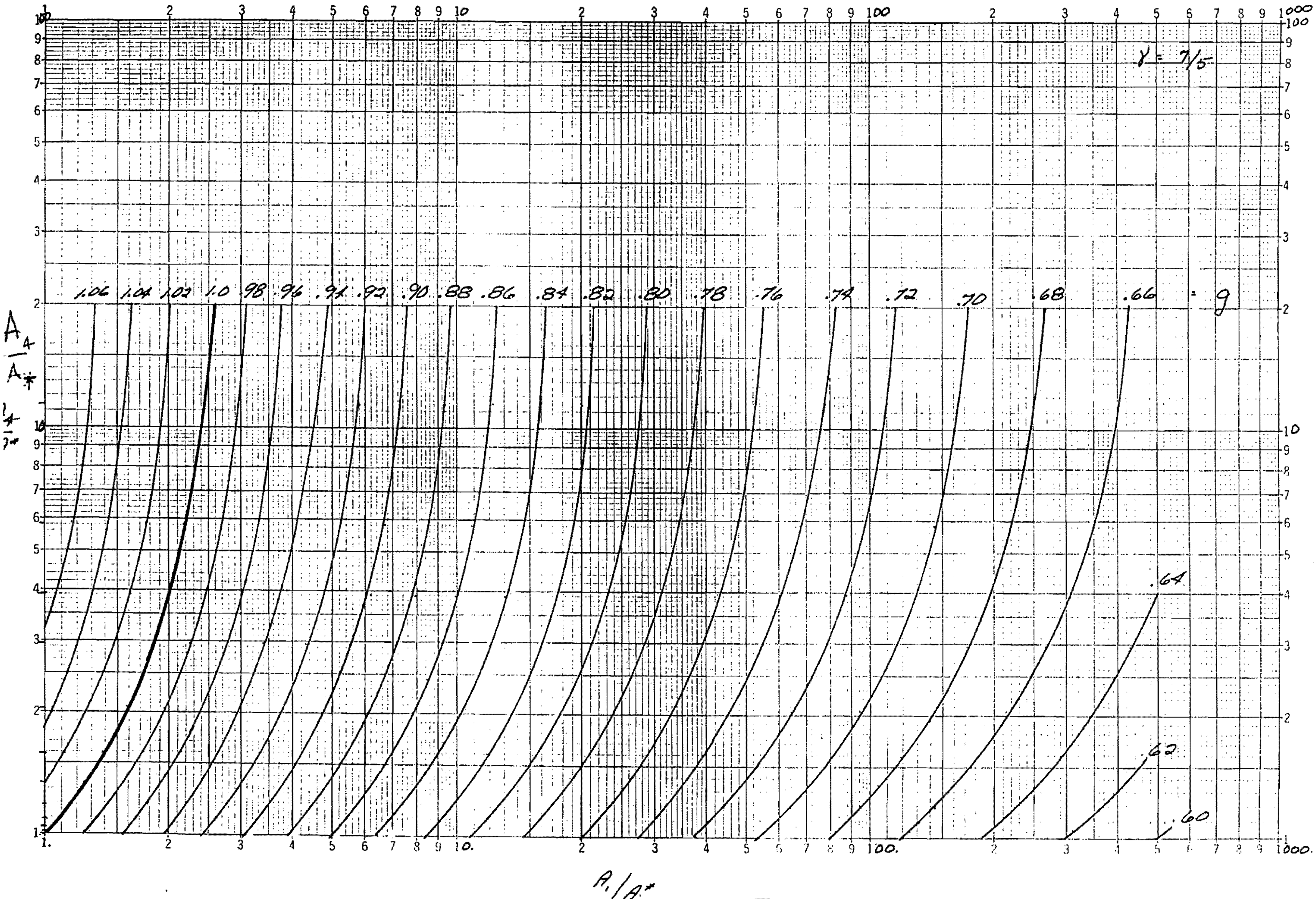
γ = 7/5
1.06 1.04 1.02 1.0 .98 .96 .94 .92 .90 .88 .86 .84 .82 .80 .78 .76 .74 .72 .70 .68 .66 = g
.64
.62
.60
A4/A*
A1/A*

Fig 9b

DOUGLAS AIRCRAFT DIVISION

JOB PAGE NO. ______ REPORT NO. ______

MODEL ______

REF. JOB PAGE NOS. ______ DATE ______

PREPARED BY ______

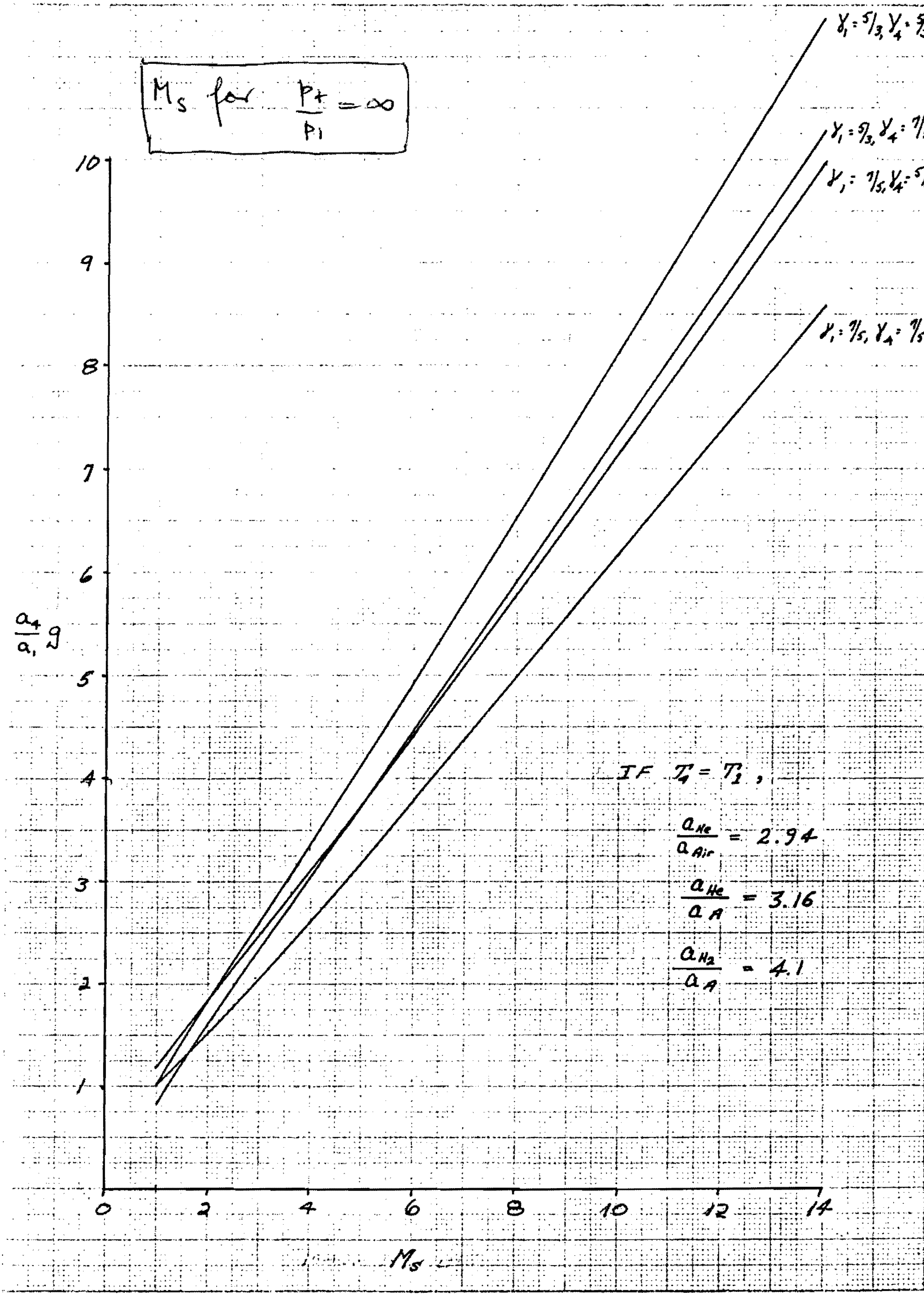

FORM 26-BP-4

K+E ALBANENE®

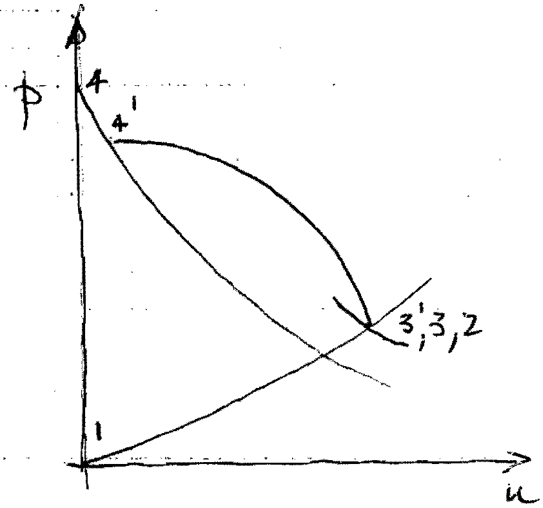

Condition for steady tailoring

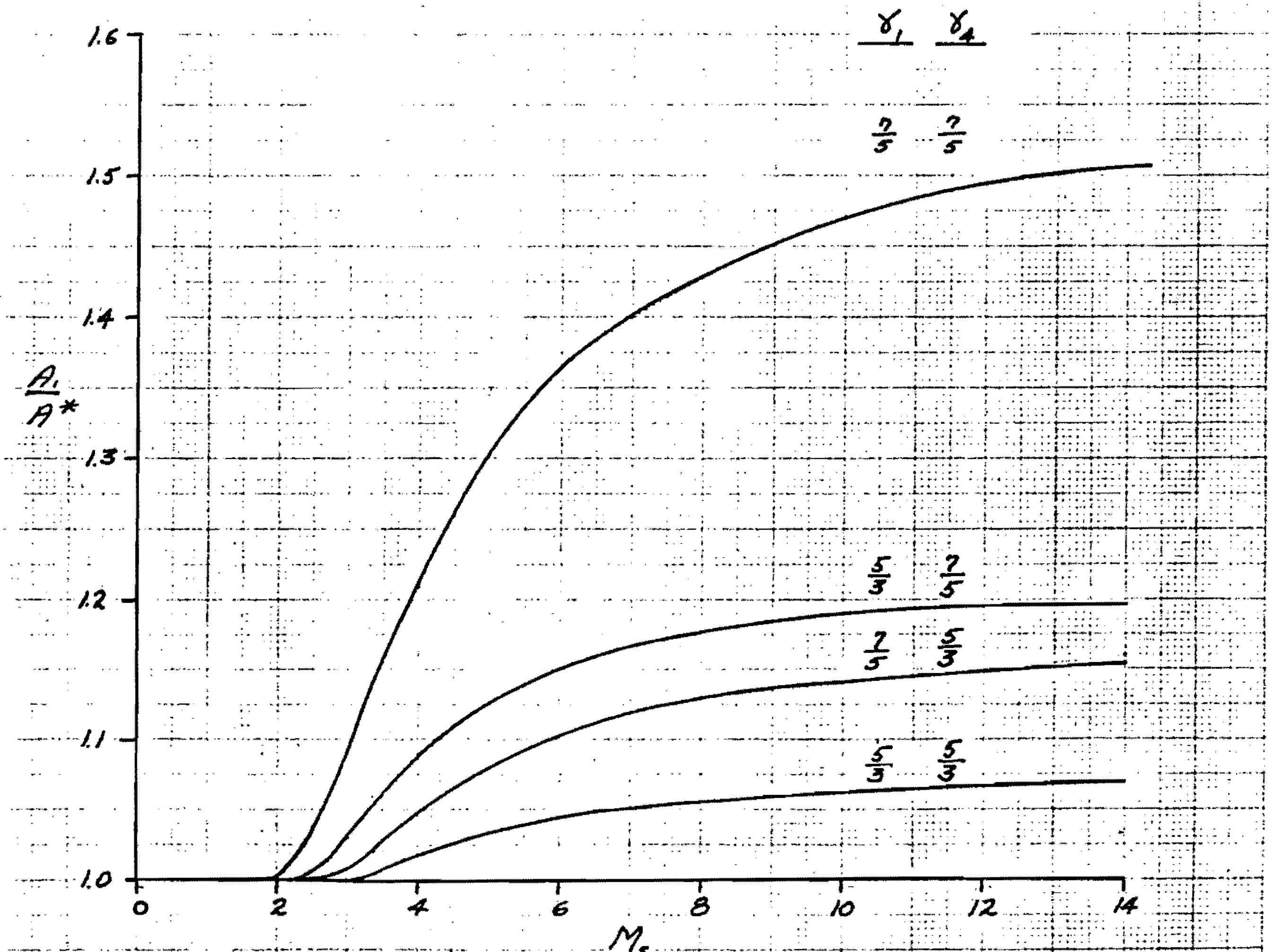

FIG. 11

(a) steady tailoring

Putting a throat at the diaphragm station therefore provides a means of adjusting the tailored-interface Mach number (see p. 152)

Interaction of a shock wave and area change

Contraction

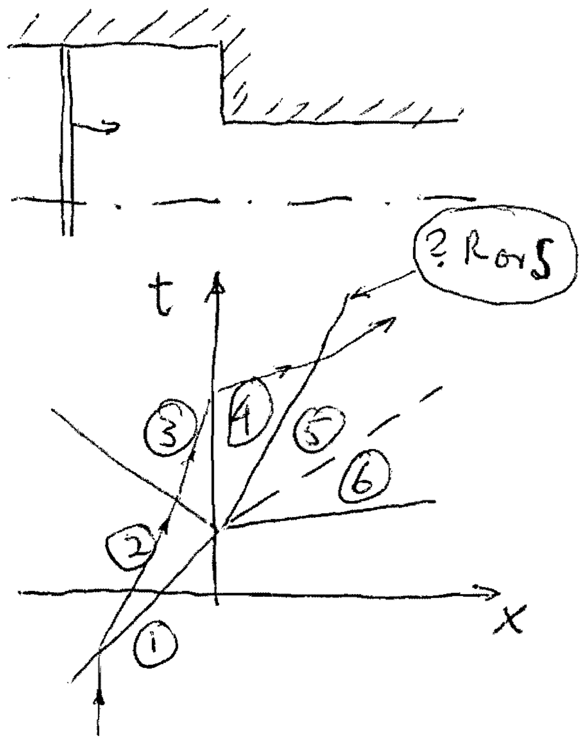

When the incident shock hits the area change a reflected shock may be propagated back. The Mach number in region 3 relative to the reflected shock is less than 1. The velocity in 3 relative to the lab is less than relative to the shock. Therefore $M_3 < 1$. Since

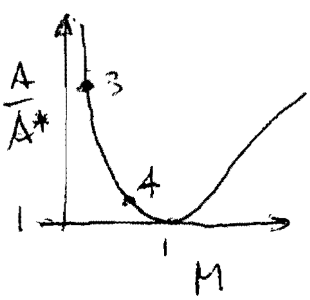

the downstream area is the minimum area in the duct, $M_4 \leq 1$. If $M_4 < 1$, the left-facing wave 45 disappears and 4 and 5 are identical. The up-diagram for this case is shown at the top of p154. The solution has to be found iteratively.

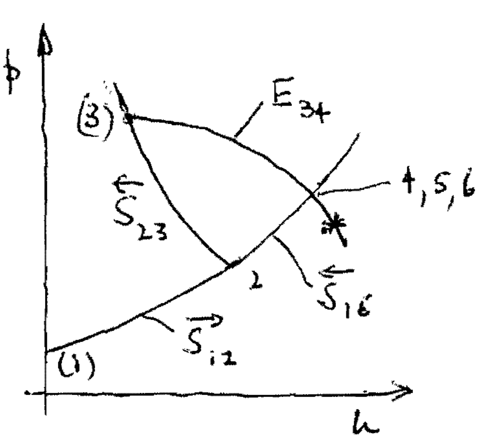

$\boxed{M_4 < 1}$

If $M_4 = 1$, the steady expansion can not take the pressure down lower than p_*, because the area does not increase. Therefore, if the region 5 has $p_5 < p_*$, an unsteady expansion has to do the job.

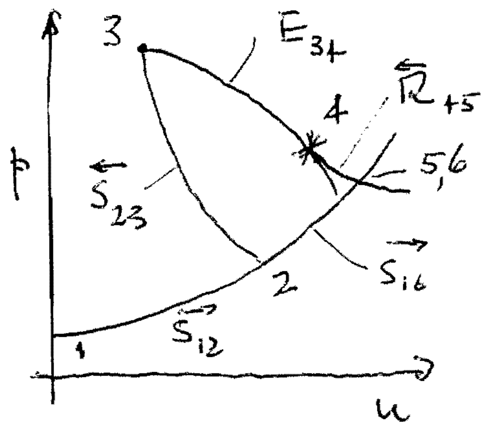

$\boxed{M_4 = 1}$

The boundary between these two cases occurs when $*$ lies on S_{16}

M_2 can be >1 or <1.

Small contraction

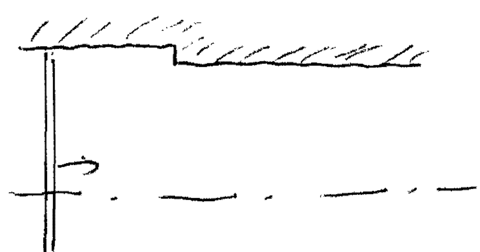

$\boxed{M_2 > 1}$

If $M_2 > 1$, The steady compression may take the point 4 to a Mach number which is

$$M_4 \geq 1.$$

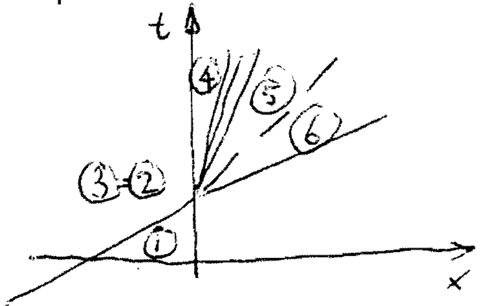

$\boxed{M_4 > 1}$

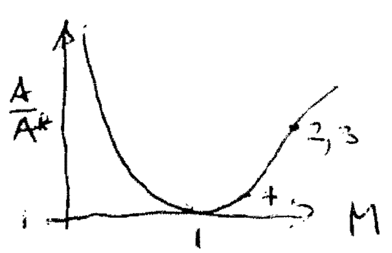

The up-diagram for $M_4 > 1$ is shown at the top of p 155

When $M_4 = 1$, the point 4 lies on the $*$ of C.

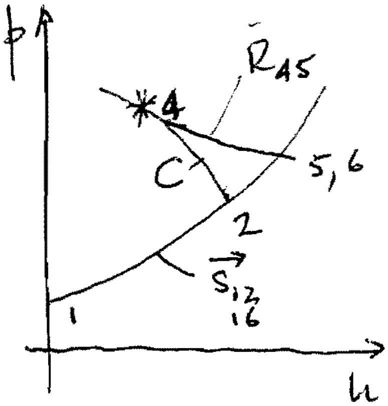

$\boxed{\begin{array}{l} M_2 > 1 \\ M_4 > 1 \end{array}}$

If $M_2 < 1$, a reflected shock occurs and the situation is the same as that shown at the top of p 154.

Area expansion

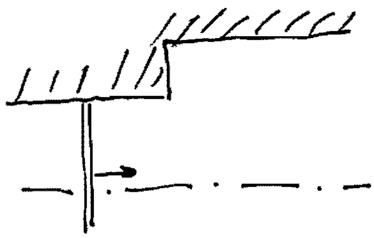

If $M_2 > 1$ there will be no left-facing wave back into the smaller area

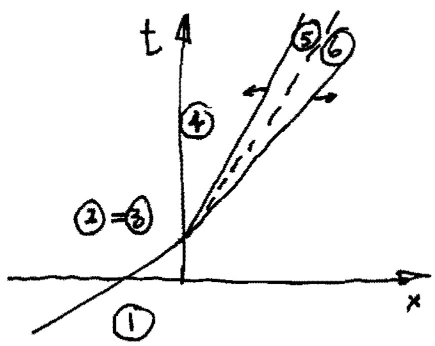

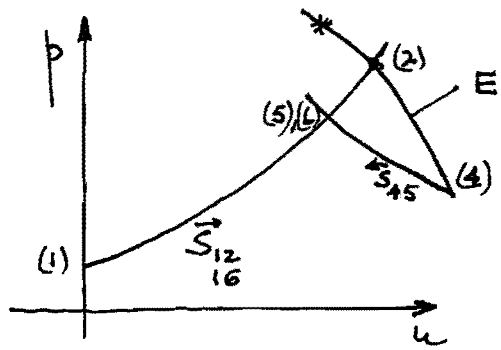

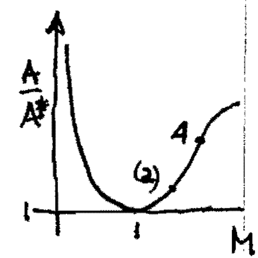

A left-facing shock $\overleftarrow{S}_{46}$ gets convected downstream because u_4 is larger than the shock speed relative to the gas in region 4. Also, the transmitted shock $\vec{S}_{16}$ precedes this and a density interface separates 5 and 6.

If the area change is gradual, it is possible that the left-facing shock becomes stationary and sits in the area expansion. The location of the shock depends on the strength of $\vec{S}_{12}$.

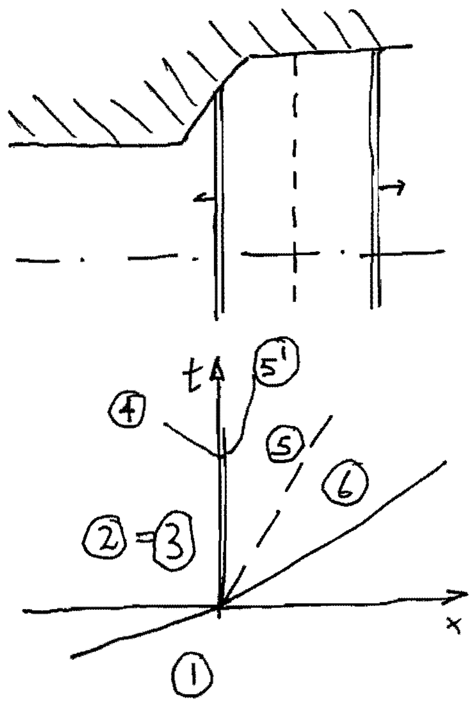

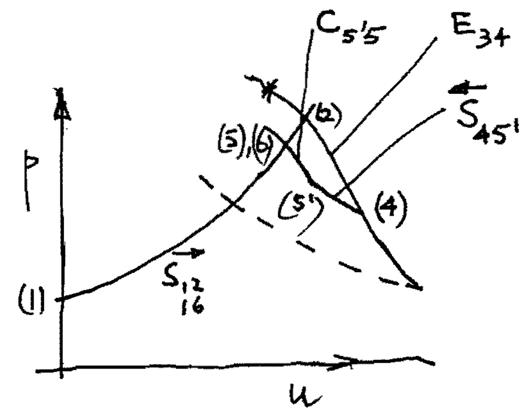

<u>If $M_2 < 1$</u> an unsteady expansion will propagate to the left. Since the left area is the minimum area

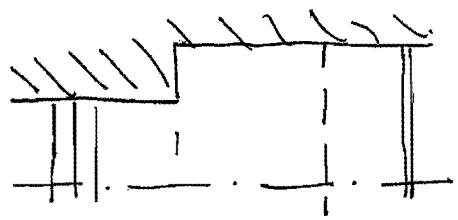

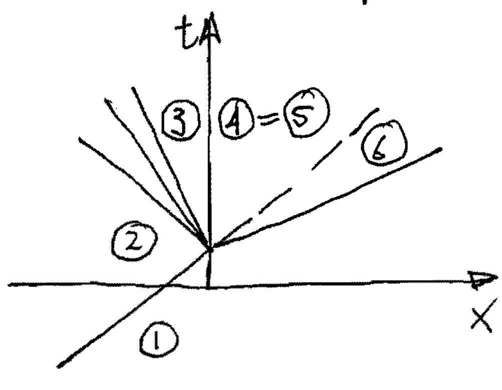

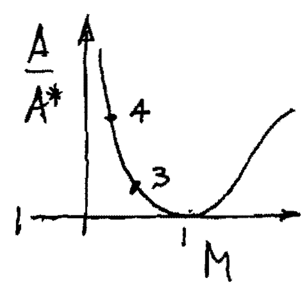

M_3 must be less than or equal to 1. If $M_3 < 1$ so that $M_4 < M_3$, then region 4 is subsonic. In that case, the up-diagram is as shown here, with $\overleftarrow{R}_{23}$ not reaching the sonic point on the ~~extension~~ of the steady compression C_{34}

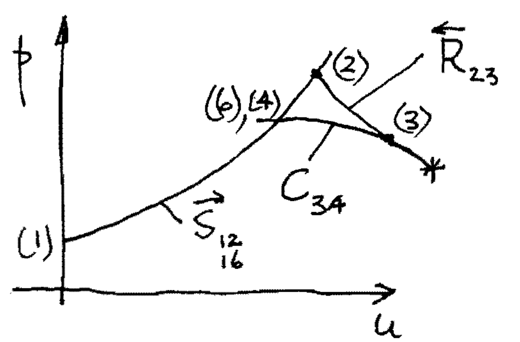

On the other hand, if $M_3 = 1$, it is possible that the flow becomes supersonic in the larger area, giving rise to a left-facing shock

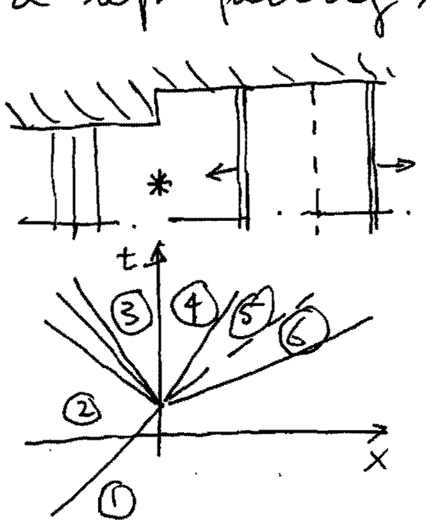

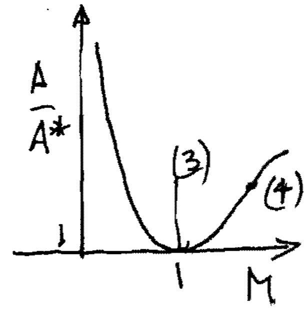

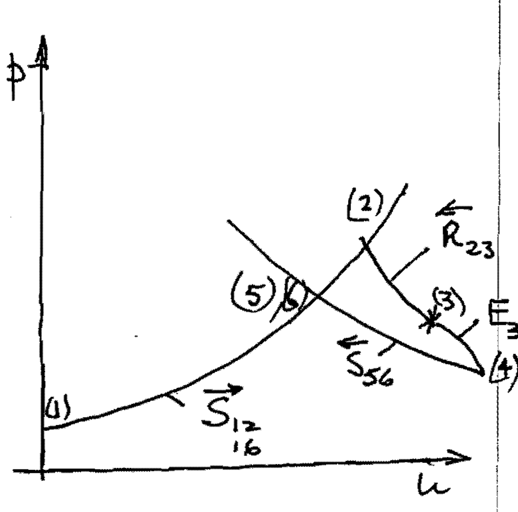

In this case, a gradual area increase would also afford the possibility of the left-facing shock sitting at some point in the area expansion.

<u>The starting process in a shock tunnel nozzle.</u>

In a shock tunnel a nozzle is attached to the downstream end of a shock tube, so that the reflected-shock region of the shock tube acts as the reservoir for a supersonic wind tunnel. In order to make the nozzle flow start

properly, the pressure at the downstream end must be low initially.

It is therefore necessary to separate this low p_D from the higher p_1 by a light diaphragm at the throat. The area of the throat is usually small compared to the shock tube area, so that the reflected shock conditions can be approximated by a closed end. At early times, i.e., when the transmitted shock is still close to the throat, the processes can be modelled crudely by a double step in area.

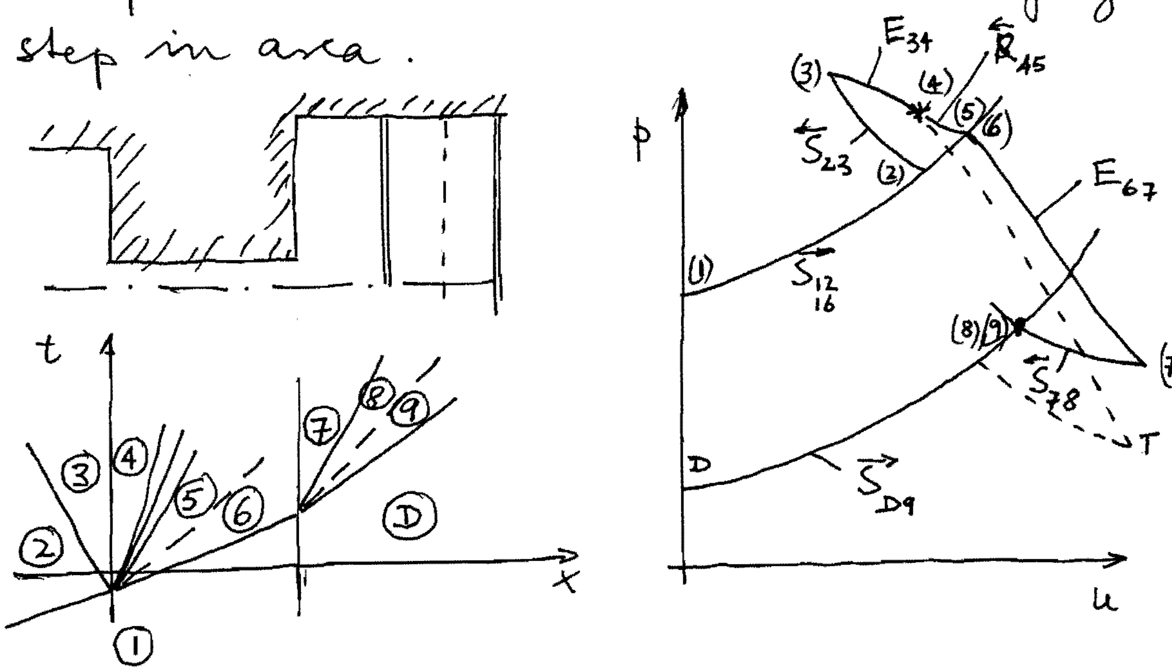

The complex pattern of waves generated will eventually all be washed down through the nozzle, and only a steady expansion from 4 to the test section condition T and the backward facing shock (downstream of the test section) will remain. (see dashed lines in the up-diagram). When this condition is established the flow is considered to have "started", because it is the beginning of steady flow in the test section. The starting process is important because it reduces available test time.

Small area change

When the area change is small, the waves 23 and 45 are weak, even if the incident and transmitted shock are strong. In that case we can make

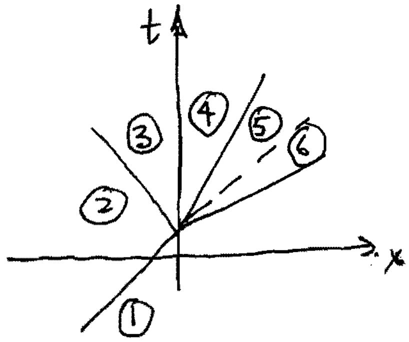

use of the fact that, in steady flow,

$$\Delta p = \rho u \, \Delta u$$

and in unsteady flow,

$$\Delta p = \rho a \, \Delta u ,$$

and treating ρu and ρa as constant average values across the wave, so that both of these will be short straight lines in the up-diagram. The result may be summarized in the following table.

Contraction | Expansion

$M_2 < 1$

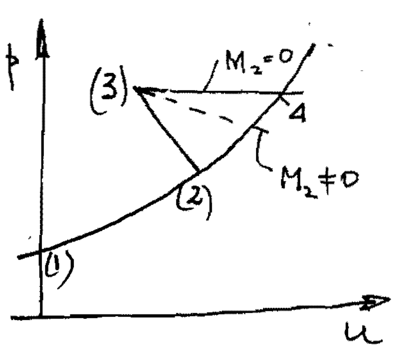

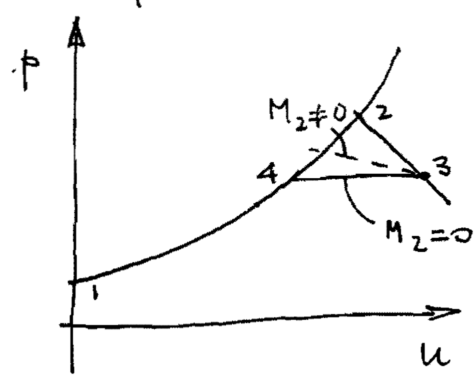

$M_2 > 1$

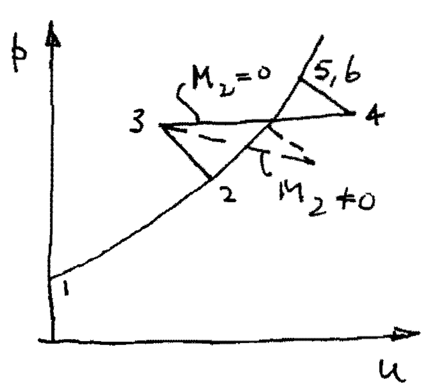

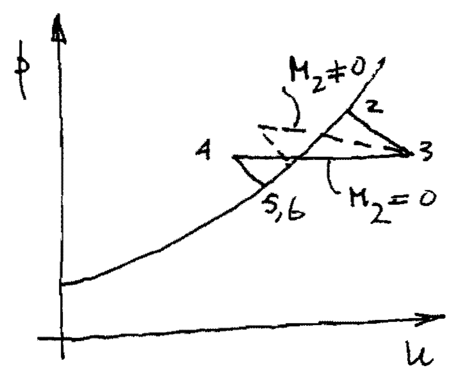

Ae237 Regions in which different shock-area change interactions occur. 160

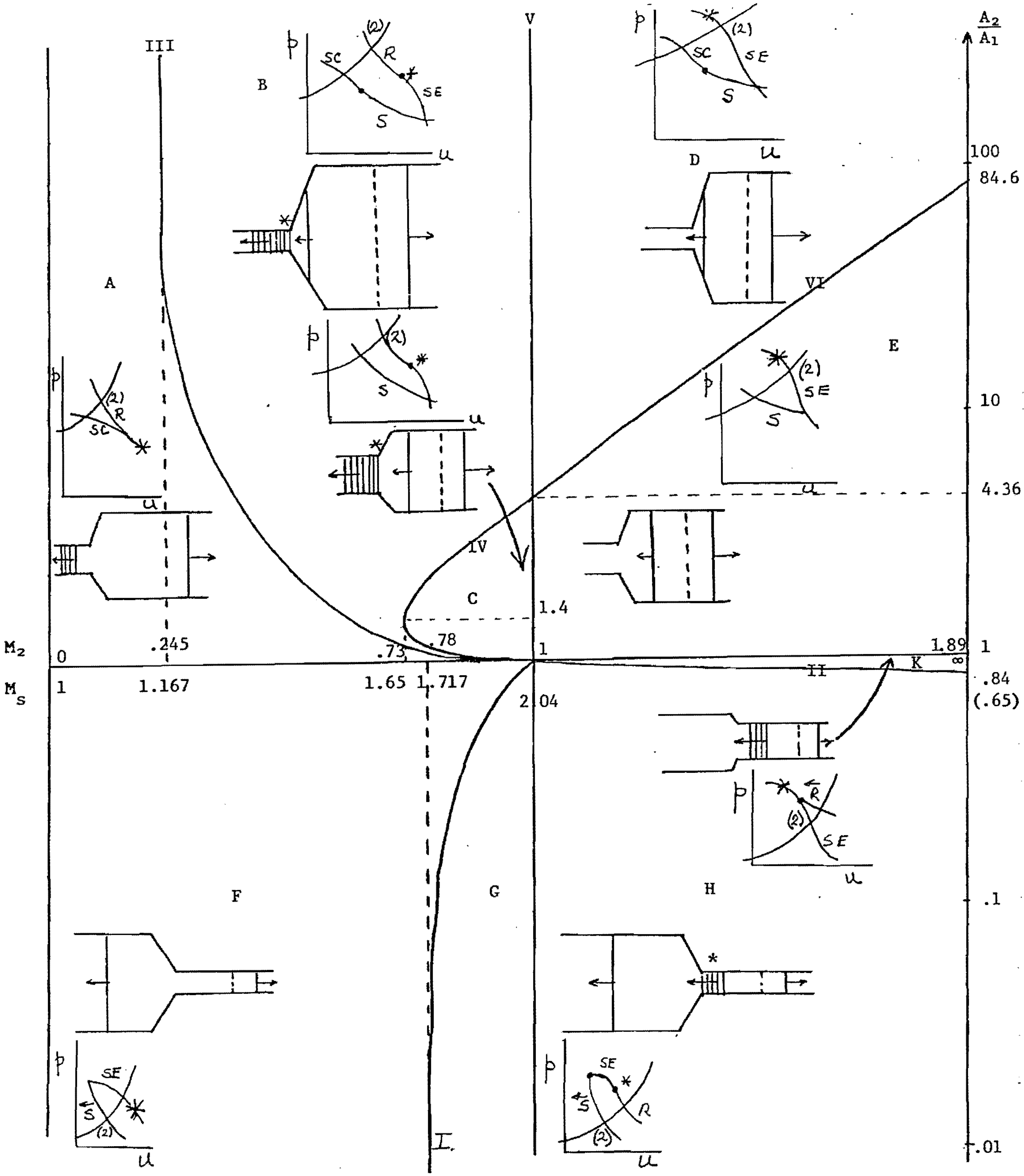

The graph on p. 160 is a plot of A_2/A_1 in a duct with area change against the incident shock Mach number for $\gamma = 7/5$. ~~Thes~~ M_S ranges from 1 to ∞ and A_2/A_1 from 0.01 to 100. Also plotted on the abscissa is M_2. The graph shows as insets the wave configurations after the interactions as well as up-sketches. The boundaries between the interaction types are plotted, separating eight distinct types. This plot was made by a graduate student who took Ae 237 many years ago and became interested in these case distinctions (Dr John Torczinsky, now at Sandia Labs)

Weak waves

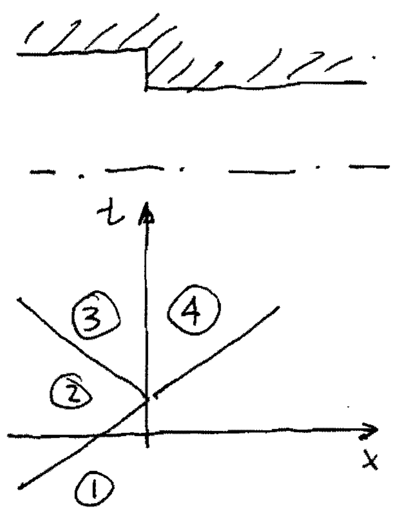

For weak waves the post-shock Mach number is well approximated by $M_2 = M_4 = 0. = M_3$
Therefore a steady process will be a horizontal line in up-space

$$\Delta p = \pm \rho u \Delta u$$

Also, the density will be constant except across waves, so that a steady process gives $uA = \text{const.}$

A non-steady wave obeys $\Delta p = \pm \rho a \Delta u$

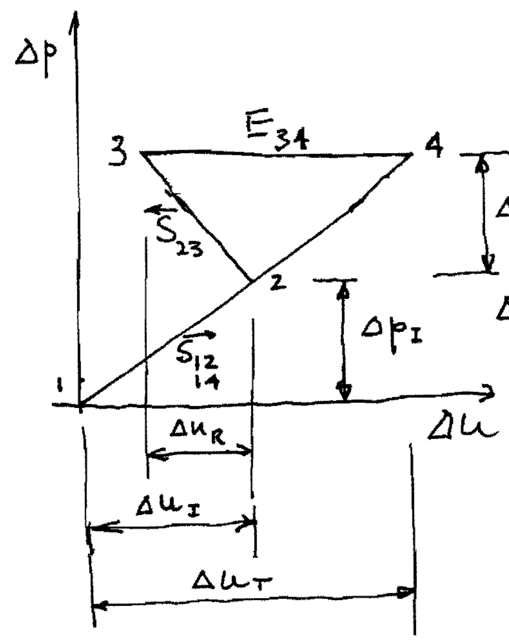

Denoting the incident and reflected waves by subscripts I and R respectively, the up-diagram is as shown here for a contraction. Subscript T for transmitted wave

For the unsteady waves,

$$\Delta p_I = \rho a \,\Delta u_I \quad \text{or} \quad \Delta p_{12} = \rho a \,\Delta u_{12}$$

$$\Delta p_R = -\rho a \,\Delta u_R \quad \text{or} \quad \Delta p_{23} = -\rho a \,\Delta u_{23}$$

$$\Delta p_T = \rho a \,\Delta u_T \quad \text{or} \quad \Delta p_{14} = \rho a \,\Delta u_{14}$$

for the steady process,

$$u_3 = u_4 \frac{A_2}{A_1}$$

$$= (u_4 - u_3 + u_3)\frac{A_2}{A_1}$$

$\Delta u_R = u_3 - u_2$

$u_3 - u_4 = 2(u_3 - u_2)$

$$= (-2\Delta u_R + u_3)\frac{A_2}{A_1}$$

or $$u_3\left(1 - \frac{A_2}{A_1}\right) = -2\Delta u_R \frac{A_2}{A_1}$$

i.e. $$(u_3 - u_2 + u_2 - \underbrace{u_1}_{=0})\left(1 - \frac{A_2}{A_1}\right) = -2\Delta u_R \frac{A_2}{A_1}$$

$$(\Delta u_R + \Delta u_I)\left(1 - \frac{A_2}{A_1}\right) = -2\Delta u_R \frac{A_2}{A_1}$$

$$\Delta u_R\left(1 + \frac{A_2}{A_1}\right) = \Delta u_I\left(\frac{A_2}{A_1} - 1\right)$$

$$\boxed{\Delta u_R = \Delta u_I \cdot \frac{\frac{A_2}{A_1} - 1}{\frac{A_2}{A_1} + 1}}$$

Also:
$$\Delta u_T = \Delta u_I - \Delta u_R$$

$$\Delta p_T = \Delta p_I + \Delta p_R$$

$$\boxed{\frac{\Delta p_R}{\Delta p_I} = -\frac{\Delta u_R}{\Delta u_I} = \frac{1 - \frac{A_2}{A_1}}{\frac{A_2}{A_1} + 1}}$$

<u>Pressure transmission coefficient</u>

This is defined by $\quad T_p \equiv \frac{\Delta p_T}{\Delta p_I}$

$$T_p = \frac{\Delta p_T}{\Delta p_I} = 1 + \frac{\Delta p_R}{\Delta p_I}$$

$$= 1 + \frac{1 - \frac{A_2}{A_1}}{\frac{A_2}{A_1} + 1}$$

$$\boxed{T_p = \frac{2}{\frac{A_2}{A_1} + 1}}$$

Similarly

$$R_p = \frac{1 - A_2/A_1}{1 + A_2/A_1} \quad \text{reflection coefficient}$$

$$T_u = \frac{2}{\frac{A_2}{A_1} + 1} \quad \text{velocity transm coeff.}$$

$$R_u = \frac{\frac{A_2}{A_1} - 1}{\frac{A_2}{A_1} + 1} \quad \text{vel. refl. coeff.}$$

Limiting cases for weak waves

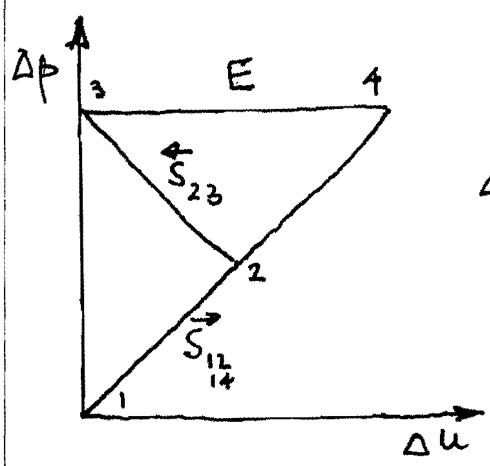

$\boxed{\dfrac{A_2}{A_1} = 0}$

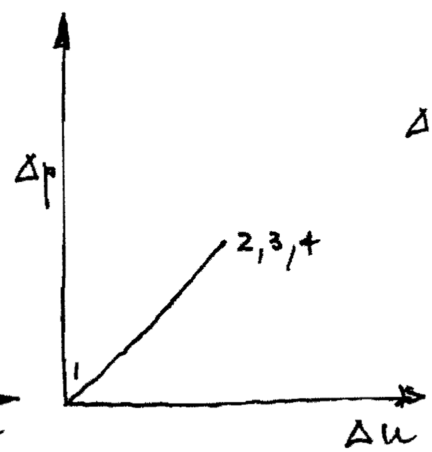

$\boxed{\dfrac{A_2}{A_1} = 1}$

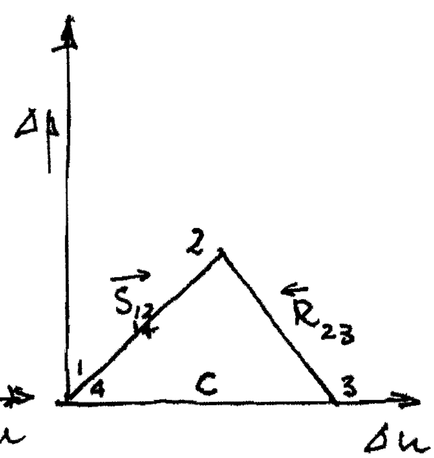

$\boxed{\dfrac{A_2}{A_1} = \infty}$

In the limiting case $A_2/A_1 = 0$, the reflected weak shock has the same strength as the incident weak shock, so 3 lies on the Δp axis. $T_p = 2$, so the transmitted shock has twice the strength of the incident shock $\Delta p_T = 2\,\Delta p_I$, $\Delta u_T = 2\Delta u_I$.

The case $A_2/A_1 = 1$ is trivial.

If $A_2/A_1 = \infty$, a reflected expansion occurs, with the same strength as the incident shock, and $T_p = 0$ so S_{14} has zero strength. The steady area increase decreases Δu to zero.

Two-dimensional flows

Interaction of shock waves with bodies and interfaces

Examples:

Shock diffracting around a cylinder.

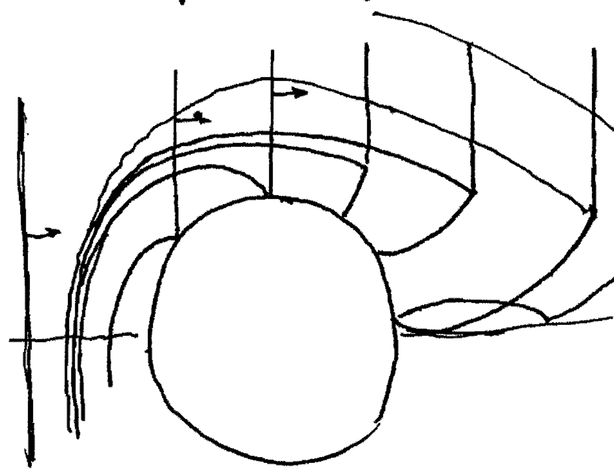

This flow starts with the incident shock being reflected in a regular reflection that later becomes a Mach reflection that exhibits a point where three shocks meet. The Mach stem then reflects from the symmetry plane behind the cylinder. If the body were a sphere instead of a cylinder, the convergence of the Mach stem onto the symmetry axis would cause it to become very strong and produce a local hot spot at the downstream end of the sphere.

Shock refraction at a density interface

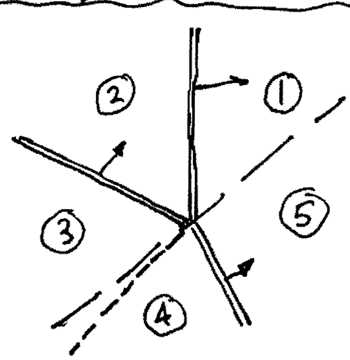

In this flow, a number of possibilities exist. The one shown here is rela tively simple, exhibiting three shocks and an interface deflection. If the speed of sound in 5 is much larger than that in ①, the shock S_{54} will move ahead of S_{12} and itself will interact with the interface, generating a weak precursor wave P.

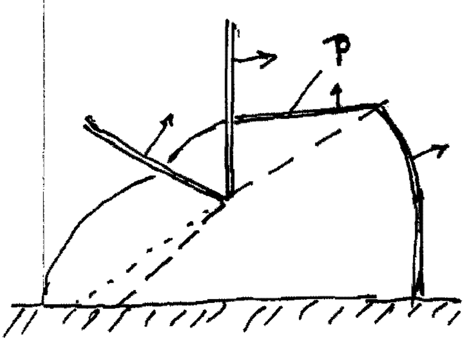

Shock focussing

Whenever, through interaction with a concave body or for other reasons, a shock is deformed to be concave toward the front, it will focus to form a regular reflection if it is weak or a Mach reflection if it is stronger. This is used, for example, in the focussing of weak shocks for the "non-intrusive" breaking of kidney stones.

Interaction of a shock with a wedge.

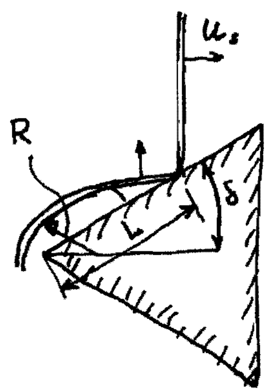

If the wedge angle δ is sufficiently large, a regular reflection will occur. This flow has a number of interesting features. First, if we consider this to be a flow in which no gas imperfections occur, and viscous and heat-conduction effects may be neglected, then any dimensionless quantity Q may be written

$$Q = Q(\gamma, M_s, \delta)$$

Thus, the dimensionless radius of curvature R/L

$$\frac{R}{L} = \frac{R}{L}(\gamma, M_s, \delta)$$

will be independent of time. Hence $R \propto L \propto t$. All length scales exhibited by the flow grow linearly with time, though the flow is unsteady.

However, we can also view the flow in the immediate vicinity of the reflection point as viewed from a reference frame that moves with the reflection point. Then we see a <u>steady</u> flow

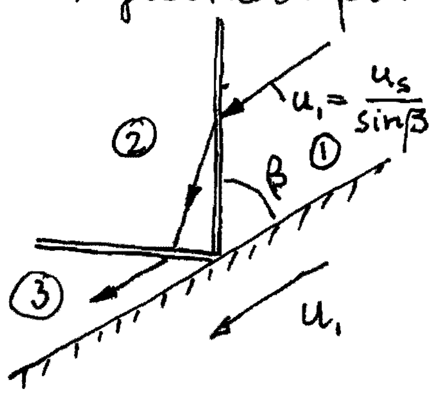

in which the wall moves parallel to itself with a speed

$$u_1 = \frac{u_s}{\sin\beta}$$

as does the gas to the right of the incident shock. The "incident" shock deflects the flow toward the wall, and we need a reflected shock to deflect the flow back to a direction parallel to the wall. In this frame the shocks are fixed and this part of the flow is steady.

Note that this is not true for the whole flow field, since, as we have seen, e.g., the radius of curvature of the shock near the wedge tip grows linearly with time. The only part of the flow field that may be transformed to a steady flow by the Galilean transformation is that which contains no length scales. Any conclusions drawn from the similarity of this flow with a steady one must therefore be treated with extreme caution and be restricted to topics that do not involve boundaries.

We now ask the following question:
Since there <u>is</u> a characteristic length scale in this problem (L), how come we can find a region of the flow in which it doesn't manifest itself?

The reason must be that this region does not know anything about L. Thus, if the reflection point moves away from the wedge tip faster than the sonic signal can follow, then there is a region ahead of the sonic signal that knows nothing about recent developments at the wedge tip, or even of its existence.

Therefore, a necessary condition for regular reflection with a locally straight reflected shock is that $M_3 > 1$.

<u>Oblique Shock Waves.</u>

To study shock reflection in more detail we need to recall the shock jump conditions for oblique shocks.

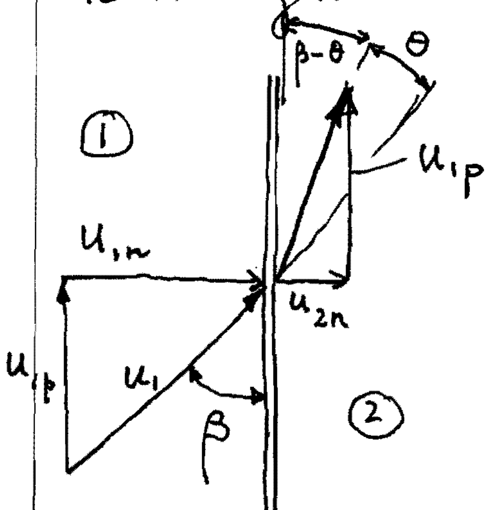

Take a steady normal shock with inflow u_{1n}, outflow u_{2n}. Perform a Galilean transformation to a frame moving parallel to the shock at a speed $-u_{1p}$. The flow seen by an observer in this frame is the normal shock flow with a superimposed uniform velocity field of $+u_{1p}$. The angle β between the shock and the upstream flow is therefore
$$\beta = \arctan \frac{u_{1n}}{u_{1p}}$$
and the flow deflection angle θ can be found from
$$\beta - \theta = \arctan \frac{u_{2n}}{u_{1p}}$$
This immediately gives the useful result
$$\frac{u_{1n}}{u_{2n}} = \frac{\rho_2}{\rho_1} = \frac{\tan\beta}{\tan(\beta-\theta)}.$$
Since the uniform superposed flow does not change the jump conditions of the normal shock, they may be written down straightforwardly by replacing M_1 in the normal-shock

relations by $M_1 \sin\beta$ for the oblique-shock relations.

$$\frac{p_2}{p_1} = 1 + \frac{2\gamma}{\gamma+1}\left(M_1^2 \sin^2\beta - 1\right)$$

$$\frac{\rho_2}{\rho_1} = \frac{\gamma+1}{\gamma-1 + 2/(M_1^2 \sin^2\beta)} = \frac{\tan\beta}{\tan(\beta-\theta)}$$

$$\frac{T_2}{T_1} = \frac{p_2}{p_1} \cdot \frac{\rho_1}{\rho_2}$$

$$M_2^2 \sin^2(\beta-\theta) = \frac{1 + \frac{\gamma-1}{\gamma+1}\left(M_1^2 \sin^2\beta - 1\right)}{1 + \frac{2\gamma}{\gamma+1}\left(M_1^2 \sin^2\beta - 1\right)}$$

$$\tan\theta = \cot\beta \cdot \frac{M_1^2 \sin^2\beta - 1}{\frac{\gamma+1}{2} M_1^2 - \left(M_1^2 \sin^2\beta - 1\right)}$$

In earlier discussions the up-plane was a useful tool, because p and u are continuous across density interfaces in non-steady flows. In steady flows, pressure and flow angle are continuous across density interfaces. Therefore, the θp-plane will be a useful tool in this topic, as we will see later. The locus of an oblique shock in the θp-plane is as shown here for a given M_1 and γ.

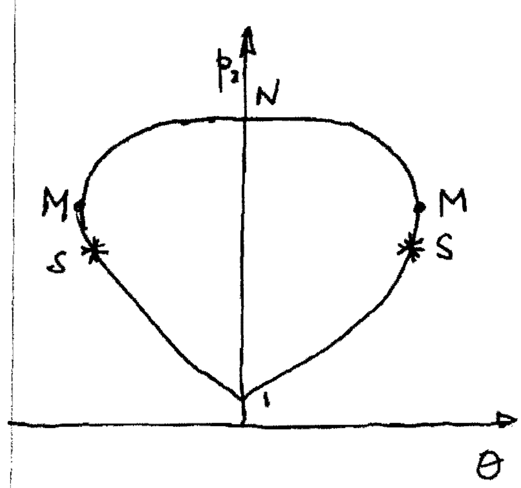

At the point 1, the wave is infinitesimally weak so that $\beta = \arcsin(1/M_1)$. As we increase β, the flow deflection ~~angle~~ θ increases and the downstream Mach number decreases, while p_2 increases, until $M_2 = 1$ at the point $*S$. Just a little more increase in β brings us to the maximum deflection point M. Further increase in β causes θ to decrease and p_2 to increase until we reach the normal-shock point N on the p_2-axis. The curve is symmetrical around the p_2-axis, of course.

Weak-shock limit.

Here, θ and $M_1^2 \sin^2\beta - 1$ are small, so that we may approximate

$$\sin\beta = \frac{1}{M_1} \quad , \quad \tan\beta = \frac{1}{\sqrt{M_1^2-1}}$$

$$\theta \doteq \tan\theta = \sqrt{M_1^2-1} \cdot \frac{2}{\gamma+1} \, \frac{M_1^2\sin^2\beta - 1}{M_1^2}$$

$$\frac{p_2-p_1}{p_1} = \frac{2\gamma}{\gamma+1}\left(M_1^2\sin^2\beta - 1\right)$$

i.e.

$$\boxed{\frac{\Delta p}{p_1} = \frac{\gamma M_1^2}{\sqrt{M_1^2-1}}\,\theta}$$

This may be used to get the slope of the shock locus in the θp-plane near the point 1.

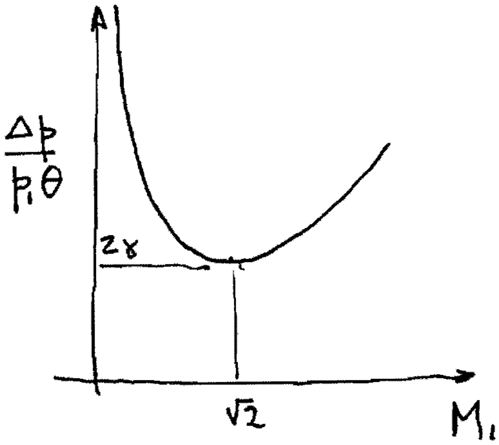

This slope has a minimum value of 2γ at $M_1 = \sqrt{2}$.

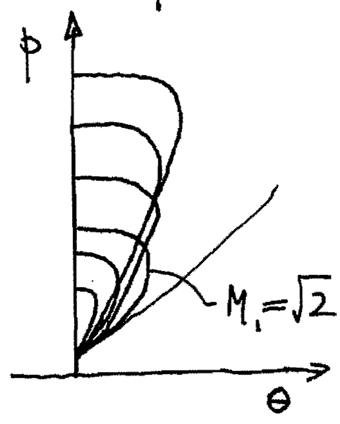

Similarly, it may be shown that

$$\frac{\Delta u}{u_1} = -\theta \tan\beta = -\frac{\theta}{\sqrt{M_1^2 - 1}}$$

and
$$\frac{\Delta M}{M_1} = -\frac{\theta}{\sqrt{M_1^2-1}}\left(1 + \frac{\gamma-1}{2}M_1^2\right)$$

In the isentropic limit (infinitesimally weak wave) this becomes
$$\frac{dM}{M} = -\frac{1+\frac{\gamma-1}{2}M^2}{\sqrt{M^2-1}}\,d\theta$$

Integrating this, we get

$$\boxed{\begin{aligned} \text{const} - \theta &= \nu(M) \quad \text{the Prandtl-Meyer function} \\ \nu(M) &= \sqrt{\frac{\gamma+1}{\gamma-1}}\arctan\sqrt{\frac{\gamma-1}{\gamma+1}(M^2-1)} - \arctan\sqrt{M^2-1} \end{aligned}}$$

Plotting this in the θp-plane, we may compare it with the shock locus. The expansion part of the PM flow exhibits a maximum turning angle θ_m which depend on M_1 and γ.

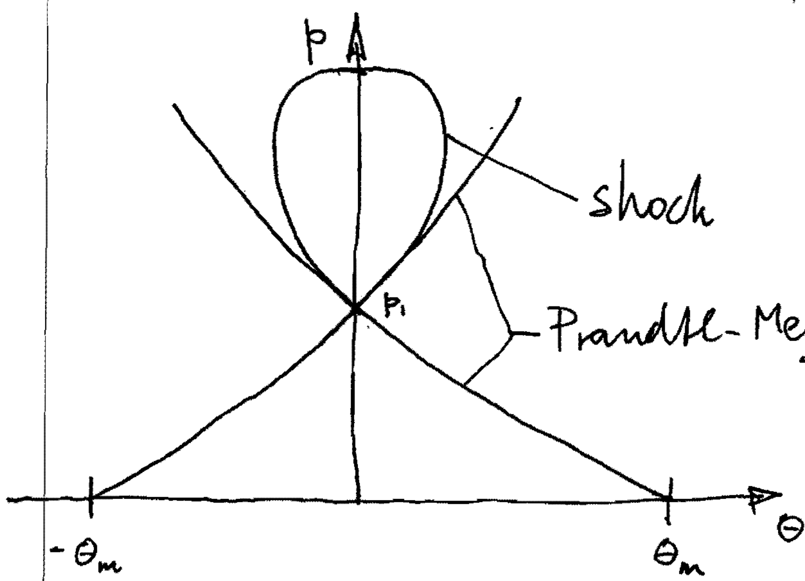

Now return to shock reflection

Regular reflection

Consider the problem in the local steady frame.

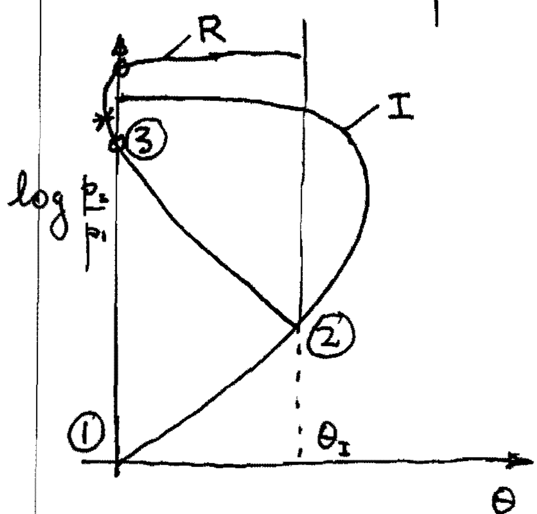

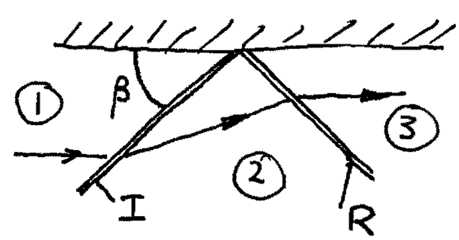

All the states ② that can be reached from ① via an oblique shock lie on the shock locus I of the incident shock. for a particular M_1 and γ. With a given β, this fixes the point ②, and the deflection angle θ_I. We can now draw a second shock locus for condition ② as the upstream condition. This is the curve R. The reflected shock has the job of

turning the flow back to a direction parallel to the wall, so that $\theta_R = -\theta_I$. The intersection of R with the p axis therefore provides the solution. Note that there are two possible solutions, one with $M_3 > 1$ and one with $M_3 < 1$ in the case shown.

The θp-plane is also useful for solving reflection from a constant pressure surface or a slip line in steady flow

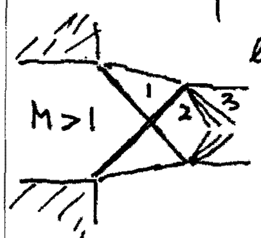

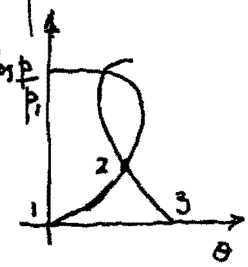

At the constant-pressure surface the incident shock raises the pressure so that the reflected wave must be an expansion, but in the case of the slip line the wave 23 can be a shock (dashed curve) or an expansion (full line) depending on whether the shock locus 04 lies outside or inside the shock locus 12.

const. p. surface

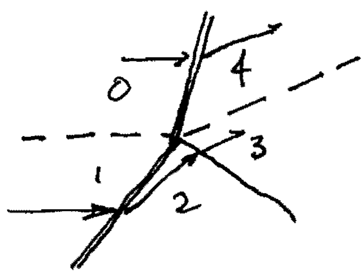

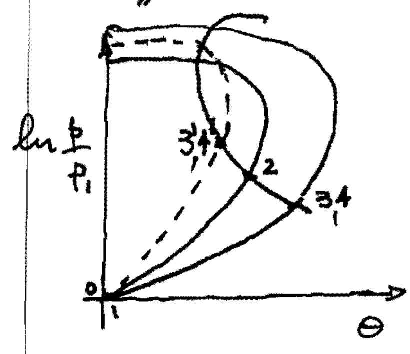

Now return to shock reflection from a wedge. If we decrease the wedge angle (i.e. increase β) sufficiently, there comes a point at which the maximum deflection through the reflected shock is insufficient to redirect the flow to be parallel to the wall. An example of the θp diagram for such a case is shown here.

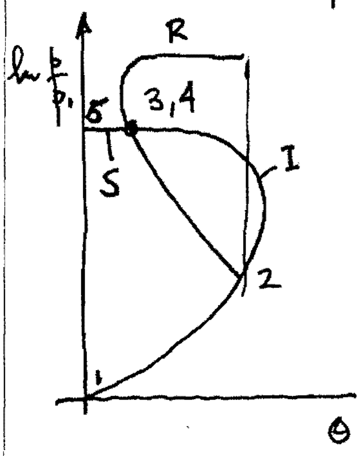

This leads to the mismatch of the flow direction and the wall boundary condition

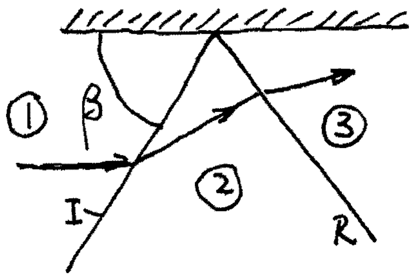

shown in the physical plane here. This is clearly not possible. The manner in which nature adjusts the transition of the flow direction from θ_3 to zero is to move the reflection point away from the wall, inserting a small subsonic region between the reflection point and the wall.

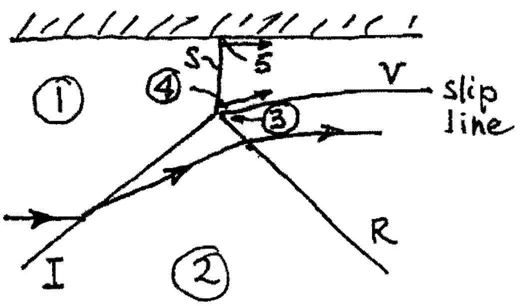

Mach reflection

A short, very slightly curved nearly normal shock takes the flow from condition 1 to 4 at the triple point and to 5 at the wall. This "Mach stem", S, is mapped in the θp-plane to the line 45 on the incident shock locus I. We now recognize the value of using the θp-plane. It lies in the fact that θ and p are variables that are continuous across the slipline. The latter comes about because conditions 4 and 3 are clearly different, so that the flow speed is not continuous across the slip line. Nor are density, temperature, entropy etc.. The sketch of the physical plane has been drawn here for the case of steady-flow Mach reflection. In the case of shock reflection

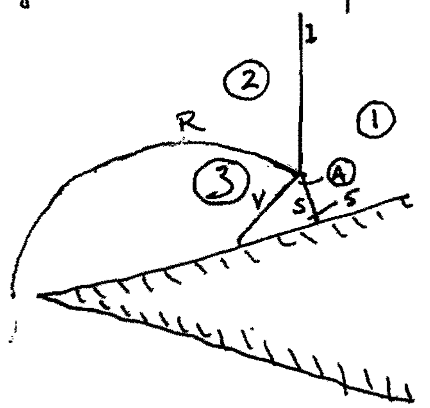

from a wedge, it looks a little different, see sketch, because the triple point moves away from the wall so that the slip line V has a different shape.

Now the question arises: How come the region near the reflection can now exhibit a length scale? The reason is that an information path now exists from the wedge tip to the reflection point. If this is truely the criterion

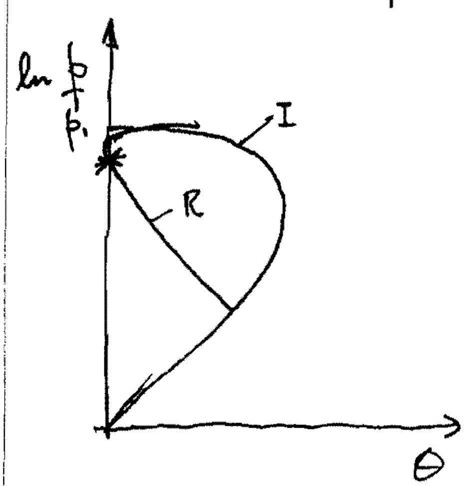

sonic criterion

for transition from regular to Mach reflection (information condition) in the case of a shock propagating into a stationary gas and reflecting from a stationary wedge, then transition will occur when the condition at the intersection point of R and the p axis is just sonic, i.e. when M_3 would be 1 in a regular reflection.

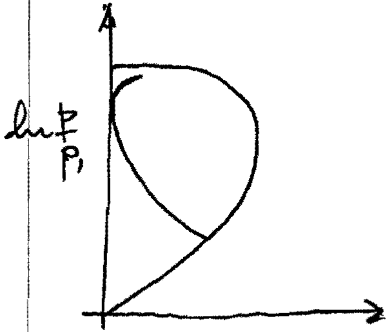

Since the sonic and detachment conditions are very close to each other, it is not possible to distinguish between them experimentally.

<u>detachment condition</u>

In the Mach reflection case, all features again grow linearly in time also, of course. This kind of flow is sometimes called "pseudo-steady".

<u>Aside on similarity coordinates for pseudosteady flow</u>

It is interesting to consider pseudo-steady flows in the coordinates that make them steady. To see how this can be done consider the continuity and momentum equations

$$\frac{D\rho}{Dt} = -\rho \nabla \cdot \underset{\sim}{u}$$

$$\frac{D\underset{\sim}{u}}{Dt} = -\frac{1}{\rho} \nabla p$$

and transform them from $(\underset{\sim}{x}, t)$ space to $(\underset{\sim}{\xi}, t)$ space, where $\underset{\sim}{\xi} = \frac{\underset{\sim}{x}}{t}$.

To make this as simple as possible, consider one-dimensional flow:

$$\frac{\partial}{\partial x} \Rightarrow \frac{\partial}{\partial \xi}\frac{\partial \xi}{\partial x} = \frac{1}{t}\frac{\partial}{\partial \xi}$$

$$\frac{\partial}{\partial t} \Rightarrow \frac{\partial}{\partial t} + \frac{\partial}{\partial \xi}\frac{\partial \xi}{\partial t} = \frac{\partial}{\partial t} - \frac{x}{t^2}\frac{\partial}{\partial \xi} = -\frac{\xi}{t}\frac{\partial}{\partial \xi}$$

since the explicit time-dependence will drop out. The continuity equation

$$\frac{\partial \rho}{\partial t} + u\frac{\partial \rho}{\partial x} = -\rho\frac{\partial u}{\partial x}$$

becomes
$$-\frac{\xi}{t}\cdot\frac{\partial \rho}{\partial \xi} + \frac{u}{t}\frac{\partial \rho}{\partial \xi} = -\frac{\rho}{t}\frac{\partial u}{\partial \xi}$$

or, for $t \neq 0$,
$$(u-\xi)\frac{\partial \rho}{\partial \xi} = -\rho\left[\frac{\partial(u-\xi)}{\partial \xi} + 1\right]$$

In two dimensions the 1 in the square brackets becomes a 2 and the continuity equation can be written as

$$\boxed{\underset{\sim}{U}\cdot\nabla^*\rho + \rho\left(\nabla^*\cdot\underset{\sim}{U} + 2\right) = 0}$$

Where $\nabla^* = \underset{\sim}{i}\frac{\partial}{\partial \xi_1} + \underset{\sim}{j}\frac{\partial}{\partial \xi_2}$, and $\underset{\sim}{U} = \underset{\sim}{u} - \underset{\sim}{\xi}$

In a similar way we get the momentum eqn.

$$\boxed{\underset{\sim}{U}\cdot\nabla^*\underset{\sim}{U} + \underset{\sim}{U} = -\frac{1}{\rho}\nabla^* p}$$

In the similarity space the flow is independent of time.

It is interesting to consider the "streamlines" in the similarity space, i.e. the integral curves of the $\underset{\sim}{U}$ field. In a region where $\underset{\sim}{u} = 0$, the transformed velocity $\underset{\sim}{U} = -\underset{\sim}{\xi}$, so that the integral curves are radial lines converging on a "sink point" at the origin $\xi = 0$. In other regions where $\underset{\sim}{u} = \text{const}$ e.g. region ② of a regular or Mach reflection, where $\underset{\sim}{u} = \underset{\sim}{u}_2$, $\underset{\sim}{U}$ will be $\underset{\sim}{u}_2 - \underset{\sim}{\xi}$. The integral curves will therefore be radial lines converging on a sink point at $\underset{\sim}{\xi} = \underset{\sim}{u}_2$, and so on. In this way the "streamline" pattern for a regular reflection is as shown here.

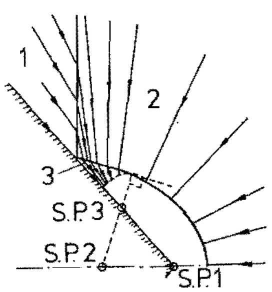

Figure 9 Regular reflection in pseudo-steady similarity space, S.P. = sink points for the uniform-flow regions 1, 2, and 3.

(End of Aside)

Types of reflection

The following pages show θp-plots of various possible solutions of the shock jump equations that give rise to different reflection configurations. These were made by Prof Sturtevant. They will be discussed in class.

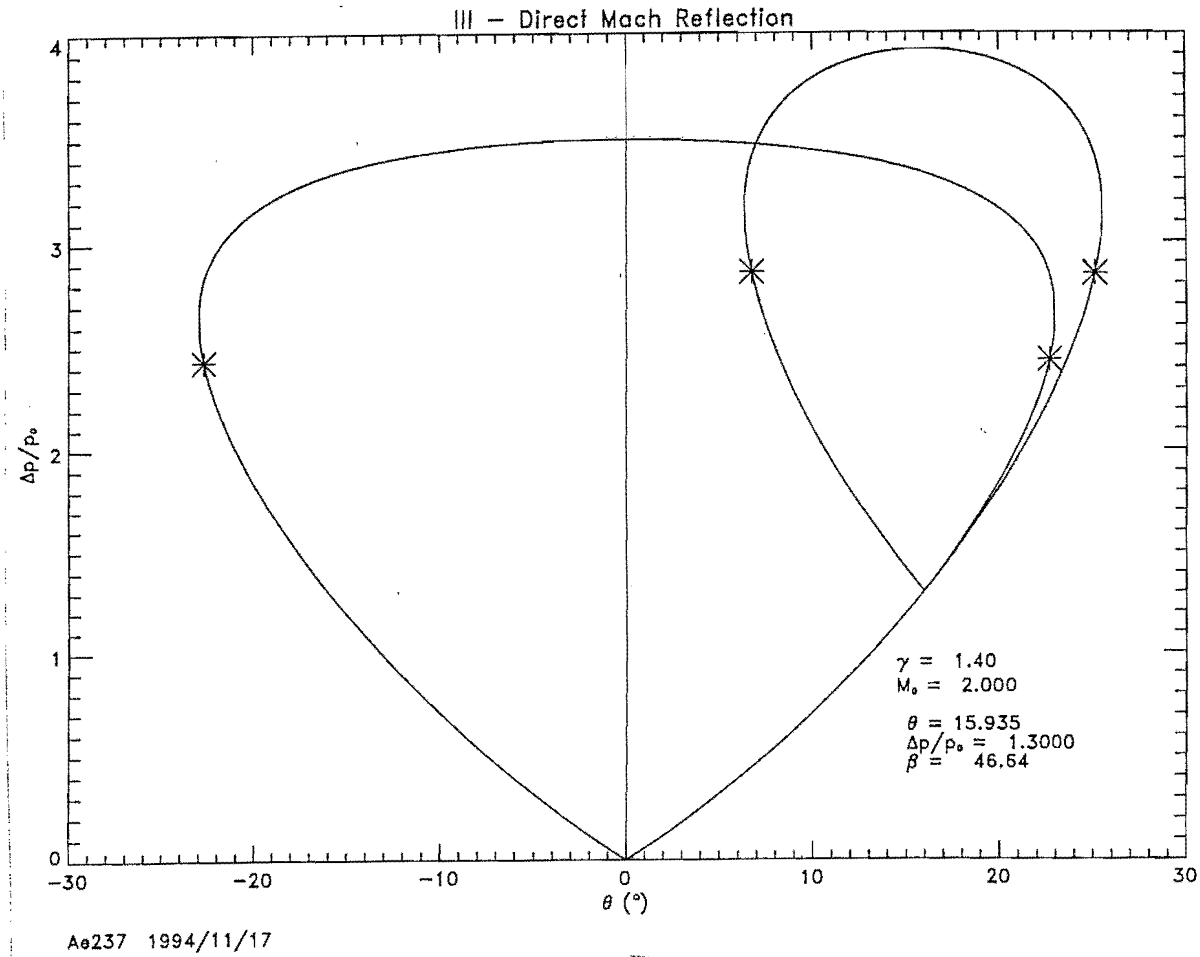
III – Direct Mach Reflection
Δp/p₀
θ (°)
γ = 1.40
M₀ = 2.000
θ = 15.935
Δp/p₀ = 1.3000
β = 46.64
Ae237 1994/11/17

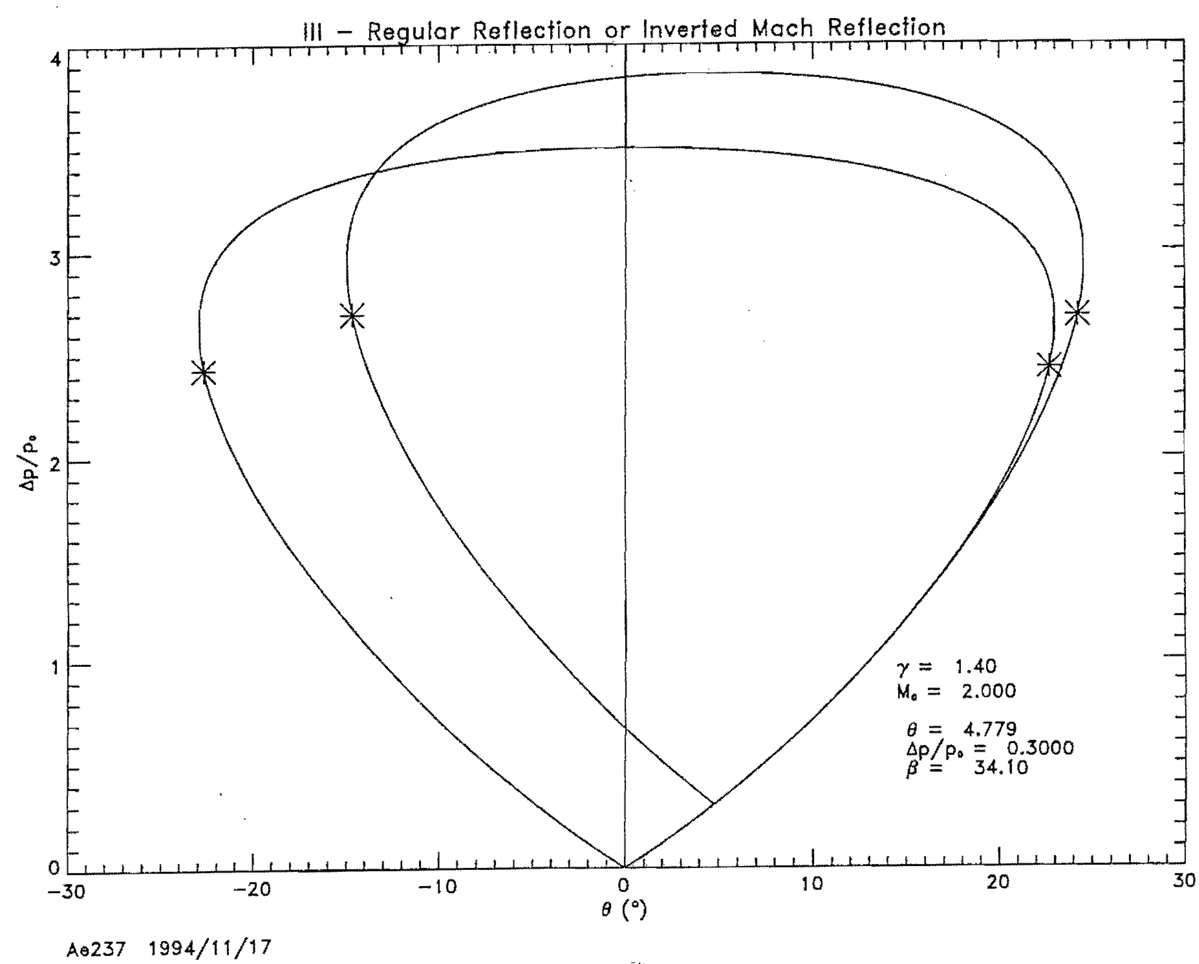
III – Regular Reflection or Inverted Mach Reflection
Δp/p₀
θ (°)
γ = 1.40
M₀ = 2.000
θ = 4.779
Δp/p₀ = 0.3000
β = 34.10
Ae237 1994/11/17

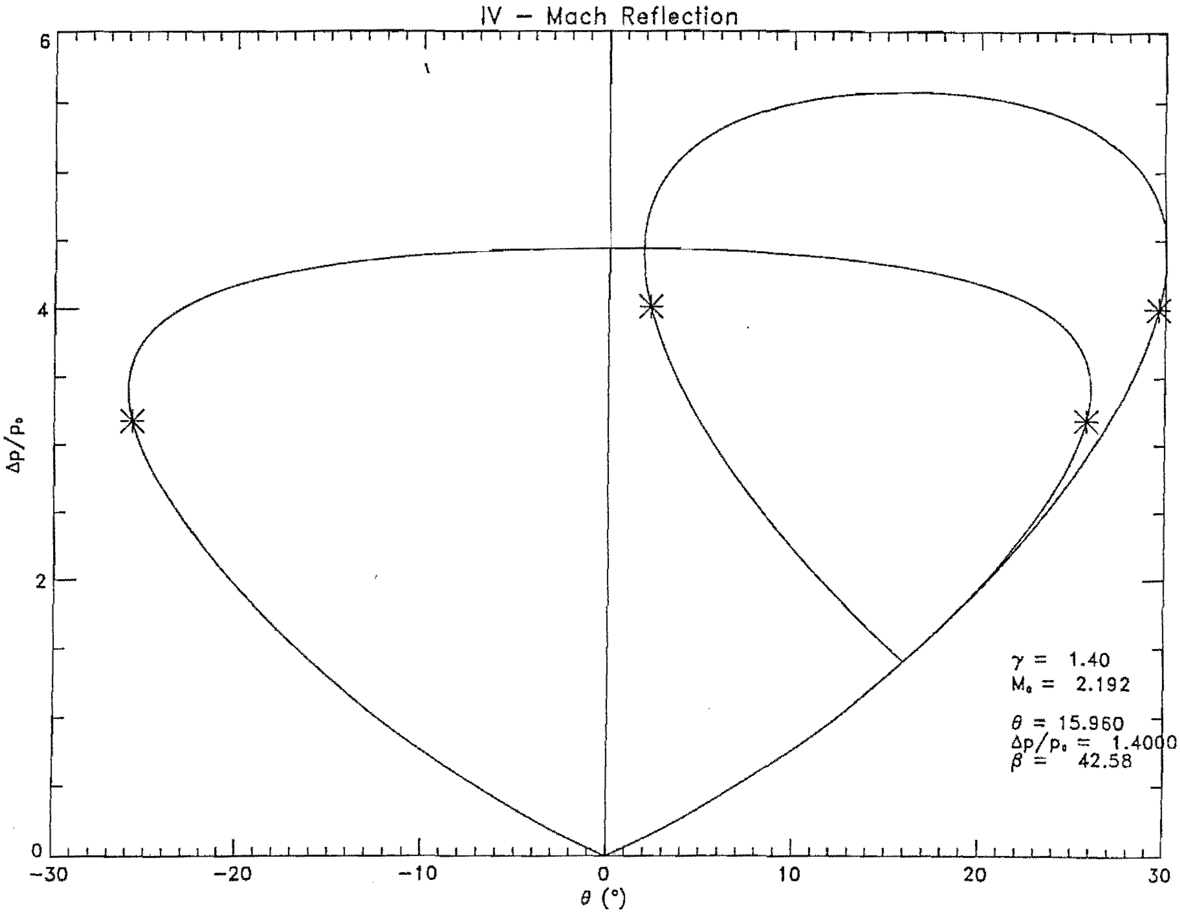

Ae237 1994/11/17

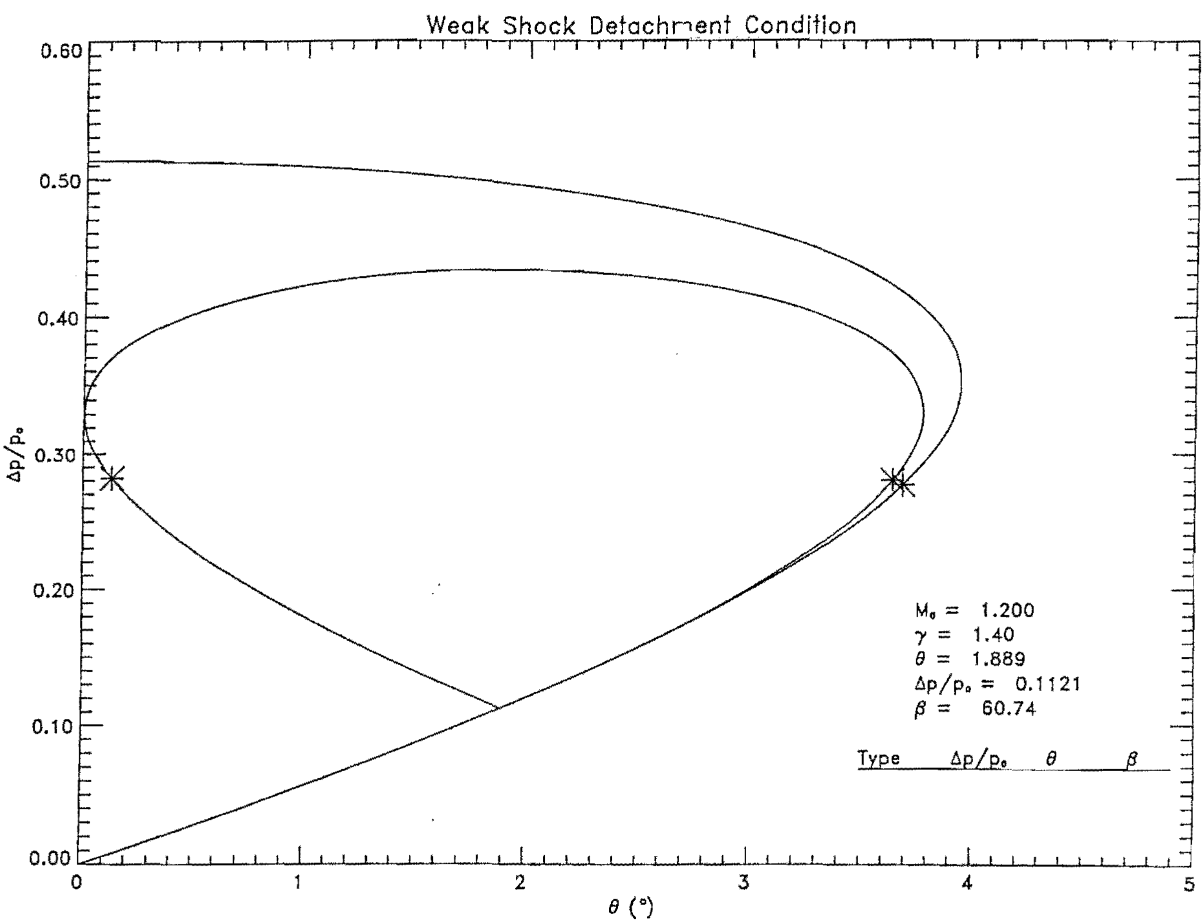

Ae237 1993/03/08

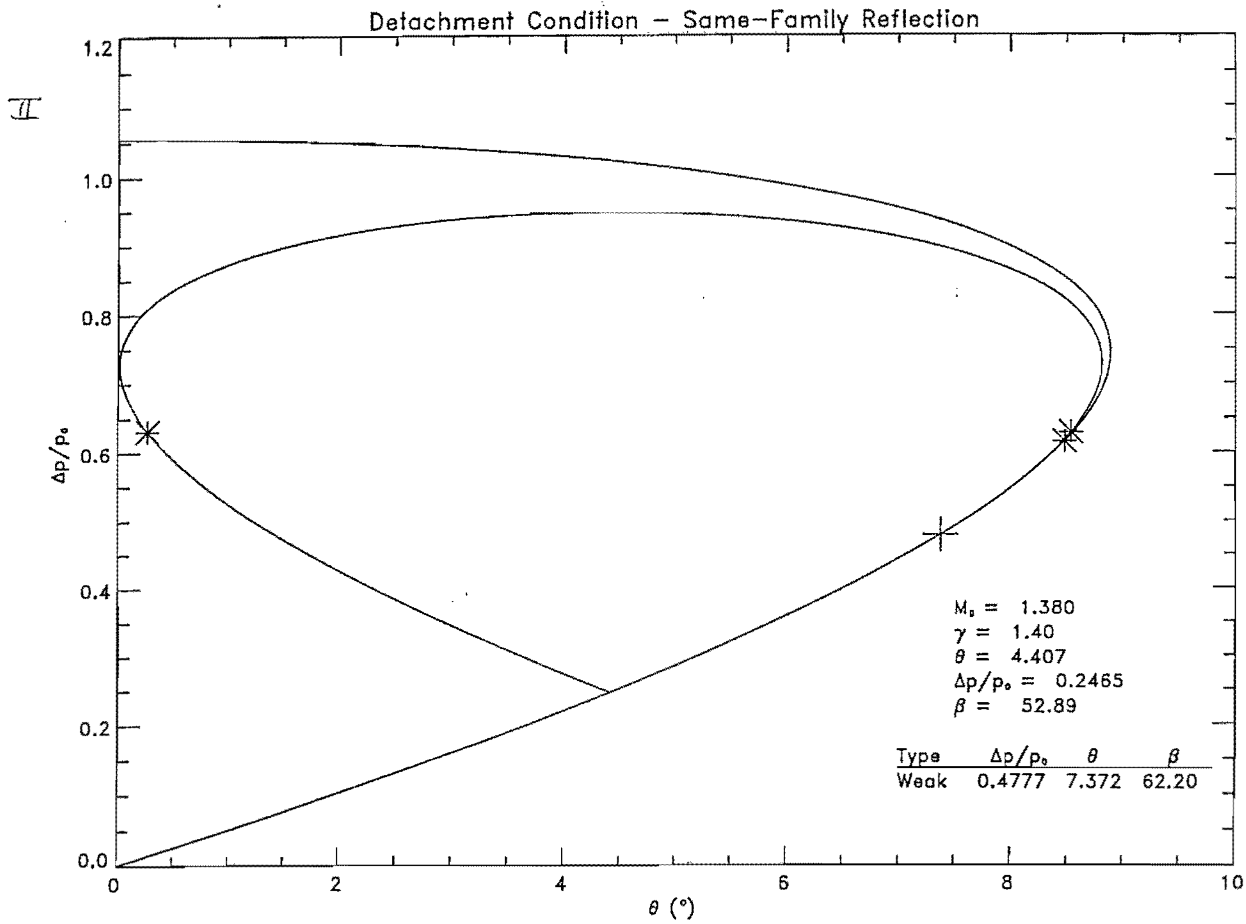

Ae237 1993/03/08

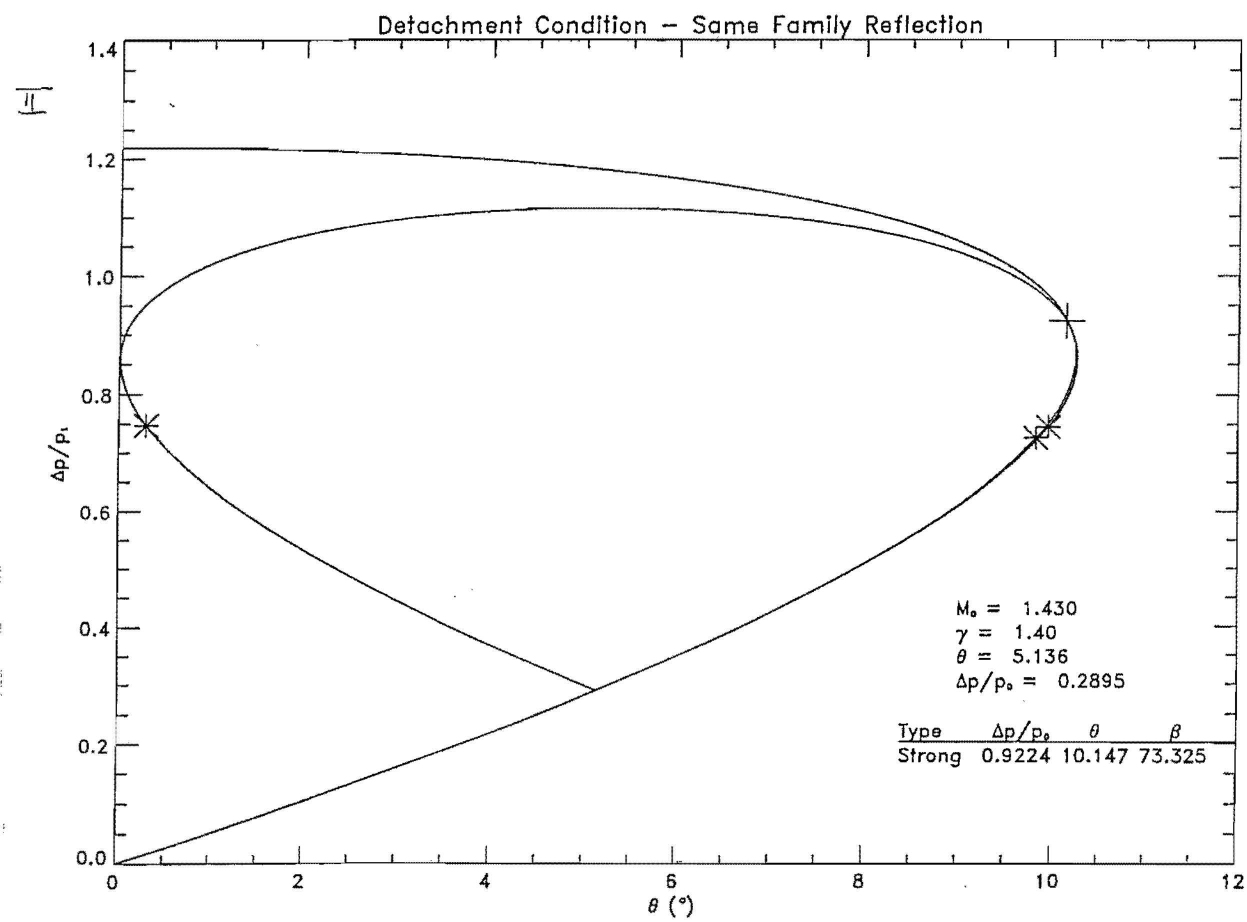

Ae237 1993/03/06

II

Same-Family Reflection?

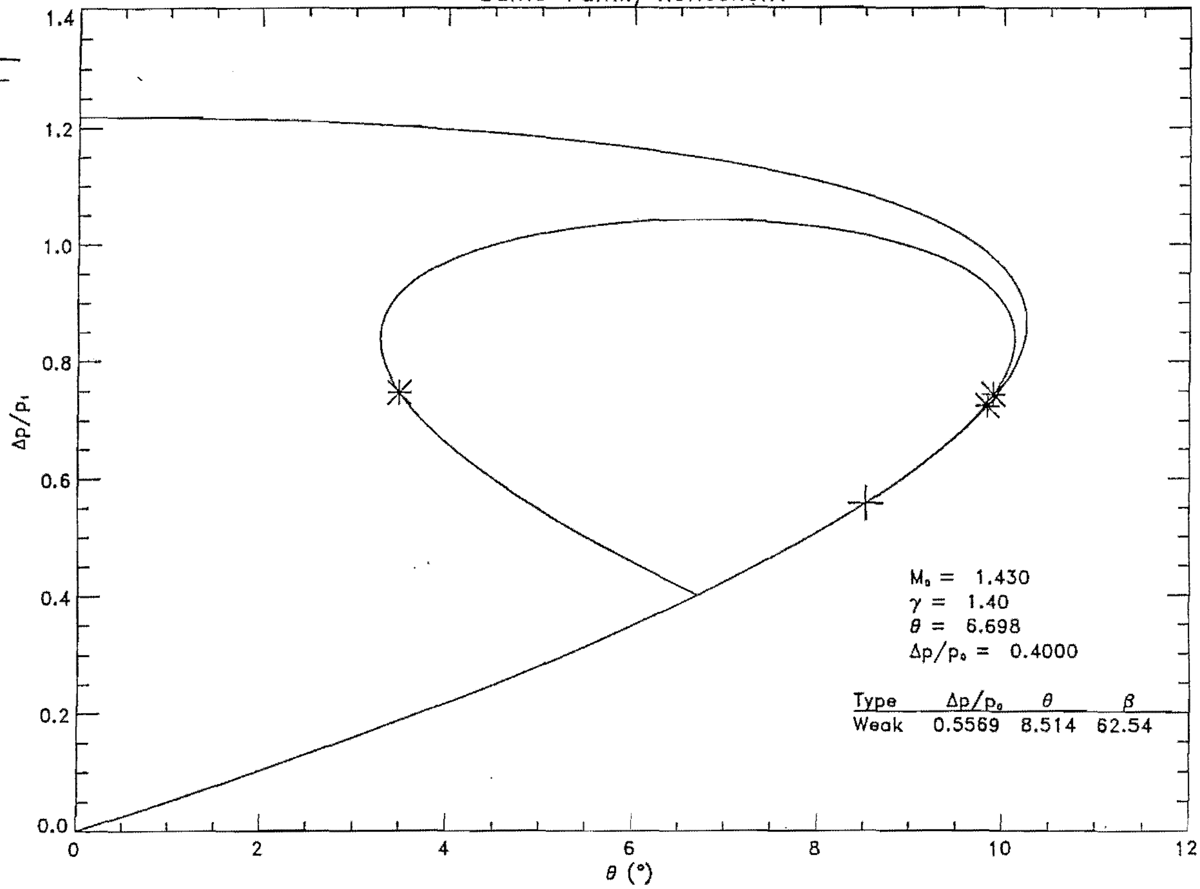

Ae237 1993/03/06

III – Detachment Condition – No-Deflection Reflection

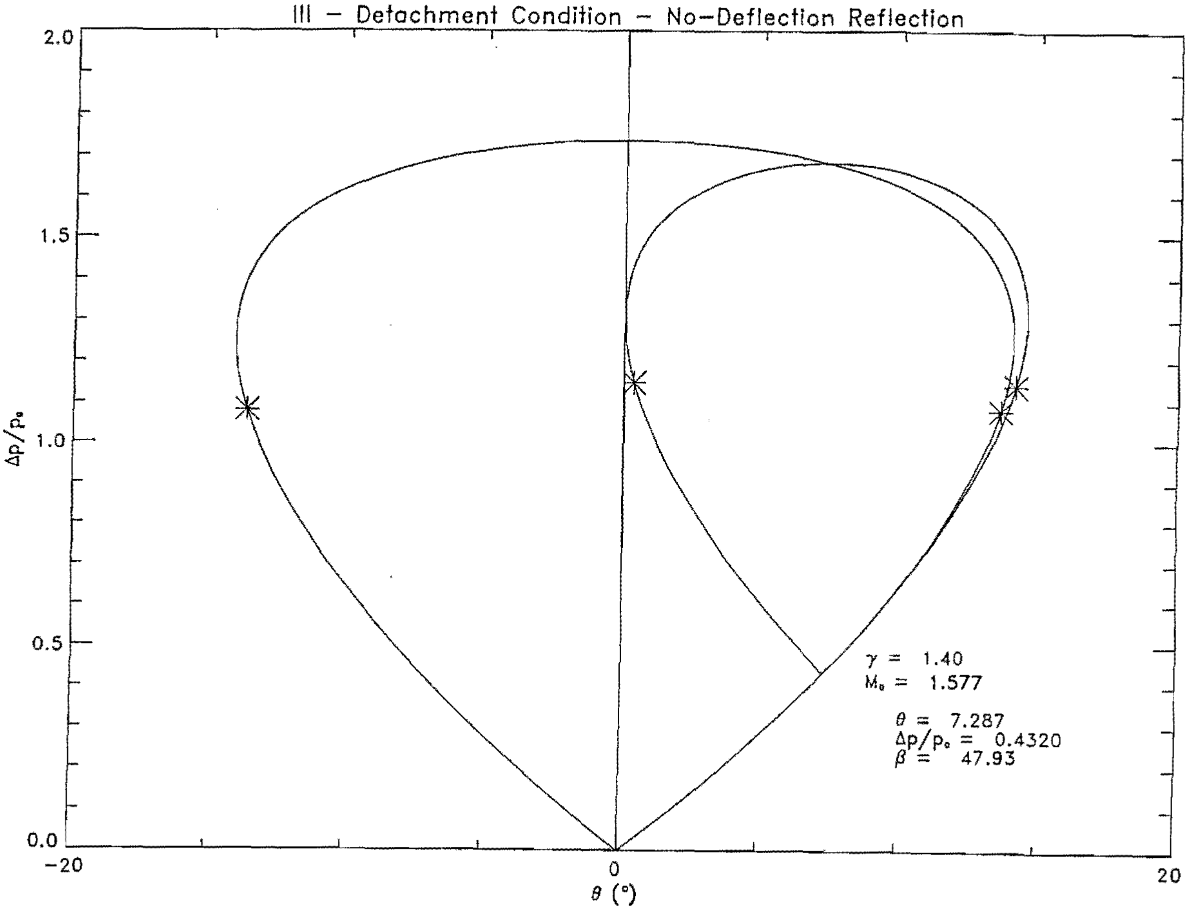

Ae237 1994/11/17

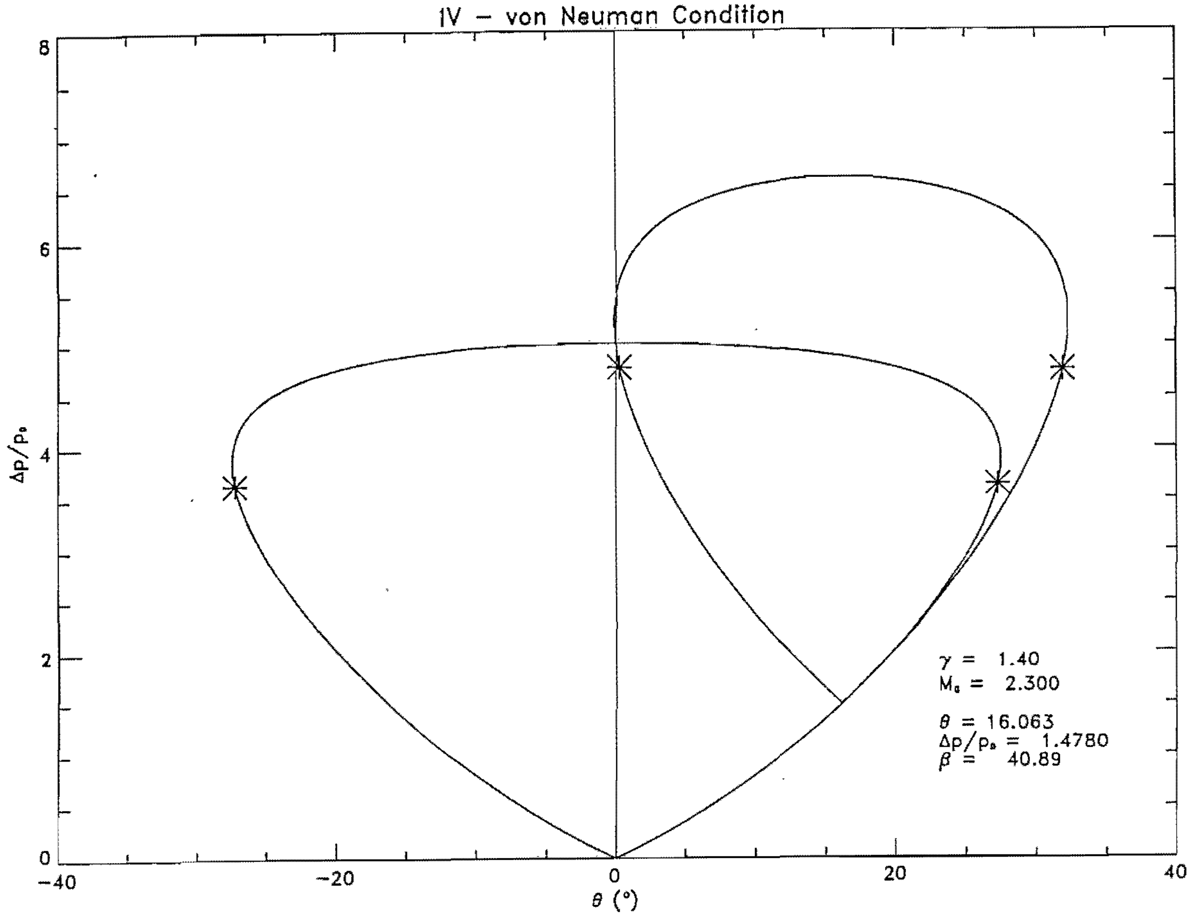

Ae237 1994/11/17

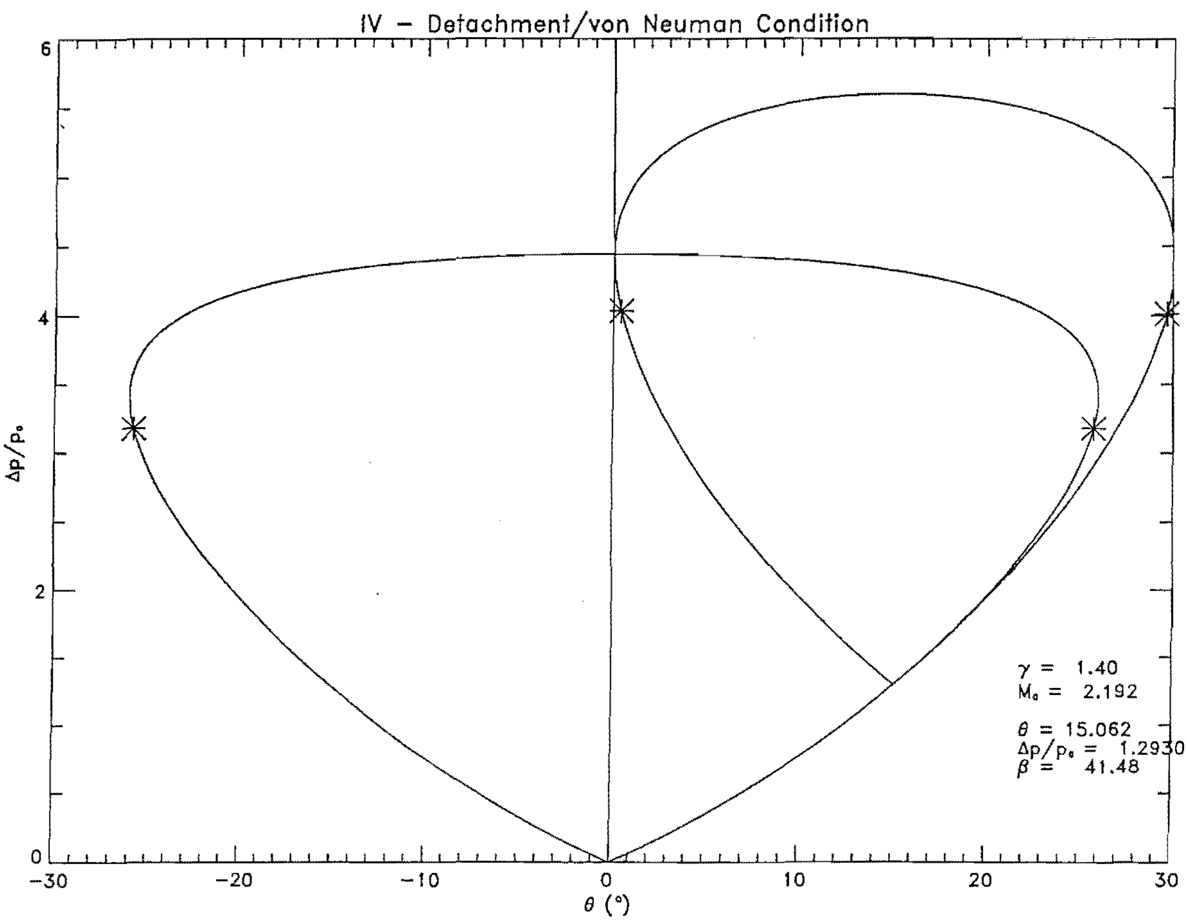

Ae237 1994/11/17

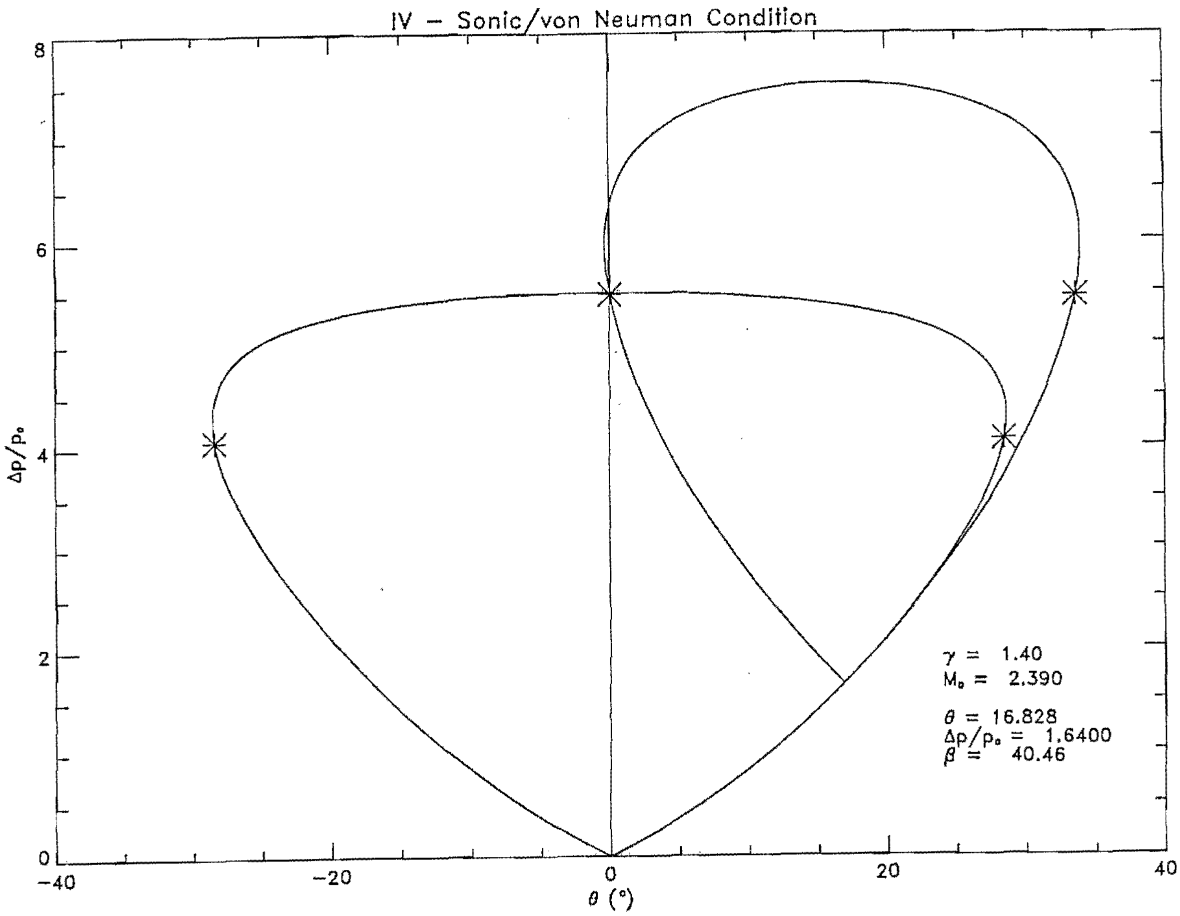

Ae237 1994/11/17

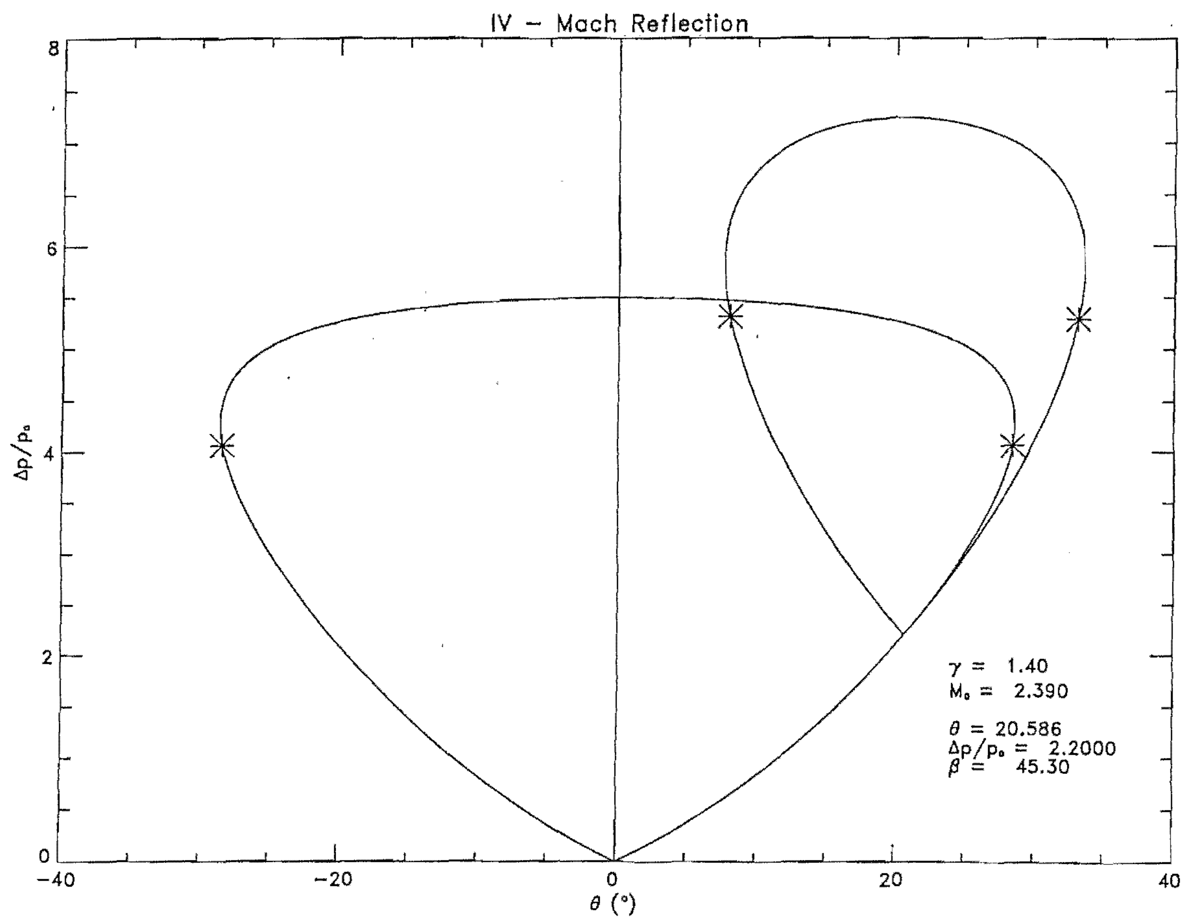

Ae237 1994/11/17

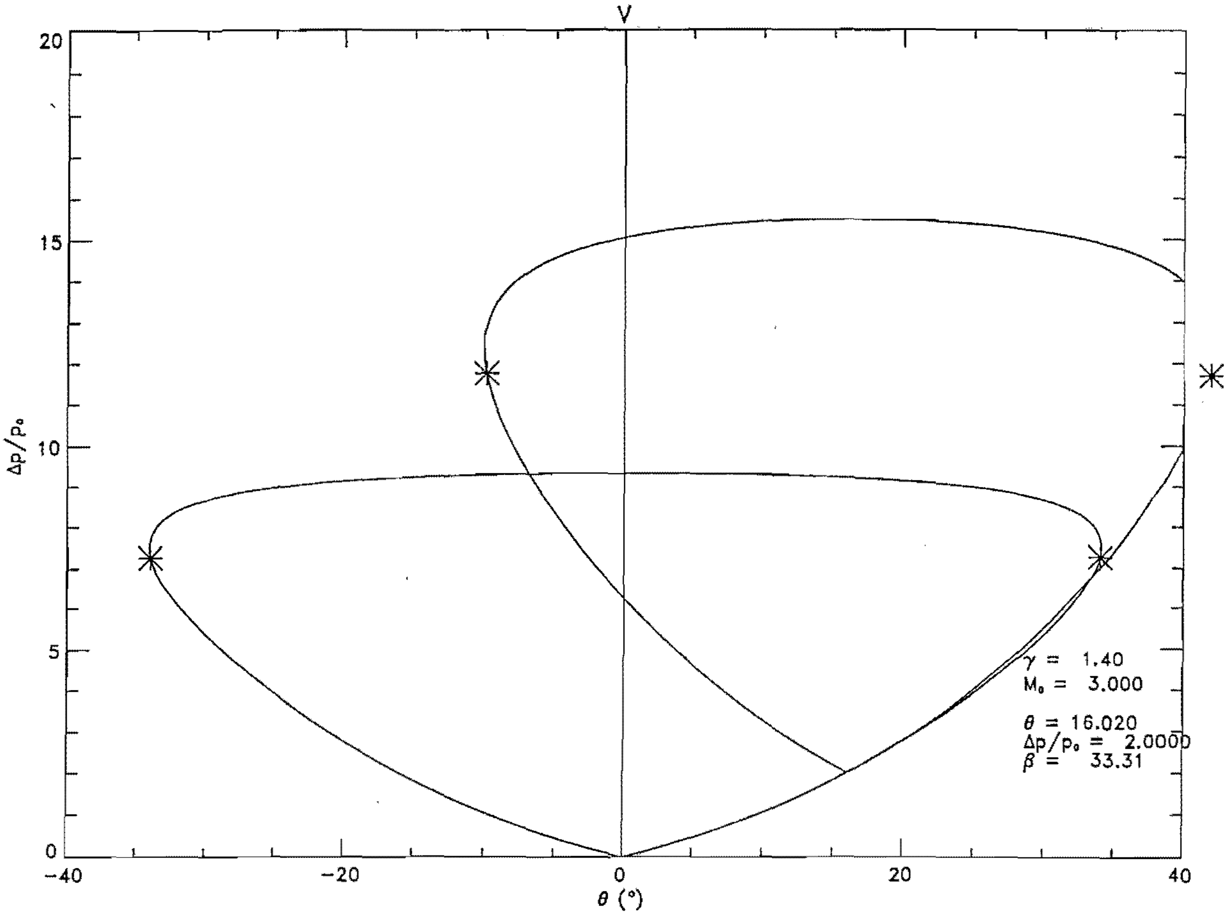

Ae237 1994/11/17

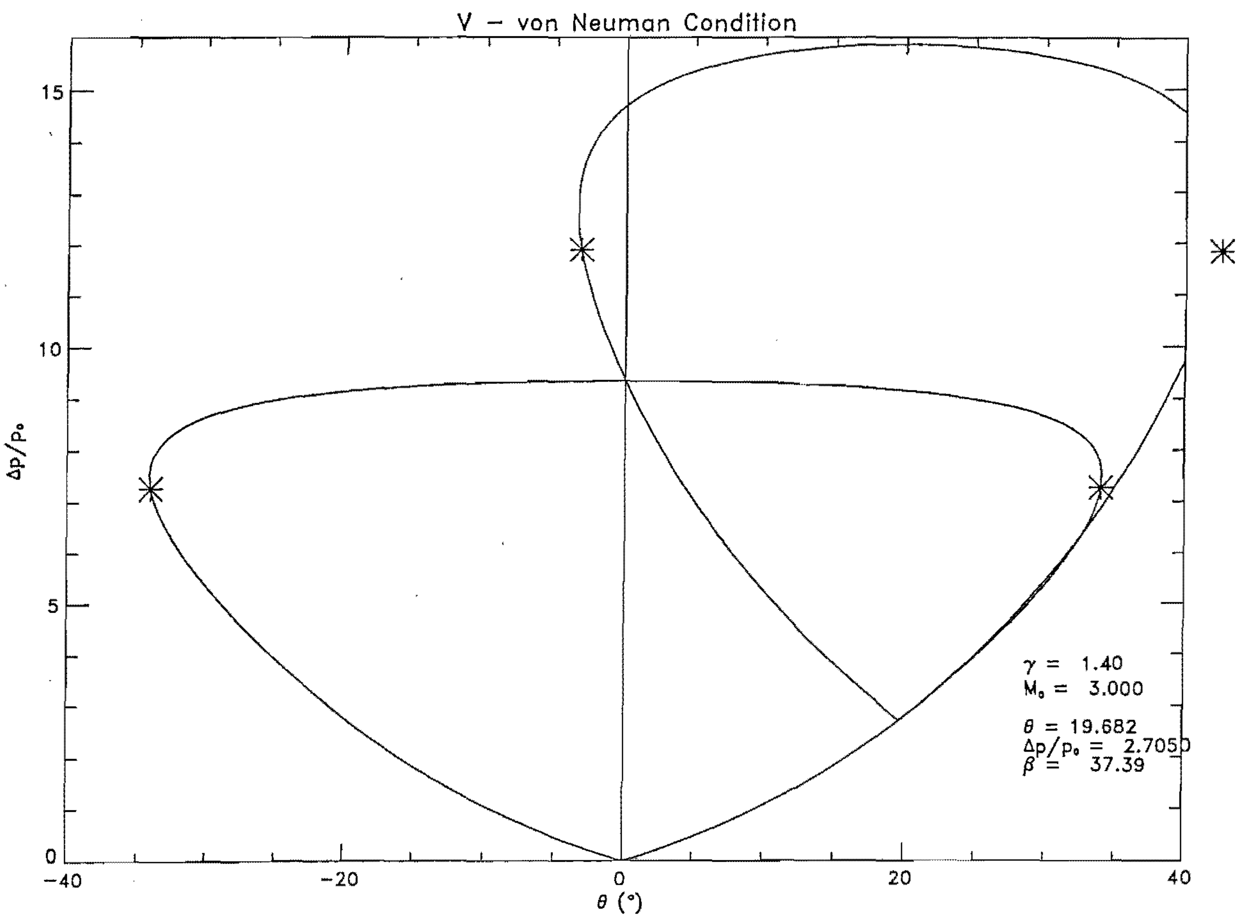

Ae237 1994/11/17

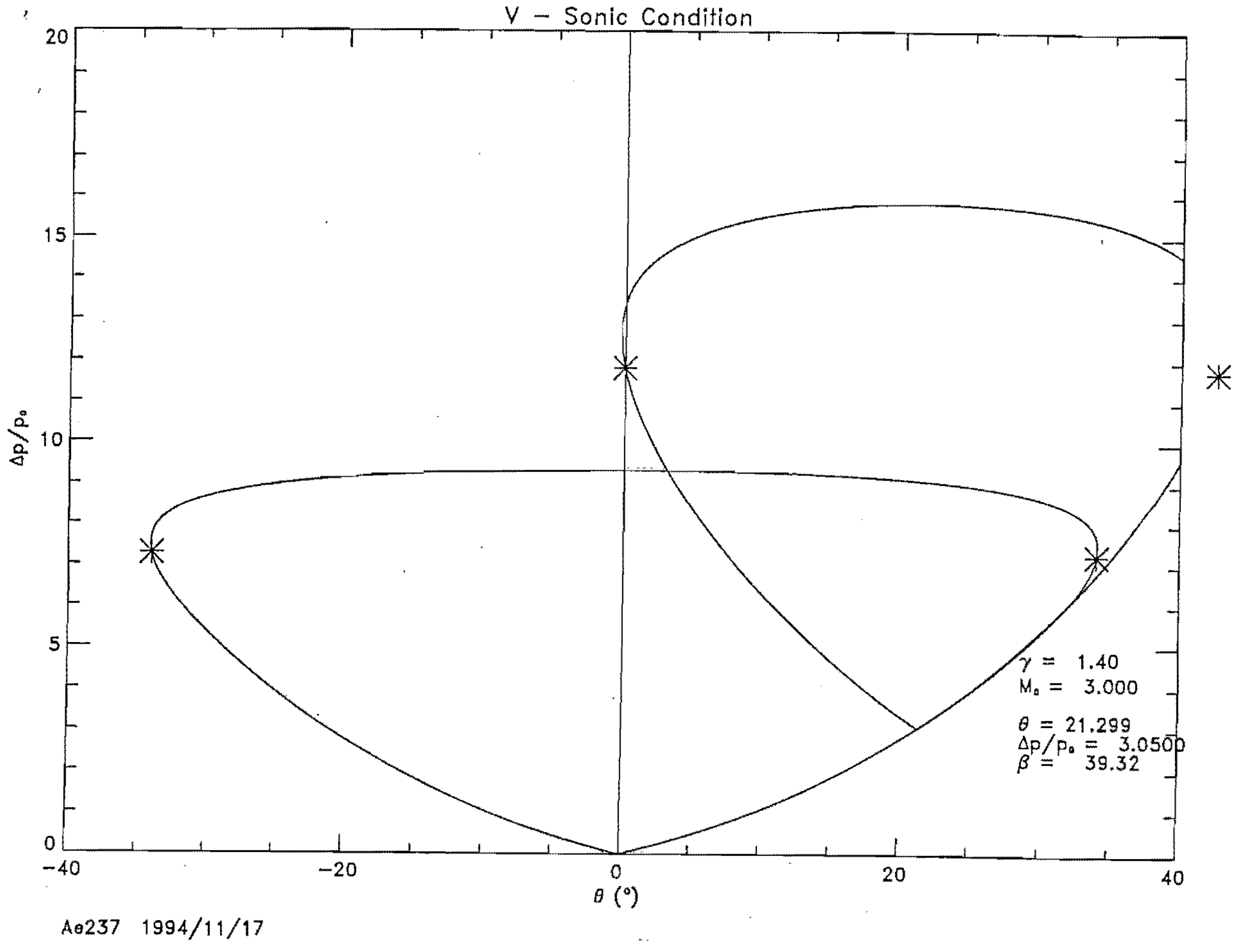

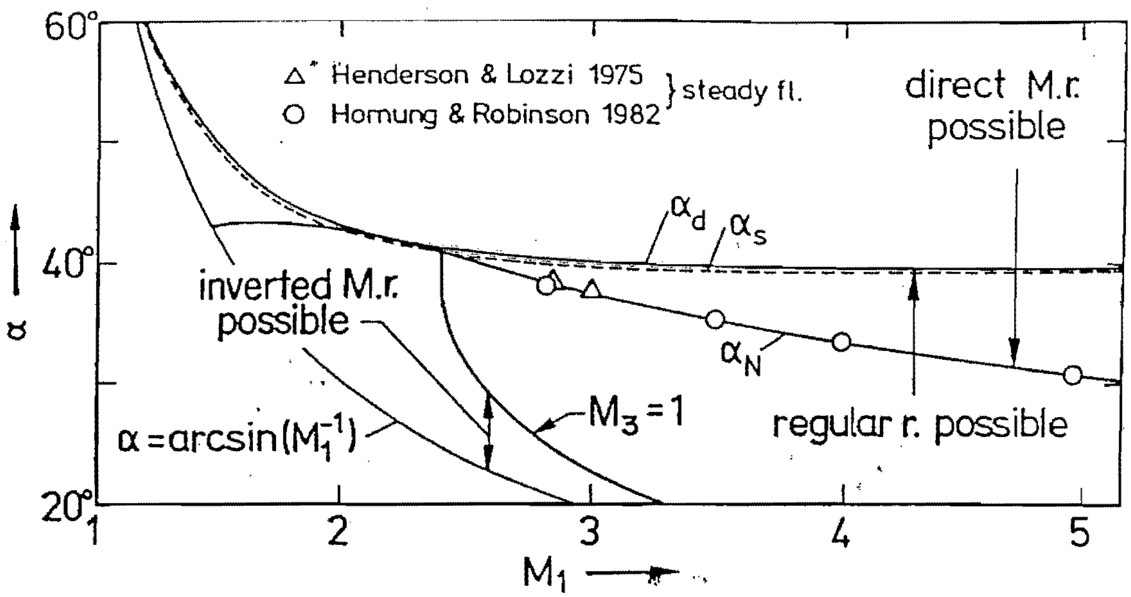

Bild 16. Die speziellen Werte von α als Funktion von M_1 bei $\gamma = 1{,}4$; die Symbole geben die α-Werte an, bei welchen in stationärer Strömung der Übergang von regulärer zu Machscher Reflexion beobachtet wurde

Mach reflection in steady flow.

In the mid 70's, Henderson at Sydney University had done some experiments at $M_\infty = 3$ in steady flow, in which he had observed that transition to Mach reflection occurred, not at the detachment condition, as textbooks said, but at what he called the "mechanical equilibrium criterion", known now as the von Neumann condition. At that time, a student of mine (George Kychakoff) and I wanted to use a symmetrical wedge configuration to study dissociative non-equilibrium effects behind regular reflection in the hypervelocity shock tunnel T3 at Canberra, Australia. Because the Mach number of this flow was much larger than Henderson's 3, (in Argon we had up to 16), the difference between β_d and β_N was much larger and way beyond the error bars. It became clear that the transition

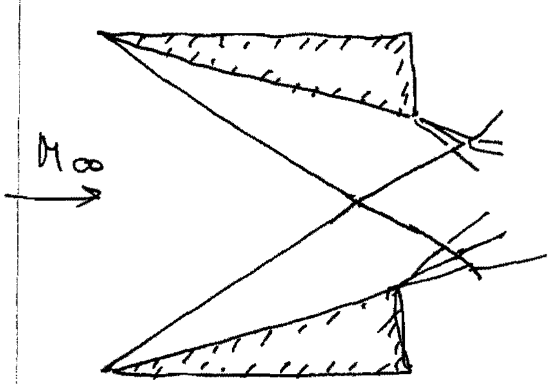

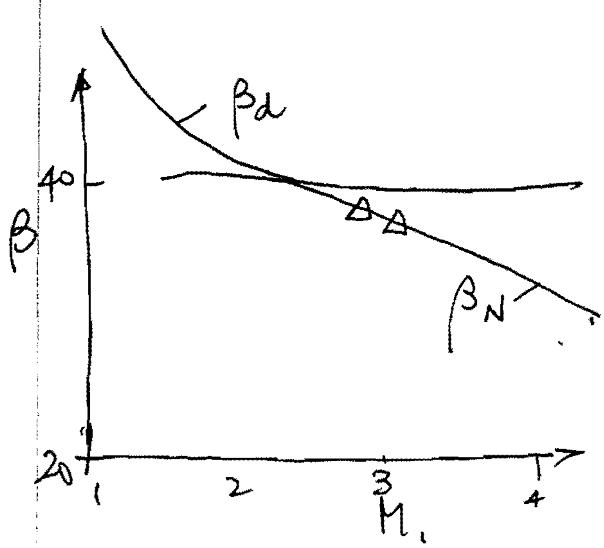

criterion for steady flow is different than for pseudosteady flow, in which the information condition gives a convincing argument for the sonic condition to be the transition criterion. Since von Neumann was the first ~ 1942 to point out that both regular and Mach reflection are possible in the range $\beta_N < \beta < \beta_d$, we referred to the "mechanical equilibrium condition" as the von Neumann condition, a name that has stuck. John Sandeman (a colleague at Canberra) and I had extensive and heated discussions about the difference between steady and pseudo-steady flows, and came to the conclusion that the information condition could explain both cases.

Consider a Mach reflection in steady flow with a symmetrical arrangement of two wedges (avoids boundary layer). In this configuration, the Prandtl-Meyer expansion from the trailing edge of the wedge causes the

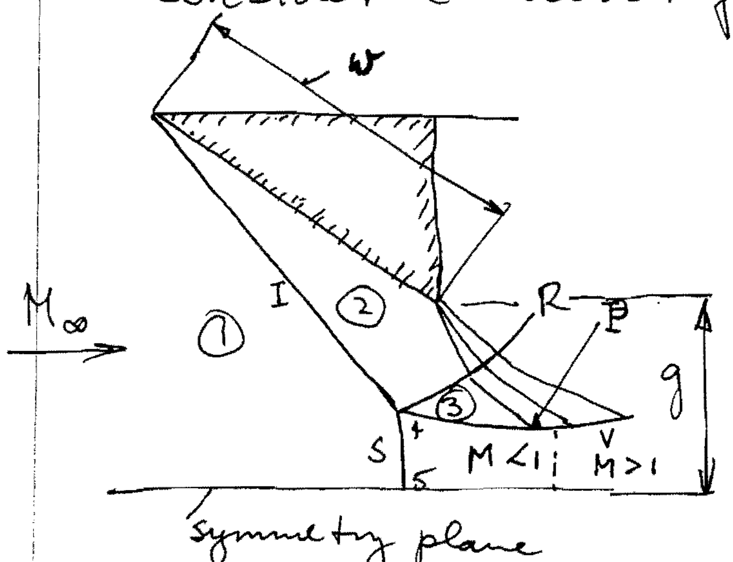

reflected shock to curve up. It also becomes refracted as it is transmitted across R. When it interacts with the slip line V, it causes the slip line to curve away from the wall. This causes the stream tube between the slip line V and the wall to have a minimum area at the dashed line. Behind the Mach stem S, the flow is subsonic. It accelerates through the minimum area to supersonic flow. Since the PM-expansion is the agency that causes V to curve away from the wall, the point P at which the most upstream characteristic from the trailing edge of the wedge reaches V lies upstream of the sonic throat. An information path therefore exists between the trailing edge of the wedge and the Mach stem.

In other words, it is o.k. for the reflection region to exhibit a length scale, since information about both the leading and trailing edge of the wedge reaches the reflection region. To illustrate this more clearly, imagine the scale of the experiment to double, i.e. both w and g to double. Then, in inviscid flow, the only length scales are w and g. Hence the length of S also has to double. It can only do so if the reflection region knows about both ends of the wedge.

The question now arises as to which reflection configuration will occur in the dual-solution regime $\beta_N < \beta < \beta_d$. In order to understand this, consider the following thought experiment. Let there be a regular reflection in the dual-solution domain, with ③ supersonic. In that case the reflection point can have no knowledge about the trailing edge of the wedge, since the leading characteristic borders a supersonic region 3.

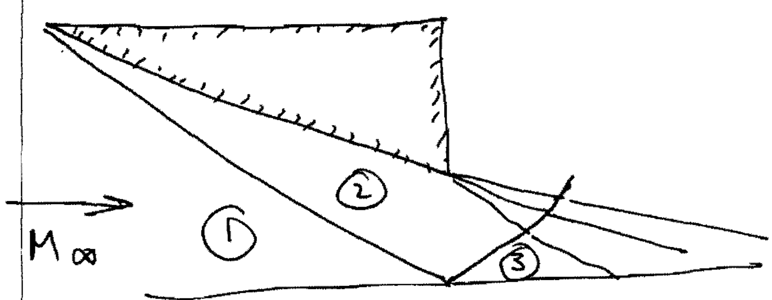

Now give the flow some suitable disturbance so that a Mach reflection temporarily occurs. Such a disturbance would immediately establish an information path to the reflection point, telling it how long to make S. (Note that this mechanism wouldn't help the reflection point to know about the wedge tip in pseudo-steady flow)

These discussions led us to do a whole flot of new experiments that established the difference once and for all (between pseudosteady and steady flow) At the end of the publication of this work in Hornung, Oertel, Sandeman, JFM 1979 I stuck my neck out and predicted that there would be a hysteresis in Mach reflection

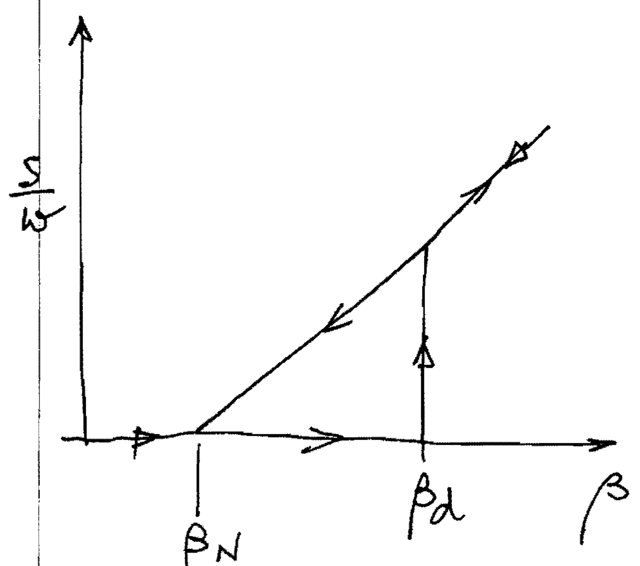

i.e. that, increasing β from below β_N, the transition to Mach reflection in steady flow would occur at β_s (or β_d) and the Mach stem length would jump discontinuously, while when decreasing β from above β_d, the Mach stem length would decrease smoothly to zero at $\beta = \beta_N$.

To test this, we did experiments in a continuous tunnel (Hornung & Robinson JFM 1982). We did not observe the hysteresis, but found that transition occurred at $\beta = \beta_N$ in all cases. These are the circular symbols at the bottom of p 187.

In the mid 1990's people started to get interested in the hysteresis again, and now it has been established that it does occur, provided that the wind tunnel is sufficiently free of disturbances. Russian, French, Japanese and German groups have confirmed it convincingly, both experimentally and computationally. It seems from Japanese experiments that dust or ice particles make ~~are~~ the most effective disturbances for causing transition to Mach reflection in the dual-solution domain.

The field has become a real cottage industry. There is now a Mach reflection symposium every 2 years and the 15th took place in Aachen, Germany in September 2002.

The next 4 pages shows some of the results that have contributed to the history described in the last pages.

Ae237

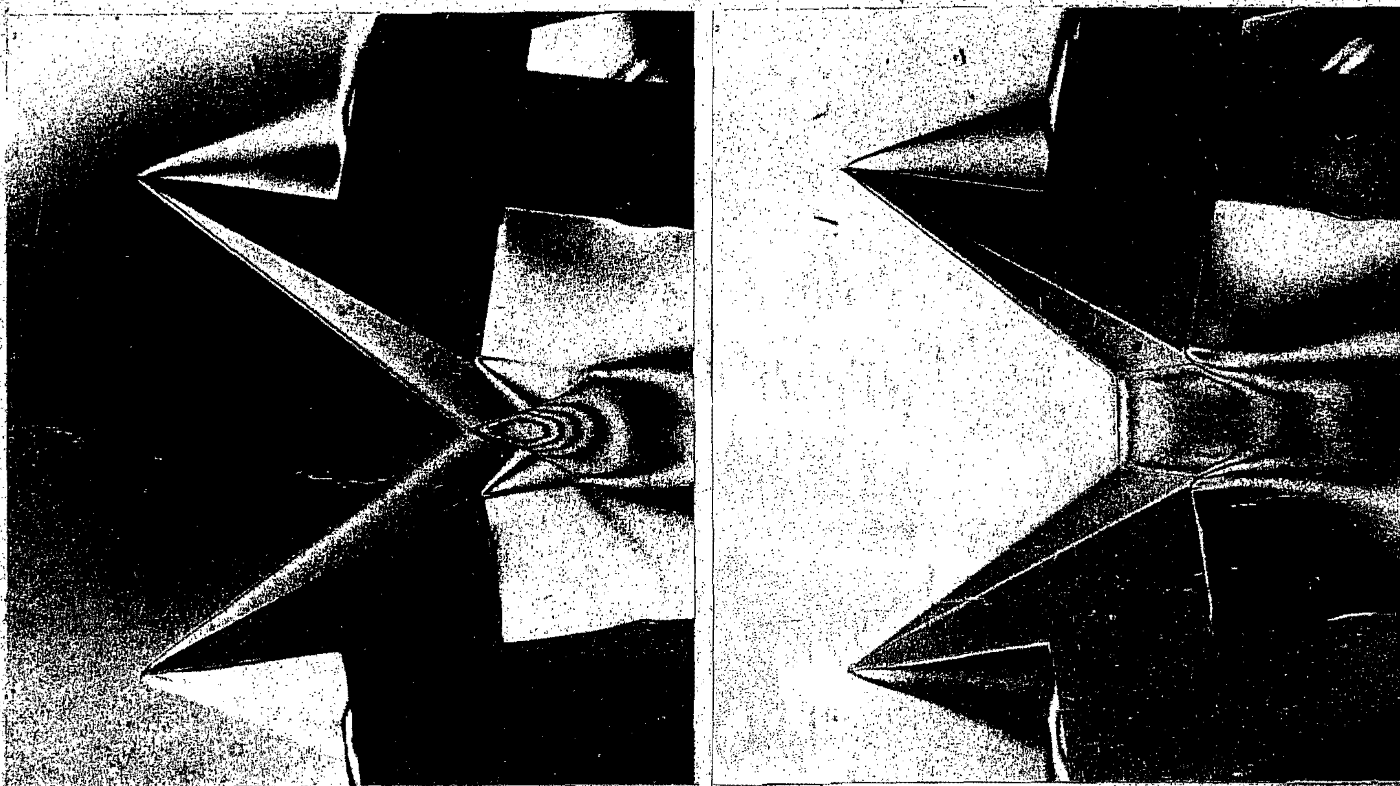

(a) $\alpha = 36{\cdot}2^0$, $g/w = 0{\cdot}37$ (b) $\alpha = 36{\cdot}5^0$, $g/w = 0{\cdot}37$

Interferograms of regular and Mach reflection in steady flow. Note how leading characteristic from trailing edge makes the slip line curve to form a sonic throat in Mach reflection.

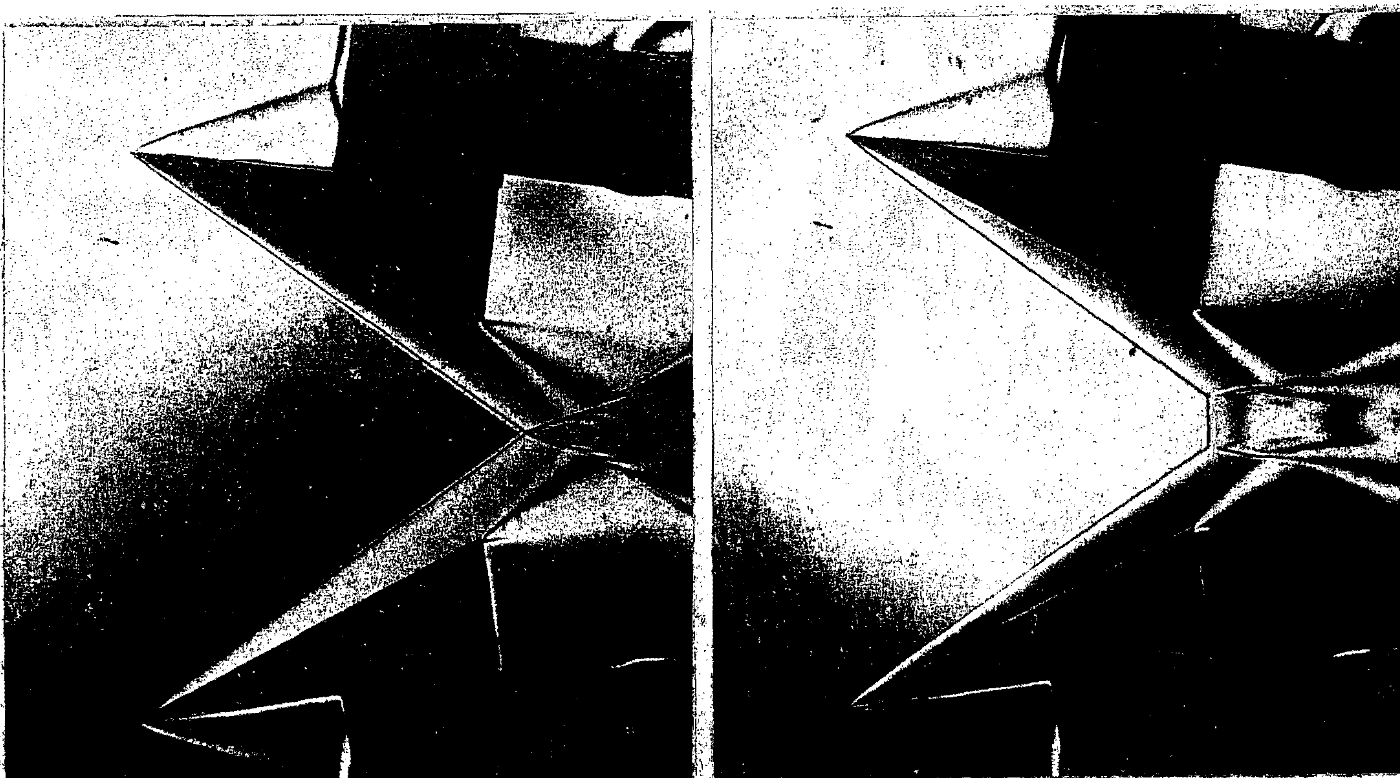

(c) $\alpha = 35{\cdot}1^0$, $g/w = 0{\cdot}56$ (d) $\alpha = 35{\cdot}3^0$, $g/w = 0{\cdot}56$

from Hornung, Oertel, Sandeman JFM 1979

Ae237

195

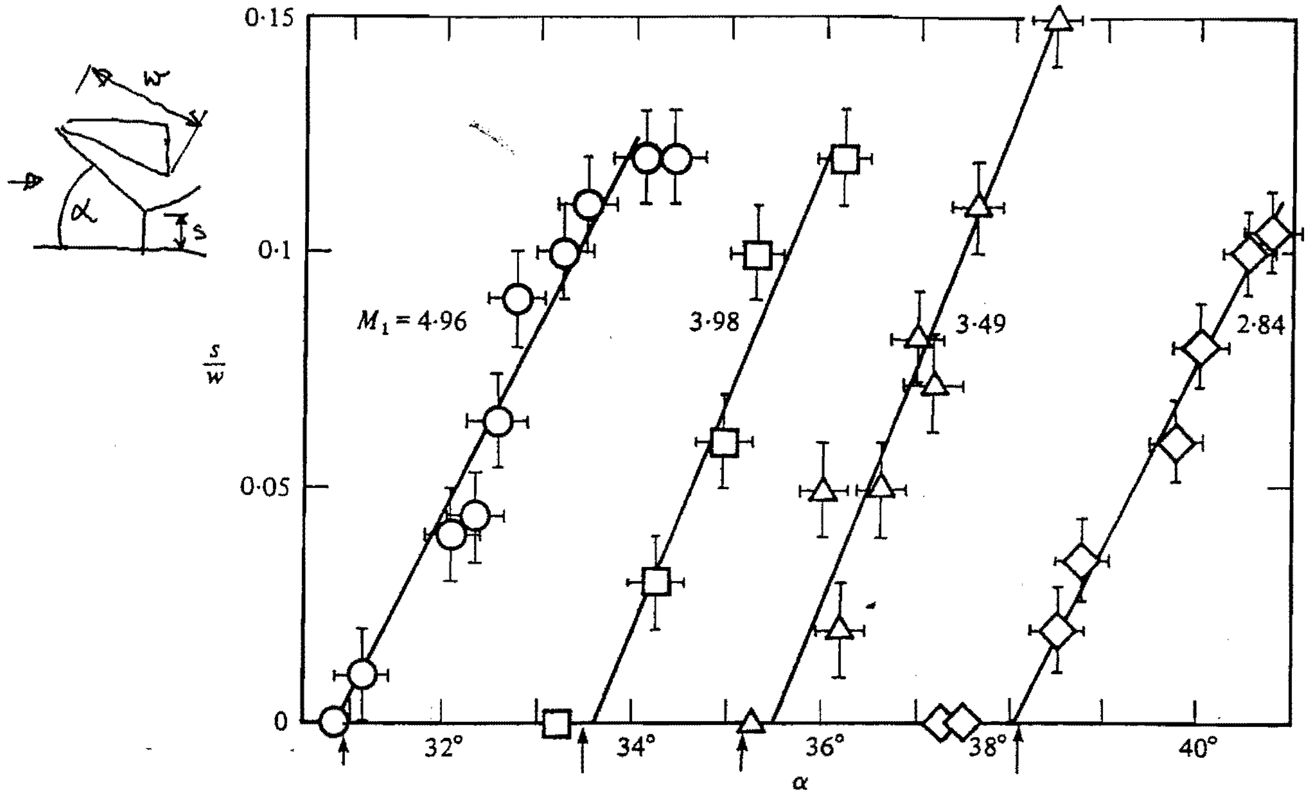

FIGURE 6. Measured dimensionless Mach stem lengths. The straight lines are least-squares fits to the experimental points. The arrows indicate corresponding values of α_N.

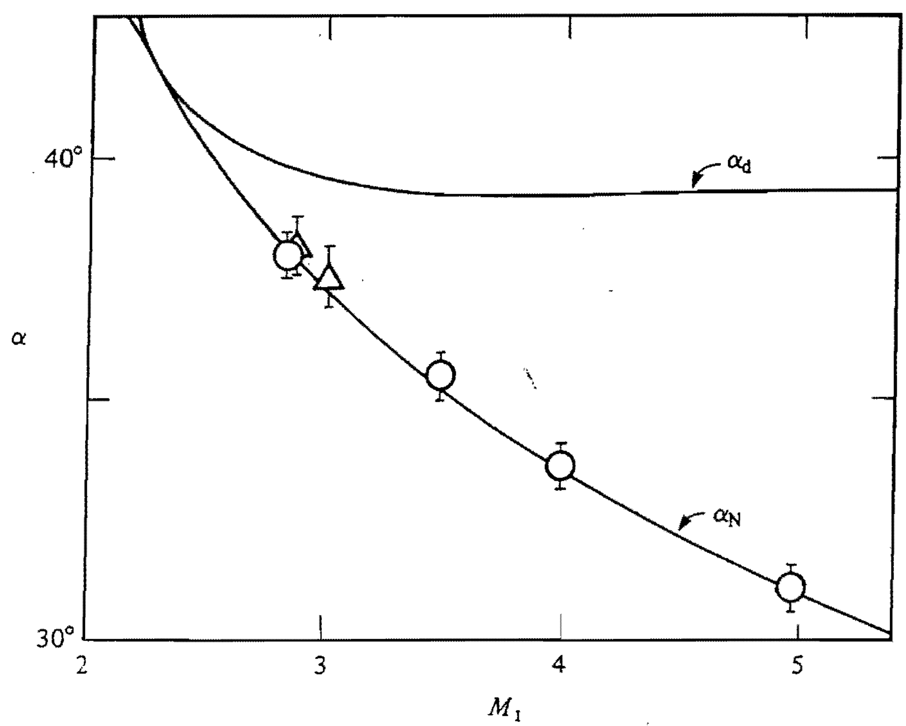

FIGURE 7. Measured transition angle compared with theory. △, Henderson & Lozzi (1975); ○, our data.

Steady flow experiments to look for hysteresis which was not found. Probably, tunnel too noisy
JFM 1982

Ae237

Previous work (1)

Hysteresis in asymmetric arrangement

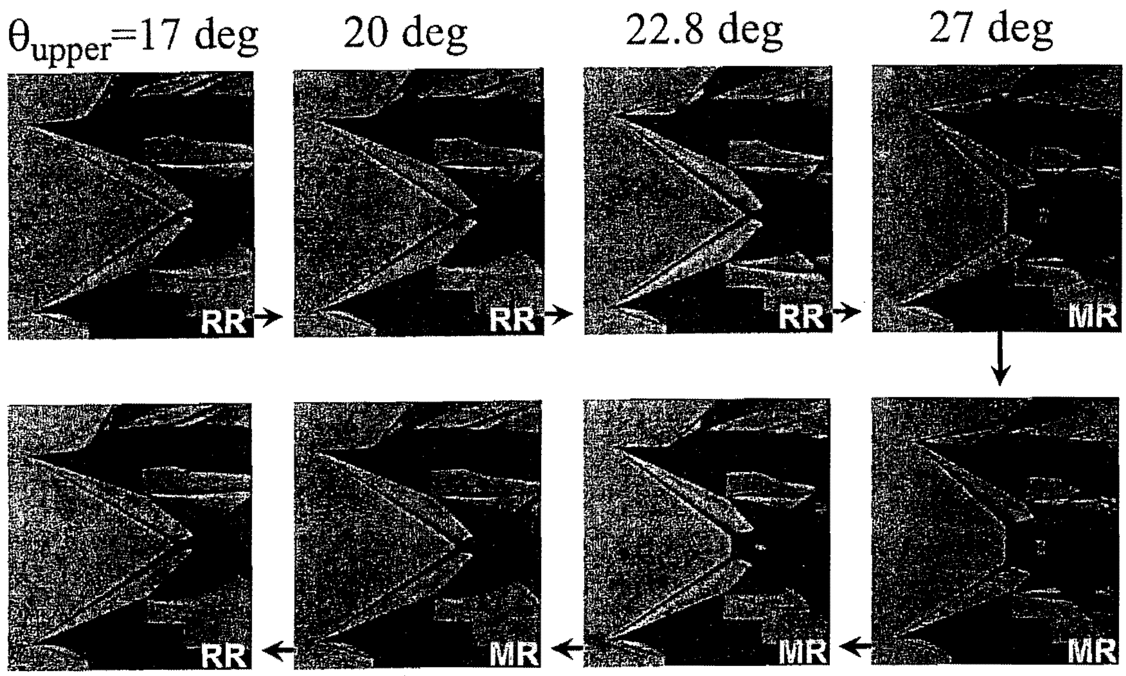

Hysteresis obcerved in experiment Sudani 2002 (*M*=4.0)

"Irregular" transition from RR to MR

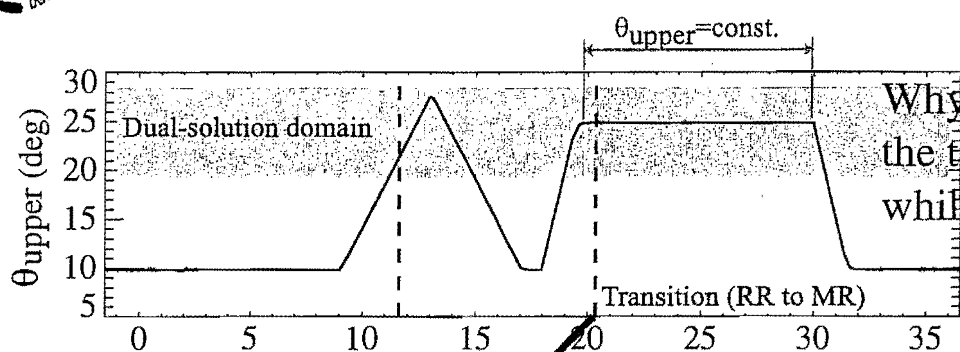

t = 20.3 s

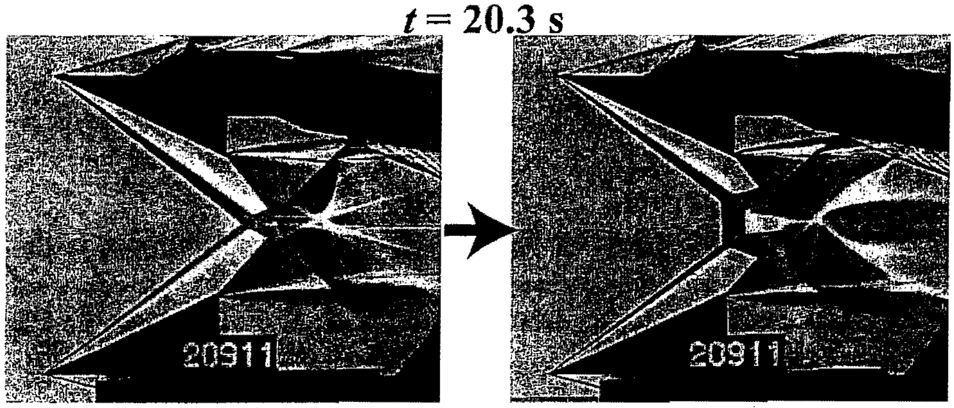

Why does the transition happen while θ_{upper}=const ?

↓

"Irregular" disturbance
or
low frequency disturbance

(*M*=4.0)

Previous work (3)

Effects of water vapors

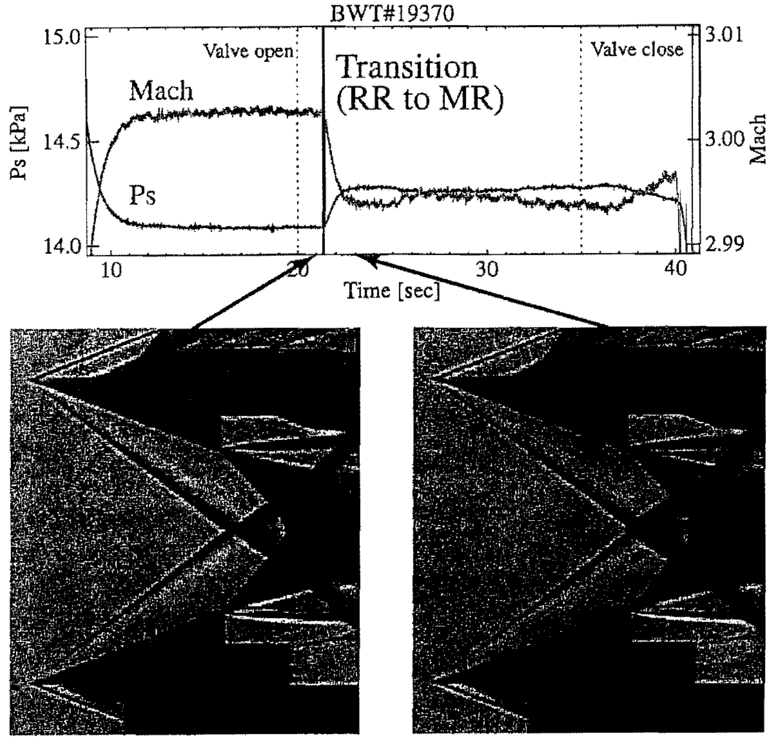

Water vapors (droplets) can be causes for the transition.

(M=3.0)

High speed movie of the transition by a needle

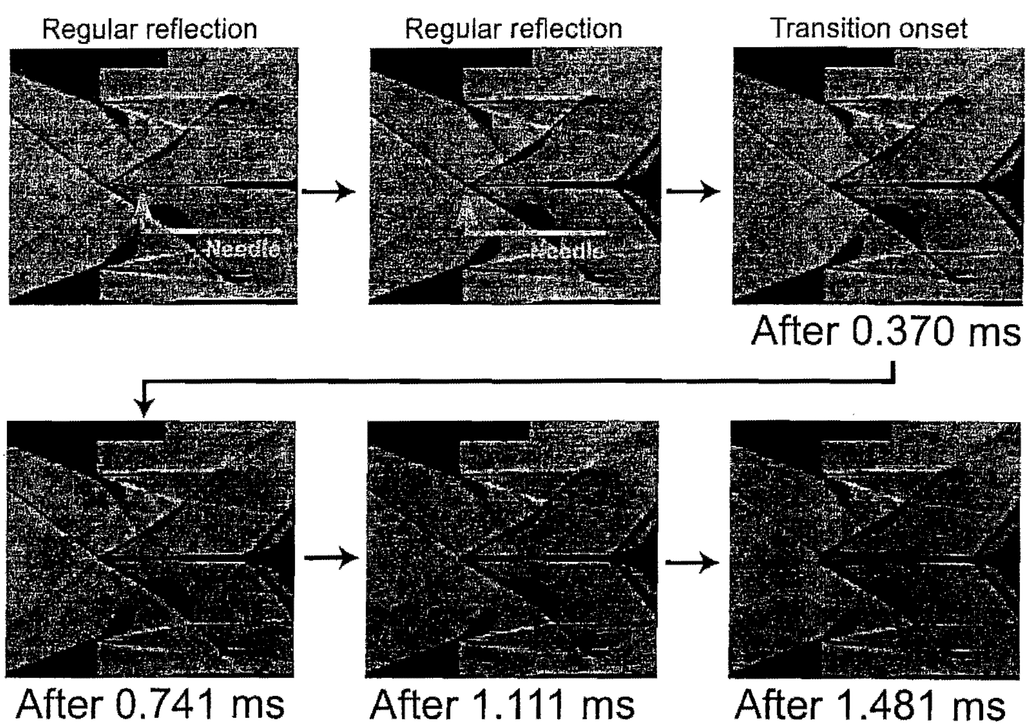

Double Mach Reflection

Consider a Mach reflection in the strong-shock range ($M_1 > 2.4$ in $\gamma = 1.4$) in pseudo-steady flow.

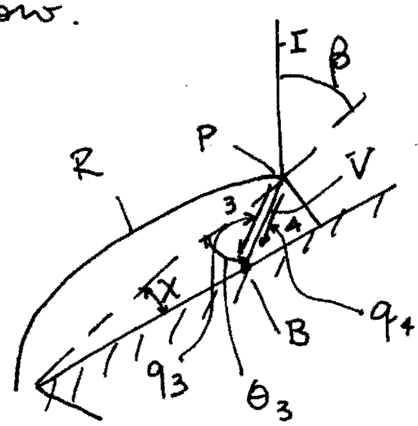

In the frame of reference of the triple point P, region 3 is supersonic and the wall has a finite normal component to its own plane. Assume for the moment that the flow in region 4 is uniform so that PB is a straight slip line that makes an angle θ_3 with the triple-point path (dashed line). Since θ_3 is determined by the shock locus intersection,

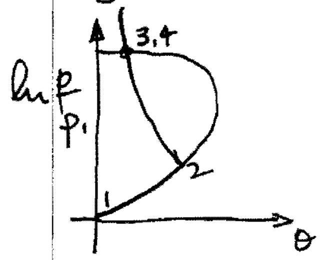

the position of B and its velocity $\underset{\sim}{q}_B$ are known

$$\theta_3 = \theta_3(M_1, \gamma, \beta, \chi),$$

$$\underset{\sim}{q}_3 = \underset{\sim}{q}_3(M_1\,\gamma, \beta, \chi),$$

where χ is the angle of the triple-point path.

The assumption that 4 is uniform and the wall impermeability demand that the wall velocity normal to its own plane, q_w, be equal to the component of $\underset{\sim}{q}_B = \underset{\sim}{q}_4$ normal to the wall:

$$q_w = q_B \sin(\theta_3 + \chi)$$

However, the velocity along the slip line V in region q_3 is different from that in region 4, q_B. Therefore the component of q_3 normal to the wall is not the same as the wall-normal component of the wall's velocity. Therefore, the flow in region 3 has to be accelerated away from or toward the wall, depending on the sign of $q_3 - q_4$. As seen from the frame of reference of B, this means that the flow needs to be deflected to a direction parallel to the wall.

In the strong shock-reflection range $q_3 - q_4 > 0$ the need to ~~decelerate~~ deflect the flow from q_3 to a wall-parallel direction causes a pressure rise near B. The consequence of this is that most of the flow is deflected toward the wedge tip, but some is deflected toward the Mach stem. A stagnation point is formed near B. The result is that V curls up toward the Mach stem. This violates the assumption that region 4 is uniform, and we will return to this.

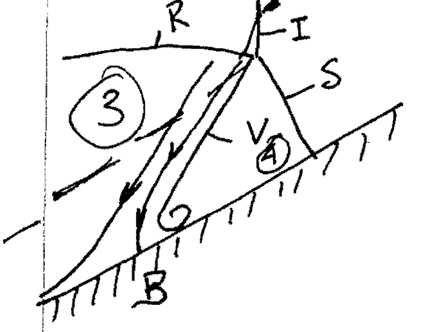

If $q_3 - q_4$ is smaller than a_3, the speed of sound in region 3, the deflection will occur without a shock. The resulting reflection configuration is sometimes called

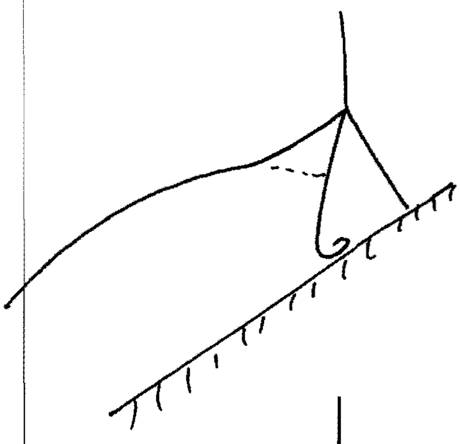

complex Mach reflection shown here. If $q_3 - q_4 > a_3$ but the incoming Mach number $\frac{q_3-q_4}{a_3}$ is too small to manage the deflection required, (deflection > max deflection for that Mach no) then

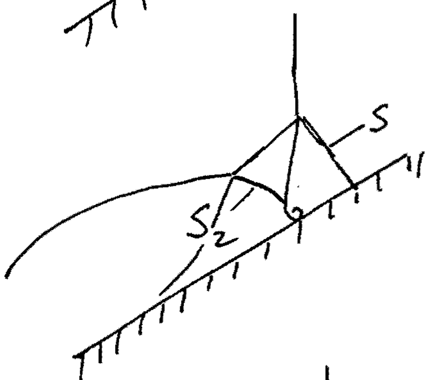

the second Mach stem S_2 will be a curved shock. If $(q_3 - q_4)/a_3$ is sufficiently large, the second Mach stem will be straight

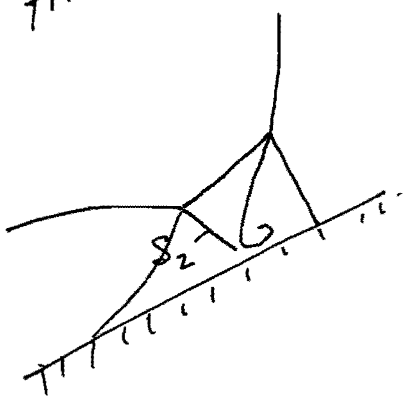

as shown here. From the second triple point, a second slip line is generated in the last two cases, of course. The momentum of the jet deflected toward the Mach stem can be so large that it causes a bulge in the Mach stem as shown here.

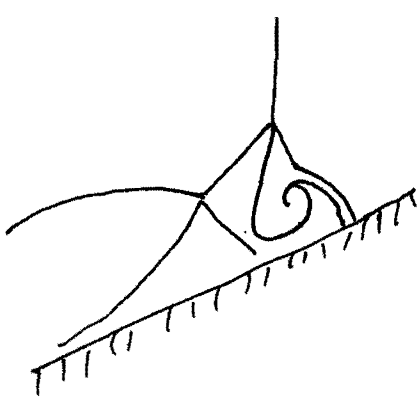

This was discovered experimentally by a 4th year undergraduate student Alison Leitch (1978). When I saw it, I told her to repeat the experiment because I didn't believe it. Soon after, numerical computations also found this phenomenon.

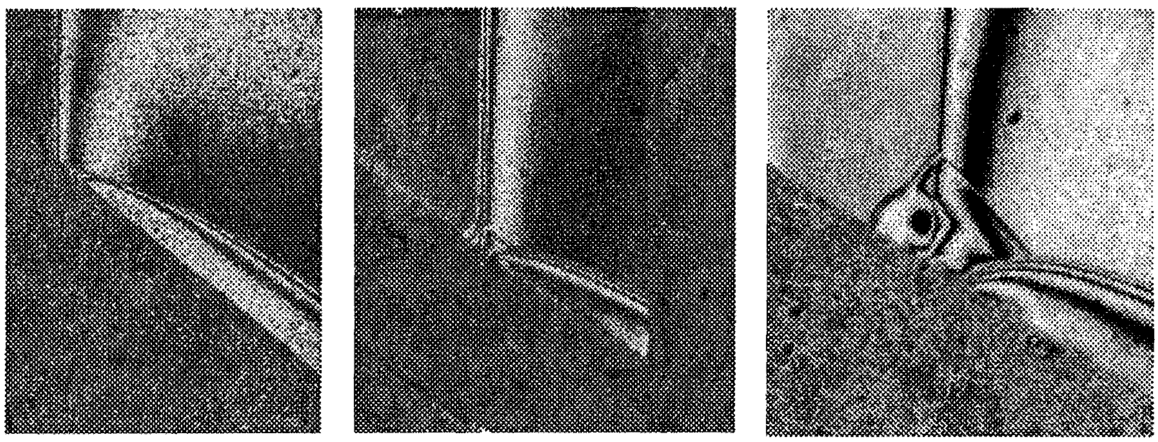

Each of the three images shows an infinite–fringe interferogram of a shock propagating from right to left at 6 km/s into nitrogen, and reflecting from a wedge of decreasing angle to the horizontal from left to right. The fringes following the shock indicate the density rise accompanying dissociation of the nitrogen. LEFT: Regular reflection, MIDDLE: small scale double Mach reflection, RIGHT: Double Mach reflection with distinctly visible bulge of the Mach stem that characterizes the phenomenon in this regime of flow. This image was the first experimental evidence of Mach stem bulge.

By making the ~~assumption~~ assumption that the Mach stem (first one in double Mach reflection) is straight and normal to the wall, Law and Glass were able to divide the parameter space up into regions where simple, complex, or double Mach reflection, or regular reflection occurs.

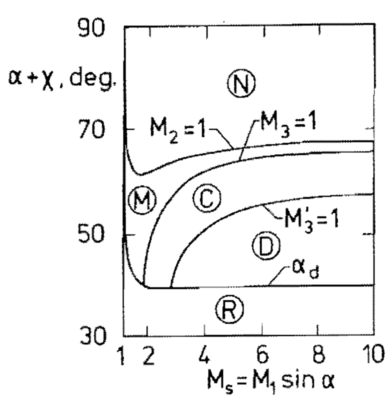

Figure 20 The structure of the direct Mach-reflection range (cf. Figure 16) for pseudosteady flow at $\gamma = 1.4$. (After Ben-Dor 1978.) R = regular, D = double Mach, C = complex Mach, M = single Mach, and N = no reflection. M'_3 is the Mach number relative to the second triple point.

In this plot, the vertical axis is $\beta+\chi$, where χ is the triple-point path angle. Thus, $\beta+\chi$ is $90°-\delta$, where δ is the wedge angle.

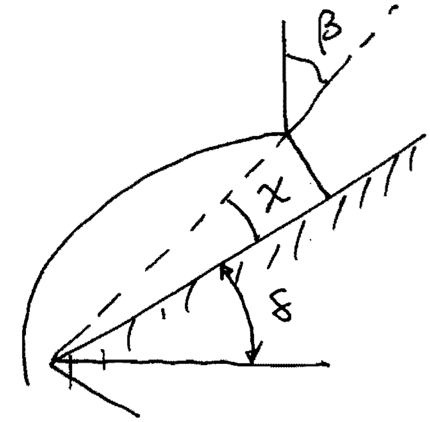

The region labelled (N) is one in which they said no reflection would occur. Indeed, this is the region where the reflected shock locus does not intersect the incident shock locus in the θp-plane, so that the three-shock theory of von Neumann gives no solution.

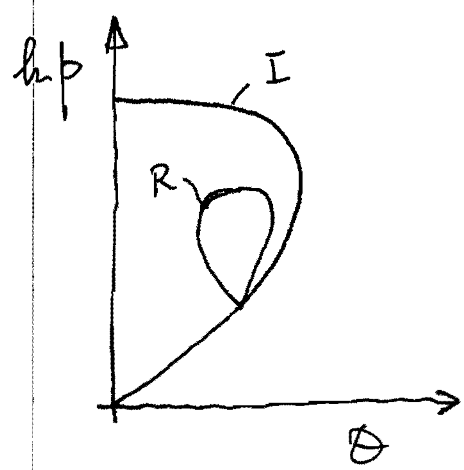

However, in experiments a clear reflected shock is observed. This inconsistency between experiment and theory is sometimes called the von Neumann paradox. Guderley 1947 had already suggested a resolution of this problem, which required a fourth wave to occur at the intersection of the reflected shock with the incident shock

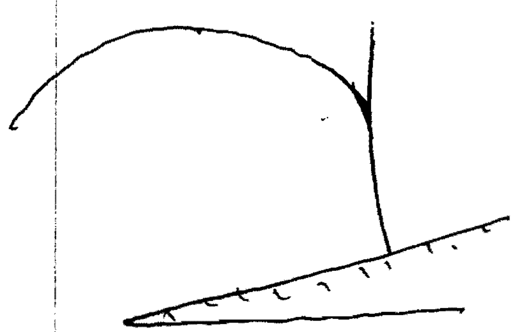

This fourth wave is an expansion fan. Locally the solution he gives looks like

this sketch. The expansion fan accelerates the flow to form a supersonic pocket. For a long time, numerical solutions were not able to support Guderley's solution. Only recently John Hunter of UC Davis and his group have discovered that the supersonic pocket is extremely small, so that the resolution of the computation has to be incredibly good to see it. Hunter started from the transonic small-disturbance equations. He discovered that the downstream side of the supersonic pocket was closed by a weak shock, so that a second expansion fan and a second supersonic pocket is necessary, and so on. These supersonic pockets get smaller and smaller, and the closing shocks get weaker and weaker. The following pages show some of these results.

203 a

conclusions in section 6.

2. The asymptotic shock reflection problem. The asymptotic shock reflection problem [11, 12, 14, 20] consists of the unsteady transonic small disturbance equation

$$\begin{aligned} &u_t + \left(\frac{1}{2}u^2\right)_x + v_y = 0, \\ &u_y - v_x = 0 \end{aligned} \tag{2.1}$$

in the half space $y > 0$ with the initial and boundary conditions

$$u(x, y, 0) = \begin{cases} 0 & \text{if } x > ay, \\ 1 & \text{if } x < ay, \end{cases} \tag{2.2}$$

$$v(x, y, t) = 0 \qquad \text{if } x > \sigma(y, t), \tag{2.3}$$

$$v(x, 0, t) = 0. \tag{2.4}$$

Here, $x = \sigma(y, t)$ is the location of the incident and Mach shocks. The location of the incident shock is given by

$$x = ay + \left(\frac{1}{2} + a^2\right) t. \tag{2.5}$$

The incident shock strength, as measured by the jump in u, is normalized to one. This problem depends on a single parameter a, the inverse slope of the incident shock.

These equations may be derived by a systematic asymptotic expansion of the shock reflection problem for the full Euler equations for weak shock reflection off thin wedges [12]. The variables $u(x, y, t)$, $v(x, y, t)$ are proportional to the x, y fluid velocity components, respectively, and pressure perturbations are proportional to u. The flow is irrotational and isentropic to leading order in the shock strength.

If the Mach number of the incident shock is M, and the wedge angle in radians is θ_w, then (2.1)–(2.4) is obtained in the limit $M \to 1$ and $\theta_w \to 0$, with

$$a = \frac{\theta_w}{2\sqrt{M - 1}} \tag{2.6}$$

fixed. Because of transonic similarity, the asymptotic problem depends on a single combination of the incident shock strength and the wedge angle. A regularly reflected solution of (2.1)–(2.4) is impossible when $a < \sqrt{2}$, and triple point solutions of (2.1), in which three plane shocks separated by constant states meet at a point, do not exist.

The problem (2.1)–(2.4) is self-similar, so the solution depends only on the similarity variables

$$\xi = \frac{x}{t}, \qquad \eta = \frac{y}{t}.$$

Writing (2.1) in terms of ξ, η, and a pseudo-time variable $\tau = \log t$, we get

$$\begin{aligned} &u_\tau - \xi u_\xi - \eta u_\eta + \left(\frac{1}{2}u^2\right)_\xi + v_\eta = 0, \\ &u_\eta - v_\xi = 0. \end{aligned} \tag{2.7}$$

Ac237 203

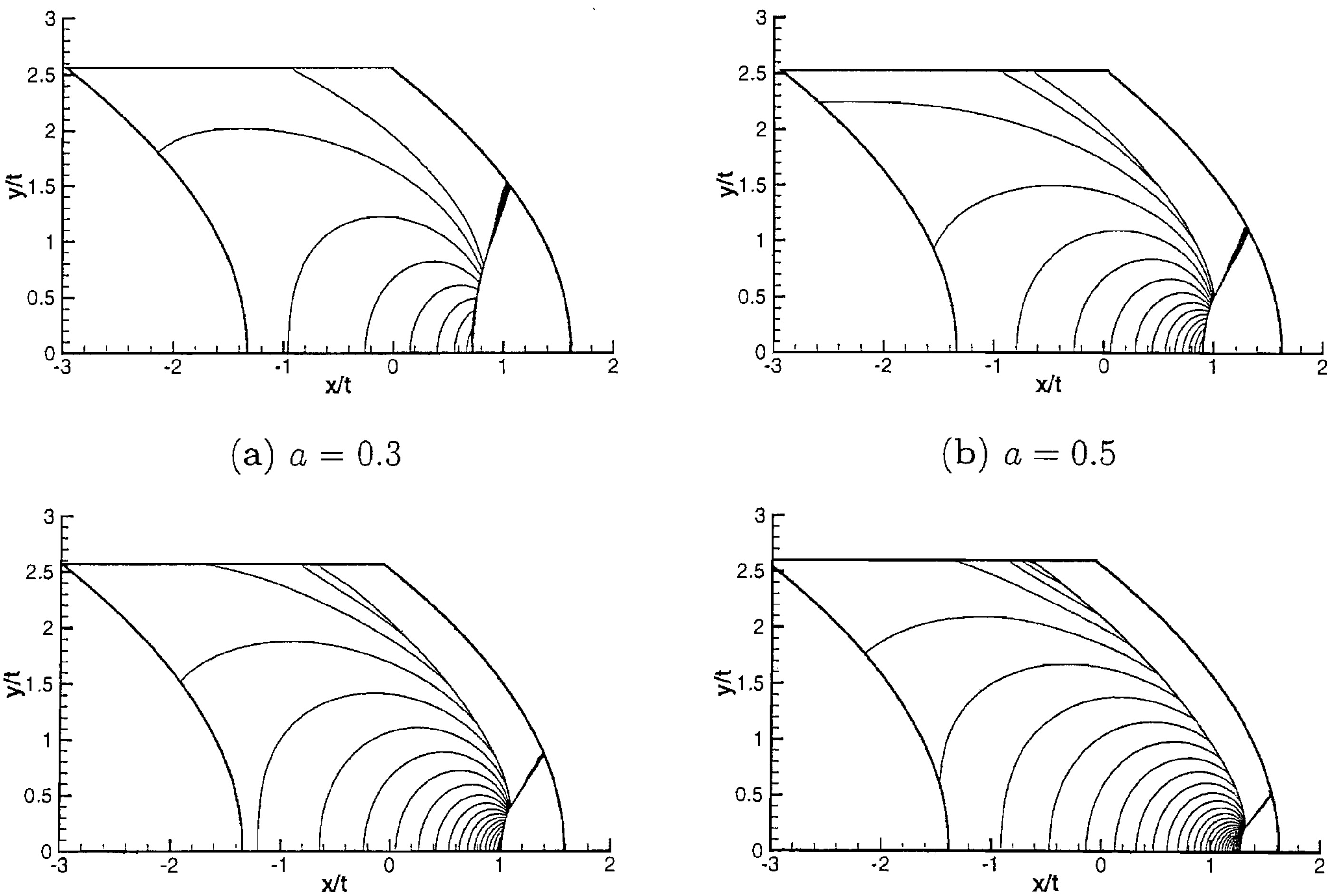

(a) $a = 0.3$ (b) $a = 0.5$

(c) $a = 0.6$ (d) $a = 0.8$

FIG. 2. *Contour plots of u for increasing values of a, showing the full numerical domain. The u-contour spacing is* 0.05.

TABLE 4.1

Numerically computed values of the size of the supersonic region at the triple point, the triple point location, and the strength $[u]_r$ *of the reflected shock at the sonic point. The shock strength is measured by the jump* $[u]$ *in u.*

Ae 237

204

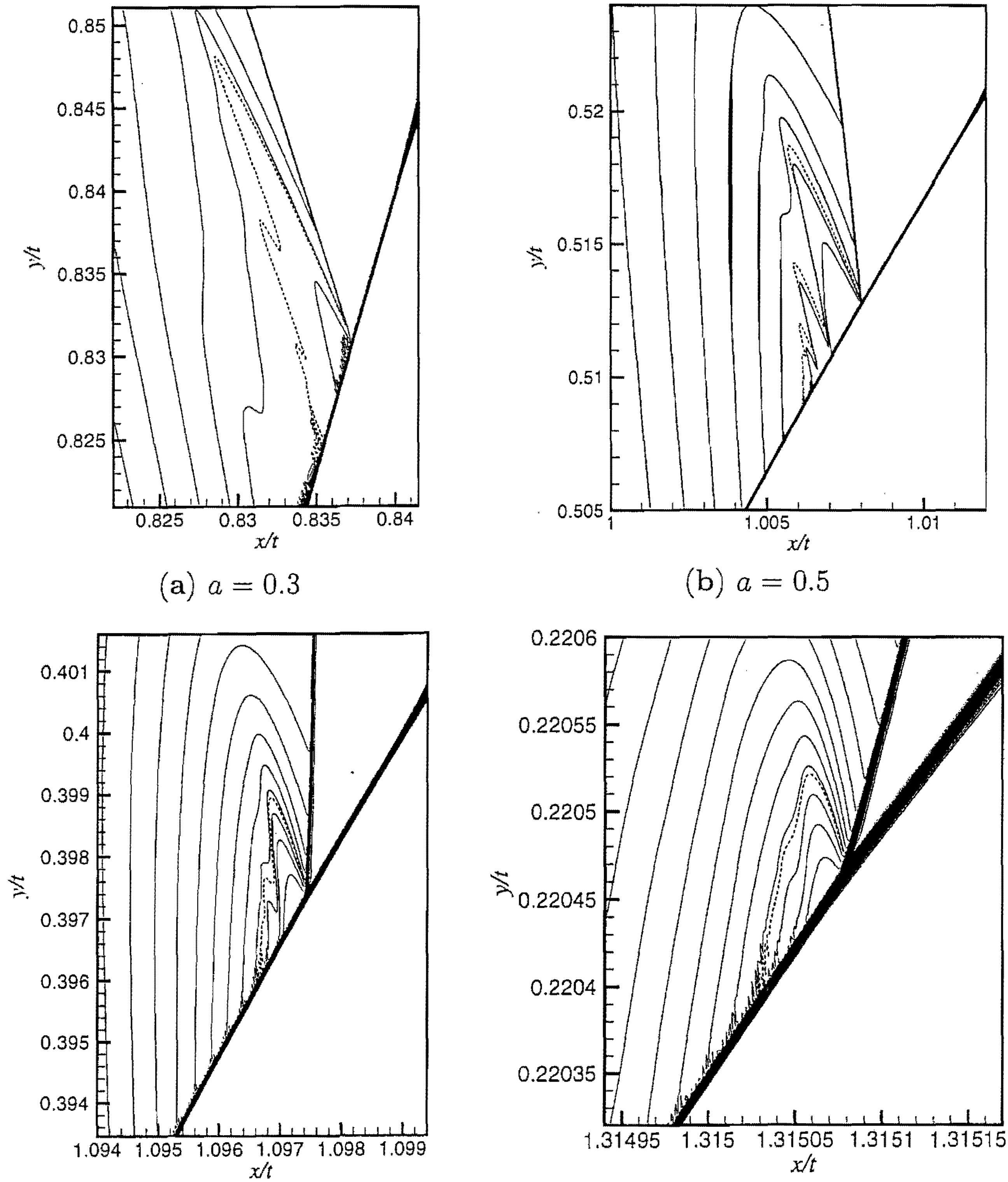

(a) $a = 0.3$

(b) $a = 0.5$

(c) $a = 0.6$

(d) $a = 0.8$

FIG. 3. *Contour plots of u near the triple point for increasing values of a. The u-contour spacing is* 0.005 *in* (a), *and* 0.01 *in* (b)–(d). *The dotted line is the sonic line. The regions shown contain the refined uniform grids, which have the following numbers of grid points:* (a) 620×480; (b) 768×608; (c) 346×260; (d) 245×150.

Ae 237 205

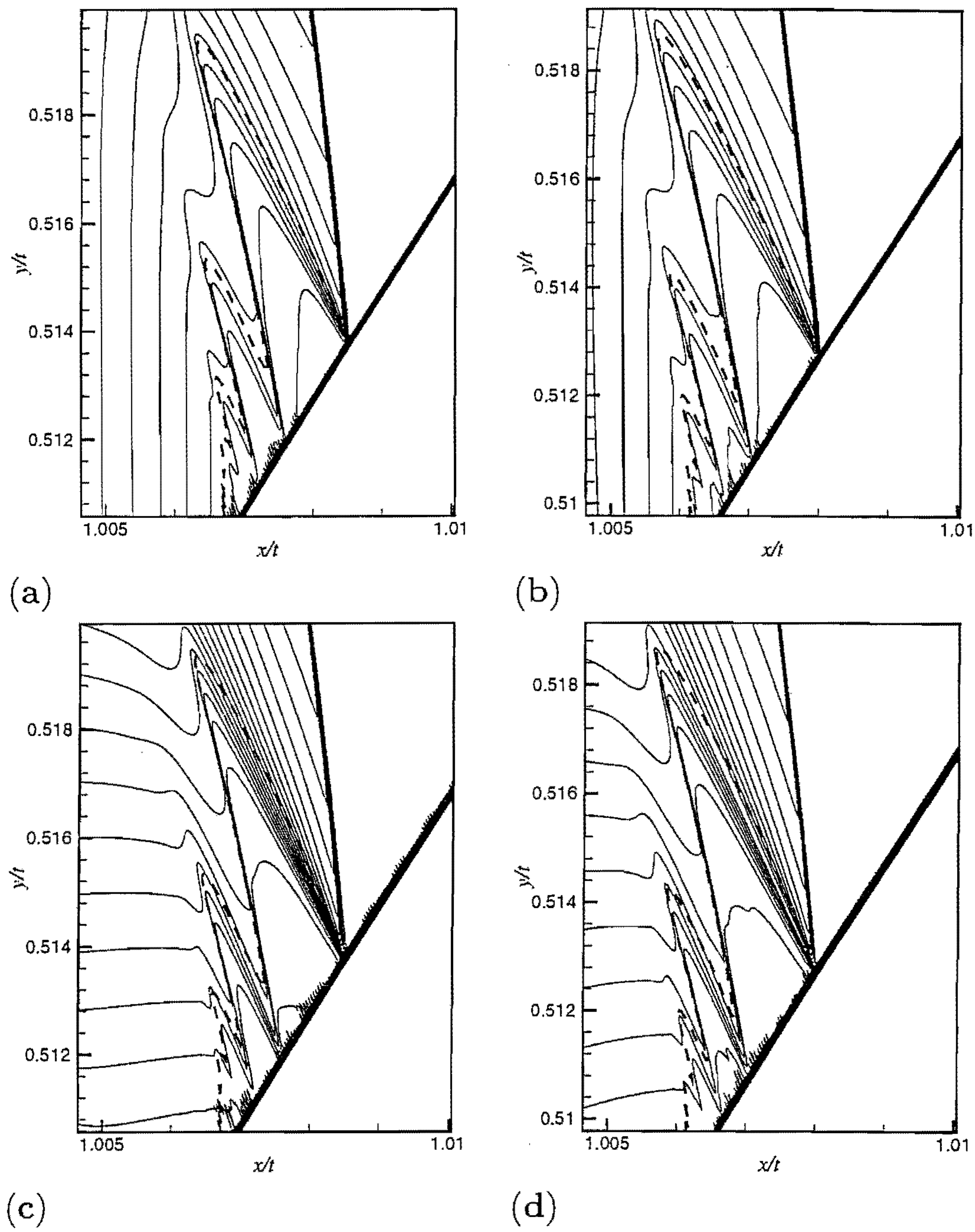

FIG. 10. *A comparison of u- and v-contours near the triple point for the two solutions shown in Figure 9. The plots in* (a) *and* (b) *show u-contours for the solutions computed on the larger and smaller domains, respectively, plotted at the same levels of u. The plots in* (c) *and* (d) *show v-contours for the solutions computed on the larger and smaller domains, respectively, plotted at the same levels of v. The dashed line in* (a)–(d) *is the sonic line. The u-contour spacing in* (a)–(b) *is* 0.005, *and the v-contour spacing in* (c)–(d) *is* 0.001.

Ae237

206

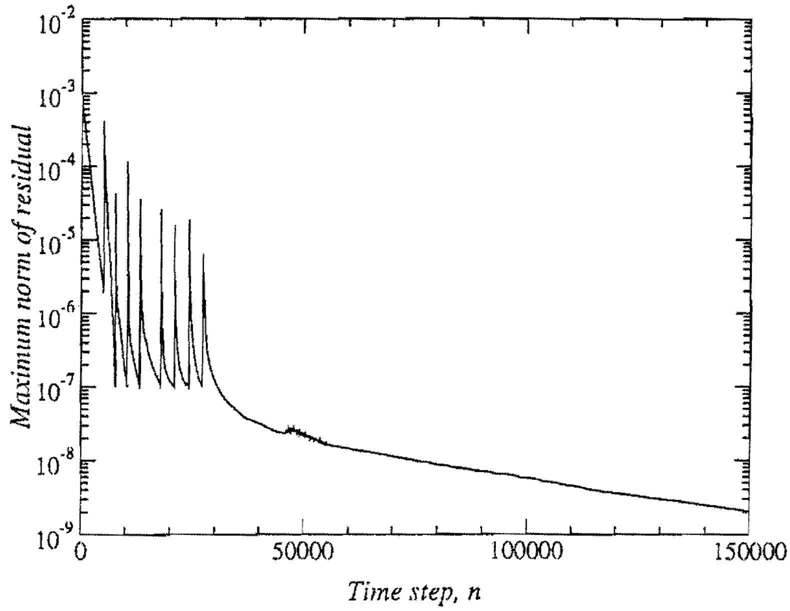

FIG. 8. *A plot of the maximum norm of the residual, showing partial convergence on a sequence of grids, followed by convergence on the most refined grid. The sharp local peaks correspond to interpolations onto more refined grids. The computation on the most refined grid begins at approximately* $n = 30000$. *The final stage of convergence to a value for the maximum norm of the residual of less than* 10^{-9} *is not shown in the plot.*

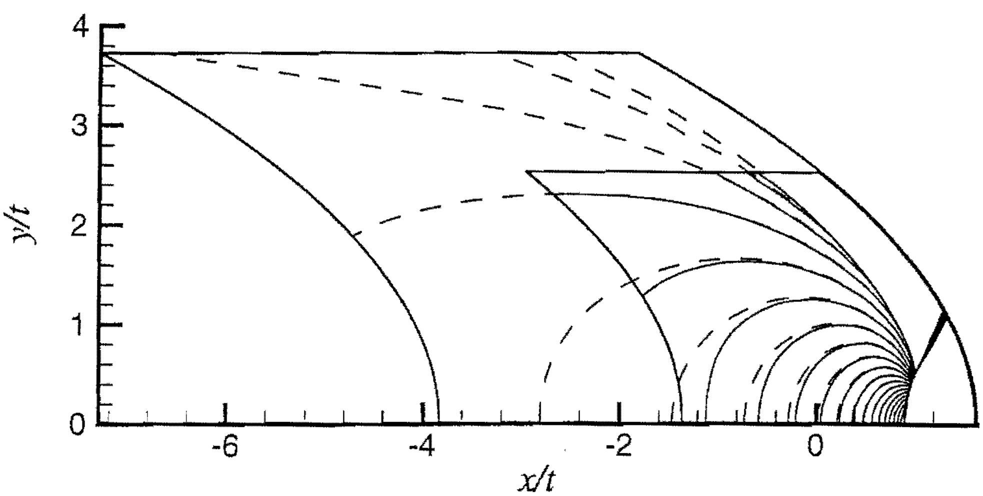

FIG. 9. *A check of the sensitivity of the solutions to the size of the numerical domain, showing u-contours for two solutions computed on different sized domains, for* $a = 0.5$. *The full numerical domains are shown, with u-contours for the large domain solution (dashed lines) and the small domain solution (solid lines) plotted at the same values of u. Contour lines for u and v near the triple point for both solutions shown here are compared in Figure* 10.

Viscous effects, shock-generated boundary layer

The shock-tube problem in a perfect gas inviscid flow is a one-dimensional problem and, if the diaphragm bursts instantaneously, the problem is pseudo-steady as well. A plot of the velocity distribution in such an inviscid flow looks as shown here for $t = t_1$. In the real case, the no-slip condition applies at the walls of the shock tube, so that $u = 0$ at the wall. A boundary layer therefore develops along the shock tube wall.

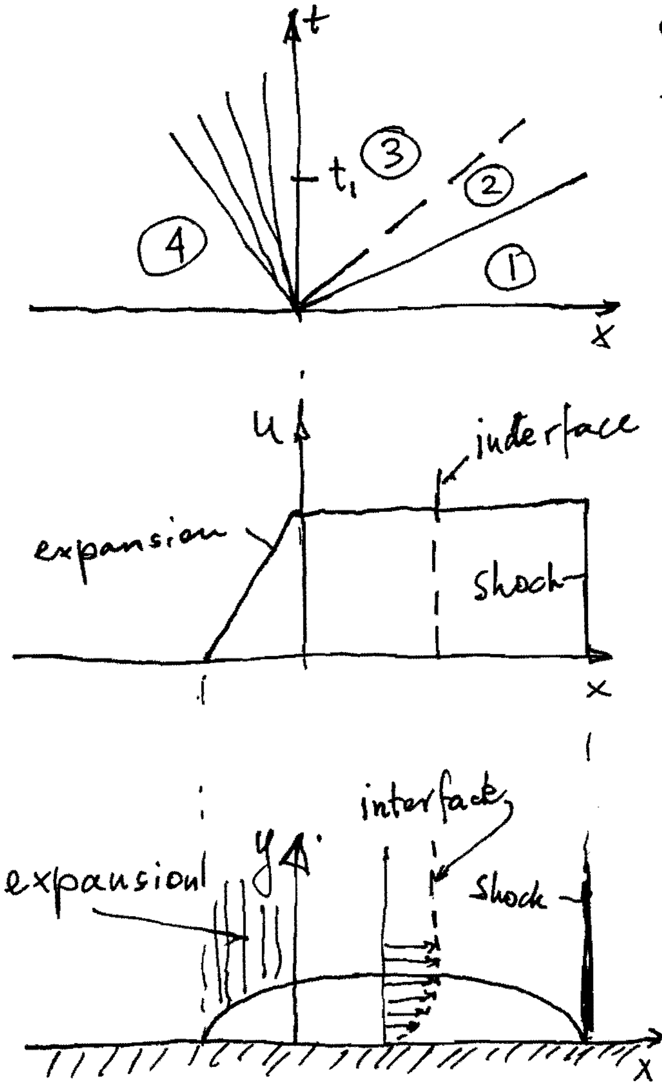

The propagation of the expansion wave into the driver gas to the left generates a boundary layer in the driver gas and the shock propagating into the test gas to the right generates a boundary layer in the test gas. The interface is distorted in the boundary layer by the velocity profile.

The problem has become very much more difficult, since, instead of being a one-dimensional pseudo-steady one, it is now a three-dimensional one (two-dimensional unsteady). However, we may reduce portions of it to two-dimensional steady flow.

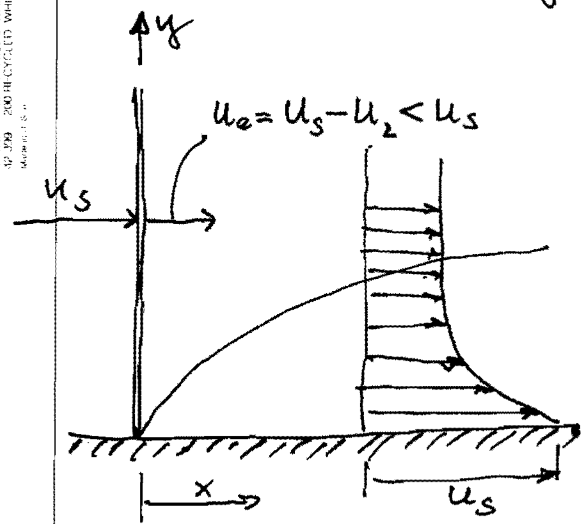

In particular, consider the shock-generated boundary layer in the frame of reference of the shock. Let the shock speed in the frame of the wall be u_s to the left, and the post-shock speed be u_2 in the wall frame. Now go to the shock-fixed frame. The gas to the left of the shock and the wall move with speed u_s to the right, and the post-shock speed outside the b. l. is $u_s - u_2$. This is smaller than the speed of the wall, so that the resulting velocity profile looks as shown. In the shock-fixed frame, the problem becomes steady if we are not interested in the far field.

One feature of this boundary layer can be seen immediately. The displacement thickness

$$\delta^* \equiv \int_0^\infty \left(1 - \frac{\rho}{\rho_e}\frac{u}{u_e}\right) dy$$

is usually negative, since $u/u_e > 1$ throughout the layer. The wall temperature is always lower than the edge temperature, so the density is higher in the b. l. than ρ_e. Thus, the displacement effect is negative, and the b. l. acts like a mass sink.

To find a solution for the shock-generated b. l. proceed as for other compressible b. l.'s

$$C \qquad \frac{\partial \rho u}{\partial x} + \frac{\partial \rho v}{\partial y} = 0$$

$$M_x \qquad \frac{\partial \rho u^2}{\partial x} + \frac{\partial \rho u v}{\partial y} = \frac{\partial \tau}{\partial y} \qquad \left[\frac{\partial p}{\partial x} = 0\right.$$

$$E \qquad \frac{\partial \rho u J}{\partial x} + \frac{\partial \rho v J}{\partial y} = \frac{\partial}{\partial y}(\tau u - q)$$

where $J \equiv h + \frac{u^2}{2}$, τ = shear stress, q = heat flux in the y direction. Now introduce a stream function such that

$$\rho u \equiv \rho_e \frac{\partial \psi}{\partial y}$$

$$\rho v \equiv -\rho_e \frac{\partial \psi}{\partial x}$$

Introduce new space coordinates X, Y such that

$$u = \frac{\partial \psi}{\partial Y}, \quad v = -\frac{\partial \psi}{\partial X}$$

This makes $\quad Y = \int_0^y \frac{\rho}{\rho_e} dy \quad , \quad X = x$

Substitute into the equations for a Newtonian fluid with simple heat conduction, to get

$$M_x \qquad \rho u \frac{\partial u}{\partial x} + \rho v \frac{\partial v}{\partial y} = \frac{\partial}{\partial y}\left(\mu \frac{\partial u}{\partial y}\right)$$

in the original space coordinates. Transform to X, Y

$$\rho u \left(\frac{\partial u}{\partial X} + \frac{\partial u}{\partial Y}\frac{\partial Y}{\partial x}\right) + \rho v \frac{\rho}{\rho_e}\frac{\partial u}{\partial Y} = \frac{\rho}{\rho_e}\frac{\partial}{\partial Y}\left(\frac{\rho}{\rho_e}\mu \frac{\partial u}{\partial Y}\right)$$

$$\text{now} \quad \rho v = -\rho_e \frac{\partial \psi}{\partial x} = -\rho_e\left(\frac{\partial \psi}{\partial X} + \frac{\partial \psi}{\partial Y}\frac{\partial Y}{\partial x}\right)$$

Substitute and rewrite terms

$$\rho \frac{\partial \psi}{\partial Y}\left(\frac{\partial^2 \psi}{\partial X \partial Y} + \frac{\partial u}{\partial Y}\frac{\partial Y}{\partial x}\right) - \rho \frac{\partial u}{\partial Y}\left(\frac{\partial \psi}{\partial X} + \frac{\partial \psi}{\partial Y}\frac{\partial Y}{\partial x}\right) = \frac{\rho}{\rho_e}\frac{\partial}{\partial Y}\left(\frac{\rho \mu}{\rho_e}\frac{\partial^2 \psi}{\partial Y^2}\right)$$

The two circled terms cancel, and, dividing by ρ,

$$\boxed{\frac{\partial \psi}{\partial Y}\frac{\partial^2 \psi}{\partial X \partial Y} - \frac{\partial^2 \psi}{\partial Y^2}\frac{\partial \psi}{\partial X} = \frac{\mu_e}{\rho_e}\frac{\partial}{\partial Y}\left(\frac{\rho \mu}{\rho_e \mu_e}\frac{\partial^2 \psi}{\partial Y^2}\right)}$$

Introduce $\quad \eta \equiv \dfrac{Y}{\delta(X)} \quad , \quad \delta(X) \equiv \sqrt{\dfrac{\nu_e X}{\frac{1}{2}(u_w + u_e)}}$

$\nu_e = \mu_e/\rho_e$, u_w = wall velocity.

This makes $\quad \dfrac{d\delta}{dX} = + \dfrac{\delta}{2X}$.

Consider $\psi(\eta, X)$, and introduce $f(\eta)$

such that

$$\psi \equiv \delta(X)\left[(u_w - u_e) f(\eta) + u_e \eta\right]$$

making $u = \dfrac{\partial \psi}{\partial Y} = (u_w - u_e) f'(\eta) + u_e$

and $f'(\eta) = \dfrac{u - u_e}{u_w - u_e}$ $= 1$ at the wall, $= 0$ at edge of b.l.

With these, we can write

$$\frac{\partial \psi}{\partial X} = -\overset{\partial\eta/\partial X}{\left(\frac{\eta}{2X}\right)}\delta\left[(u_w - u_e) f' + u_e\right] + \frac{\delta}{2X}\left[(u_w - u_e) f + u_e \eta\right]$$

$$\frac{\partial \psi}{\partial Y} = (u_w - u_e) f' + u_e$$

$$\frac{\partial^2 \psi}{\partial Y^2} = \frac{u_w - u_e}{\delta} f''$$

Substitute these into the box and simplify:

$$\boxed{f''\left[(u_w - u_e) f + u_e \eta\right] + (u_w + u_e)\left(\frac{\rho\mu}{\rho_e \mu_e} f''\right)' = 0}$$

with boundary conditions: $f'(0) = 1$

$f'(\infty) = 0$

$f(0) = 0.$

The assumption introduced by Chapman and Rubesin that $\rho\mu = \rho_e \mu_e$ is a good

approximation and simplifies matters greatly.
Putting $\varepsilon \equiv \dfrac{u_e}{u_e + u_w}$, the equation becomes

$$\boxed{f''' + \left[(1-2\varepsilon) f + \varepsilon\eta\right] f'' = 0}$$ same b.c.'s.

This differs from the regular flat-plate b. l. equation only in the parameter ε, which for the regular b. l. is zero.

Now consider the energy equation. Rewrite it using continuity and Newtonian fluid:

$$u\frac{\partial J}{\partial \cancel{x}} + v\frac{\partial J}{\partial y} = \frac{1}{\rho}\frac{\partial}{\partial y}\left(\mu u \frac{\partial u}{\partial y} + k\frac{\partial T}{\partial y}\right)$$

or

$$\frac{D\left(h + \frac{u^2}{2}\right)}{Dt} = \frac{1}{\rho}\frac{\partial}{\partial y}\left(\mu\frac{\partial u^2/2}{\partial y} + \frac{k}{c_p}\frac{\partial h}{\partial y}\right)$$

$$= \frac{1}{\rho}\frac{\partial}{\partial y}\left(\frac{k}{c_p}\frac{\partial\left(h+\frac{u^2}{2}\right)}{\partial y} + \left(\mu - \frac{k}{c_p}\right)\frac{\partial \frac{u^2}{2}}{\partial y}\right)$$

$$= \frac{1}{\rho}\frac{\partial}{\partial y}\left(\frac{\mu}{Pr}\frac{\partial\left(h+\frac{u^2}{2}\right)}{\partial y} + \frac{k}{c_p}(Pr - 1)\frac{\partial\frac{u^2}{2}}{\partial y}\right)$$

where $Pr = \mu c_p / k$

Put $Pr = 1$ $\longrightarrow$ $$= \frac{1}{\rho}\frac{\partial}{\partial y}\left(\frac{\mu}{Pr}\frac{\partial\left(h+\frac{u^2}{2}\right)}{\partial y}\right)$$

With $Pr = 1$, a good assumption for gases, one solution of this equation is

$$h + \frac{u^2}{2} = \text{constant} = h_w$$

With this result, we can write down a relation between h and u as follows

$$\frac{h}{h_e} - 1 = \left(\frac{h_w}{h_e} - 1\right)\frac{u^2 - u_e^2}{u_w^2 - u_e^2}$$

We now proceed to find an expression for the displacement thickness

$$\delta^* = \int_0^\infty \left(1 - \frac{\rho u}{\rho_e u_e}\right) dy = \int_0^\infty \left(\frac{\rho_e}{\rho} - \frac{u}{u_e}\right) dY$$

For a perfect gas $\frac{h}{h_e} = \frac{\rho_e}{\rho}$, and

$$\delta^* = \delta \int_0^\infty \left[\left(\frac{h}{h_e} - 1\right) - \left(\frac{u}{u_e} - 1\right)\right] d\eta$$

Put $H = h_w/h_e$ and $U = u_w/u_e$

$$\delta^* = \delta \int_0^\infty \left[(H-1)\frac{u^2 - u_e^2}{u_w^2 - u_e^2} - \frac{u - u_e}{u_w - u_e}\,\frac{u_w - u_e}{u_e}\right] d\eta$$

$$= \delta \int_0^\infty \left[(H-1)\frac{(u - u_e)}{u_w - u_e} \cdot \frac{(u - u_e + 2u_e)}{u_w - u_e} \cdot \frac{u_w - u_e}{u_w + u_e} - f'(U-1)\right] d\eta$$

$$= \delta \int_0^\infty \left[(H-1) f'\left(f' + \frac{2}{U-1}\right)\frac{U-1}{U+1} - f'(U-1)\right] d\eta$$

$$= (U-1)\delta \int_0^\infty \left\{ \frac{H-1}{U+1} f'^2 + \left[2\,\frac{H-1}{U^2-1} - 1\right] f' \right\} d\eta$$

Now write this in a form that can be integrated by parts. Note first, that

$$(ff')' = f'^2 + ff''$$

So $$f'^2 = (ff')' - ff''$$

The b.l. equation gives $ff'' = \frac{-1}{1-2\varepsilon}\left[f''' + \varepsilon \eta f''\right]$

So, using $\varepsilon = \frac{1}{U+1}$,

$$f'^2 = (ff')' + \frac{U+1}{U-1} f''' + \frac{\eta f''}{U-1}$$

Substitute these back into the δ^* equation:

$$\frac{\delta^*}{\delta} = (U-1)\int_0^\infty \left\{ \frac{H-1}{U+1}(ff')' + \frac{H-1}{U-1} f''' + \frac{H-1}{U^2-1}\eta f'' \right.$$
$$\left. + \left[2\frac{H-1}{U^2-1} - 1\right] f' \right\} d\eta$$

The contribution from the first term is zero since $f'(\infty) = 0$ and $f(0)=0$. The third term can be integrated by parts to give $\int_0^\infty \eta f'' d\eta = \eta f' \Big|_0^\infty - \int_0^\infty f' d\eta = -f\Big|_0^\infty = -f(\infty)$

$$\frac{\delta^*}{\delta} = (U-1)\left\{ -\frac{H-1}{U-1} f''(0) + f(\infty)\left[2 \cdot \frac{H-1}{U^2-1} - 1 - \frac{H-1}{U^2-1}\right]\right\}$$

$$\boxed{\frac{\delta^*}{\delta} = -(U-1) f(\infty)\left\{1 + \frac{1-H}{U-1}\left[\frac{1}{U+1} - \frac{f''(0)}{f(\infty)}\right]\right\}}$$

Next we obtain an expression for the shear stress at the wall, τ_w.

$$\tau_w = \mu_w \left(\frac{\partial u}{\partial y}\right)_w$$

$$= \mu_w \frac{\rho_w}{\rho_e} \left(\frac{\partial^2 \psi}{\partial Y^2}\right)_w$$

$$= \mu_e \frac{u_w - u_e}{\delta} f''(0)$$

Therefore the local skin friction coefficient

$$C_f \equiv \frac{\tau_w}{\frac{1}{2}\rho_e u_e^2} = 2 \frac{\nu_e}{u_e \delta} \frac{u_w - u_e}{u_e} f''(0)$$

$$\boxed{C_f = 2 \frac{\nu_e}{u_e \delta} (U - 1) f''(0)}$$

Also, if $Pr = 1$, the energy equation gives

$$q = \tau u$$

so that $\boxed{q_w = \tau_w u_w}$

Define the Stanton number

$$St \equiv \frac{q_w}{(h_e - h_w)\rho_e u_e}$$

$$= \frac{\tau_w u_w}{\frac{1}{2}\rho_e u_e^2} \cdot \frac{\frac{1}{2}\rho_e u_e^2}{(h_e - h_w)\rho_e u_e}$$

$$\boxed{St = \frac{1}{2} C_f \cdot \frac{U}{1-H} \cdot \frac{u_e^2}{h_e}}$$

$$= \cancel{4} C_f \frac{U}{1-H} \cdot \frac{(\gamma-1)}{2} M_e^2$$

Velocity profiles in limiting cases

$$f''' + \left[(1-2\varepsilon) f + \varepsilon \eta\right] f'' = 0$$

Shock generated boundary layer:

Weak shock: $\quad \frac{u_w}{u_e} = 1, \quad \varepsilon = \frac{1}{2}$

$$f''' + \frac{\eta}{2} f'' = 0$$

gives $f' = \operatorname{erfc} \frac{\eta}{2}$

Rayleigh b. l.

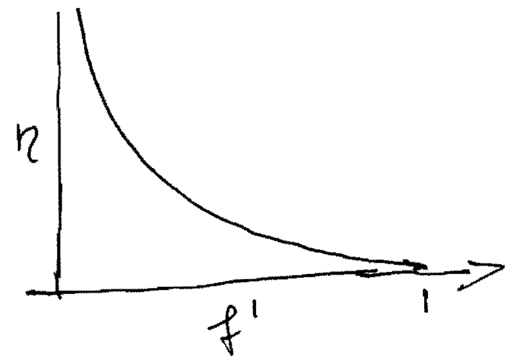

Very strong shock:

$u_w \gg u_e, \quad \varepsilon = 0$

$$f''' + f f'' = 0$$

Blasius equation
with different b.c.'s

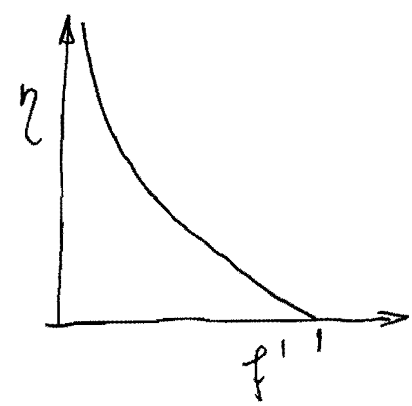

The following three pages give quantitative results for velocity profiles, $f''(0)$ and $f(\infty)$ from Prof. Sturtevant's calculations.

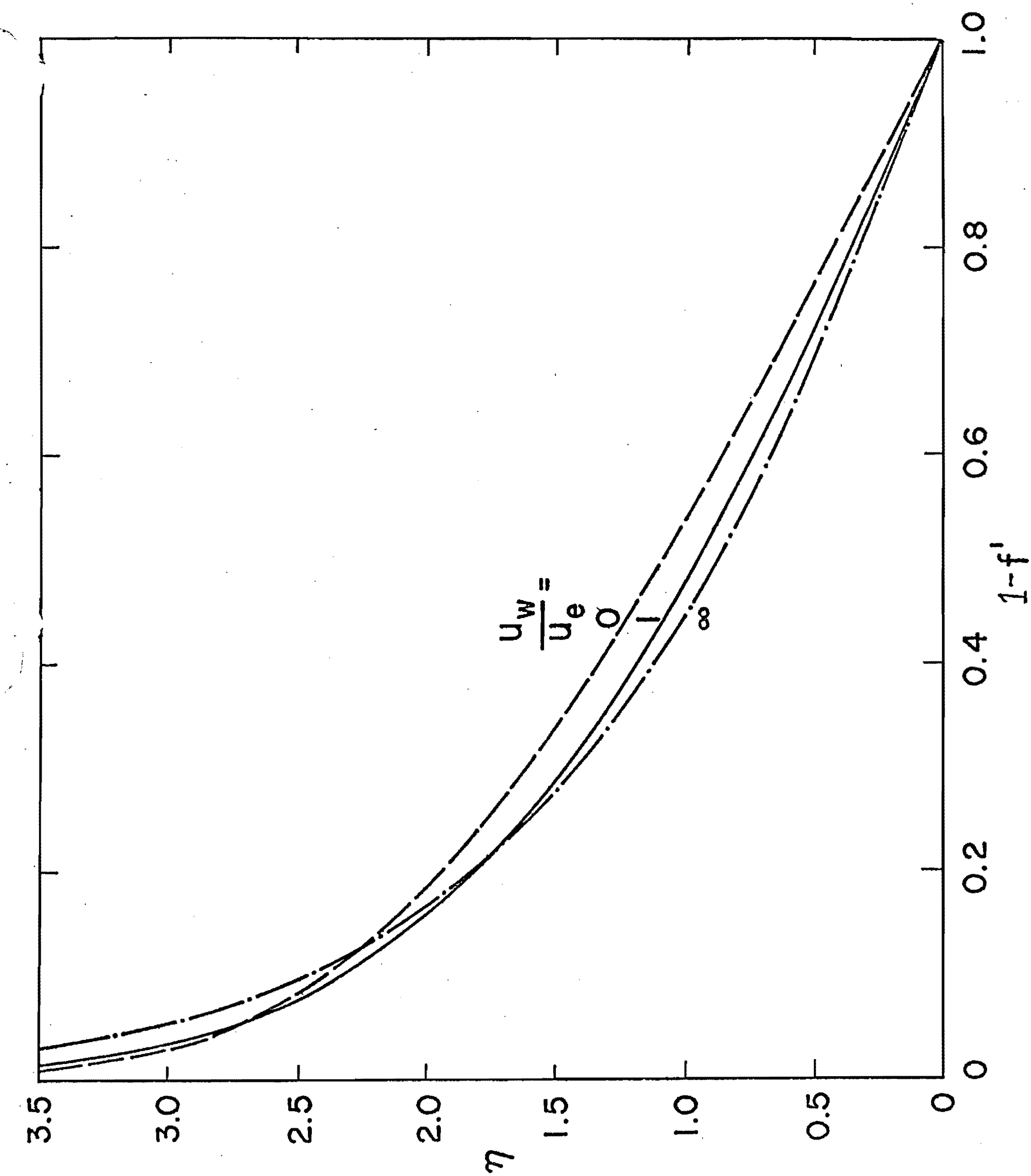
$\frac{u_w}{u_e}$ =
0
1
∞
$1-f'$
η
0
0.2
0.4
0.6
0.8
1.0
0.5
1.0
1.5
2.0
2.5
3.0
3.5

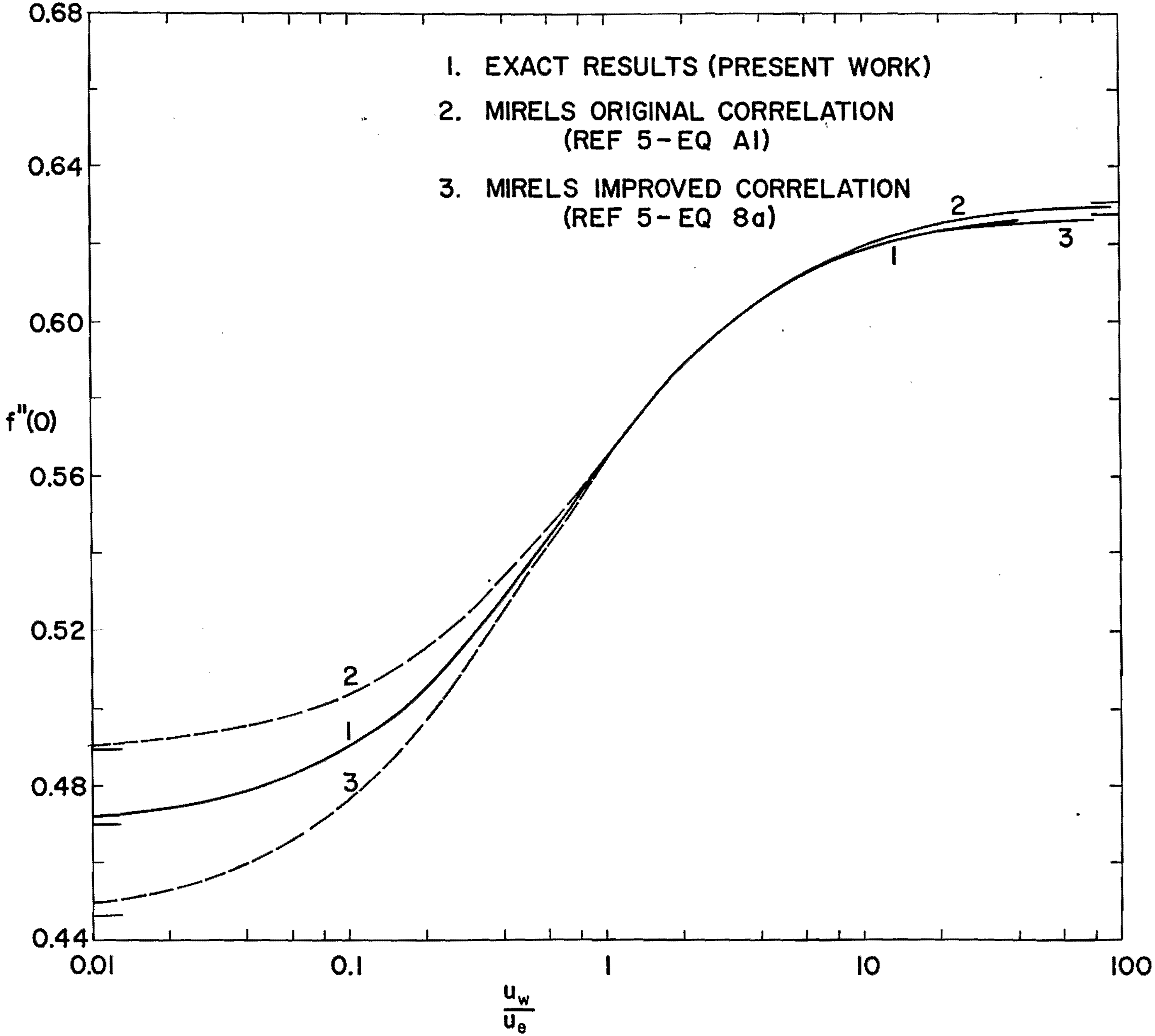

1. EXACT RESULTS (PRESENT WORK)
2. MIRELS ORIGINAL CORRELATION (REF 5-EQ A1)
3. MIRELS IMPROVED CORRELATION (REF 5-EQ 8a)
f''(0)
0.68
0.64
0.60
0.56
0.52
0.48
0.44
0.01
0.1
1
10
100
$\frac{u_w}{u_e}$
1
2
3

Ae237

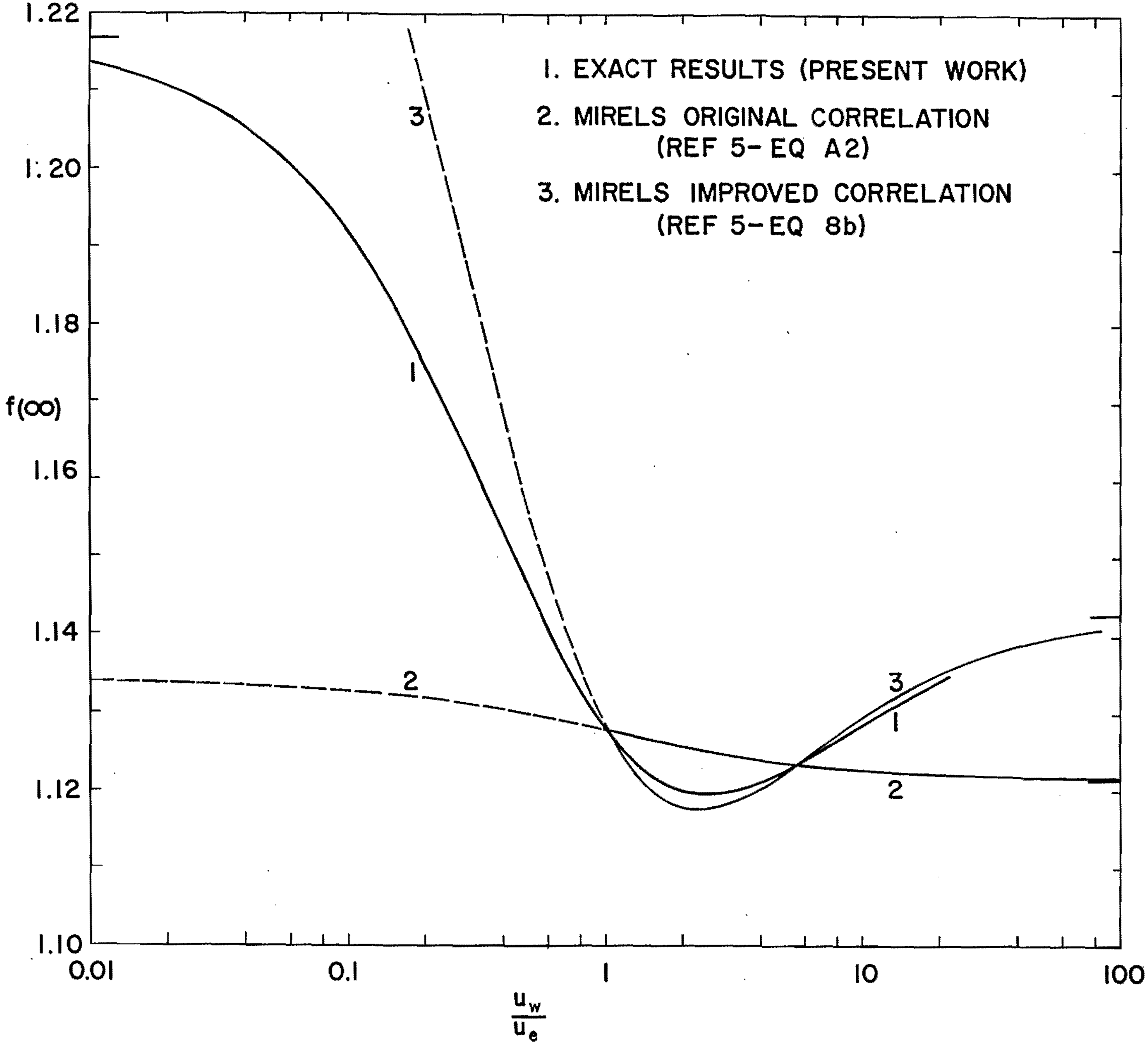
1. EXACT RESULTS (PRESENT WORK)
2. MIRELS ORIGINAL CORRELATION (REF 5- EQ A2)
3. MIRELS IMPROVED CORRELATION (REF 5- EQ 8b)
f(∞)
1.22
1.20
1.18
1.16
1.14
1.12
1.10
0.01
0.1
1
10
100
$\frac{u_w}{u_e}$
1
2
3

Ae237

Displacement thickness

Weak shock: $M \to 1$

Evaluate the quantities involved in the formula:

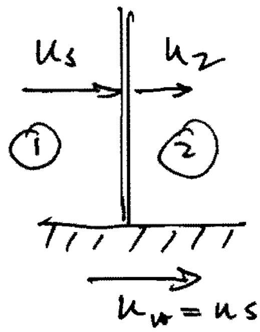

$$U-1 = \frac{u_w}{u_e} - 1 = \frac{u_s}{u_2} - 1 = \frac{\rho_2}{\rho_1} - 1$$

$$= \frac{\gamma+1}{\gamma-1+\frac{2}{M^2}} - 1$$

$$= \frac{\gamma+1-\left[\gamma-1+\frac{2}{M^2}\right]}{\gamma-1+\frac{2}{M^2}}$$

$$= \frac{2(M^2-1)}{\gamma+1+(M^2-1)}$$

$$\doteq \frac{2}{\gamma+1}(M^2-1) \qquad M \to 1$$

$$1-H = 1-\frac{h_w}{h_e} = 1-\frac{h_1}{h_2}$$

$$= 1-\frac{1}{1+\frac{2(\gamma-1)}{\gamma+1}(M^2-1)}$$

$$= \frac{1+2\frac{\gamma-1}{\gamma+1}(M^2-1)-1}{1+\frac{2(\gamma-1)}{\gamma+1}(M^2-1)} \doteq 2\,\frac{\gamma-1}{\gamma+1}(M^2-1)$$

$$\frac{\delta^*}{\delta} = -(U-1)\,f_1(\infty)\left\{1+\frac{1-H}{U-1}\left[\frac{1}{U+1}-\frac{f_1''(0)}{f_1(\infty)}\right]\right\}$$

$$= -\frac{2}{\gamma+1}(M^2-1)\,f_1(\infty)\left\{1+(\gamma-1)\left[\frac{1}{2}-\underbrace{0.496}_{\text{for that case}}\right]\right\}$$

$$\boxed{\frac{\delta^*}{\delta} = -\frac{2}{\gamma+1}(M^2-1)\,f_1(\infty)}$$

Note: using f_1 ok. because $f_2 \simeq f_1$

Strong shock. $M \to \infty$

For a strong shock, $h_e \gg h_1 = h_w$. The upstream specific enthalpy h_1 and the specific enthalpy at the wall are the same, since the wall has had no time to get hot, and the gas temperature at the wall is equal to the wall temperature. Also, the density ratio across the shock $\rho_2/\rho_1 = (\gamma+1)/(\gamma-1)$, since $M \to \infty$. Therefore $U = (\gamma+1)/(\gamma-1)$.

$$\therefore\ U-1 = \frac{2}{\gamma-1}, \qquad U+1 = \frac{2\gamma}{\gamma-1}$$

$$\frac{\delta^*}{\delta} = -\frac{2}{\gamma-1} f(\infty)\left\{1 + \frac{\gamma-1}{2}\left[\frac{\gamma-1}{2\gamma} - \frac{f''(0)}{f(\infty)}\right]\right\}$$

Now look at $\{\ \}$ for different values of γ

$\gamma = 1.4$: $\quad f(\infty) = 1.123$, $\frac{\gamma-1}{2} = 0.2$, $\frac{\gamma-1}{2\gamma} = \frac{1}{7}$, $\frac{f''(0)}{f(\infty)} = \frac{0.612}{1.123}$

Resulting value of $f(\infty)\{\ \} = 1.033$

$\gamma = 5/3$: $\quad f(\infty) = 1.122$, $\frac{\gamma-1}{2} = \frac{1}{3}$, $\frac{\gamma-1}{2\gamma} = \frac{1}{5}$, $\frac{f''(0)}{f(\infty)} = \frac{0.603}{1.122}$

$$f(\infty)\{\ \} = 0.996$$

Effect of γ is negligible,

$$\boxed{\frac{\delta^*}{\delta} = -\frac{2}{\gamma-1}} \quad \boxed{= -\frac{u_w}{u_e}}$$

The effect of the shock-generated b.l. on shock tubes

The velocity profile across the shock tube immediately after the shock is uniform as shown here, $u = u_2$. However some distance downstream of the shock, the profile looks as shown here. The effect of the negative displacement thickness is to make the shock tube look (to the flow outside the b.l. as if the diameter were to increase with distance from the shock by twice the displacement thickness. In the shock-fixed frame ② is always subsonic, so area increase causes velocity decrease and density increase.

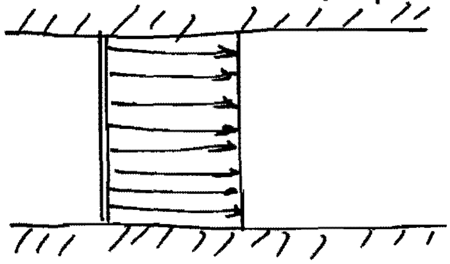

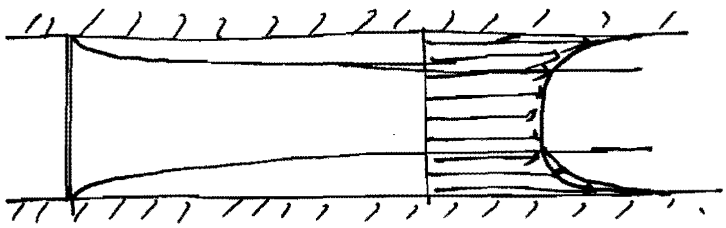

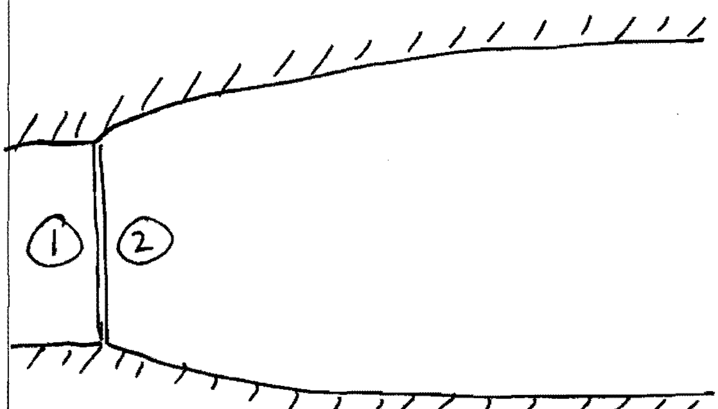

Now consider a control volume in a two-dimensional shock tube. The velocity $u_e(x)$ outside the b.l. decreases with increasing x, and $\rho_e(x)$ increases.

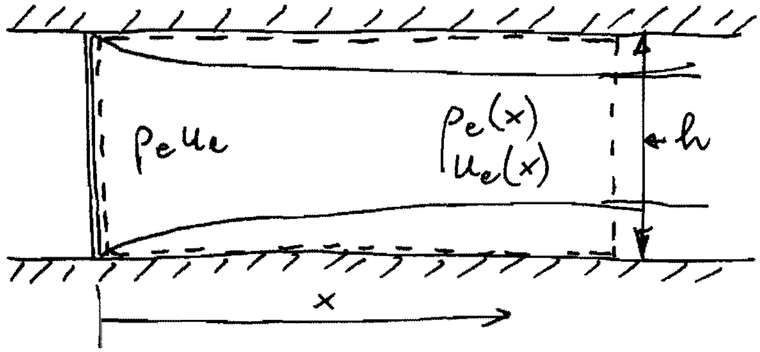

Conserve mass for control volume shown dashed.

$$\rho_e(0)\, u_e(0)\, h = \rho_e(x)\, u_e(x)\, h - 2\rho_e(x)\, u_e(x)\, \delta^*(x)$$

This is a consequence of the definition of δ^*. As x increases there comes a point when $u_e(x)$ becomes zero (negative δ^*). When this point is reached,

$$u_e(x) = \frac{\rho_e(0)\, u_e(0)}{\rho_e(x)}\left[1 + 2\frac{\rho_e(x)\, u_e(x)}{\rho_e(0)\, u_e(0)}\frac{\delta^*}{h}\right] = 0$$

At this condition, the interface between driver gas and test gas moves with the same speed as the shock wave. Note: as $u_e(x) \to 0$, $\delta^* \to -\infty$, but their product remains finite.

Now consider the case of a strong shock. $u_w \gg u_e$, $\rho_e(\ell) \approx \rho_e(0)$. In that case let ℓ be the distance between the shock and the contact surface. Substituting for δ^* from strong shock result,

$$u_e(\ell) = \frac{d\ell}{dt} \doteq u_e(0)\left[1 - 2\frac{u_w}{u_e(0)}\frac{\delta(\ell)}{h}\right]$$

For a laminar b.l., $2\dfrac{u_w}{u_e(0)}\dfrac{\delta(\ell)}{h} = \sqrt{\dfrac{\ell}{\ell_m}}$, where ℓ_m is the value of ℓ at which $u_e(\ell) \to 0$.

$$\boxed{u_e(\ell) = \frac{d\ell}{dt} = u_e(0)\left[1 - \sqrt{\frac{\ell}{\ell_m}}\right]}$$

Recall that $\delta(l) = \sqrt{\frac{2\nu_e l}{(u_w + u_e)}}$ (laminar b.l.)

so with $u_w >> u_e$, $\frac{dl}{dt} = 0$ is reached when $l = l_m$ at

$$4 \frac{u_w^2}{u_e^2(0)} \cdot \frac{2\nu l_m}{u_w h} = 1$$

or $$\boxed{\frac{l_m}{h} = \frac{1}{8} \frac{u_e(0)}{u_w} \cdot \frac{u_e(0) h}{\nu_e}}$$ $f(\infty) \doteqdot 1.12$

Since $\frac{u_e(0)}{u_w} \doteqdot \frac{\gamma - 1}{2}$, l_m greatest for monatomic gas. Also l_m increases with Reynolds number.

Return to the equation at the bottom of p. 223. Write $L = l/l_m$, $T = \frac{u_e(0)t}{l_m}$

to get $$\frac{dL}{dT} = 1 - \sqrt{L}$$

Integrate: $$T = -2\left\{ \ln(1-\sqrt{L}) + \sqrt{L} \right\}$$

put $L = 1 - \varepsilon$ $$T = -2\left\{ \ln\left(1 - \left(1 - \frac{\varepsilon}{2}\right)\right) + 1 - \frac{\varepsilon}{2} \right\}$$

$$= -2\left\{ \ln\frac{\varepsilon}{2} + 1 - \frac{\varepsilon}{2} \right\}$$

$$e^{-\frac{T}{2}} = \frac{\varepsilon}{2} \cdot e^{1 - \frac{\varepsilon}{2}}$$

$$\boxed{\lim_{T \to \infty} L = 1 - 2e^{-\frac{T}{2}}}$$

The maximum distance between shock and contact surface is reached asymptotically. In many papers it is assumed that the average speed of the test gas slug is constant, and that consequently the shock slows down and the contact surface speeds up. This is wrong!

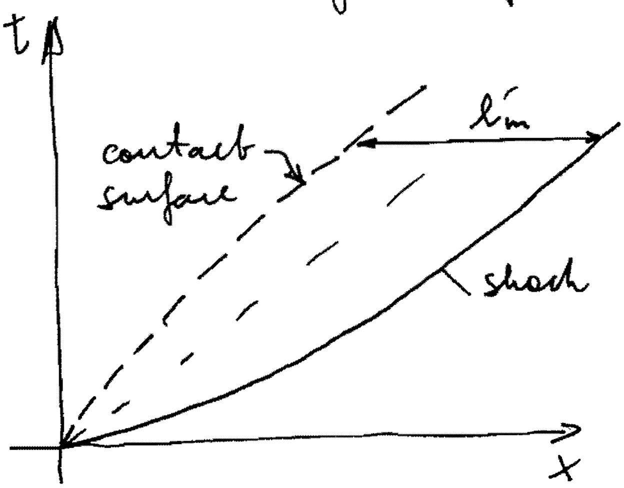

Often assumed WRONG behavior.

In actual fact, the shock wave is observed to slow down to speeds that are smaller than the initial contact surface speed ($u_c(0)$). The reason is that there is a boundary layer in the driver gas too. The friction associated with this slows down the driver gas, so that the "piston" driving the test gas is decelerated also. A more realistic picture is therefore as shown here.

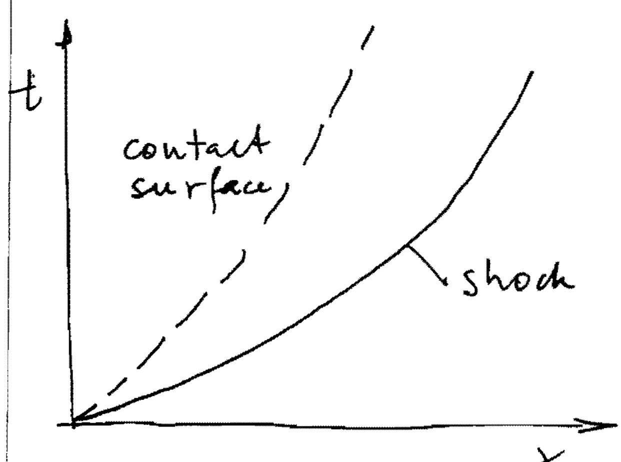

By making a momentum balance in a control volume that includes the driver gas in a circular shock tube, a simple, very useful formula can be derived for strong shocks:

$$\frac{\Delta M_s^2}{M_s^2} \doteq 2 \frac{L}{d} C_f$$

where C_f is the local skin friction coefficient. In the shock tube of T5, $Re_x \sim 10^9$ and C_f is $\sim 1.7 \times 10^{-3}$.

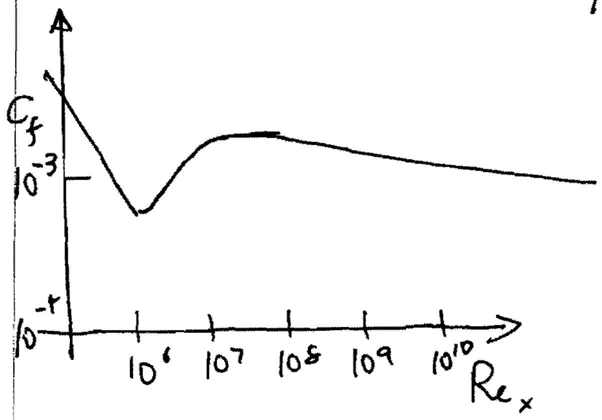

$$\frac{\Delta M_s}{M_s} \sim 1.7 \times 10^{-3} \frac{L}{d}$$

is a very good rule of thumb.

Had we known this, we would have made the L/d of T5 smaller

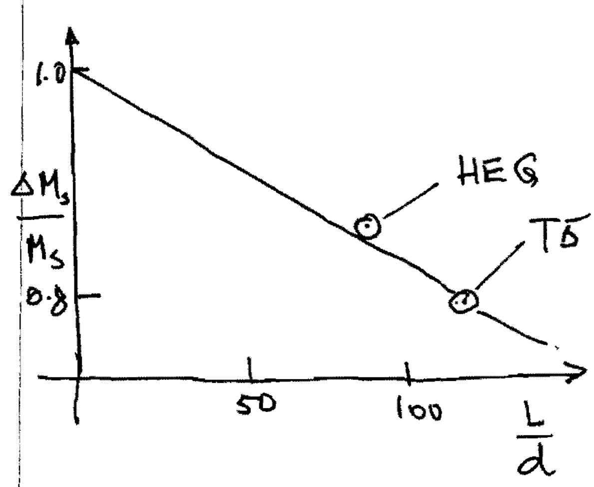

Weak Shock:

In the case of a weak shock the Mach number after the shock is nearly equal to 1, so that in the steady compression that follows the shock as a consequence of the area

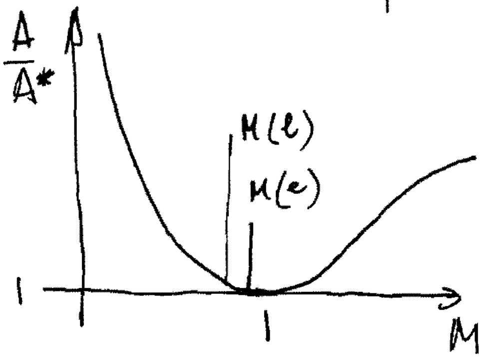

increase that occurs because of the negative displacement thickness, one may write $\rho_e(x)\, u_e(x) \doteq \rho_e(0)\, u_e(0)$ in the square brackets in the middle of page 223. Consequently the maximum slug length is reached when

$$2\frac{\delta^*}{h} = -1$$

or
$$\frac{2\delta}{\gamma+1}\left(M_e^2-1\right) f_1(\infty) = h$$

$$\frac{2\nu_e l_m}{(u_w+u_e)h^2} = \frac{(\gamma+1)^2}{4(M_e^2-1)^2 f_1^2(\infty)}$$

$$\frac{l_m}{h} = \frac{(\gamma+1)^2 (u_w+u_e) h}{8(M_e^2-1)^2 \nu_e f_1^2(\infty)}$$

$$\boxed{\frac{l_m}{h} \doteq \frac{(\gamma+1)^2}{4(M_e^2-1)^2} \frac{u_w h}{\nu_e} \cdot \frac{1}{f_1^2(\infty)}}$$

Since M_e is close to 1, attenuation of the shock is not a serious problem for weak shocks.

Ae237 Non-steady gasdynamics, 2003, Topics covered

1. Discrete waves in a medium, general shock jump conditions
2. Causality, stability, relation between Hugoniot, Rayleigh line, isentrope in dependence of Grüneisen parameter and fundamental derivative
3. General properties of the Hugoniot, Chapman-Jouguet points
4. Strong and weak detonations, deflagrations
5. Phase transitions, normal and retrograde fluids
6. Sound speed in mixed and vapor phase, expansion shocks, shock structure
7. Conditions near a critical point
8. Weak shock theory
9. Waves in traffic
10. Viscous dispersion, shock structure
11. Simple waves in one-dimensional flow, dependence on fundamental derivative, comparison of steady and unsteady waves
12. Wave interactions, shock tube, *up*-diagram, tailored interface operation
13. Evolution of a simple compression into a shock, more wave interactions
14. Wave interaction with an area change
15. Interaction of a shock with an area change
16. Two-dimensional flows, oblique shock, shock reflection from a wedge
17. Pseudo-steady flow, Mach reflection, case distinctions, information condition
18. Mach reflection in steady flow, von Neumann condition, dual solution domain, hysteresis, information condition again
19. Double Mach reflection, von Neumann paradox for very weak Mach reflection, resolution of v. N. paradox
20. Viscous effects, shock-generated boundary layer, displacement thickness and wall shear stress
21. Viscous effects in Mach reflection

Viscous effects in Mach reflection.

During the 1970's a number of researchers confirmed an observation first made by Smith (1959), that the transition from regular to Mach reflection ~~on~~ pseudosteady flow occurred at a slightly larger value of β than β_d. In particular, Takayama and Sekiguchi obtained experimental results that showed qualitatively the behavior sketched here, where the experimental points lie clearly above the value of β_d. The points indicate the angle β at which transition was observed to occur.

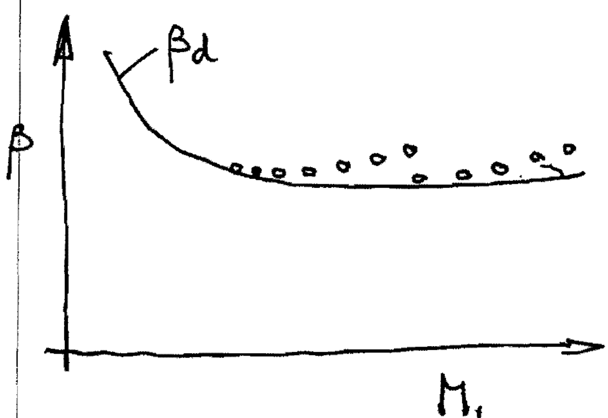

In 1978 we explained this behavior qualitatively by the negative displacement effect of the shock-generated boundary layer, see figure. The viscous case requires the reflected shock to produce only a smaller deflection angle

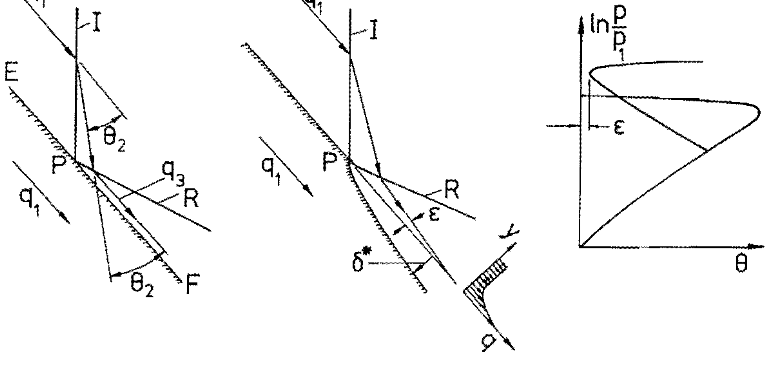

Figure 23 Regular reflection viewed from P's reference frame. (*left*) Inviscid. (*center*) Viscous displacement effect as seen by flow outside the boundary layer. (*right*) Viscosity causes transition to Mach reflection to be delayed.

than the inviscid one. Transition will therefore be delayed to a point where the reflected shock locus does not need to intersect the p axis. If the transition delay is truly a viscous phenomenon, then the delay should be reduced at higher Reynolds number. This made us look again at the peculiar feature of Takayama & Sekiguchi's data, which exhibit a step in the effect at a particular Mach number. Looking at their data in more detail, we found that, at that particular Mach number they switched from an air to a helium driver gas in order to be able to achieve the higher Mach numbers in their shock tube with reasonable

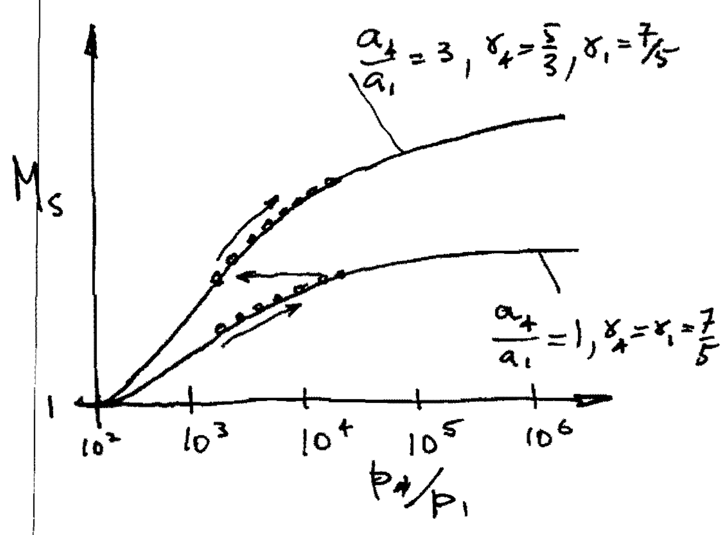

values of p_4/p_1. Now recall the shock tube equation, two solutions of which are sketched here, one with air driver, and one with Helium driver. So usually the maximum value of p_4 is fixed, and to increase M_s, one lowers p_1, thus lowering the Reynolds-number and increasing the displacement effect. So to keep increasing the shock Mach number, T+S first kept decreasing p_1 until it became too small, and then switched to helium drive to be able to operate with reasonable p_1 and get higher M_s. Thus, since $Re \sim p_1$, there is a step increase in Re at this Mach number, which we thought was the reason for the step change in the transition delay.

We therefore did an experiment in the shock tunnel T3, in which we were able to vary the Reynolds number at fixed shock Mach number. A plot of the transition angle against $1/\sqrt{Re}$ showed straight line behavior as it should for laminar boundary layers, and extrapolating the line to $Re = \infty$ gives almost exactly the inviscid value. This made us believe that it is truly the viscous effect that is responsible for the transition delay.

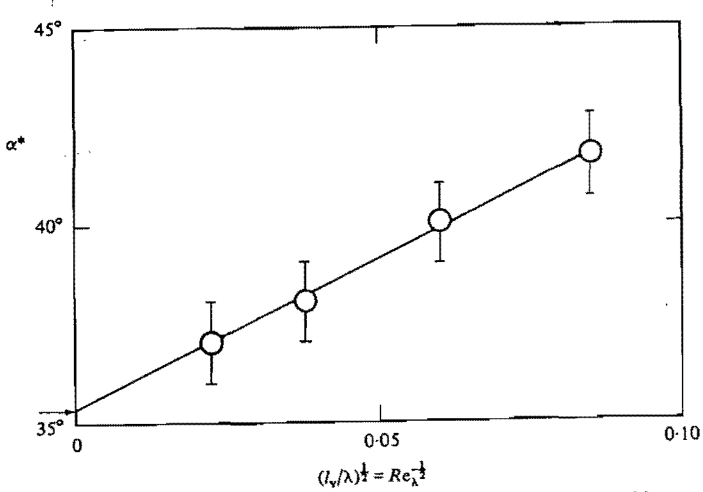

GURE 10. Experimental results: transition angle as a function of Reynolds number. Note the lculated inviscid value of α^* indicated by an arrow. Choosing $\lambda = 0{\cdot}22$ mm gives agreement of ›pe with theoretical estimate (11), (12).

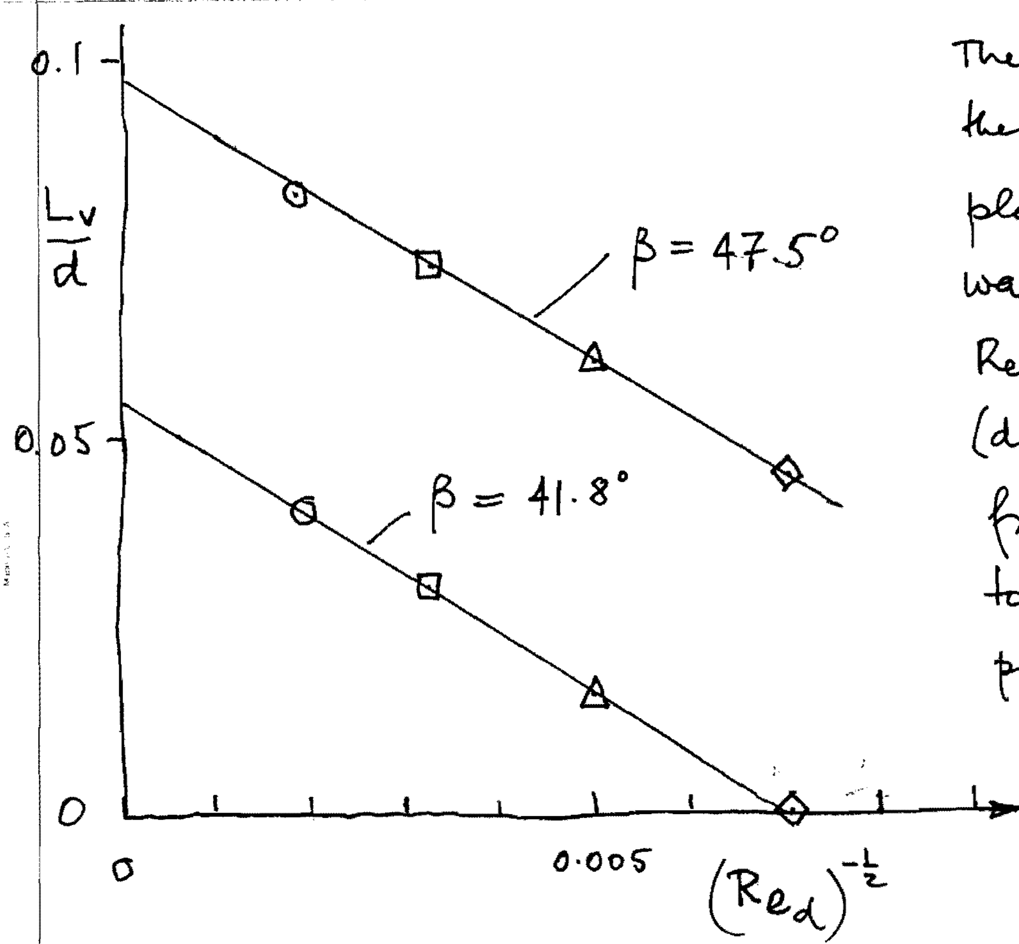

The data obtained there may also be plotted in a different way: Varying the Reynolds number (d is the distance from the wedgetip to the reflection point) at constant β, the Mach stem length L_v normalized by d varies as shown. Again we get a clear behavior of the form

$$\frac{L_v}{d} = \frac{L_i}{d} - \frac{c}{\sqrt{Re_d}}$$

Where L_v is the Mach stem length in viscous flow, L_i in inviscid flow and c is a constant.

THE EFFECT OF VISCOSITY ON THE MACH STEM LENGTH IN UNSTEADY STRONG SHOCK REFLECTION

Hans Hornung
Institut für Experimentelle Strömungsmechanik
DFVLR-AVA, 3400 Göttingen, Bunsenstr. 10

Introduction

Consider a plane shock wave I travelling from right to left with a constant speed q_s into a uniform gas at rest relative to an inertial frame. Let the shock strike a plane wedge whose leading edge is parallel to the plane of the shock, see *Figure 1*. Let the wedge be at rest relative to the same inertial frame. The interaction of the shock wave with the wedge usually causes a reflected shock R to be generated. In the situation shown in *Figure 1* this occurs as a so-called regular reflection. The reason for the

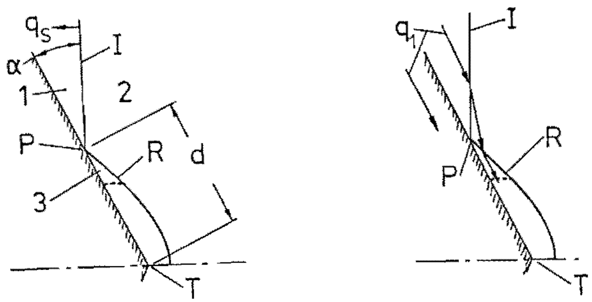

Figure 1 Regular shock reflection viewed from an inertial frame fixed in T (left) and from an inertial frame fixed in P (right)

reflected shock becomes evident when the flow in the vicinity of the reflection point P is observed from a frame of reference moving with P. In this frame the flow is steady in the neighbourhood of P, see *Figure 1*. In region 1, the undisturbed gas moves with velocity q_1 towards the shock I. It is then deflected towards the wedge surface by I (region 2), and the reflected shock performs the function of returning the flow direction to the wall direction in region 3. In the reference frame of P the wall also has the velocity q_1, of course.

We consider situations in which the flow is well approximated by the model of an ideal, viscous, heat-conducting gas with a constant ratio of specific heats γ, shear viscosity μ, heat conductivity k and density ρ. Let the wall temperature be T_w and a representative reservoir temperature be T_o.

In such situations any global dimensionless quantity Q may be expressed as a function of five parameters:

$$Q = Q\,(q/a,\ \gamma,\ \rho q d/\mu,\ \mu c_p/k,\ T_w/T_o), \quad \text{or}$$

$$Q = Q\,(M,\ \gamma,\ Re,\ Pr,\ T_w/T_o), \tag{1}$$

where c_p is the specific heat at constant pressure and $a^2 = \gamma p/\rho$, p being the pressure. In the inviscid (and non-conducting) limit this reduces to

$$Q = Q\,(M,\ \gamma)\ . \tag{2}$$

We now return to shock reflection: As the wedge angle is reduced, so that the angle α between I and the wedge surface (wall) is increased, an angle $\alpha = \alpha_d(M_1,\ \gamma)$ is reached, beyond which it is not possible for the second shock to return the streamline direction to that of the wall. The streamline direction in region 3 thus has a finite component towards the wall. As a consequence a third shock, the "Mach stem" S appears, opening up a fourth region between the wall and the triple shock point P which now lies off the wall, see *Figure 2*. The velocities in regions 3 and 4 are different, but the pressures and streamline directions are the same. The streamline from the triple point is thus a vortex sheet V in inviscid flow. This reflection configuration is called Mach reflection.

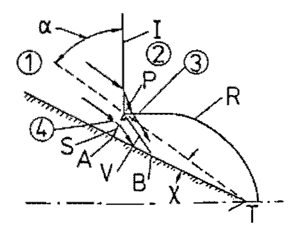

Figure 2 Mach reflection viewed from inertial frame fixed in P.

The different manifestations of shock reflection are too numerous to be discussed here. The interested reader is referred to [1] and the extensive list of references given in it. For our purposes it suffices to treat the two configurations illustrated in *Figures 1-2*, because we wish to single out the effect of viscosity.

In the inviscid limit, the only characteristic length in the problem is d. This increases linearly with the time t that has elapsed from the instant of contact of the shock with the wedge tip. Hence the geometrical configuration of the flow also grows linearly with t if the wedge surface is straight and smooth. Flows which exhibit this kind of selfsimilarity are called pseudosteady. Their particular feature is that the flow becomes independent of time in coordinates which are stretched by dividing the

232

space coordinates by t. For inviscid pseudosteady flows the transition from regular to Mach reflection occurs at

(3) $$\alpha = \alpha^*_{ps} = \alpha_d\ (M_1,\ \gamma).$$

The introduction of any second characteristic length into the problem necessarily destroys the selfsimilarity of pseudosteady flows. For example, if the gas is so rarefied that the mean free path λ is not extremely small compared with d, the reflection configuration will look different when it is near the tip than when it is far from the tip (see [2], [3]). Indeed, this effect is intimately connected with the problem at hand, since the introduction of viscosity brings into the problem the viscous length scale

(4) $$\ell_v = \mu/(\rho q),$$

which is related to the mean free path by

(5) $$\ell_v = b\lambda/M,$$

where, for a given gas, b is a numerical constant of order one.

Consequences to be expected from the introduction of viscosity into the problem are therefore:

1. that the angle α^*_v, at which transition from regular to Mach reflection occurs in viscous flow, is different from $\alpha^*_{ps}(M_1,\ \gamma)$, and

2. that α^*_v depends on the additional parameters d/ℓ_v = Re, Pr and T_w/T_o.

The first of these effects has been amply confirmed by [4] through experiments conducted with a systematic variation of ℓ_v, holding other parameters constant. As regards the second, [4] makes the mistake of not recognizing the fact that the destruction of the selfsimilarity through the introduction of viscosity means that the transition angle varies with the distance from the tip. This is because it had been tacitly assumed that the effect of viscosity is local to the reflection, and a local charateristic length was sought for the Reynolds number. In [4] the length chosen was the length of the Mach stem at observed transition, i.e. the observer's smallest resolvable length.

This turns out to be an incorrect description of the facts. However, the form of the variation of the viscous effect with ℓ_v was correctly modelled by [4], and agrees well with experiment. The mistake was not discovered because both d and the observer's smallest resolvable length were constant in the experiments of [4].

The crucial quantity in the measurement of the condition for transition to Mach reflection is the length of the Mach stem. The aim of the present work is to determine the dependence of this quantity on the parameters in equation (1) for Re >> 1.

The free shear layer

Consider the Mach reflection shown in *Figure 2*. The velocity discontinuity of the vortex sheet will be smeared out by the action of viscosity, so that the rotational region grows in thickness with distance along V from the triple point P. For laminar flow, this growth will be parabolic. In fact, such shear layers become unstable after quite short distances and roll up into discrete vortices thereafter. This effect may be observed in some schlieren photographs of Mach reflection.

The effect of viscous diffusion on the streamline shape in a shear layer in the region upstream of the point where the instability manifests itself, is to cause a displacement towards the faster side. This displacement may be expected to grow as the square root of the product of ℓ_v and the distance from P. However, in schlieren photographs e.g. of [4] it was not possible to observe any such displacement, the vortex sheet V being clearly visible and having no discernible curvature. In the following, the effect of viscosity at the vortex sheet is ignored, because the viscous effect at the wall produces much larger, and certainly observable angular changes, see [4].

The shock-induced boundary layer at the wall

Consider Mach reflection from a frame of reference fixed relative to the foot of the Mach stem, point A, see *Figure 3*. Let us focus attention on the flow in the immediate vicinity of A. The velocity of the wall, v_w, and of the gas in region 1, v_1, are equal. The Mach stem causes v_4, the velocity in region 4 to be smaller than v_w. For inviscid flow this means that a velocity discontinuity exists at the solid boundary. In viscous flow this is smeared out to form a boundary layer. In our shock-fixed frame of reference the flow in the vicinity of A is steady. The velocity in the shock-induced boundary layer is everywhere greater than the free stream velocity v_4. If the wall temperature is uniform and equal to the static temperature in region 1, the wall will be colder than the free stream, so that the density will also be greater within the boundary layer than in the free stream. Hence the displacement thickness of this boundary layer is negative. Becker [5] gives a detailed treatment of such shock-induced boundary layers. He shows that the displacement thickness δ^* may be expressed in the following form for laminar flow.

(6) $$\delta^*/x = -f_4\,(M,\ \gamma,\ Pr,\ T_w/T_o)\,(\ell_{v4}/x)^{1/2},$$

where x is the distance from A in the downstream direction along the wall, and the subscript 4 signifies that ℓ_v and the function f are to be evaluated at the conditions in region 4 outside the boundary layer.

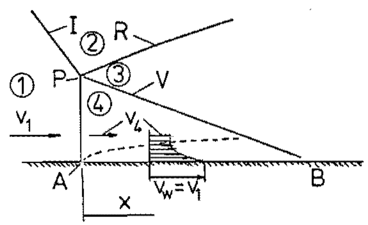

Figure 3 The Mach stem generates a velocity discontinuity which is smeared out by viscosity to form a boundary layer. Viewed from a frame of reference fixed in A

The influence of displacement thickness on Mach stem length

We now determine the mass of gas that has passed through the Mach stem during its traverse of the distance d from the wegde tip, see *Figure 2*. We do this for both the inviscid (pseudosteady, subscript ps) and the viscous case. In the pseudosteady case the triple point path is straight, and in the viscous case it describes a curve of so far unknown shape. Let L_v and L_{ps} be the Mach stem lengths in the viscous and pseudosteady case respectively. Since the conditions in region 1 are independent of whether the flow is viscous or not, the ratio of the masses m_v and m_{ps} swept up by the Mach stem in the viscous and pseudosteady case respectively is equal to the ratio of the corresponding volumes swept through. I.e.

(7) $$m_v/m_{ps} = 2\int_0^d L_v\,dz/(L_{ps}\,d),$$

where z = d - x is the coordinate measured from T.

Now let us obtain another expression for this mass ratio. The mass that has been swept up by the Mach stem is all contained in the region P'AB' in the pseudosteady case and in the region PAB in the viscous case, see *Figure 4*. That is, the vortex sheet V separates the gas that has been processed by S from that which has been processed by I and R. We now assume that the angle β between S and V is independent of viscosity and return to this assumption later. We further assume that the conditions in region 4 are

uniform except for the region occupied by the boundary layer. We also note that, if we wished to accommodate the mass m_v of gas at the conditions 4,

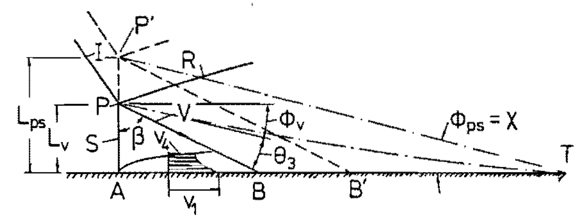

Figure 4 Showing viscous, ——, and inviscid flow, — — —, in the vicinity of the Mach stem, viewed from a frame of reference fixed in A. —·—·—, triple point paths

we would require a volume that is larger than the volume PAB by the displacement volume of the boundary layer, i.e. by

(8) $$\left|\int_0^{L_v\tan\beta}\delta^*dx\right| = \tfrac{2}{3}\,f_4\,\ell_{v4}^{1/2}(L_v\tan\beta)^{3/2}.$$

Hence,

$$m_v/m_{ps} = [L_v^2\tan\beta + \tfrac{4}{3}\,f_4\,\ell_{v4}^{1/2}\,(L_v\tan\beta)^{3/2}]/(L_{ps}^2\tan\beta),\quad\text{or}$$

(9) $$m_v/m_{ps} = [L_v^2 + \tfrac{4}{3}\,f_4\,(\ell_{v4}\tan\beta)^{1/2}L_v^{3/2}]\,/L_{ps}^2.$$

We may now equate (9) and (7) to get

(10) $$\int_0^z L_v dz' = [L_v^2 + \tfrac{4}{3}\,f_4\,L_v^{3/2}(\ell_{v4}\tan\beta)^{1/2}]/(2\tan\chi),$$

where the upper limit of integration has been changed from d to z for convenience.

Let us now introduce the dimensionless variables

(11) $$\zeta = z/d,\quad g(\zeta) = L_v/d,\quad g' = dg/d\zeta.$$

Assuming that β is independent of ℓ_{v4} (see later), we substitute (11) into (10) and differentiate w.r.t. ζ to obtain

(12) $$g\tan\chi = gg' + a\,Re_4^{-1/2}\,g^{1/2}g',$$

where $Re_4 = d/\ell_{v4}$ and $a = f_4(\tan\beta)^{1/2}$. Rewriting (12) in the form

(13) $$g'(1 + a\,Re_4^{-1/2}\,g^{-1/2}) = \tan\chi,$$

234

we may see that direct integration is possible, giving

$$g + 2a\,Re_4^{-1/2}\,g^{1/2} = \zeta \tan\chi + C, \tag{14}$$

where C is a constant of integration. Let us choose the boundary condition $g = 0$ at $\zeta = 0$ suggested by the fact that, at the wedge tip, the Mach stem length must be zero, and return to this choice later. This boundary condition puts $C = 0$. Solving (14), we obtain

$$g = \zeta \tan\chi\,[\,1 - 2a\,Re_4^{-1/2}/(\zeta \tan\chi)^{1/2}\,] + O(Re_4^{-1}), \text{ or} \tag{15}$$

$$L_v = z \tan\chi\,[1 - 2f_4\,(\tan\beta)^{1/2}\,Re_4^{-1/2}/(z \tan\chi/d)^{1/2}], \tag{16}$$

to the accuracy permitted here (boundary layer assumptions). This result is shown in *Figure 5*. It deserves some comment. In the inviscid limit, $Re = \infty$, it gives the correct behaviour that $L_v = z \tan\chi = L_{ps}$. In the viscous

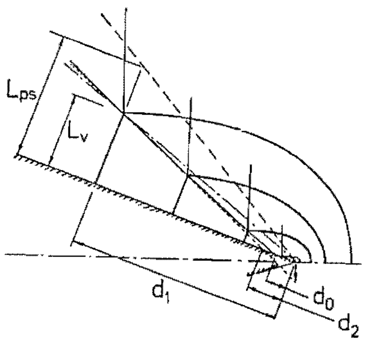

Figure 5 Effect of viscosity on triple point path: ——, viscous flow; — — —, inviscid flow; —·—·—, according to observer assuming inviscid flow; ------, by the procedure of [6]

case it predicts that the triple point path describes a curve which is concave away from the wall. A tangent to this curve extrapolated back towards the tip intersects the wall. In fact, the curve itself intersects the wall at $z = d_o$. However, this occurs in a region where our asymptotic theory is not valid, and where equation (16) does not give a good description of the facts, since higher order terms in $Re_4^{-1/2}$ would become important. A tangent to the curve at a point $z = d_1$ cuts the surface at a point

$$z = d_2 = f_4\,(d_1\,\ell_{v4} \tan\beta)^{1/2}\,(\tan\chi)^{-3/2}\,. \tag{17}$$

With the help of [5] and inviscid Mach reflecton theory, the right hand sides of (16) and (17) can be evaluated for a given set of the parameters M, γ, Re, Pr, T_w/T_o and α.

Revision of assumptions made

Three assumptions made in the argument leading to the results of the previous section need to be discussed. The first is, that the Mach reflection is assumed to have existed all the way from the tip, and this assumption is contradicted by the results. This contradiction arises because of the limitations of boundary layer theory. Consider equation (17). It is clear that $d_o = O(\ell_{v4})$, so that the Reynolds number based on d_o is $O(1)$. The results of the theory are restricted to large Reynolds numbers, so that the theory must not be expected to be valid in the region $z = O(d_o)$. In the range $z \gg d_o$ the negative contribution to the integrations in (7) and (8) which arise from $0 < z < d_o$ are $O(Re_4^{-1})$. Hence they appear only in higher order terms of the asymptotic theory and must be neglected for consistency.

The second assumption was that β is independent of viscosity. To investigate its effect, consider the angles ϕ_v and ϕ_{ps} made by the paths of P and P' relative to the wall. In the inviscid case, this is $\phi_{ps} = \chi$. In the viscous case it is

$$\begin{aligned}\phi_v &= [\arctan(dL_v/dz)]_{z=d}\\ &= \arctan[\tan\chi - f_4(\ell_{v4}\tan\beta\,\tan\chi/d)^{1/2}]\\ &= \chi - f_4(\ell_{v4}\tan\beta\,\tan\chi/d)^{1/2}/(1+\tan^2\chi),\end{aligned}$$

$$\phi_v = \chi - b_1 Re_4^{-1/2} + O(Re_4^{-1}). \tag{18}$$

The angle θ_3 between V and the direction of the triple point path is given by the shock jump conditions applied in a frame of reference attached to the triple point. Provided that $d \gg d_o$, it is possible to show that

$$\theta_{3v} = \theta_{3ps} + b_2\,Re_4^{-1/2}. \tag{19}$$

The quantities b_1 and b_2 do not depend on Re_4. Since

$$\beta = \pi/2 - (\phi + \theta_3), \tag{20}$$

$$\beta_v = \beta_{ps} + (b_1 - b_2)\,Re_4^{-1/2}. \tag{21}$$

Hence the error in β incurred by the assumption is $O(Re_4^{-1/2})$. Since β only occurs in a term $O(Re_4^{-1/2})$ in the results, the assumption is valid in the asymptotic sense.

The third assumption was that the conditions in region 4 are independent of viscosity. By considering the speed of the Mach stem in the two cases from a frame of reference fixed in the wall, it may be seen that this is not quite correct. In all our considerations we took the viscous and inviscid Mach stems to be at the same position, see *Figure 4.* Since the viscous Mach stem is shorter, it must lag behind the inviscid one, however, because the incident shock is in the same position for both cases. The separation of the Mach stems is

$$\Delta = (L_{ps} - L_v)\tan(\alpha + \chi), \tag{22}$$

so that this too is $O(Re_4^{-1/2})$, see equation (16). An error in the free stream conditions of this order affects the displacement thickness only in higher orders, so that again, the assumption is valid in the asymptotic sense.

The experimental evidence

Apart from the experimental results of [4] which support the parabolic dependence of the viscous effects on Reynolds number, there are two items of evidence worth noting here.

The first is in the experiments of Henderson and Gray [6] who showed that the measured shock and vortex sheet angles did not agree with the shock jump conditions if the triple point path was assumed to be a straight line through the wedge tip. They adjusted the slope of the triple point path to minimize the discrepancy. The resulting triple point path was found to cut the wedge surface. This is in agreement with the behaviour described by equation (16), and equation (17) gives a quantitative expression for the intersection point.

The second item of evidence is the behaviour of the Mach stem length in rarefied gas flows. Such flows have been examined by Walenta [2] and Schmidt [3], who found that the triple point path emerges from the surface at a distance from the tip which is of the order of $100\ \lambda$. In unpublished work, Walenta relates this effect to the dependence of the speed of shocks of finite thickness on shock curvature. It is likely, however, that it is at least partly due to the effect of shear viscosity at the wall.

Conclusions

An asymptotic theory for large Reynolds number is presented, which yields an expression for viscous and heat conduction effects on the triple point path of Mach reflection. The result predicts that viscosity and heat

transfer to the wall cause the Mach stem length to be reduced by an amount which increases as the square root of the distance from the tip of the reflecting wedge. Some qualitative features of this solution are confirmed by independent experiments. The results are of considerable importance in the interpretation of experimental results on Mach reflection.

References

[1] Hornung, H.: "Regular and Mach reflection of shock waves." To be published in Ann. Rev. Fluid Mech. (1986)

[2] Walenta, Z.A.: "Formation of the Mach-type reflection of shock waves." Arch. Mech. 35, (1983) 187 - 196

[3] Schmidt, B.: "Stoßwellenübergang von regulärer Reflektion zur Mach Reflektion auf der Flanke eines Keils." ZAMM 65 (1985)

[4] Hornung, H.G.; Taylor, J.R.: "Transition from regular to Mach reflection of shock waves. Part 1. The effect of viscosity in the pseudosteady case." J.Fluid Mech. 123 (1982) 143-153

[5] Becker, E.: "Instationäre Grenzschichten hinter Verdichtungsstößen und Expansionswellen." In: "Progress in Aero. Sci." eds. Ferri, Küchemann, Sterne, 1 (1961) 104-153

[6] Henderson, L.F.; Gray, P.M.: " Experiments on the diffraction of strong blast waves." Proc. Roy. Soc. Lond. A 377 (1981) 363-378